Quantitative MRI in the assessment of healthy and diseased muscle

Matthew Farrow

Submitted in accordance with the requirements for the degree of Doctor of Philosophy

The University of Leeds
Faculty of Medicine
Leeds Institute of Rheumatic and Musculoskeletal Medicine

September 2020

Intellectual Property and Publication Statements:

The candidate confirms that the work submitted is his own, except where work which has formed part of jointly authored publications has been included. All figures in this thesis were produced by Matthew Farrow unless stated otherwise. The contributions of the candidate and the other authors to this work have been explicitly indicated below. The candidate confirms that appropriate credit has been given within the thesis where reference has been made to the work of others.

Chapter 1, Chapter 2, and **Chapter 9** include work from a jointly authored publication by "**Farrow, M**. Biglands, JD. Alfuraih, A. Wakefield, R. Tan, AL. Novel muscle imaging in inflammatory rheumatic diseases. Frontiers in Medicine. 2020" (1). Matthew Farrow and Ai Lyn Tan wrote the first draft of the manuscript. Matthew Farrow and John Biglands contributed figures. All authors revised the work critically and approved the final version of the manuscript.

Chapter 4 is based on work from a jointly authored publication by "**Farrow, M**. Grainger, A. Tan, AL. Buch, MH. Emery, P. Ridgway, JP. Feiweier, T. Tanner, SF. Biglands, JD. Normal values and test-retest variability of stimulated-echo diffusion tensor imaging and fat fraction measurements in the muscle. British Journal of Radiology. 2019" (2). Matthew Farrow and John Biglands recruited participants. John Biglands developed the post-processing software, and all cases were processed by Matthew Farrow. John Biglands conducted the MR spectroscopy analysis. Matthew Farrow and Andrew Grainger drew the regions of interest. Matthew Farrow completed the statistical analysis and generated the results. Matthew Farrow wrote the first draft of the manuscript. All authors revised the manuscript critically and approved the final version of the manuscript.

Chapter 5 is based on work from a jointly authored publication by "**Farrow, M**. Biglands, JD. Tanner, SF. Clegg, A. Brown, L. Hensor, EMA. O'Connor, P. Emery, P. Tan, AL. Ageing Clinical and Experimental Research. 2020" (3). Matthew Farrow was involved in the study protocol development and ethics application. Care 75+ provided a database of healthy controls over the age of 75 who had consented to take part in research. Matthew Farrow developed the muscle function testing protocol. Matthew Farrow recruited participants. Matthew Farrow and Abdulrahman Alfuraih completed the muscle function testing. John Biglands developed the post-processing software, and Matthew Farrow processed all cases and compiled the cohort database. Matthew Farrow drew the regions of interest, completed the statistical analysis, generated the results, and wrote the first draft of the manuscript. Elizabeth Hensor provided statistical advice. All authors revised the manuscript critically and approved the final version of the paper.

Chapter 6 is based on work from a jointly authored publication by "**Farrow, M**. Biglands, JD. Grainger, A. O'Connor, P. Hensor, EMA. Ladas, A. Tanner, SF. Emery, P. Tan, AL. Quantitative MRI in myositis patients: A comparison with healthy volunteers and radiological visual assessment. Clinical Radiology. 2020" (4). Matthew Farrow was involved in the study protocol development and ethics application. Matthew Farrow developed the muscle function testing protocol. Matthew Farrow and Abdulrahman Alfuraih recruited participants and completed the muscle function testing. John Biglands developed the post-processing software, and Matthew Farrow processed all cases and compiled the cohort database. Matthew Farrow drew the regions of interest, completed the statistical analysis, generated the results, and wrote the first draft of the manuscript. Elizabeth Hensor provided statistical advice. Philip O'Connor and Andreas Ladas scored the myositis images. All authors revised the manuscript critically and approved the final version of the paper.

Chapter 7 is based on work from a jointly authored publication by "**Farrow, M**. Biglands, JD. Tanner, SF. Hensor, EMA. Buch, MH. Emery, P. Tan, AL. Muscle deterioration due to rheumatoid arthritis: Assessment by quantitative MRI and strength testing. Rheumatology. 2020" (5, 6). Matthew Farrow was involved in the study protocol development and ethics application. Matthew Farrow developed the muscle function testing protocol. Matthew Farrow recruited the patients. Matthew Farrow and Abdulrahman Alfuraih completed the muscle function testing. John Biglands developed the post-processing software, and Matthew Farrow processed all cases and compiled the cohort database. Matthew Farrow drew the regions of interest, completed the statistical analysis, generated the results, and wrote the first draft of the manuscript. Elizabeth Hensor provided statistical advice. All authors revised the manuscript critically and approved the final version of the manuscript.

Chapter 8 is based on work from a jointly authored manuscript currently in preparation by "**Farrow, M.** Biglands, JD. Hensor, EMA. Tanner, SF. Mackie, SL. Emery, P. Tan, AL. Muscle differences in patients with giant cell arteritis on glucocorticoids as assessed by quantitative MRI: a pilot study." Matthew Farrow was involved in the study protocol development and ethics application. Matthew Farrow developed the muscle function testing protocol. Matthew Farrow and Abdulrahman Alfuraih recruited participants and completed muscle function testing. John Biglands developed the post-processing software, and Matthew Farrow processed all cases and compiled the cohort database. Matthew Farrow drew the regions of interest, completed the statistical analysis, generated the results, and wrote the first draft of the manuscript. Elizabeth Hensor provided statistical advice. All authors revised the manuscript critically and approved the final version of the manuscript.

List of published articles arising from this thesis:

1. Normal values and test-retest variability of stimulated-echo diffusion tensor imaging and fat fraction measurements in the muscle
   Farrow, M. Grainger, AJ. Tan, AL. Buch, MH. Emery, P. Ridgway, JP. Feiweier, T. Tanner, SF. Biglands, JD.
   The British Journal of Radiology, 2019.
   (The data from this paper are discussed in Chapter 4 of this thesis)

2. Novel muscle imaging in inflammatory rheumatic diseases
   Farrow, M. Biglands, JD. Alfuraih, A. Wakefield, R. Tan, AL.
   Frontiers in Medicine, 2020.
   (Components of this paper are included in Chapter 1, Chapter 2, and Chapter 9)

3. The effect of ageing on skeletal muscle as assessed by quantitative MR imaging: an association with frailty and muscle strength
   Farrow, M. Biglands, JD. Tanner, SF. Clegg, A. Brown, L. Hensor, EMA. O'Connor, P. Emery, P. Tan, AL.
   Ageing Clinical and Experimental Research, 2020.
   (The data from this paper are discussed in Chapter 5 of this thesis)

4. Quantitative MRI in myositis patients: A comparison with healthy volunteers and radiological visual assessment
   Farrow, M. Biglands, JD. Grainger, A. O'Connor, P. Hensor, EMA. Ladas, A. Tanner, SF. Emery, P. Tan, AL.
   Clinical Radiology, 2020.
   (The data from this paper are discussed in Chapter 6 of this thesis)

5. Muscle deterioration due to rheumatoid arthritis: Assessment by quantitative MRI and strength testing
   Farrow, M. Biglands, JD. Tanner, SF. Hensor, EMA. Buch, MH. Emery, P. Tan, AL.
   Rheumatology, 2020.
   (The data from this paper are discussed in Chapter 7 of this thesis)

6. *Commentaries on Viewpoint: The interaction between SARS-CoV-2 and ACE2 may have consequences for skeletal muscle viral susceptibility and myopathies*
   *Tan, AL. **Farrow, M**. Biglands, J.*
   Journal of applied physiology, 2020.

List of articles in preparation for publication arising from this thesis:

1. Muscle differences in patients with giant cell arteritis as assessed by quantitative MRI: a pilot study (in preparation)
   Farrow, M. Biglands, JD. Hensor, EMA. Tanner, SF. Mackie, SL. Emery, P. Tan, AL.
   (The data from this paper are discussed in Chapter 8 of this thesis)

Annual conference oral presentations

1. Quantitative MRI and dynamometer measurements can distinguish myositis from healthy control muscle
   Farrow, M. Biglands, JD. Grainger, A. O'Connor, P. Hensor, EMA. Ladas, A. Tanner, SF. Emery, P. Tan, AL.
   British Association of Clinical Anatomists. 2018.
   Recipient of award - Conrad Lewin Prize

2. The effect of ageing on skeletal muscle as assessed by quantitative MR imaging: an association with frailty and muscle strength
   Farrow, M. Biglands, JD. Tanner, SF. Clegg, A. Brown, L. Hensor, EMA. O'Connor, P. Emery, P. Tan, AL.
   The Anatomical Society. 2019.

3. Muscles in myositis patients with normal MRI appearance have higher quantitative T2 compared to those in healthy controls
   Farrow, M. Biglands, JD. Grainger, A. O'Connor, P. Hensor, EMA. Ladas, A. Tanner, SF. Emery, P. Tan, AL.
   International Society of Magnetic Resonance Imaging in Medicine. 2019.
   Recipient of award - Educational award

4. Quantitative MRI of muscles is different in rheumatoid arthritis patients compared to healthy controls
   Farrow, M. Biglands, JD. Tanner, SF. Hensor, EMA. Buch, MH. Emery, P. Tan, AL.
   British Association of Clinical Anatomists. 2019.

5. The effect of ageing on skeletal muscle as assessed by quantitative MR imaging: an association with frailty and muscle strength
   Farrow, M. Biglands, JD. Tanner, SF. Clegg, A. Brown, L. Hensor, EMA. P O'Connor. Emery, P. Tan, AL.
   International conference of Frailty and Sarcopenia. 2020.

6. Muscle deterioration due to rheumatoid arthritis: Assessment by quantitative MRI and strength testing
   Farrow, M. Biglands, JD. Tanner, SF. Hensor, EMA. Buch, MH. Emery, P. Tan, AL.
   European Congress of Rheumatology. 2020.
   Recipient of award - Conference bursary

Annual conference poster presentations

1. Repeatability and Reproducibility of Diffusion Tensor MRI and two-point Dixon Fat Fraction measurements in the muscle
   Farrow, M. Grainger, AJ. Tan, AL. Buch, MH. Emery, P. Ridgway, JP. Feiweier, T. Tanner, SF. Biglands, JD.
   International Society of Magnetic Resonance Imaging in Medicine 2018.

2. Quantitative MRI measurements can distinguish myositis from healthy control muscle
   Farrow, M. Biglands, JD. Grainger, A. O'Connor, P. Hensor, EMA. Ladas, A. Tanner, SF. Emery, P. Tan, AL.
   British Chapter- International Society of Magnetic Resonance Imaging in Medicine. 2019.

3. Muscles in myositis patients with normal MRI appearance have higher quantitative T2 compared to those in healthy controls
   Farrow, M. Biglands, JD. Grainger, A. O'Connor, P. Hensor, EMA. Ladas, A. Tanner, SF. Emery, P. Tan, AL.
   European Congress of Rheumatology. 2019.
   Recipient of award - Conference bursary

4. Quantitative MRI measurements can distinguish myositis from healthy control muscle
   Farrow, M. Biglands, JD. Grainger, A. O'Connor, P. Hensor, EMA. Ladas, A. Tanner, SF. Emery, P. Tan, AL.
   Experimental Biology. 2019.
   Recipient of awards - 1) Abstract award 2) Conference bursary

5. Quantitative MRI of muscles is different in rheumatoid arthritis patients compared to healthy controls
   Farrow, M. Biglands, JD. Tanner, SF. Hensor, EMA. Buch, MH. Emery, P. Tan, AL.
   The anatomical society. 2019.

6. Variability of Diffusion Tensor MRI, 2-Point Dixon fat fraction and T2 relaxation in ROIs of thigh muscles in rheumatoid arthritis patients
   Bertham, D. **Farrow, M**. Tan, AL. Tanner, S. Emery, P. Biglands, J.
   International Society of Magnetic Resonance Imaging in Medicine. 2020.

7. The effect of ageing on skeletal muscle as assessed by quantitative MR imaging: an association with frailty and muscle strength
   Farrow, M. Biglands, JD. Tanner, SF. Clegg, A. Brown, L. Hensor, EMA. O'Connor, P. Emery, P. Tan, AL.
   International Society of Magnetic Resonance Imaging in Medicine. 2020.
   Recipient of award - Educational award

8. Muscles in myositis patients with normal MRI appearance have higher quantitative T2 compared to those in healthy controls
   Farrow, M. Biglands, JD. Grainger, A. O'Connor, P. Hensor, EMA. Ladas, A. Tanner, SF. Emery, P. Tan, AL.
   British Society of Rheumatology. 2020.

9. Quantitative MRI of muscles is different in rheumatoid arthritis patients compared to healthy controls
   Farrow, M. Biglands, JD. Tanner, SF. Hensor, EMA. Buch, MH. Emery, P. Tan, AL.
   British Society of Rheumatology. 2020.

10. Quantitative MRI of muscles is different in rheumatoid arthritis patients compared to healthy controls
    Farrow, M. Biglands, JD. Tanner, SF. Hensor, EMA. Buch, MH. Emery, P. Tan, AL.
    International Society of Magnetic Resonance Imaging in Medicine. 2020.
    Recipient of award - Educational award

11. Differences in muscle properties in GCA patients compared to healthy controls as assessed by quantitative MRI
    Farrow, M. Biglands, JD. Tanner, SF. Hensor, EMA. Mackie, SL. Emery, P. Tan, AL.
    European Congress of Rheumatology. 2020.
    Recipient of award - Conference bursary

Acknowledgements

This PhD would not have been possible without the valuable input of my supervisors and colleagues, and the support of my family. Firstly, I would like to thank my supervisors sincerely, Dr Ai Lyn Tan, Dr John Biglands, Professor Paul Emery, and Professor Maya Buch for their tireless support and guidance, and providing me with the opportunity to conduct research within the internationally acclaimed Leeds Institute of Rheumatic and Musculoskeletal Medicine. Their guidance over the past four years has been unwavering, and it has been a great privilege to work with such high calibre academics and incredibly kind people.

I am immensely thankful to Dr Steven Tanner and Dr John Ridgway, who provided MRI physics advice. I am also incredibly thankful to Dr Elizabeth Hensor (department statistician) who provided expert statistical guidance.

I am indebted to Dr Andrew Grainger and Dr Philip O'Connor, who provided invaluable expert radiological support during this PhD. This PhD would not have been possible without the brilliance of the Leeds Biomedical Research Centre radiographers: Mr Dominic Bertham, Mr Brian Chaka, and Mr Robert Evans.

I have made many sincere friends throughout this PhD. I would like to thank everybody who has made the last four years enjoyable, of which there are too many to mention. Therefore, I will limit myself to mentioning only those with whom I shared an office with: Dr Gabriele De Marco, Dr Sayam Dubash, Dr Hannah Mathieson, Dr John Arnold, and Miss Annie Dou.

I would like to particularly express my gratitude to fellow researcher and great friend Dr Abdulrahman Alfuraih who worked alongside me on the MUSCLE project. It has been a pleasure to collaborate with Dr Alfuraih over the past four years.

I would like to thank the University of Leeds, the Leeds Institute of Rheumatic Medicine (LIRMM), and the Leeds National Institute of Health Research (NIHR) Biomedical Research Centre (BRC) for awarding me the generous funding to pursue this PhD. The PhD scholarship has provided me with financial support to conduct this research and supported numerous opportunities for me to present my research at national and international conferences.

I would like to thank the University of Bradford, School of Pharmacy and Medical Sciences, Faculty of Life Sciences, for offering me a permanent post as Lecturer in Anatomy, Physiology, and Musculoskeletal Sciences during the final year of this PhD. Thanks to this lectureship, I have gained valuable experience lecturing on the Clinical Sciences, Foundation in Medicine, and the Master of Pharmacy programmes. This experience has helped me during the write up of this thesis and provided significant insight into the workings of an academic career.

Finally, I am deeply grateful to the study participants and patients who generously volunteered their time without reimbursement to take part in this study.

Matthew Farrow

Abstract

Skeletal muscle health is intrinsically associated with physical function and quality of life. A decrease in skeletal muscle health is associated with functional loss and often occurs with ageing, disease, and the effects of medication. In recent years, medical imaging has played an increasing role in the clinical management of patients with rheumatic disease. However, compared to research investigating the joints (7, 8), research into muscle imaging is significantly less established, even though muscle symptoms are similarly prevalent and debilitating within the spectrum of rheumatic diseases.

Magnetic resonance imaging (MRI) can provide information regarding muscle health. Conventional MRI relies on the visual interpretation of disease activity and is, therefore, qualitative and susceptible to subjective bias. Quantitative MRI has the potential to offer a non-invasive measurement of muscle status, which may be more sensitive and reliable than conventional MRI.

The work presented in this thesis aimed to explore the use of quantitative MRI measurements in the assessment of skeletal muscle in healthy controls and rheumatic patients. This research used specific MRI measurements that focus on some of the known muscle pathologies that occur with muscle disease. These muscle pathologies include: muscle oedema, myosteatosis, changes to muscle microstructure, and muscle atrophy. The quantitative MRI measurements used in this thesis include: T2, fat fraction, diffusion tensor imaging, and muscle volume. In addition to the quantitative MRI measurements, this research project has also collected quantitative physiological data on knee extension, knee flexion, and handgrip strength.

The first study within this thesis is based on a new MRI protocol that was tested within a cohort of healthy controls. This first study demonstrated differences in muscle properties within the hamstrings and quadriceps and demonstrated that quantitative MRI measurements have excellent test-retest, inter-rater, and intra-rater reliability. Following this first study, which established the normal values and the excellent reliability of the quantitative MRI measurements, these measurements were utilised in healthy controls and patients with myositis, rheumatoid arthritis (RA), and giant cell arteritis (GCA). The results of this research demonstrate that quantitative MRI measurements can identify substantial differences within the muscle between young, middle-aged, and older participants, and can identify substantial differences between patients with rheumatic conditions and age- and gender-matched healthy controls. Furthermore, this research found that quantitative MRI measurements correlate with muscle strength and the English Longitudinal Study of Ageing frailty index. In addition, this research found that in myositis patients diagnosed by radiologists as having unaffected muscles, there were substantial differences in T2 measurements compared to matched healthy controls. Therefore, T2 measurements may be more sensitive than current radiologist semi-quantitative scoring using conventional MRI. Furthermore, this research found that RA and GCA patients who are newly diagnosed may have muscle pathology during the initial stages of the disease, which is a pathological process not previously reported in the literature. In addition, this research demonstrated that RA patients who achieve clinical remission may still have muscle pathology.

In conclusion, this research has found preliminary data that indicates that muscle health can decrease due to ageing, myositis, RA, and GCA. This thesis demonstrates that quantitative MRI has the potential to be an excellent tool to assess for degenerative changes within the muscle and may correlate with muscle function and frailty.

Table of Contents

List of Figures

List of Tables

List of Abbreviations

ACR	American College of Rheumatology
ANOVA	Analysis of variance
ATPase	Adenosine triphosphatase
AUC	Area under the curve
BF	Biceps femoris
BMI	Body mass index
BRC	Biomedical Research Centre
BSR	British Society for Rheumatology
CARE 75+	Community ageing research - 75+
CI	Confidence intervals
CK	Creatine kinase
CLES	Common language effect size
cm	Centimetre
CRP	C-reactive protein
CT	Computed tomography
d	Cohen's delta
D	Diffusion coefficient
DAS28	Disease activity score 28
DG	Diffusion-sensitising gradients
DM	Dermatomyositis
DMARDs	Disease-modifying anti-rheumatic drugs
DOMS	Delayed onset muscle soreness
DTI	Diffusion tensor imaging
DWI	Diffusion-weighted imaging
DXA	Dual-energy X-ray absorptiometry
ELSA	English longitudinal study of ageing
EMG	Electromyography
EPI	Echo planar imaging
ESR	Erythrocyte sedimentation rate
EULAR	European League Against Rheumatism
EWGSOP	European Working Group on Sarcopenia in Older People
FA	Fractional anisotropy
FF	Fat fraction
FI	Frailty index

g	Hedge's g
G	Magnitude
GCA	Giant cell arteritis
GIM	Glucocorticoid-induced myopathy
GRAPPA	Generalised auto-calibrating partial parallel acquisition
Hz	Hertz
IBM	Inclusion body myositis
ICC	Intraclass correlation coefficient
IIM	Idiopathic inflammatory myopathies
IL	Interleukin
IPAC	International physical activity questionnaire
IQR	Interquartile range
ISRCTN	International standard randomised controlled trial number
IU/L	International units per litre
LIRMM	Leeds Institute of Rheumatic and Musculoskeletal Medicine
LTHT	Leeds Teaching Hospitals Trust
MATLAB	Matrix laboratory
MD	Mean diffusivity
MESE	Multi-echo, spin-echo
M_f	Proton densities of fat
mg	Milligrams
mm	Millimetre
MMT	Manual muscle testing
MR	Magnetic resonance
MRI	Magnetic resonance imaging
MRS	Magnetic resonance spectroscopy
ms	Millisecond
MUSCLE	Magnetic resonance imaging and UltraSound CLinical Evaluation of muscle pathology
Mw	Proton densities of water
MyHC	Myosin heavy chain
NF-κB	Nuclear factor kappa-beta pathway
NIHR	National Institute of Health Research
Nm	Newton metres
NSAIDs	Non-steroidal anti-inflammatory drugs
PET	Positron emission tomography
pH	Potential of hydrogen

PM	Polymyositis
PMR	Polymyalgia rheumatica
PPM	Parts per million
RA	Rheumatoid arthritis
RAMRIS	Rheumatoid arthritis magnetic resonance imaging scoring system
RF	Radiofrequency
RF	Rectus femoris
ROC	Receiver operator characteristic
ROI	Regions of interest
S	Signal
S_0	MR signal at baseline
SD	Standard deviation
SE	Spin echo
S_f	Signal of fat
SM	Semimembranosus
SNR	Signal to noise ratio
SPAIR	Spectral attenuated inversion recovery
SPSS	Statistical package for the social sciences
ST	Semitendinosus
STEAM	Stimulated echo acquisition mode
STIR	Short tau inversion recovery
S_w	Signal of water
T	Tesla
TA	Acquisition time
TE	Echo time
TM	Mixing time
TNF-α	Tumour necrosis factor-alpha
TR	Repetition time
TSE	Turbo spin-echo
VAS	Visual analogue scale
VI	Vastus intermedius
VIBE	Volumetric interpolated breath-hold examination
VL	Vastus lateralis
VM	Vastus medialis
µm	Micrometre
γ	Gamma
δ	Duration

Δ	Time interval
λ	Lambda
ω_0	Larmor frequency

Chapter 1 Introduction to the thesis

This chapter serves as a brief introduction to this thesis and includes an article by Matthew Farrow, John Biglands, Abdulrahman Alfuraih, Richard Wakefield, and Ai Lyn Tan. "Novel muscle imaging in inflammatory rheumatic diseases" published in Frontiers in Medicine, 2020 (1).

1.1 Introduction

A decline in muscle health can significantly affect the quality of life for people and is associated with increased mortality and morbidity (9). For this thesis, the term muscle health shall be defined as 'a state of physical capability influenced by intrinsic muscle properties and muscle mass. Decreases in muscle health are often assessed by blood tests (creatine kinase), muscle biopsies, and medical imaging such as ultrasound, computed tomography, and magnetic resonance imaging (MRI). Muscle health can also be evaluated by assessing muscle function and muscle quality. Muscle function can be examined by strength tests, such as with the use of dynamometers, or by functional tests, such as gait speed tests. The assessment of muscle quality can encompass several aspects, such as muscle oedema, myosteatosis (fat infiltration), and muscle atrophy. All of which can be assessed by MRI. For this thesis, the term 'muscle health' shall encompass muscle function (muscle strength and physical function), muscle quality (pathology within the muscle), and muscle volume. It is known that muscle health deteriorates due to ageing (10, 11), disease (12), and medication use, in particular - steroid use (13). However, the changes that occur within the muscle due to ageing and rheumatic disease are under-reported within the scientific literature, resulting in a lack of understanding of the muscle pathology, which can impede the development of effective treatments to improve muscle health (14). Within rheumatic diseases, the features of: malaise, myalgia, muscle inflammation, myosteatosis, muscle atrophy,

and decreased muscle strength are frequently observed (15). However, although muscle pathology is known to occur in rheumatic disease, the majority of research has focussed on joint pathology as opposed to muscle pathology, highlighting the need for further research in the field of muscle pathology within rheumatology.

One of the reasons that the effects of ageing and disease on the muscles are not well understood is that it is difficult to see early changes occurring in the muscle in response to ageing, disease, or treatment. It is challenging to identify these early changes because the noticeable features, such as loss of muscle strength, muscle atrophy, and myalgia, often become apparent in the later stages of the disease once a certain threshold of muscle pathology has already occurred. If these pathological changes could be identified earlier and measured quantitatively, a better understanding of muscle pathology could be achieved. Therefore, quantitative MRI measurements may result in an improved comprehension of muscle pathology due to ageing and disease and may allow for an earlier diagnosis which could enhance the clinical management, including providing an instrument for the objective monitoring of disease progression and assist in the development of future interventions.

Medical imaging modalities are often used to assess joints in rheumatology, and there is increasing emphasis on the role of the muscle in contributing to the symptoms of patients with rheumatic conditions. Types of medical imaging that have been used to assess muscle include: dual-energy X-ray absorptiometry (DXA) which costs approximately £125 per scan, positron emission tomography (PET) which costs approximately £1,400 per scan, conventional radiography (X-ray) which costs approximately £85 per scan, ultrasound which costs approximately £125 per scan, computed tomography (CT) which costs approximately £295 per scan, and magnetic resonance imaging (MRI) which costs approximately £200 per scan. These modalities are discussed in more detail in section 2.3.2.1. The research in this thesis focusses on MRI. MRI is regarded as the gold standard for the assessment of soft tissue, including muscle, as the images are often clearer

with better contrast than with other imaging techniques. MRI is well suited for assessing muscle as it can enable the visualisation of individual muscles as well as muscle groups, and is suitable for assessing myosteatosis, muscle oedema (inflammation), and muscle atrophy. Furthermore, MRI can also provide quantitative measurements which may be sensitive to some of the known muscle pathologies, such as inflammation, fat infiltration, muscle atrophy and changes to muscle microstructure.

Moreover, MRI is a frequently used medical imaging technique and has been utilised since the 1980s as a useful tool for the diagnosis and monitoring of musculoskeletal disease progression (16). Therefore, MRI could be suitable in filling the currently unmet need to distinguish the pathological processes within diseased muscle due to ageing and rheumatic disease. Within skeletal muscle, MRI has been shown to provide information relating to morphology and physical function, with unparalleled tomographic capabilities and the ability to define different soft tissue structures (17-22). The benefits of MRI include that it is non-invasive, ionising radiation-free, and provides images with good contrast between anatomical structures. Limitations of MRI include patient claustrophobia and the high cost.

In this research, several quantitative MRI techniques have been used. These include: T2, fat fraction (FF), diffusion tensor imaging (DTI), and muscle volume. These quantitative MRI measurements could be used in the future to characterise and monitor muscle disease. They could also assist in the development of interventions by acting as a modality to assess early or subclinical changes in response to disease or treatment. Quantitative MRI T2 provides information on the relaxation time of tissue and provides an indirect assessment of fluid levels within the muscle. Therefore, MRI T2 is a surrogate measure of muscle oedema and inflammation. Fat fraction measurements are made using Dixon fat/water MR imaging and measures the fraction of a voxel which is fat and is, therefore, sensitive to myosteatosis (23, 24). DTI provides an assessment of muscle tissue

microstructure by measuring water diffusion. There has been previous research to suggest that DTI may be sensitive to muscle fibre type populations (25) and muscle pathology (26). Quantitative muscle volume provides an assessment of the total volume of the muscles and can assess muscle atrophy. These MRI measurements (discussed in section 2.4) have been previously used in other regions of the body, notably the liver for fat fraction (27, 28) and the brain for diffusion tensor imaging (29-33) and T2 (34). However, their use in the field of muscle disease is sparse.

Certain medical conditions were chosen for this thesis based on several key features of the disease. The conditions include sarcopenia, myositis, rheumatoid arthritis (RA), and giant cell arteritis (GCA). The key features of these diseases can include: muscle oedema, myosteatosis, muscle atrophy and changes in muscle microstructure, which are features generally accepted to be sensitive to MR imaging. These key features have clinical significance as they may impair physical function and decrease quality of life. Muscle oedema may occur due to inflammatory processes within each of these diseases. Myosteatosis and muscle atrophy may occur due to disease processes or due to a reduction in physical activity. Changes in muscle microstructure could occur due to denervation of muscle motor units or because of alteration in the shape and structure of muscle fibres. These key features can occur either in isolation or together and may result in a decrease in physical function.

In summary, this research project investigated the potential of quantitative MRI measurements in helping to detect the pathophysiological changes of muscle due to ageing and rheumatic disease. This topic is relevant as detectable muscle changes may be amenable to interventions that may improve general health and increase patient quality of life (35); however, further research is required to provide evidence to support this hypothesis.

1.2 Thesis hypothesis

The over-arching hypothesis of this research was that specific quantitative MRI techniques (T2, fat fraction, diffusion tensor imaging, and muscle volume) could provide useful information on muscle status. This was investigated by testing several hypotheses:

1. Diffusion tensor imaging and fat fraction measurements differ between the hamstrings and the quadriceps, and have excellent test-retest, inter-rater, and intra-rater reliability.

2. Differences in the muscle caused by the effects of ageing can be detected using quantitative MRI measurements between young, middle-aged, and older people.

3. Quantitative MRI measurements can detect differences in muscle properties in patients with myositis compared to age- and gender-matched healthy controls.

4. Subclinical changes to the muscle in patients with rheumatoid arthritis can be demonstrated using quantitative MRI.

5. Quantitative MRI can detect differences in muscle properties of patients with giant cell arteritis compared to age- and gender-matched healthy controls.

1.3 Aims of the thesis

The primary aim of this research was to identify if specific quantitative MRI techniques (T2, fat fraction, diffusion tensor imaging, and muscle volume) can quantify differences between patients and healthy controls in various participant groups. This thesis consists of five chapters. Each chapter has two aims. The ten aims of this thesis are as follows:

- Aim 1: To identify differences in normal values between the muscles of the thigh in healthy participants.

- Aim 2: To assess the reliability of diffusion parameters and fat fraction estimates in healthy muscle.

- Aim 3: To investigate whether quantitative MRI can detect differences within the muscles between three age groups.

- Aim 4: To assess how these measures compare with frailty index, gait speed, and muscle power in healthy participants.

- Aim 5: To assess whether quantitative MRI can detect differences between the muscles of patients with myositis and healthy controls.

- Aim 6: To assess how T2 and fat fraction compares to radiologist scoring for muscle oedema and fat infiltration in patients with myositis.

- Aim 7: To explore whether quantitative MRI can detect differences between the thigh muscles of patients with rheumatoid arthritis and healthy controls.

- Aim 8: Establish whether these measures are sensitive enough to assess the muscle phenotype of different disease stages in patients with rheumatoid arthritis.

- Aim 9: To identify whether quantitative MRI can detect differences within the muscle between newly diagnosed giant cell arteritis patients and healthy controls.

- Aim 10: Identify whether these measures can detect changes in muscle properties in giant cell arteritis patients on glucocorticoid therapy.

1.4 Structure of the thesis

Chapter 1 serves as a brief introduction to this thesis. This chapter includes published work by Farrow et al (1). “Novel muscle imaging in inflammatory rheumatic diseases. Frontiers in Medicine. 2020.”

Chapter 2 describes the anatomy, muscle pathology, and MRI theory relevant to the investigation of muscle changes. This chapter includes published work by Farrow et al (1). “Novel muscle imaging in inflammatory rheumatic diseases. Frontiers in Medicine. 2020.”

Chapter 3 describes the general methodology used across all four studies, including recruitment of participants, MR imaging sequences, and muscle strength assessments. Specific details regarding the study methodology are outlined in their respective chapters.

Chapter 4 identifies the importance of understanding normal values and assessing the reliability of measures and describes a research study conducted as part of this thesis identifying normal values and the reliability of diffusion tensor imaging and two-point Dixon fat fraction imaging in healthy controls. This chapter includes published work by Farrow et al (2). British Journal of Radiology. 2019.”

Chapter 5 provides background information on age-related decreases in muscle health and describes a research study conducted as part of this thesis investigating the differences in quantitative MRI within the muscles between young, middle-aged, and older healthy participants, and to assess how these measures compare with frailty index, gait speed, and muscle power. This chapter includes published work by Farrow et al (3). Ageing Clinical and Experimental Research, 2020.”

Chapter 6 provides background information on myositis and describes a research study conducted as part of this thesis investigating if quantitative MRI can detect differences in patients with myositis compared to healthy controls and how this compares to current radiologist semi-quantitative scoring. This chapter includes published work by Farrow et al (4). “Quantitative MRI in myositis patients: A comparison with healthy volunteers and radiological visual assessment. Clinical Radiology. 2020.”

Chapter 7 provides background information on rheumatoid arthritis and describes a study investigating if quantitative MRI can detect differences in the thigh muscles of patients with rheumatoid arthritis compared to healthy controls and establish whether these measures are sensitive enough to assess the muscle phenotype of different disease stages. This chapter includes published work by Farrow et al (5). “Muscle deterioration due to rheumatoid arthritis: Assessment by quantitative MRI and strength testing. Rheumatology. 2020.”

Chapter 8 provides background information on giant cell arteritis and describes a study investigating if quantitative MRI can detect differences in patients with giant cell arteritis compared to healthy controls and identify whether these measures could detect longitudinal muscle changes in patients on long term glucocorticoid therapy. The manuscript for this research study is in preparation for publication.

Chapter 9 summarises and discusses the main research findings of this thesis and highlights potential future directions.

Chapter 2 Background

This chapter describes the anatomy, muscle pathology, and MRI theory relevant to this thesis. This chapter includes published work by Matthew Farrow, John Biglands, Abdulrahman Alfuraih, Richard Wakefield, and Ai Lyn Tan. "Novel muscle imaging in inflammatory rheumatic diseases" published in Frontiers in Medicine, 2020 (1).

2.1 Introduction

Muscle participates in multiple human functions, from the cardiovascular system to locomotion. The types of muscle found in humans are broadly categorised as smooth and striated muscle. Striated muscle is so-called due to the striated appearance of the myocytes under the microscope. There are two types of striated muscle: cardiac and skeletal (36). The large thigh skeletal muscles have been chosen to be the muscles of interest for this research project as they are easily accessible and are a frequent site for a muscle biopsy to confirm a diagnosis of muscle pathology. Furthermore, the muscles of the thigh are easily identifiable on MRI and are vital for daily activities, such as walking.

Skeletal muscles are under voluntary neural control and attach to bones via tendons. There are approximately 680 skeletal muscles in the human body which contribute to typically 40% of an individual's body weight (36, 37). Each skeletal muscle consists of individual muscle fibres. Each muscle fibre is surrounded by connective tissue and blood vessels and has a single connection to the nervous system via a motor neuron (36).

Skeletal muscle can become compromised from injury, inactivity, ageing, disease, and medication. Musculoskeletal complications affect more than one out of every two adults (38) across their lifetime and can present with muscle pathology (39, 40). Pathology affecting skeletal muscles can result in a decreased quality of life and may increase the risk of injuries due to falls (41). Rheumatic diseases (diseases treated within the speciality of rheumatology) can frequently present with myalgia, malaise, and fatigue (42), which could indicate subclinical muscle involvement. The impact of this decrease in muscle health in response to rheumatic disease is detrimental to the functional capacity of patients. This potential decrease in muscle health suggests that there may be a significant unmet need for an improved understanding of muscle pathology observed in rheumatic diseases.

Historically, when considering rheumatic conditions, the skeletal components, including bone and joints, have been the primary area of interest, with muscle involvement in rheumatic disease not being a main focus of research. This lack of interest in researching muscle has contributed to a lesser understanding of how muscle is involved in certain diseases, such as rheumatoid arthritis, compared to the joints. This lack of understanding has limited the development of methods to assess and improve muscle health in the majority of rheumatic diseases due to not appreciating the severity of concurrent muscle pathology. In the limited literature available, myopathic clinical features, including: muscle inflammation, myosteatosis (fat infiltration), changes in muscle microstructure, muscle loss, myalgia, and loss of physical function have been reported to occur in several rheumatic diseases (1). In addition to the decrease in quality of life due to rheumatic disease (43), hospitalisation and treatment also pose a substantial economic burden, with musculoskeletal complications being a significant cause of absence from work (44-46) and accounts for 20% of primary care consultations (47).

Advances in diagnostic imaging in rheumatology, particularly in the area of inflammatory arthritis, have contributed to significant clinical benefits to patients and improved our knowledge of rheumatic disease pathogenesis. Despite the

usefulness of MRI in diagnosing arthritis, and monitoring disease progression in the joints, and related joint structures, the role of muscle imaging has conventionally been centred around the diagnosis of inflammatory muscle diseases (48), such as polymyositis and dermatomyositis. However, with an increasing appreciation of the impact and prevalence of muscular symptoms in rheumatic diseases (49), and due to developments in medical imaging, recent attention has been directed towards the utility of medical imaging for the identification and monitoring of muscle pathology in rheumatic disease, in particular, quantitative medical imaging.

MRI is ideal in the study of muscle health as it is non-invasive and can be used to detect differences, diagnose disease, monitor changes, and assist in the development of interventions to improve muscle health. MRI is frequently used in the assessment of muscle health; however, conventional MRI is subjective and may lack the sensitivity to detect subtle differences. The term conventional MRI will be used throughout this thesis to describe the process by which a radiologist will visually assess MR images for pathology, possibly using a semi-quantitative scoring system such as the rheumatoid arthritis magnetic resonance imaging scoring system (RAMRIS) (50) or the foot osteoarthritis MRI score (FOAMRIS) (51). Quantitative MRI may be more sensitive and be able to detect more subtle differences which currently go unseen by conventional MRI. As mentioned, the quantitative MRI techniques within this thesis include T2, two-point Dixon (fat fraction), diffusion tensor imaging, and muscle volume. These measurements were chosen as they may be able to detect known muscle pathologies, such as muscle oedema, myosteatosis (fat infiltration), changes in microstructure, and muscle atrophy. If it can be demonstrated that quantitative MRI is capable of detecting subtle differences within the muscle, then this could be useful in future research studies in assessing disease progression. This future research could increase knowledge of the rheumatic diseases and assist in the diagnosis of disease by calculating receiver operator characteristic (ROC) curves and cut-off values for diagnosis.

Within this thesis, the application of quantitative MRI techniques in the thigh is explored in the context of age-related muscle disease (sarcopenia) and three inflammatory rheumatic conditions in which the muscle is of interest. The first inflammatory rheumatic condition is myositis, a primary inflammatory condition of the muscle; the second is rheumatoid arthritis in which patients often complain of comorbid muscle-related symptoms, and the third is giant cell arteritis in which patients frequently present with polymyalgia rheumatica and are at risk of the complications of prolonged high-dose steroid therapy.

2.2 Skeletal muscle

All physical activities that a person performs involve voluntary contraction of skeletal muscle. Skeletal muscle consists of long fibres running the length of the muscle. These muscle fibres are 10 - 40mm in length and 10 - 80µm in diameter and are arranged in a parallel fashion within the tissue (36). Each muscle fibre contains several hundred to several thousand polymerised proteins known as myofibrils. These myofibrils are composed of myosin and actin filaments. The configuration of actin and myosin filaments located between two z discs is known as a sarcomere (Figure 2-1). Muscles produce motion by the myosin filaments and actin filaments contracting, a concept known as the sliding filament theory (36). As the contractile capability of skeletal muscle is reliant on the contraction of the sarcomeres, comprehension of the muscle microstructure is of the utmost importance in understanding muscle function (52).

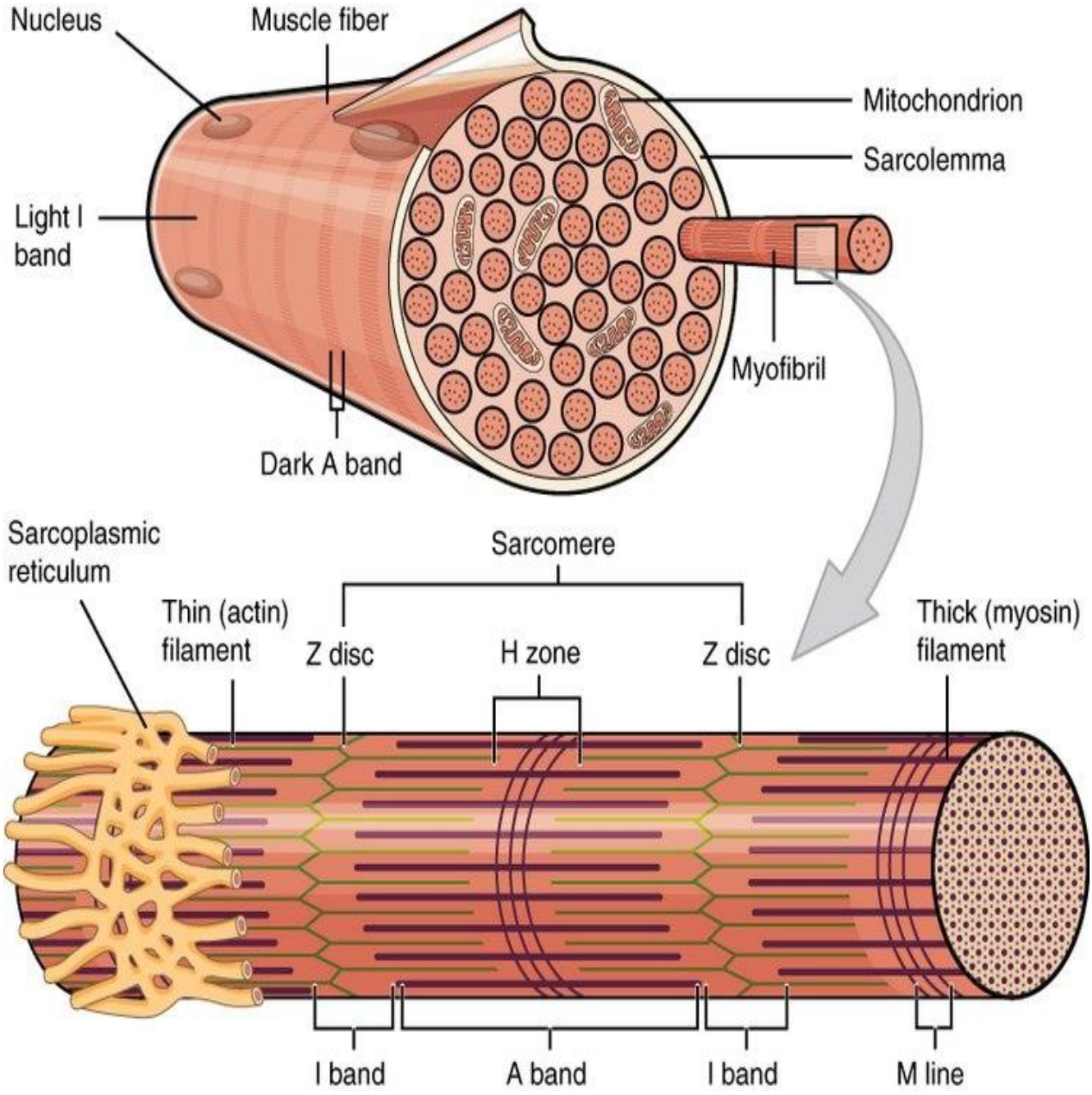

Figure 2-1: Microstructure of skeletal muscles

Skeletal muscles have classically been described as having two types of fibre phenotype, known as type I (slow-twitch) and type II (fast-twitch) muscle fibres. Skeletal muscles have varying percentages of type I and type II muscle fibres, depending on the function of the muscle, and the genetic disposition of the individual (53). Type I (slow-twitch) muscle fibres are often found in high quantities in muscles that maintain posture and can sustain prolonged contractions. Type II (fast-twitch) muscle fibres are designed for short, rapid, and powerful contractions. The type of muscle fibre can be identified by studying the enzyme activity using myosin adenosine triphosphatase (ATPase). Fibres which stain strongly following pre-incubation at pH 10.4 are referred to as type II, whilst fibres which show low ATPase activity at pH 10.4 are referred to as type I. Type II muscle fibres are comprised of three subtypes: type IIA, IIX, and IIB. It is known that in addition to pure fibre types, skeletal muscles can contain hybrid muscle fibres with mixed myosin heavy chain (MyHC) composition, demonstrating the existence of a spectrum of fibre types (54). It is known that skeletal muscle fibres can change their phenotype within this spectrum due to the influence of: hormones, medication, nutrition, exercise, disease, ageing, and due to motor neuron firing (55-58).

2.2.2 Anatomy of the human thigh

The thigh can be divided into three compartments: anterior, medial, and posterior. The research within this thesis is focussed predominantly on the anterior and posterior compartments, and to a lesser extent, the medial compartment of the thigh (only used for thigh muscle volume measurements) (Table 2-1 and Figure 2-2). The thigh muscles were chosen as they are involved in daily tasks such as walking, and a decrease in thigh muscle health can result in a decreased quality of life (59). The anterior and posterior compartments of the thigh were primarily chosen as they are easily identifiable on MRI, are important for knee flexion and knee extension, and are frequently used sites of muscle biopsy to confirm the

diagnosis of muscle pathology (60). The medial aspect of the thigh received less attention in this research project as it can be difficult to demarcate the individual medial muscles in patients with muscle pathology without subcutaneous fat contaminating the regions of interest.

Within the anterior compartment, the quadriceps femoris is the primary extensor muscle of the knee joint and assists in hip flexion. The quadriceps femoris consists of four muscles: rectus femoris, vastus medialis, vastus intermedius, and vastus lateralis. In addition to the quadriceps, the sartorius muscle is also located within the anterior compartment. The posterior compartment of the thigh is separated from the anterior compartment by the lateral intermuscular septum. Within the posterior compartment, the hamstring muscles are the principal flexors of the knee joint and consist of three muscles: semimembranosus, semitendinosus, and biceps femoris. The medial thigh muscles are responsible for leg rotation and adduction of the thigh. The medial compartment is composed of 4 muscles: adductor brevis, adductor longus, adductor magnus, and gracilis.

Table 2-1: Origin, insertion, and nerve supply of the muscles that make up the quadriceps and hamstrings

Muscles of thigh	Origin	Insertion	Nerve supply
Quadriceps			
Rectus femoris	Anterior inferior iliac spine	Quadriceps tendon	Femoral nerve (L2,3,4)
Vastus medialis	Intertrochanteric line		
Vastus lateralis			
Vastus intermedius	Shaft of femur		
Hamstrings			
Semimembranosus	Ischial tuberosity	Medial condyle of tibia	Sciatic nerve (L5, S1,2)
Semitendinosus		Upper shaft of tibia	
Biceps femoris	Short head: linea aspera of femur Long head: ischial tuberosity	Head of fibula	

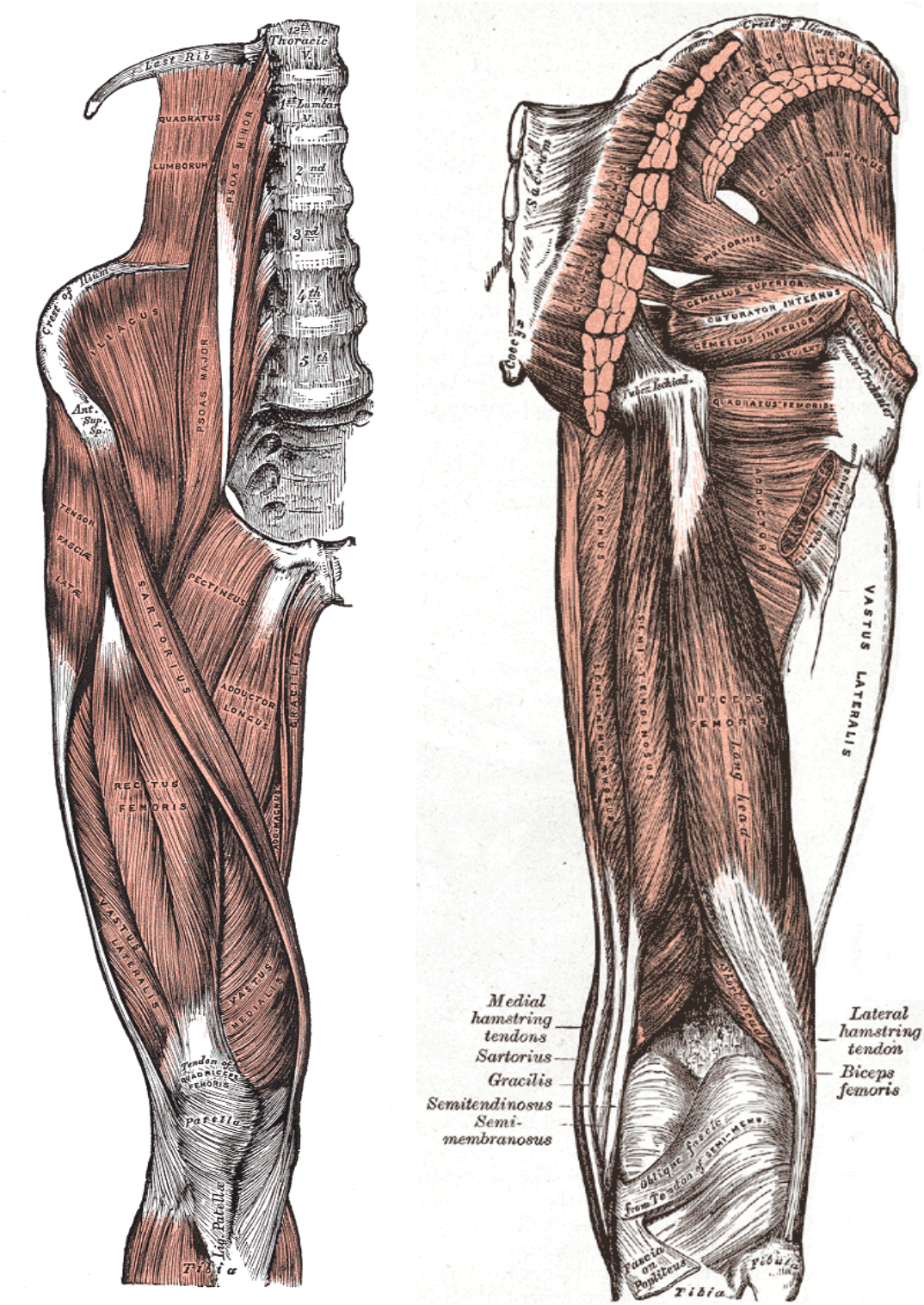

Figure 2-2: Muscles of lower limb

Thigh muscle front and back by Henry Gray and Henry Carter (1858) is in the public domain and has no copyright protection.

Muscles of interest in this thesis are the quadriceps (anterior), hamstrings (posterior), and to a lesser extent, the muscles of the medial compartment.

2.3 Muscle pathology

Rheumatic muscle disease can arise due to primary disease, for example, where muscle tissue is the primary site of pathology, such as polymyositis, or from secondary causes as a sequela to another disease process, such as disuse myopathy from immobility. Patients with rheumatic disease can experience: muscle inflammation, myosteatosis, changes in muscle microstructure, muscle atrophy, and loss of muscle strength (5, 58). In this thesis, four groups were investigated to identify the presence of muscle pathology due to: ageing (sarcopenia), myositis, rheumatoid arthritis, and giant cell arteritis. Each group was compared to matched healthy controls. Sarcopenia, a condition in which there is an age-related decrease in muscle health, was selected as it has implications for public health. Sarcopenia is caused by muscle atrophy, low muscle quality, and decreased physical function and muscle strength. Myositis was selected as it is defined by inflammation of the muscle. Rheumatoid arthritis was selected because it is a common rheumatic disease, and comorbid muscle atrophy and fatigue are associated symptoms (61), suggesting subclinical disease effects on the muscles that are little explored to date. Giant cell arteritis was selected because it is a systemic inflammatory disease often concurrent with polymyalgia rheumatica – a condition that presents with muscle stiffness, and is treated with glucocorticoids, which can cause glucocorticoid-induced myopathy. These conditions can result in the loss of functional capability, which can cause difficulty in routine daily tasks, and necessitate healthcare, occupational, and social modifications and services (13, 62-64).

2.3.1 Diseases researched in this thesis

2.3.1.1 Age-related decrease in muscle health

Ageing is characterised by a decline in muscular capabilities (65, 66). The effect of ageing on muscles is an important field to research, as many older individuals function close to their maximum physical capability during normal daily activities (67, 68). Demographic shifts in the population have resulted in an expansion in the number of older adults. The population aged above 60 is estimated to increase from 841 million in 2013 to over 2 billion by 2050 (69). Sarcopenia, first described in 1989, comes from the Greek translation of σάρξ (sarx): “flesh”, and πενία (penia): “penury”. Therefore, sarcopenia translates to ‘extreme poverty of flesh’. Sarcopenia is described as the progressive loss of muscle mass and reduction in muscle function. It has been suggested that sarcopenia may occur in up to 13% of individuals aged between 60 and 70, and 50% of those aged over 80 (70, 71). These age-related changes decline faster in the lower extremities than the upper extremities, affecting ambulatory function and increasing the risk of falls and fractures (72-76). As well as increased mortality and falls, sarcopenia is a major contributor to frailty and depression (77-79) and imposes a significant economic burden on healthcare services (80).

The loss of physical function observed in sarcopenia is speculated to be attributed to a reduction in muscle quality, due to the infiltration of fat (myosteatosis) and other non-contractile tissue (myofibrosis), changes in muscle fibres, and muscle atrophy (81-84). However, a direct relationship between muscle quality assessed by MRI and age-related muscle weakness has not yet been established. Therefore, further research into the relationship between muscle quality assessed by MRI and physical function is required. One of the potential mechanisms explaining how fat tissue decreases muscle function is the increased production of tumour necrosis factor-alpha (TNF-α). It has been suggested that TNF-α, which also has an

influential role in rheumatic disease, may act directly on muscle fibres, disrupting excitation-contraction coupling by altering intracellular calcium stores (85).

Specific changes in muscle fibres due to ageing, are caused by a decrease in the motor neurons innervating type II (fast-twitch) muscle fibres, as they are recruited less frequently than type I (slow-twitch) muscle fibres. With the loss of their motor unit, type II muscle fibres either atrophy or become innervated by a branch that emerges from a healthy axon nearby, which is innervating a type I muscle fibre. This reinnervation ultimately results in a higher quantity of type I (slow-twitch) muscle fibres in older individuals compared to type II (fast-twitch) muscle fibres (86-89). This reinnervation results in the grouping of muscle fibre types, which describes the phenomenon that certain fibre types appear to be distributed in clusters rather than in the random fashion as seen in young, healthy muscle (90). In addition to a decrease in the quantity of type II (fast-twitch) muscle fibres, the size of the muscle fibres also decrease. This decrease in muscle fibre size is demonstrated by a 10-40% reduction in type II muscle fibre size compared to young controls (91-93). In contrast, type I muscle fibre size is mostly unaffected (37, 94, 95). This evidence suggests that there may be a selective preservation of type I (slow-twitch) muscle fibres for their mechanical properties, as these fibres are required for low force activities, such as walking.

There is ongoing research into the best approach for diagnosing sarcopenia. Historically, sarcopenia has been diagnosed based on the loss of muscle mass. The limitation with this approach, however, is that although muscle strength and muscle mass are correlated, the loss of muscle strength occurs at a faster rate than that of muscle loss, which suggests that other factors, in conjunction with muscle mass, are influencing muscle strength. The European Working Group on Sarcopenia in Older People (EWGSOP) developed the sarcopenia European consensus on definition and diagnosis guidelines in 2010. These guidelines include three diagnostic aspects: body composition analysis, muscle strength assessment, and physical performance (Table 2-2) (71). However, there have been criticisms of

these guidelines that suggest new diagnostic tools should be used (96-98). In 2019, the EWGSOP updated their diagnostic guidelines to include ‘low muscle quality’ and the addition of a ‘probable’ sarcopenia diagnosis for individuals with low muscle strength (99). The EWGSOP defines the term muscle quality as the microscopic and macroscopic properties of muscle, muscle mass, and muscle function. However, there is currently no universal consensus on methods to assess or define muscle quality, demonstrating a significant unmet need to develop new tools to measure muscle quality accurately. The EWGSOP 2019 criteria highlight the potential use of MRI to assess muscle quality, including by assessing infiltration of fat into muscle (Table 2-3). It could be speculated that many older individuals will meet the diagnosis of probable sarcopenia due to individuals having low muscle strength.

Although physical activity, especially strength training, can help slow the rate of development of sarcopenia (100), even active older individuals succumb to progressive loss of muscle mass and strength (101, 102), which can affect their ability to perform daily tasks (103, 104). These findings suggest a need to research different types of interventions to combat age-related changes within the muscle.

Table 2-2: EWGSOP 2010 diagnosis for sarcopenia

EWGSOP 2010 diagnosis for sarcopenia is based on documentation of criterion one plus either criterion two or criterion three (71)		
	Criterion	Assessed by
1	Low muscle mass	CT
		MRI
		DXA
		BIA
		Body potassium per fat-free soft tissue
		Anthropometry
2	Low muscle strength	Handgrip strength
		Knee flexion/knee extension
		Peak expiratory flow
3	Low physical performance	Short Physical Performance Battery
		Gait speed
		Get-up-and-go test
		Stair climb power test

Table 2-3: EWGSOP 2019 diagnosis for sarcopenia.

Probable sarcopenia is identified by criterion one Definite sarcopenia if criteria one and two present Severe sarcopenia if all criteria are met (99)				
	Criteria	Assessed by	Cut-off points for males	Cut-off points for females
1	Low muscle strength	Grip strength	<27kg	<16kg
		Chair stand test	>15 seconds for five raises	
2	Low muscle quantity or quality	Appendicular skeletal muscle mass by DXA	<20kg	<15kg
		Whole-body skeletal muscle mass predicted by BIA	Depending on the population	
		appendicular skeletal muscle mass by MRI	<20kg	<15kg
		Mid-thigh cross-sectional area by CT or MRI	No cut-off developed	
		Lumbar muscle cross-sectional area by CT or MRI	No cut-off developed	
		Muscle biopsy of thigh	No cut-off developed	
		MRS of thigh	No cut-off developed	
3	Low physical performance	Gait speed	≤0.8m/s	
		Short Physical Performance Battery	≤8point score	
		Timed-up-and-go test	≥20 seconds	
		400-metre walk	Non-completion or ≥6 minutes for completion	

2.3.1.2 Myositis

The idiopathic inflammatory myopathies (IIM) are the most prevalent inflammatory muscle disease group seen within rheumatology. IIM are a heterogeneous group of autoimmune inflammatory muscle diseases comprising primarily of dermatomyositis and polymyositis. Idiopathic inflammatory myopathies, also known as myositis, present with: muscle weakness, raised muscle enzymes, abnormal electromyography (EMG), abnormal muscle biopsies, and myositis-related antibodies (105). MRI has become an integral imaging tool in the diagnosis and monitoring of disease activity of myositis due to its ability to non-invasively detect affected muscles and identify the most suitable site for muscle biopsies required to confirm the diagnosis (Figure 2-3) (106-110). Reassuringly in myositis, MRI correlates with biopsy results (111) and is more sensitive than muscle enzymes and EMG in diagnosing myositis (112).

Nevertheless, the interpretation of MR images can be subjective (113), and MRI findings in isolation may not be specific enough for diagnostic purposes (114). Quantifying parameters such as fluid, myosteatosis, diffusion of water molecules, and muscle mass by utilising quantitative MRI techniques such as T2, fat fraction, diffusion tensor imaging, and muscle volume may provide a more accurate description of muscle pathology (109, 115, 116). It can also be used to guide muscle biopsies more precisely, which may increase the likelihood of a positive biopsy. It could be speculated that quantitative MRI may be of greater importance in patients with low-grade pathology, which may currently go undetected with conventional MRI, as it may be more sensitive to subtle changes.

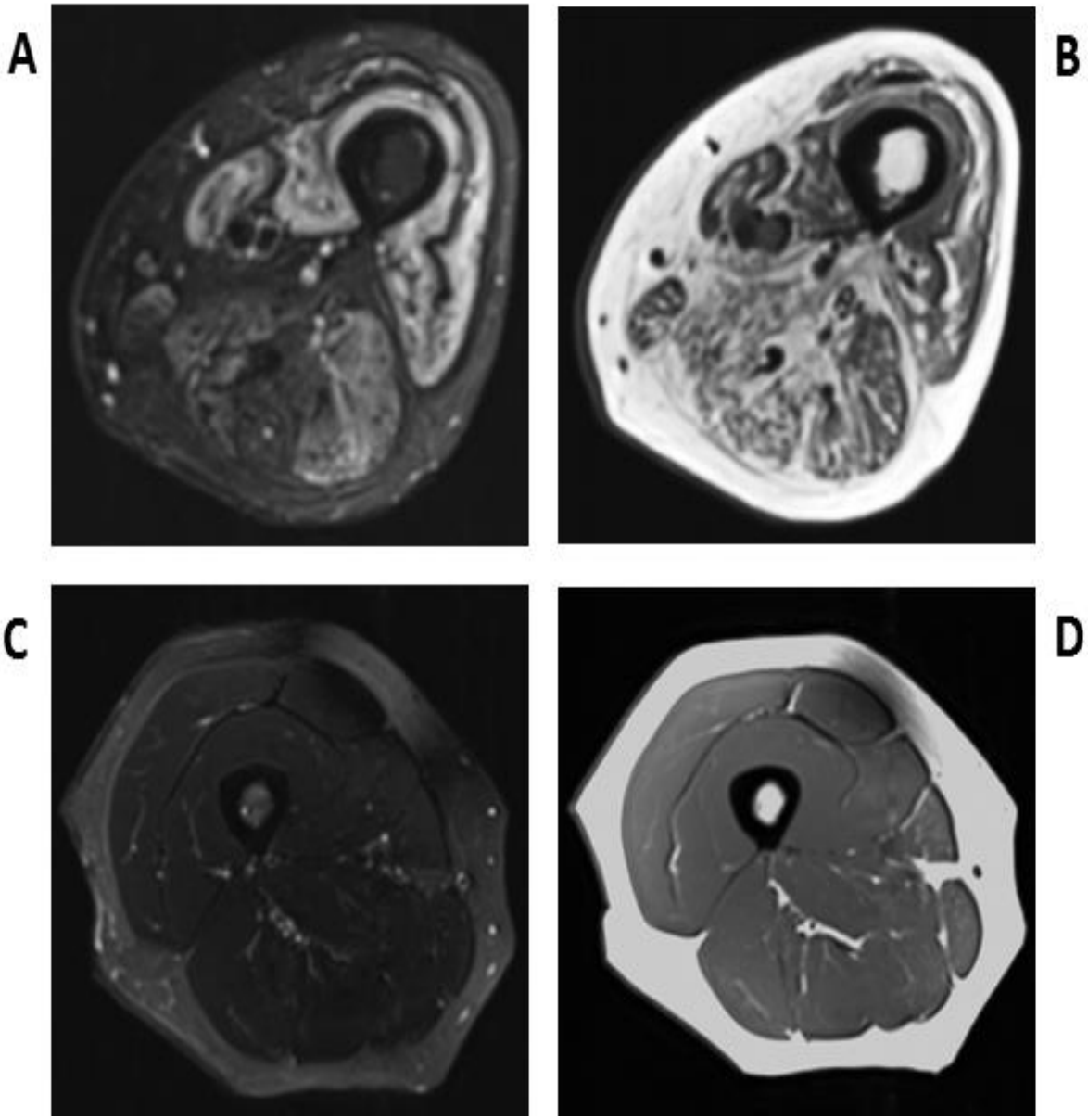

Figure 2-3: Conventional MRI of the right thigh

(A) T2-weighted STIR and (B) T1-weighted images of a 60 year-old male with active myositis, compared to (C) T2-STIR and (D) T1-weighted images of a 45 year-old healthy female.

Muscle oedema (T2-STIR) and fat infiltration (T1-weighted) is present in patients with myositis compared to healthy controls.

2.3.1.3 Rheumatoid arthritis

Rheumatoid arthritis (RA) is a chronic inflammatory joint disease that presents with inflammatory arthritis. The predominant site of pathology in RA is in the synovial joints. The joints are, therefore, the most imaged structure in RA. However, there are many reasons for patients with RA to have weaker muscles, such as joint pain and impaired physical function resulting in a greater tendency towards physical inactivity (117, 118), inflammatory processes of the disease, and medication - in particular steroids which can cause myopathy. Rheumatoid arthritis patients often present with lower muscle mass (119) and report experiencing muscle problems or myopathy (120). Fatigue is a common symptom in many rheumatic conditions, including rheumatoid arthritis, and imparts a significant burden on patients' lives (121). Histologically, RA is also associated with atrophy of type II (fast-twitch) muscle fibres, similar to the effects of sarcopenia on the muscle (58, 122). In addition, the pro-inflammatory state in inflammatory arthritis predisposes patients to the cachectic body composition, which is another reason for compromised muscles in rheumatoid arthritis (123, 124).

Despite reduced muscle strength being associated with increased disease activity in patients with RA, there is little muscle imaging data from studies in patients with RA. Quantitative MRI offers a different imaging perspective of muscle and can provide further insight into the pathogenesis of muscle pathology in RA. Indeed, quantitative MRI could be used to identify if patients with RA are in remission or still have muscle pathology, such as muscle inflammation or myosteatosis. Furthermore, quantitative MRI could identify whether current treatment has any effect on improving muscle health, or if additional interventions, such as exercise, should be developed for a more comprehensive approach in patients with RA. Although treatment, including biological therapy and exercise, can help improve symptoms of fatigue, it is not effective in all patients (125, 126). The fact that exercise can improve fatigue suggests that modifying the muscles in patients with RA is a potential route to improving clinical symptoms for patients. Therefore, it

could be speculated that interventions to improve muscle health in patients with RA could have clinical benefit, and quantitative MRI may be beneficial in providing further insight into their application and efficacy.

2.3.1.4 Giant cell arteritis

Giant cell arteritis (GCA), which often presents with concurrent polymyalgia rheumatica, is a systemic vasculitis and autoimmune inflammatory disease that affects older people. Patients with GCA are often disabled by muscle weakness and fatigue from the disease process (127). It would, therefore, be reasonable to hypothesise that, despite not demonstrating a classical myositic picture with abnormal blood markers or EMGs (128), the muscles of patients with GCA are likely to be compromised. Due to the inflammatory nature of GCA, it is possible that muscle oedema, a surrogate biomarker (a biological characteristic that is objectively measured and used as an indicator of pathology) of inflammation, could be present in patients with GCA and identifiable on fluid-sensitive sequences such as quantitative T2.

Patients with GCA are treated with high doses of glucocorticoids (steroids). British Society for Rheumatology (BSR) guidelines suggest that glucocorticoid treatment should start at 40-60 mg/day of prednisolone for GCA (129). However, glucocorticoids can result in glucocorticoid-induced myopathy. It is important, therefore, to consider that there may be a combination of the effects of inflammation from the disease (GCA) and the catabolic effects of therapy (glucocorticoids) on the muscle of patients with GCA.

2.3.1.4.1 Glucocorticoid-induced myopathy

Glucocorticoids are potent anti-inflammatory steroid agents and have a variety of uses in rheumatology, most commonly acting as bridging therapy before replacement with other longer-term treatments. Whilst numerous diseases are treated with glucocorticoids, such as myositis and rheumatoid arthritis, GCA is an example for which high doses of glucocorticoids are prescribed. As a result, many GCA patients often develop a proximal myopathy, in the absence of typical inflammatory laboratory markers such as muscle enzyme abnormalities or myositis-related antibodies. The effects of glucocorticoids on the muscle itself can present as myopathy or muscle weakness. However, due to the lack of a standardised definition of glucocorticoid-induced myopathy, reporting of myopathies due to prednisolone treatment can prove inconsistent (130). Therefore, the management of glucocorticoid-induced myopathy can be challenging due to the difficulty in identifying myopathy with the current means of investigation (131). Amongst the many adverse effects of glucocorticoids, a major consequence is muscle atrophy, with a particular affinity for the atrophy of type II (fast-twitch) muscle fibres (132, 133), similar to that seen in sarcopenia and rheumatoid arthritis.

Very little research regarding GCA and glucocorticoids has been published about muscle in the literature. Most studies have focussed on the diagnosis of GCA and responses to glucocorticoid therapy (134-136). The fact that type II muscle fibres tend to be affected by steroid therapy suggests that techniques such as MRI diffusion tensor imaging, which are sensitive to changes in muscle microstructure, could be useful in understanding the pathogenesis of glucocorticoid-induced myopathy (26). Furthermore, muscle atrophy due to the catabolic effects of glucocorticoids could be quantitatively measured to monitor muscle changes over time. The challenge will be interpreting the findings and elucidating if the observed imaging changes are due to therapy (glucocorticoids) or the inflammatory disease process (GCA).

Steroid-sparing immunosuppressant regiments have been investigated against long term steroid monotherapy in the treatment of RA, and it has been possible to tell that steroid-receiving recipients had weaker strength compared to patients who did not receive steroid therapy (137, 138). However, due to the complexities of current therapy and the ethical limitations in withholding treatment, such direct comparison studies in GCA patients may not be feasible. The confounding impact of glucocorticoid therapy in the muscle health of patients with GCA highlights an unmet need to identify the exact cause of the myopathy to optimise management – this an area for further exploration where quantitative MRI may be useful.

2.3.2 Assessment of muscle health

Patients with rheumatic disease can present with muscle weakness, fatigue, malaise, and myalgia. There are numerous ways of investigating the health of muscles in addition to medical imaging, such as conducting muscle biopsies, blood biomarker testing (creatine kinase [CK]), electromyography (EMG), and clinical examination.

Muscle biopsies are the gold standard in assessing muscle health. Muscle biopsies involve removing a small sample of muscle tissue, often from the vastus lateralis, to assess the muscle's appearance under a microscope (60). This sample of muscle is examined for signs of pathology. Pathology can be identified utilising histology (appearance and structure of muscle cells), histochemistry (the activity of chemicals within muscle fibres), immunohistochemistry (presence of proteins within the muscle), and electron microscopy (structural abnormalities). Unfortunately, muscle biopsies assume that the small sample of muscle, between 20mg and 293mg in size (139), represents that of the whole muscle, which, due to the heterogeneous nature of muscle pathology, is incorrect. To improve the likelihood of successfully obtaining a sample of muscle with pathology present, ultrasound- and MRI-guided

muscle biopsies can be performed. However, a significant limitation of muscle biopsies is that they are invasive, which impedes on their frequent use to monitor changes within a research context. In addition, muscle biopsies are uncomfortable for patients (140) and have several known risks, such as infection and bleeding, and are, therefore, contraindicated in frail individuals or patients taking anticoagulant therapy (60).

EMG is an invasive procedure and consists of needles inserted through the skin into the muscle to monitor the electrical activity of the muscle in response to stimulation. EMG is frequently used in the diagnosis of neuromuscular disease (141).

Clinical examination of the muscle consists of trained health professionals conducting physical tests to measure muscle strength and muscle function such as a ‘chair sit to stand’ test (142) or the ‘get up and go’ walk test (143). Clinical examinations of muscle are often semi-quantitative, such as manual muscle tests (MMT), in which the patient opposes manual resistance supplied from an examiner (144). A major limitation of clinical examination and MMT is that they can be subjective and reliant on both participant and examiner effort. Furthermore, a clinical examination does not directly measure muscle status and quality but measures physical performance.

To assess physical capability, targeted muscle strength assessments can be conducted. ‘Maximum strength’ is defined as the maximum force or torque a muscle can generate at a specified determined velocity (145). ‘Muscle power’ is defined as a product of torque and speed (146). The three primary forms of strength testing are isotonic, isometric, and isokinetic. Isotonic contractions can be divided into concentric and eccentric contractions. Concentric contractions are when the muscle shortens as it contracts. Eccentric contractions occur when the muscle lengthens in a controlled manner as tension is produced. An example of an

eccentric contraction is on the downward phase of a bicep curl. Isometric testing requires participants to produce maximum torque against an immovable resistance. Isokinetic testing is often utilised to assess muscle strength. Isokinetic testing involves the measurement of torque during a movement in which the velocity is constant. Isokinetic testing can be either concentric or eccentric.

To assess global physical function, isometric handgrip strength is often used. However, whilst handgrip strength provides an overview of physical health, it does not provide information on muscle quality, such as the presence or degree of myosteatosis and muscle inflammation.

2.3.2.1 Muscle imaging in rheumatic disease

Medical imaging, such as computed tomography (CT), positron emission tomography (PET), ultrasound, and magnetic resonance imaging (MRI), are useful for the evaluation of muscle pathology and the monitoring of disease progression as it can provide information about a larger quantity of the muscle.

Computed tomography produces three-dimensional images by utilising ionising radiation. In muscle, it can identify the distribution of myosteatosis and assess muscle size (147). However, the high radiation burden to the patient is a complication, particularly to children and young adults who could require several CT scans throughout their lifetime. Therefore, the radiation burden involved in CT scanning precludes this technique from being used too frequently and is particularly problematic for longitudinal research (148). Whilst CT scans can provide quantitative measurements of fat and muscle mass (149); it is less suitable to assess muscle tissue microstructure and muscle oedema compared to MRI.

PET scans produce images which use radioactive materials to visualise and demonstrate metabolic processes within the body. PET scans are useful for detecting changes in physiological activities, including blood flow and metabolism, and are frequently used in the diagnosis of cancer. However, PET imaging can be utilised in the study of the musculoskeletal system to provide insight into the pathology of myopathies (150). A benefit of PET scans, in comparison to many other imaging modalities, is that they demonstrate biochemical changes compared to anatomical changes. Limitations of PET scans include the expense and the radiation burden, which, similar to CT, preclude this technique from being used too often.

Ultrasound is achieved using the emission and reflection of high-frequency sound waves within the tissue. Ultrasound is an easily applicable and safe non-invasive technique to visualise soft tissues. The benefits of ultrasound include high patient tolerance and that it is easily accessible with few contraindications, while providing images of soft tissue in real-time within the clinical setting. Important aspects to consider with ultrasound would be the selection of the ultrasound machine, settings, and probe selection which can be crucial for optimum visualisation (151, 152). Whilst ultrasound can quantitatively measure fat and muscle; there are several caveats. This modality can be affected by operator pressure on the probe, which can lead to significant changes in measured muscle thickness. Furthermore, muscle dimensions change with contraction/relaxation, so it is critical to ensure that the patient is cooperating (153). In addition, when assessing for muscle pathology, it has been reported that ultrasound can be reported as healthy whilst MRI is shown to detect pathology (154). This suggests that MRI may be more sensitive to muscle disease compared to ultrasound.

2.4 Magnetic resonance imaging

Magnetic resonance imaging (MRI) is a non-invasive imaging modality which provides excellent soft-tissue assessment and has superior image contrast for the assessment of soft tissue compared to most other imaging modalities. Furthermore, there is a wide range of image contrasts, due to T1 and T2 tissue characteristics, to enable the visualisation of the anatomy. MRI is frequently used to diagnose or evaluate joint disorders and to visualise soft tissues (muscles, tendons, and ligaments). Some of the benefits of MRI include the fact that it does not use ionising radiation and produces three-dimensional structures (155). Limitations of MRI include the potential of long scan times and limited availability.

MRI is considered the reference imaging method to assess the morphology of muscles due to its capability to demarcate different tissue (156, 157). MRI also permits the examination of deeper tissue structures compared to ultrasound. Furthermore, MRI has a role in the diagnosis and monitoring of muscle disease and is used for guiding muscle biopsy (158, 159). Aside from conventional MRI, which provides a qualitative assessment of muscle based on the difference in signal properties in various tissues and pathologies, there may also be an important role for quantitative MRI measurements, such as T2, fat fraction, diffusion tensor imaging, and muscle volume. These quantitative MRI measurements can provide objective measurements of muscle parameters, including: fluid, myosteatosis, diffusion of water molecules, and muscle atrophy. These measurements may potentially aid in the diagnosis and monitoring of muscle disease as they have the potential to provide quantitative information on the known muscle pathologies which can occur, including muscle oedema, myosteatosis, changes in muscle microstructure, and muscle atrophy (160).

2.4.1 The MRI system

MRI scanners are composed of a magnet, gradient coils, and radiofrequency (RF) transmitter and receiver coils, which help produce the MR images (Figure 2-4). The participant lies in the main magnet field (B_0) with the anatomical region of interest in the isocentre (the most homogenous part of the field) of the magnet. There are three reference axes (Figure 2-5) which illustrate the directions of the magnetic fields within an MRI scanner (161).

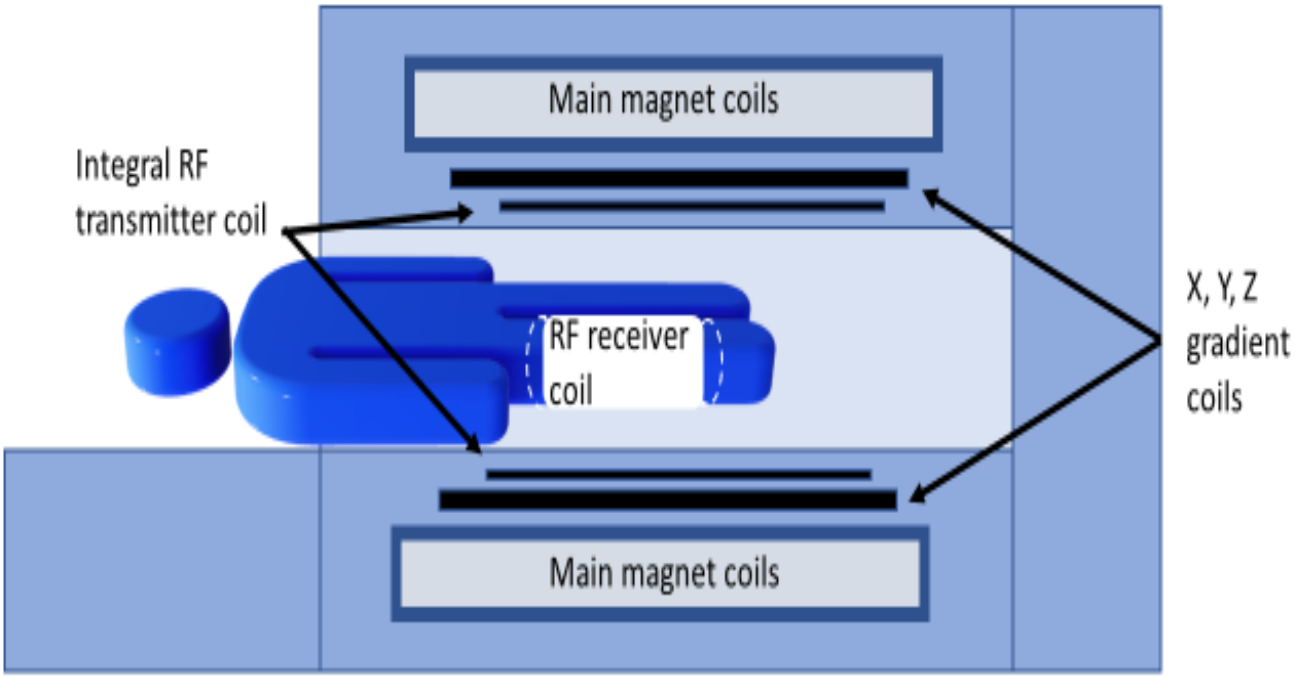

Figure 2-4: MRI system

Main components of an MRI machine

Figure 2-5: Reference coordinate axes

References axes which describe the directions of the magnetic fields

2.4.2 MRI signal production

The MRI signal is generated from the magnetic moments of the hydrogen protons within water molecules. Within the presence of an external magnetic field, these magnetic moments precess about the magnetic field (Figure 2-6). The frequency of this precession is described as the Larmor frequency (ω_0). Initially, these magnetic moments are in a random orientation.

In the presence of a strong, external magnetic field, a net magnetic field is generated from these individual magnetic moments. To generate a measurable MRI signal from the net magnetisation, an RF pulse is used to tip the net

magnetisation into a plane orthogonal to that of the main external magnetic field (B_0). Following the removal of the RF pulse, the net magnetisation returns to its ground state. The net magnetisation is frequently described as having two components, longitudinal and transverse. Two phenomena are important for the longitudinal and transverse elements: T1 is used to describe the longitudinal relaxation time and is a measure for the amount of time required to return to 66.6% of its maximum value. T2 is the time constant that describes the speed for the transverse magnetisation to decay to 37% of its value. Different tissues have different T1 and T2 values, which are the reason for the contrast in signal strength between tissues and, ultimately, for image contrast in the image. This image contrast is dictated by the echo time (TE) and the repetition time (TR). The echo time describes the interval between the centre of the RF pulse and the centre of the echo when the receiver coil receives the signal. The repetition time describes the time interval between the two, consecutive, RF pulses (Figure 2-7).

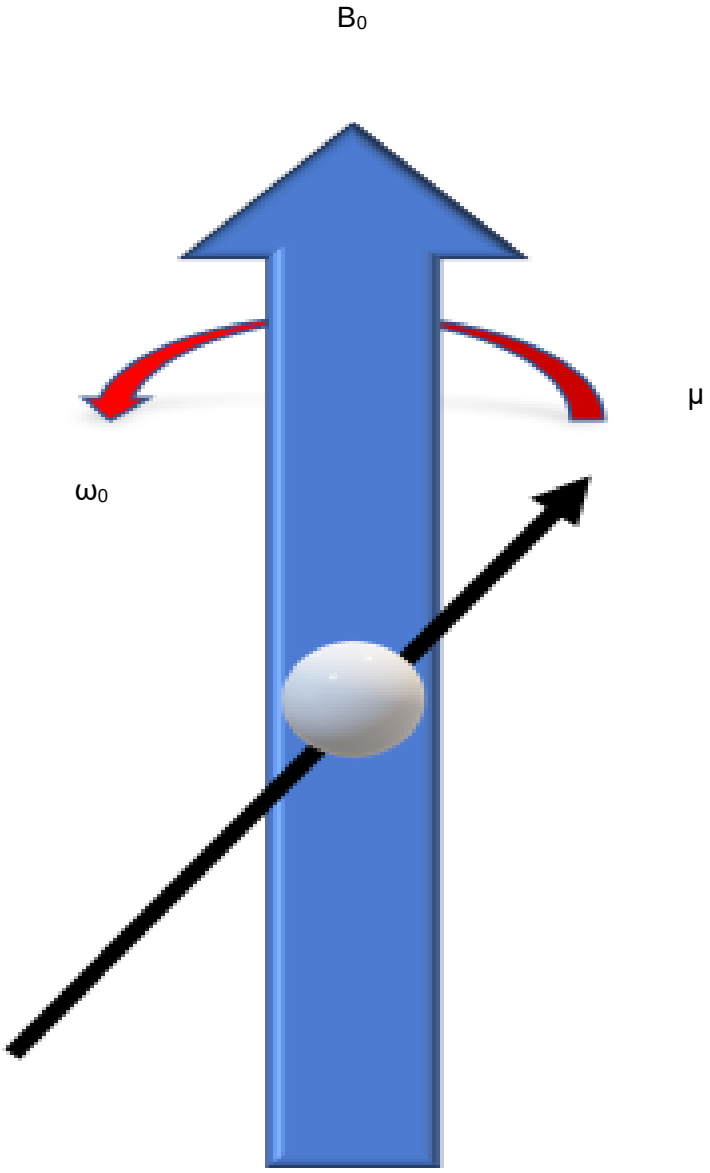

Figure 2-6: Precession of the spin magnetic moment in the presence of an external magnetic field

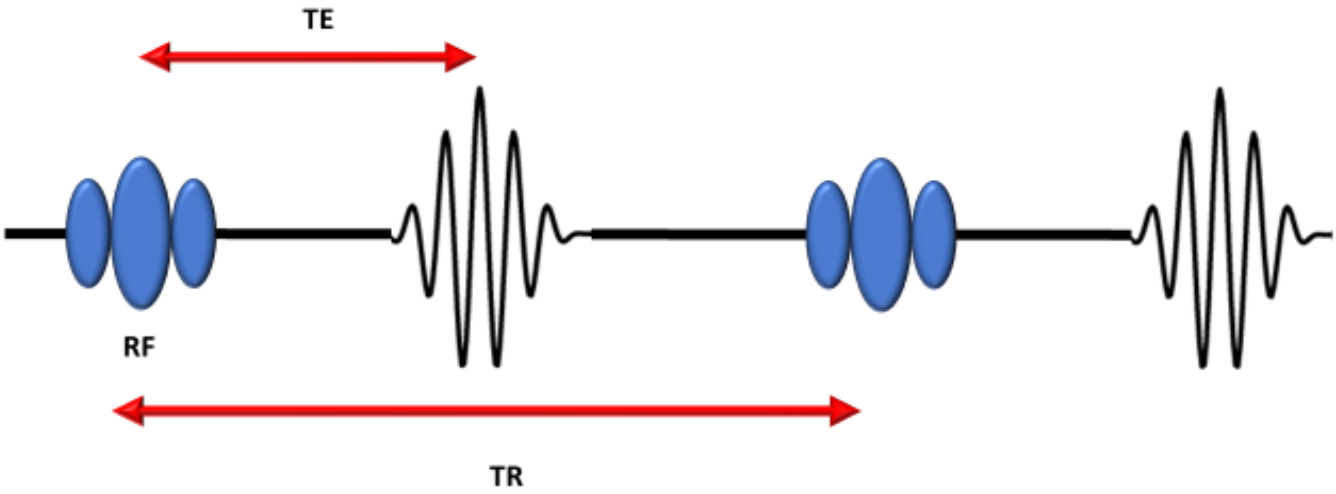

Figure 2-7: Echo time and repetition time

The echo time and repetition time are two important phenomena in MRI and allow for different image contrast between tissues. The echo time (TE) is the interval between the centre of the RF pulse and the centre of the echo. The repetition time (TR) is the time interval between two RF pulses.

2.4.3 Quantitative MRI measurements used in this thesis

2.4.3.1 Quantitative T2 MRI

T2, or the transverse relaxation time, is one of the fundamental contrast mechanisms in MRI. Quantitative T2 measurements are sensitive to fluid related to physiological or pathological changes at the macromolecular level (162). Quantitative T2 measurements can provide a map in which the value for the voxel quantitatively represents the T2-relaxation time of the tissue that is located inside the voxel. Longer T2 relaxation times are often interpreted as increased fluid due to oedema or inflammation (160). Typically, T2 measurements are performed using fat

suppression. However, fat suppression is challenging, and there is always some remnant olefinic fat in fat-suppressed MR images. Therefore, T2 measurements are usually contaminated with olefinic fat to some degree (115, 163).

The T2 describes the rate of signal decay due to spin-spin interactions within the tissue. Typically, T2 is measured using a spin-echo (SE) sequence (Figure 2-8). Spin echo uses a 180-degree pulse to refocus the dephasing of the net magnetisation due to magnetic field inhomogeneities before the signal is acquired, giving T2. The most basic T2 measurement can be made by acquiring several images of the same anatomy using spin-echo sequences with a range of echo times. For each voxel on the resulting images, T2 can be estimated by fitting an exponential decay model to the signal intensity measured across all the echo times. However, this simple method is too time-consuming to use clinically. Therefore, a turbo spin-echo (TSE) sequence is used, in which multiple 180-degree pulses (and multiple echoes) are acquired after a single read-out (Figure 2-9). With TSE, the entire train of images can be acquired in a single acquisition, therefore bringing the imaging time down, compared to a simple spin-echo. However, due to the signal decaying exponentially, the number of suitable echoes in the echo train is restrained by the T2 decay. Therefore, if images are acquired with a TE that is too great, then the acquired signal will have a weak signal-to-noise ratio (SNR), inducing errors in the fit. Therefore, noise must be dealt with in the fitting or excluded by not acquiring images with very long TE values.

Multi-echo sequences are known to overestimate T2 due to the formation of stimulated echoes (164, 165) but are used in practice to keep scan times tolerably short for participants. More elegant analysis methods that take the full extended phase graphs into account have been used (166, 167); however, these methods are complex and not readily available in routine clinical imaging.

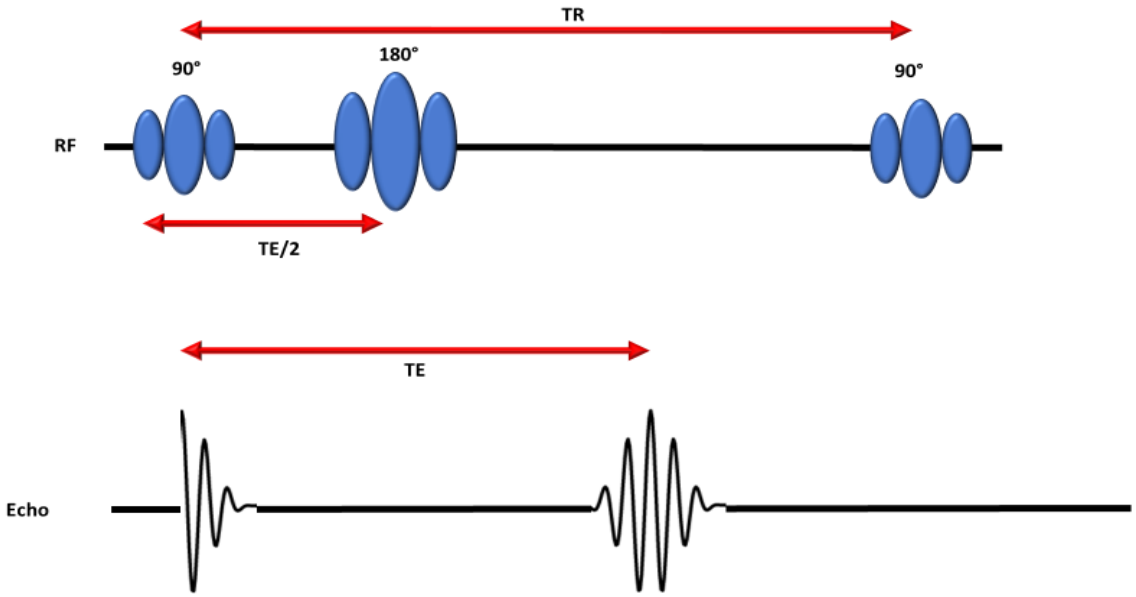

Figure 2-8: Spin echo sequence

T2 is often measured using a spin echo sequence. A spin echo sequence includes a 90- degree excitation pulse followed by a 180-degree pulse that refocuses the pulse. A single echo is measured during each repetition time.

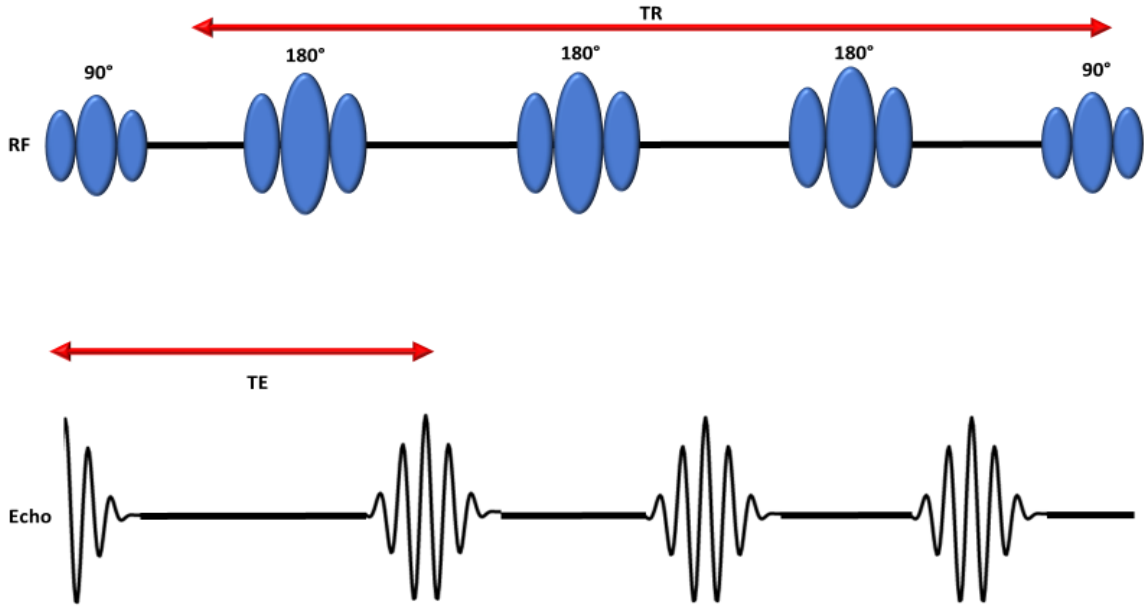

Figure 2-9: Turbo spin-echo

Turbo spin-echo is an adaptation of the spin-echo sequence used to reduce scanning time. Multiple echoes are recorded after each 90-degree excitation pulse by the use of multiple 180-degree inversion pulses.

2.4.3.2 Fat fraction MRI

Higher skeletal muscle fat accumulation is associated with lower muscle strength, lower physical function, and decreased mobility. Semi-quantitative measurements, such as the Mercuri fat infiltration scale (159), are often used as an outcome measure to assess myosteatosis but are inherently limited as they lack sensitivity and are subjective. More sensitive measurements to assess myosteatosis show potential in muscle imaging to provide a more objective measure, such as Dixon imaging (168).

Dixon imaging is a technique that exploits the differences in the resonant frequencies between fat and water in order to separate them in the image and produce fat fraction measurements (168). Fat fraction measurements using Dixon imaging have been validated in phantom experiments (169-173), have been shown to be highly reproducible in the liver (174), and have been shown to correlate well with chemical analysis (175) and the histology grading of liver steatosis (175, 176). Research into using fat fraction in skeletal muscles is an emerging and exciting topic.

2.4.3.2.1 Two-point Dixon

Two-point Dixon MRI acquires two images at two different echo times (TE-in-phase and TE-out-of-phase) using a modified gradient-echo pulse sequence. This technique exploits the fact that water and fat precess at different rates. At TE = 0, fat and water are in phase. The difference in their precessional frequencies is 3.5 parts per million (PPM) or 440Hz, in a magnetic field of 3T (Figure 2-10). As such, over time, the two signals alternate between being in-phase and out-of-phase with one another (Figure 2-11 and Figure 2-12).

If it is presumed that water is the dominant signal (i.e. there is more water signal than fat signal), then, by combining the two images, the water signal remains without the fat signal, whilst the subtraction of the out-of-phase from the in-phase will result in a fat image without the water (177):

- $S_{ip} + S_{oop} = (S_w + S_f) + (S_w - S_f) = 2S_w$
- $S_{ip} - S_{oop} = (S_w + S_f) - (S_w - S_f) = 2S_f$

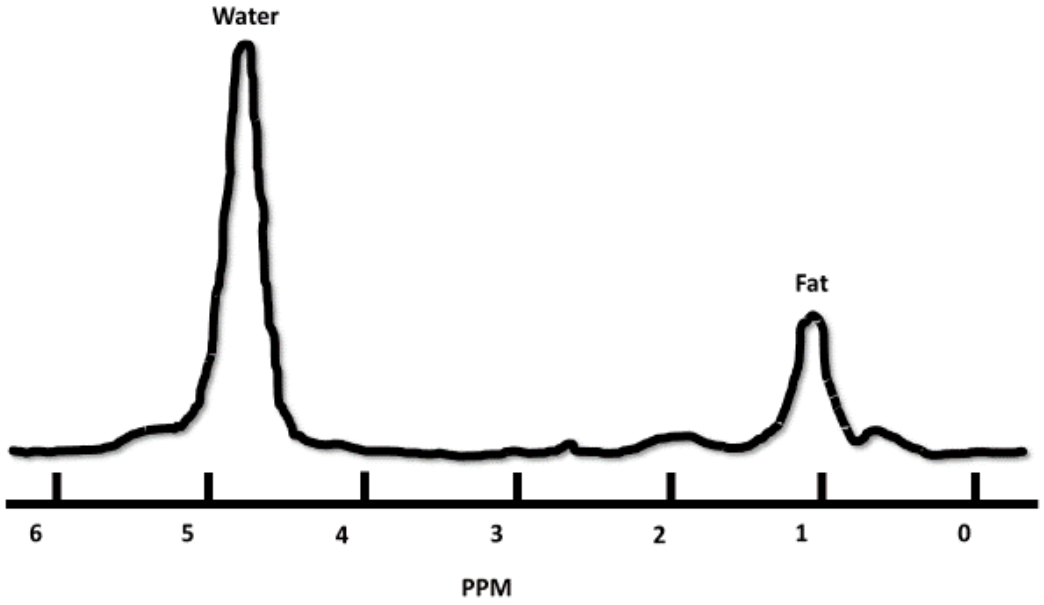

Figure 2-10: Chemical shift properties of water and fat

Water and fat precess at different rates, with water being the dominant signal. The difference in precessional frequencies is 3.5PPM in a magnetic field of 3T. This difference in precession allows for the separation of fat and water, to create fat only images and water only images.

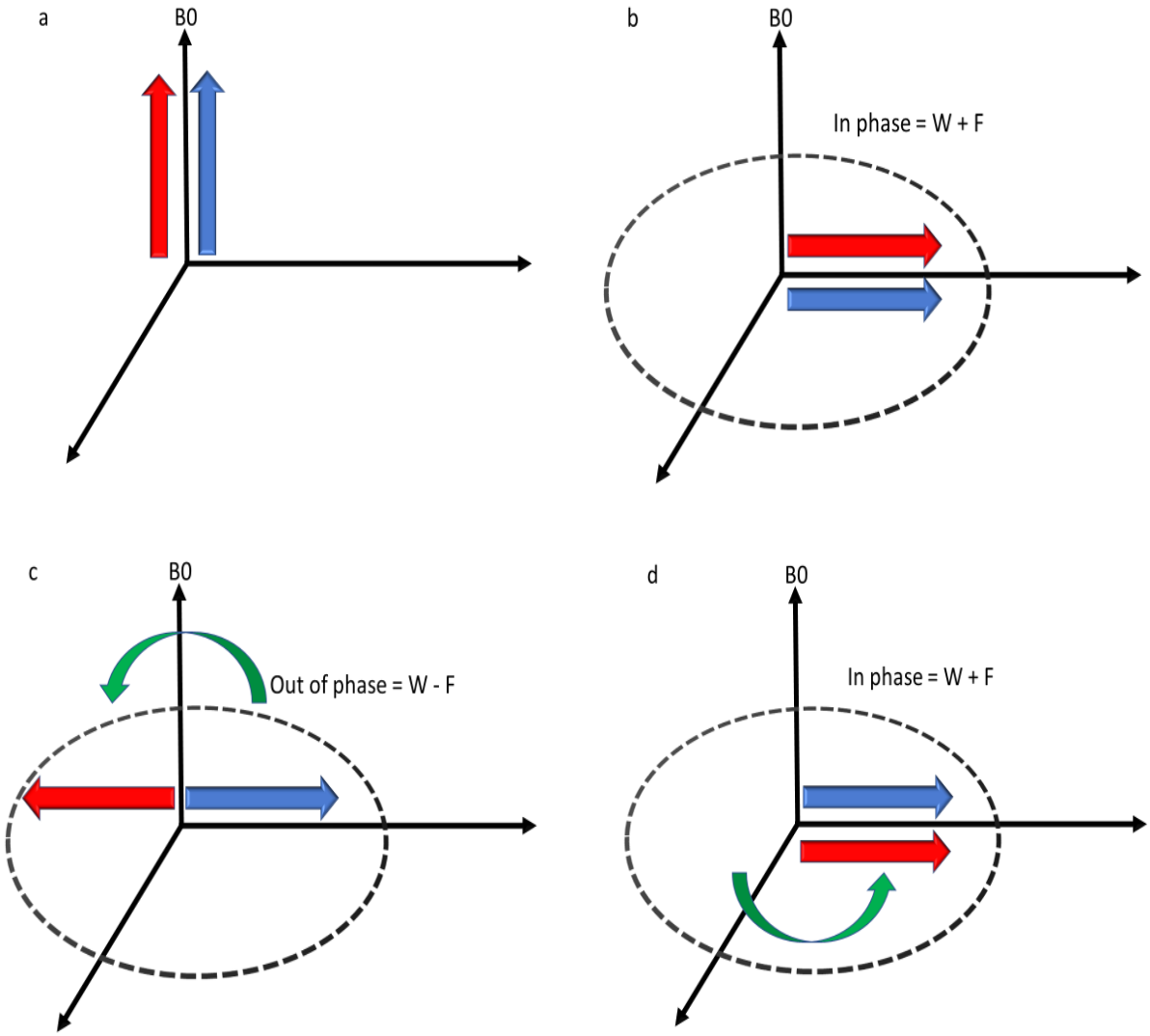

Figure 2-11: Two-point Dixon chemical shift MRI.

(a) Before the RF excitation, water and fat magnetisations are along the longitudinal axis. (b) After the RF excitation, the transverse magnetisations are in-phase. (c) Due to the slower processing of the fat signal, an echo acquired at this point would consists of a net signal of W-F. (d) Signal will transition between being in-phase and out-of-phase every 1.2 milliseconds.

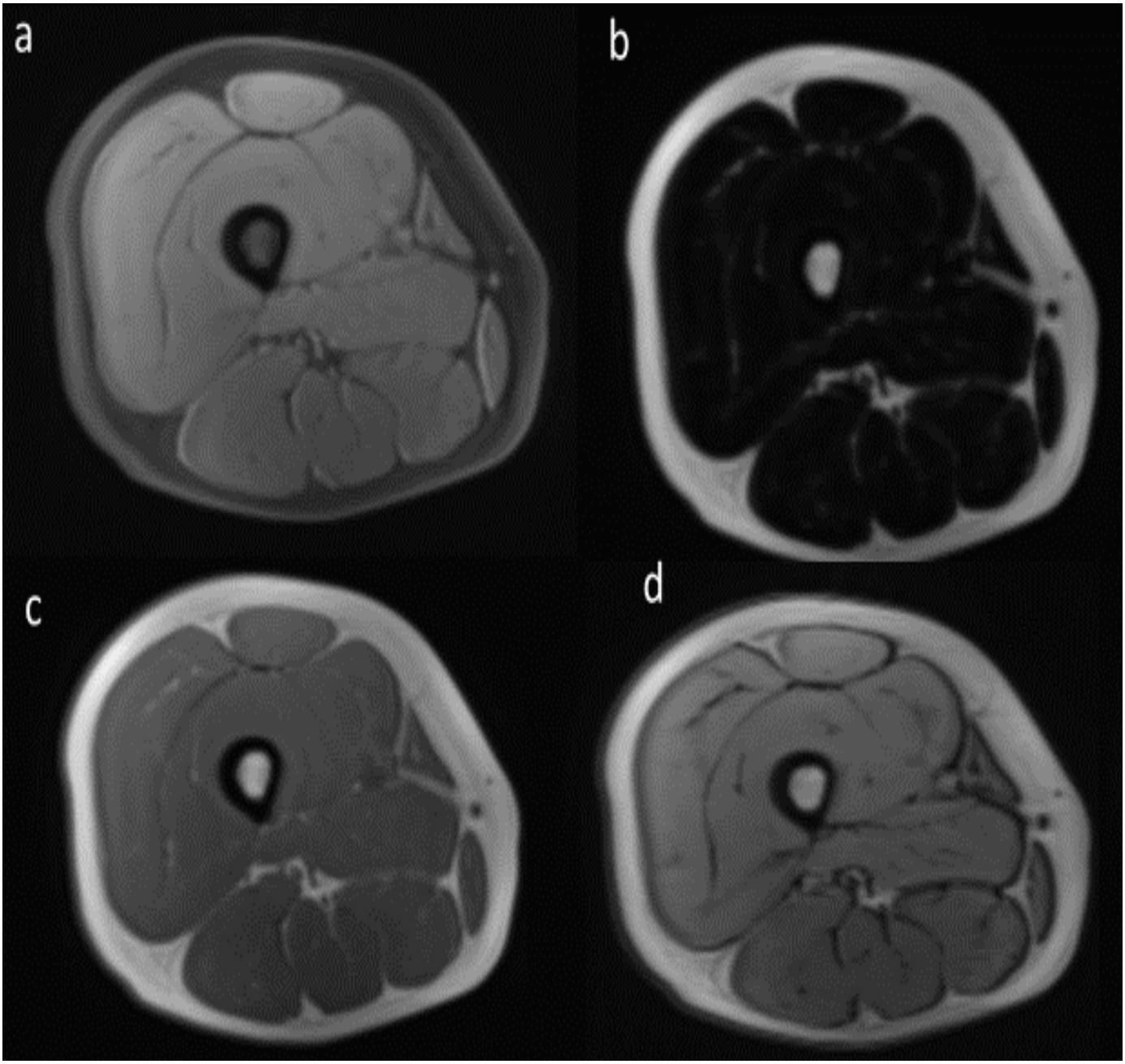

Figure 2-12: MR images of two-point Dixon chemical shift.

Two-point Dixon sequence in the same participant showing MRI images of (a) Water. (b) Fat. (c) In-phase. (d) Out-of-phase due to difference in resonance.

While two-point Dixon, which is used in this thesis, is available on all clinical scanners, it is sensitive to: errors caused by B_0 inhomogeneity, T2* effects, eddy currents, noise-related bias, and the spectral complexity of fat. However, multiple studies have failed to show that the errors inherent to two-point Dixon confound fat measurements in muscle in either ex-vivo or in-vivo analysis (178). Furthermore, two-point Dixon correlates strongly with confounder-corrected fat quantitation methods and with spectroscopy (178). Although improved accuracy in fat fraction measurements can be achieved using confounder corrected fat quantitation methods, there is no evidence to suggest that the relative differences in fat fraction with two-point Dixon are not related to genuine differences in muscle fat. More advanced methods of Dixon imaging, such as three-point Dixon and multiple echo time models, can be used to account for B_0-field inhomogeneities, T2* decay, and the fact that there are resonant fat frequencies. However, such techniques are not available on all clinical scanners.

2.4.3.3 MRI Diffusion imaging

Early pathophysiological changes can begin at the cellular level. Such changes cannot be detected by conventional MR imaging. Currently, to monitor early changes within muscle on a cellular level, histological examination is employed, requiring invasive tissue biopsies. A technique which is non-invasive but sensitive to subtle muscle changes is desirable. One possible approach is to detect the movement of molecules.

Two types of molecular movement can be observed in tissues. One is coherent bulk flow, which occurs in blood or cerebrospinal fluid. The second is the microscopic random displacement of the molecule in space (diffusion), known as Brownian motion. In biological tissues, such as muscles, the trajectory of the diffusion of water molecules is dependent on the structure and properties of the tissue. Through studying these changes in diffusion, changes can be detected. The

measurement of diffusion can be achieved using specialised MRI techniques called diffusion-weighted imaging (DWI) and diffusion tensor imaging (DTI) which are sensitive to changes in tissue microstructure and allow for the quantification and visualisation of the muscle architecture (179). To suppress chemical shift artefacts in diffusion imaging in order to improve image quality, fat suppression methods such as SPAIR are utilised.

Diffusion imaging can measure water diffusion in the muscle and permits the quantification of anisotropy of muscle fibres and muscle architectural parameters (180-182). Due to this, diffusion imaging has been utilised in the investigation of skeletal muscle physiology (26, 183-196) as it may be able to measure more subtle changes in muscle compared to conventional MRI, which could provide information on disease progression and treatment.

Moreover, muscle pathology and muscle fibre disorganisation and deterioration can be detected by diffusion measurements such as mean diffusivity (MD) and fractional anisotropy (FA) [26]. However, the interpretation of what a change in diffusion means is difficult, and there is ongoing research to analyse diffusion acquisitions to separate different properties of the muscle microstructure from diffusion measurements (197-199).

2.4.3.3.1 Diffusion-weighted imaging

Diffusion-weighted imaging (DWI), first developed by Stejskal and Tanner, is an MRI technique which permits the study regarding the microstructural organisation of tissue (31, 177, 182, 200-203). DWI has historically been used in the brain for applications such as distinguishing between an infarct and reversible ischaemia following a stroke (204).

Diffusion is often measured using spin-echo sequences (Figure 2-13) and utilises the b-value. The b-value measures the degree of diffusion weighting applied. The b-value, given by the equation $b = \gamma^2 G^2 \delta^2 (\Delta - \delta/3)$ (γ = Gamma G = magnitude, δ = duration, Δ = time interval), reflects the strength, length, and timing of the gradients used to produce diffusion-weighted images. A greater b-value is achieved by increasing the gradient, duration, and interval between pulses. Whereas b = 0 produces a non-diffusion-weighted image, a higher b-value produces greater diffusion effects. Sequences with a range of b-values can be used to calculate the quantity of signal loss due to diffusion. Specifically, if S_o is the MR baseline signal and D is the diffusion coefficient, the signal (S) following the application of the diffusion gradients is given by the equation $S = S_o e^{-bD}$.

First, a b = 0 image must be obtained, which shows no diffusion attenuation. Then, the diffusion across a minimum of three orthogonal directions (X, Y, and Z) is calculated by applying gradients symmetrically on each side of a 180-degree pulse (Figure 2-13). These gradients de-phase and then re-phase the transverse net magnetisation. This process imperfectly rephases protons that move due to diffusion in the interval between these two gradients because they experience a different field strength during dephasing than they do during rephasing.

After the second diffusion gradient, an image acquisition module is performed. The image acquisition module is often an echo-planar imaging (EPI) sequence utilising rapidly oscillating phase and frequency gradients which produce multiple gradient echoes. During this process, the net magnetic field is reduced after these gradients have been applied by an amount that depends on the degree of water diffusion within the tissue (Figure 2-14). The extent of the attenuation is reliant on the b-value and the diffusion coefficient (in millimetres squared per second).

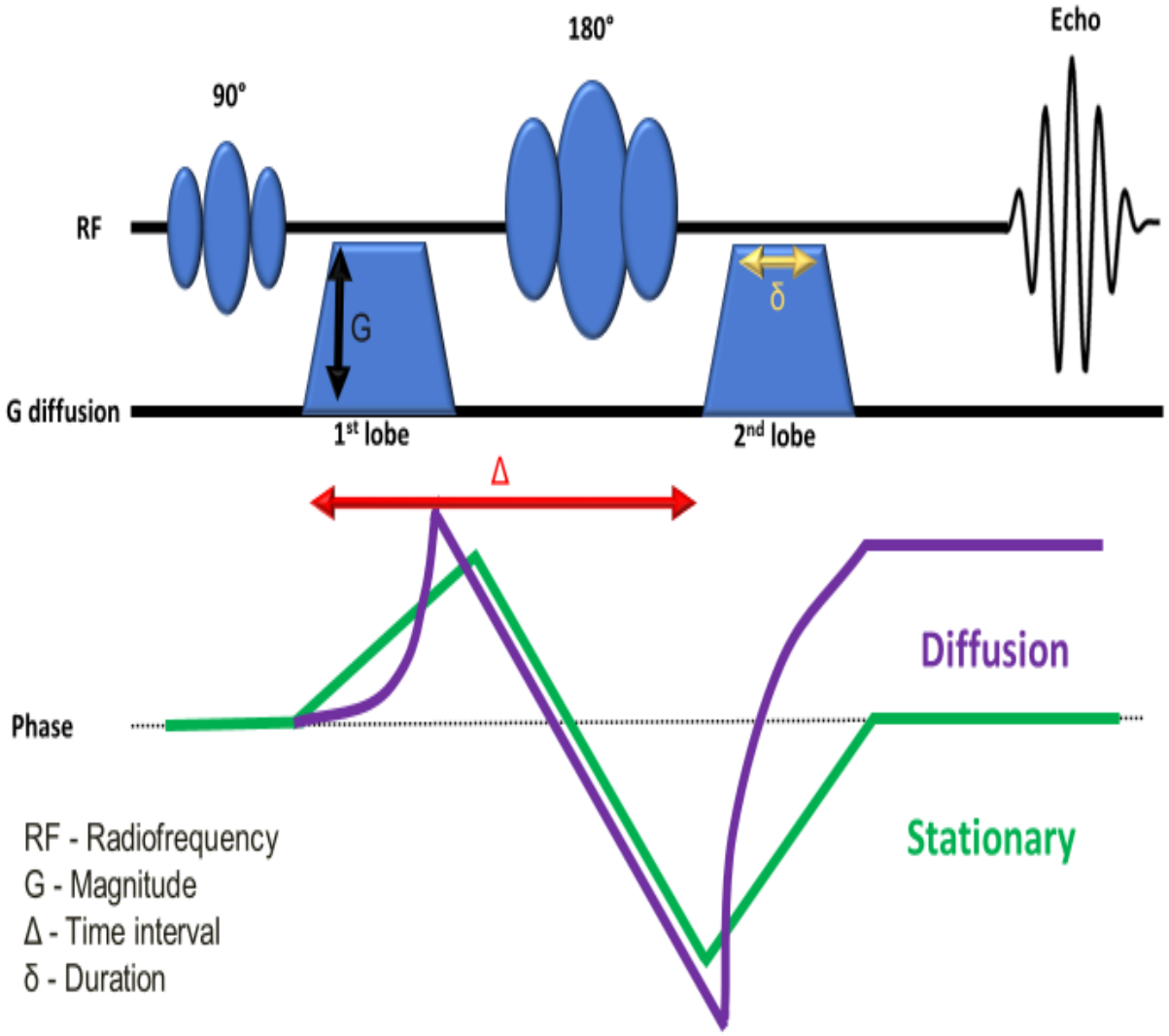

Figure 2-13: Spin echo diffusion sequence

Diffusion gradients are turned on before and after the 180-degree pulse which induces a phase shift in proton procession. After the second diffusion gradient, an image acquisition (EPI) is turned on. Molecules which diffuse move into different locations between the first and second lobes, resulting in a loss of signal.

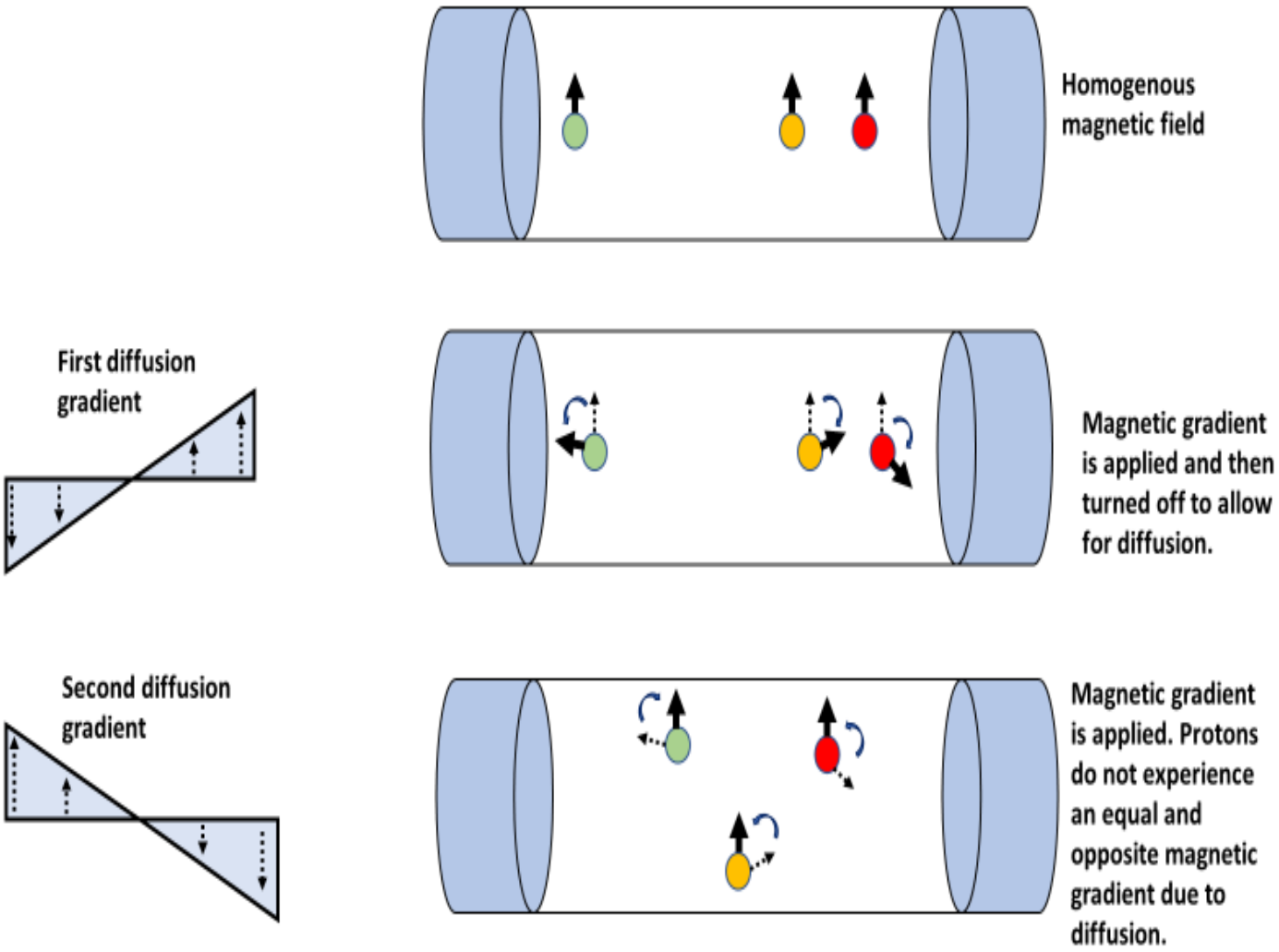

Figure 2-14: Proton movement due to gradient diffusion

2.4.3.3.2 Diffusion tensor imaging

Diffusion-weighted imaging can be extended by calculating the mean diffusivity in a minimum of six independent directions. This extension is known as diffusion tensor imaging (DTI). Diffusion tensor imaging parameters have potential as a quantitative assessment of muscle due to their sensitivity to the direction and anisotropy of

water diffusion within the muscle. The direction of the diffusion is characterised by three eigenvalues: λ1, λ2, and λ3. The principal eigenvalue, λ1, describes the direction with the highest diffusion. In healthy muscle, this corresponds to the local muscle fibre orientation (205). Eigenvalue λ2 is orthogonal to λ1 and is the next greatest component of the diffusion. Eigenvalue λ3 is the component of diffusion orthogonal to λ1 and λ2. From the three eigenvalues, the mean diffusivity (MD), and fractional anisotropy (FA) can be calculated (206-208). Mean diffusivity can be calculated as $MD = \frac{\lambda_1+\lambda_2+\lambda_3}{3}$. Mean diffusivity represents the overall amount of diffusion and is measured in units of millimetres squared per second. Tissues which have free diffusion have a higher mean diffusivity. In contrast, those that have restricted diffusion have a lower mean diffusivity. Restricted diffusion can be caused by physical barriers (e.g. fibre walls) that limit diffusion. To quantify the diffusion anisotropy, the scalar index for fractional anisotropy was introduced (180, 209). Fractional anisotropy can be calculated as follows:

$$FA = \sqrt{\frac{3}{2}}\sqrt{\frac{(\lambda_1-MD)^2+(\lambda_2-MD)^2+(\lambda_3-MD)^2}{{\lambda_1}^2+{\lambda_2}^2+{\lambda_3}^2}} .$$

Fractional anisotropy represents the shape of the ellipsoid (Figure 2-15), described by the three eigenvalues. Fractional anisotropy is dimensionless and equals zero in an isotropic medium. For a cylindrical symmetric anisotropic medium, the fractional anisotropy value approaches 1. A value of 0 indicates that all three eigenvalues are equal and indicates diffusion within a medium that is unhindered equally in all directions (a perfect sphere). A value of 1 indicates λ1 having infinite length while λ2 and λ3 have a length of 0 (a straight line).

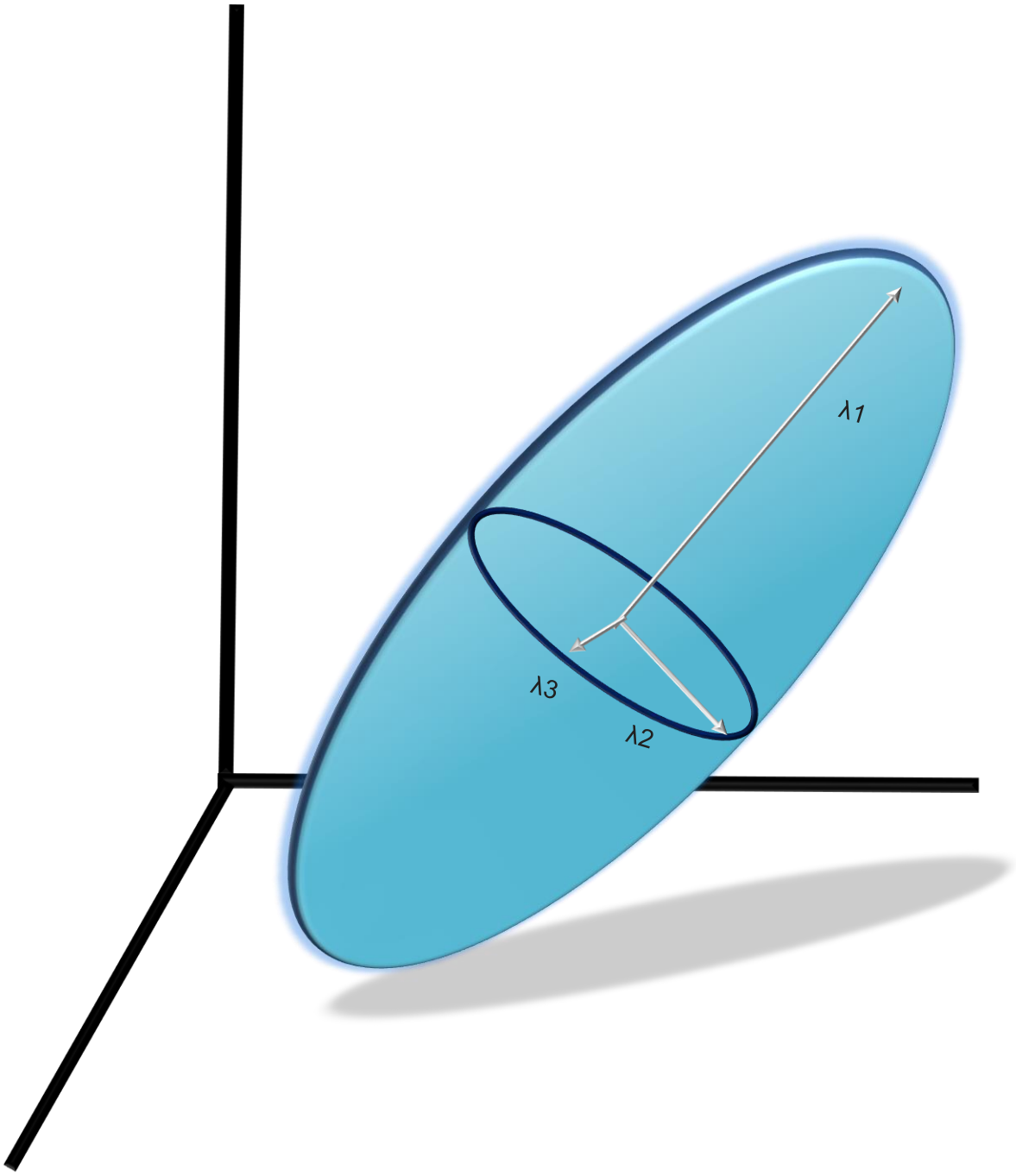

Figure 2-15: Fractional anisotropy

The direction of the diffusion is characterised by three eigenvalues: λ1, λ2, and λ3. From the three eigenvalues, the mean diffusivity, and fractional anisotropy can be calculated

2.4.3.3.3 Stimulated echo acquisition mode diffusion sequence

As muscle is made up of long muscle fibres, muscle diffusion is highly anisotropic and ordered. As muscle diameters are relatively wide, MR sequences which permit long diffusion times (the time elapsed between diffusion gradients) are necessary if the measurements are to be sensitive to restricted diffusion across the fibre. Whilst diffusion-weighted imaging typically employs a spin-echo (SE), echo-planar imaging (EPI) pulse sequence (Figure 2-13), stimulated echo acquisition mode (STEAM) pulse sequences (Figure 2-16) may be beneficial for skeletal muscle diffusion imaging due to the increased echo times that they allow. This increased echo time allows for greater diffusion across the length of the muscle fibres.

STEAM is a technique often used in spectroscopy which uses three slice-selective 90-degree pulses which are applied simultaneously with three orthogonal gradients (x, y, and z) (177). A benefit of STEAM in comparison to the more frequently used SE pulse sequence is that it can have a high b-value without incurring the TE-induced signal loss.

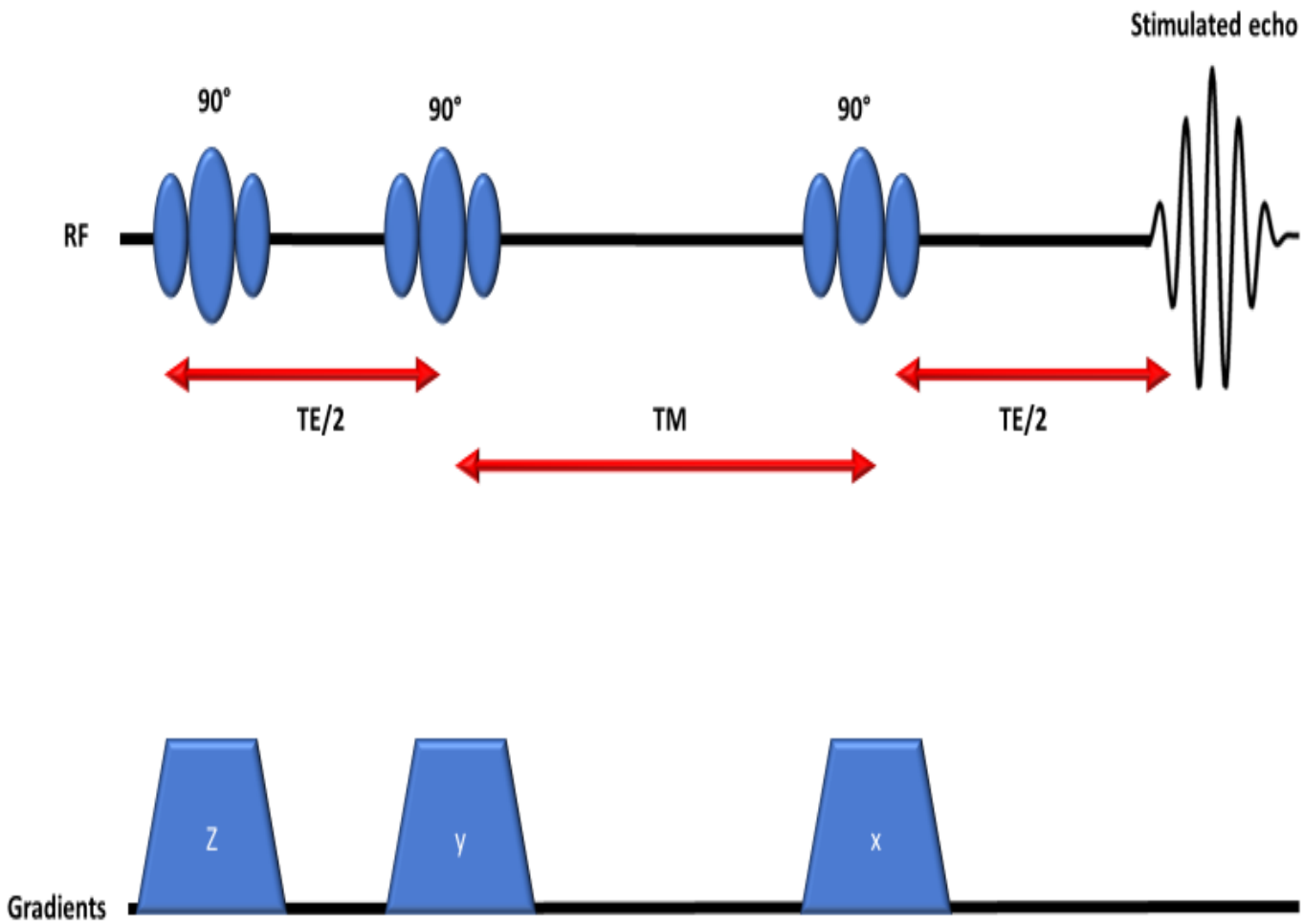

Figure 2-16: STEAM MRI

STEAM uses three 90-degree pulses applied with the three orthogonal gradients (x, y, and z) and produces a stimulated echo.

2.4.3.4 Muscle volume assessed by MRI

Muscle volume correlates with physical function in both healthy and pathological populations (52, 210-213) and is closely related to the physiological cross-sectional area, which is associated with muscle strength (52). MRI is often regarded as the gold standard for the evaluation of muscle volume and can be used to validate other imaging techniques for the assessment of muscle mass (214, 215). The majority of studies investigating muscle volume, including this research project, have utilised T1-weighted sequences due to their ability to distinguish margins between muscles and because of their capacity to contrast bone from muscle (216-218). It could be speculated that quantitative muscle volume could be used for the diagnosis of muscle disease and may enable monitoring of changes in muscle mass in response to interventions or due to disease progression (219-222). However, a potential complication of assessing muscle volume is segmentation. Whilst it may be beneficial to assess multiple slices to measure muscle volume, manual segmentation is a time-consuming process, and therefore most research studies use only one slice which is inferior to assessing the muscle volume across its entire length. Unfortunately, due to the time constraints of manual segmentation, whole muscle volume assessment would likely require an automated segmentation method. In addition, this automated process could also allow for a smaller slice thickness. This is an important consideration because it could be speculated that if the slice thickness is too large, subtle changes may be missed; however, a smaller slice thickness may result in increased scan times and a greater quantity of segmentation required, which, if done manually, could be time-consuming.

2.5 Summary

Maintaining muscle health is important for daily activities. Ageing and disease, such as rheumatic diseases, can cause a decrease in muscle health which can impact an individual's quality of life and increase the risk of falls. Therefore, research into assessing muscle pathology due to ageing and rheumatic disease may have a significant benefit to the lives of individuals. There are numerous ways to assess muscle health, such as muscle function testing and MRI. MRI has vastly improved our knowledge of joint pathology. However, the role of MRI in assessing the muscle in rheumatic diseases has been under-researched.

MRI is regarded as the gold-standard in imaging muscle and is frequently used for identifying muscle oedema, myosteatosis, and muscle atrophy, which are common features observed in patients with muscle pathology. Conventional MRI and physical function assessments are utilised clinically but can be subjective and may not be sensitive enough to detect subtle changes within the muscle, such as at the early stages of the disease. Thus, muscle pathology may already be established before it is detectable by conventional MRI or present with noticeable changes in physical function. Researching the use of quantitative MRI and muscle strength in the muscle may be able to provide information on the pathogenesis of muscle involvement due to ageing and rheumatic disease. Quantitative MRI can provide a numerical value to many of the pathological features observed within the muscle, including: muscle oedema, myosteatosis, changes to muscle microstructure, and muscle atrophy. Within the clinical setting, quantitative MRI and strength testing could hence be used as biomarkers for the assessment and monitoring of a range of musculoskeletal diseases (223-228). It may also have an important role in assessing the efficacy of potential interventions to preserve muscle function.

Chapter 3 General methodology

Chapter 3 describes the general methodology used across all four studies, including recruitment of participants, MR imaging sequences, muscle strength assessments, and analysis of data. Specific details regarding study methodology are outlined in their respective chapters.

3.1 Introduction

The data analysed in this thesis was acquired under the Magnetic resonance imaging and UltraSound CLinical Evaluation of muscle pathology (MUSCLE) research project from the Leeds Institute of Rheumatic and Musculoskeletal Medicine (LIRMM), the Leeds National Institute of Health Research (NIHR) Biomedical Research Centre (BRC), and the University of Leeds. Researchers on the MUSCLE project included Matthew Farrow and Abdulrahman Alfuraih. Both researchers recruited and consented the patients and conducted muscle function assessments. The MUSCLE project was a multi-imaging (MRI and ultrasound) research project to assess a range of medical imaging techniques for the assessment of muscle pathology due to ageing, myositis, rheumatoid arthritis, and giant cell arteritis. This thesis focusses on the MRI and muscle strength components of the MUSCLE project.

3.2 Ethical approval

The study complied with the declaration of Helsinki and was conducted in line with the principles of ‘Good clinical practice.’ This study was approved by the local research ethics committee (14-LO-1785 and 17/EM/0079).

3.3 Study group selection

Previous studies of quantitative MRI in muscle disease have mostly focussed on a single disease group, with most examining a single myopathic clinical feature of a disease. This study investigated the wide applicability of quantitative MRI by including various disease groups and assessing multiple clinical features of muscle pathology. These groups included healthy controls and patients with myositis, rheumatoid arthritis, and giant cell arteritis. Baseline demographic and clinical data were collected for all participants.

3.3.1 The rationale for patient groups

In order to have an understanding of how muscle pathology can present on quantitative MRI, this research recruited myositis patients as it is a primary inflammatory muscle disease and is, therefore, an excellent model to study muscle pathology. Furthermore, the current diagnosis of myositis involves the use of MRI to identify muscle oedema, myosteatosis, and muscle atrophy; and therefore, MRI, which can quantify these observed muscle pathologies, could be easily integrated into the clinical management of the disease.

Patients with rheumatoid arthritis (RA) often present with joint swelling, pain, and stiffness, and frequently experience fatigue and muscle weakness, which could represent underlying muscle involvement. However, muscle involvement in patients with RA has received little research interest. Therefore, patients with RA were recruited for this study to identify whether there is subclinical muscle involvement in RA patients.

Giant cell arteritis (GCA) patients frequently present with polymyalgia rheumatica which is associated with myalgia. In addition, patients with GCA are treated with high doses of glucocorticoids which are known to cause glucocorticoid-induced myopathy. However, despite the recognition of muscle involvement in GCA, little research exists regarding muscle pathology of patients with GCA. In response to this lack of understanding, GCA patients were recruited for this study to identify if muscle involvement is present in GCA patients at the start of their treatment and if the disease is affected by glucocorticoids longitudinally.

3.3.2 Healthy controls

The addition of healthy controls is vital as reported values of MRI measurements can vary between studies due to differences in participant cohort, field strength, scanner model, and sequence parameters. Therefore, it is difficult to compare results in patients to those of healthy controls in the literature. Thus, for quality control, matched healthy controls were essential for this research. In this research project, one large cohort of healthy controls provided age- and gender-matching for patient groups. Healthy controls were used multiple times across all chapters, except for Chapter 4, which had its own healthy controls. The inclusion of healthy controls in this research project allowed for the direct comparison of patient data with age- and gender-matched healthy controls. Furthermore, this research investigated if quantitative MRI measurements are sensitive enough to detect the

known changes that occur within the muscle due to normal ageing (sarcopenia), in otherwise healthy individuals.

3.4 Recruitment

All participants were 18 years of age and above and provided informed written consent. Participants were instructed to avoid physical activity for twenty-four hours prior to the study. Patients were identified when they attended clinics or wards at Leeds Teaching Hospitals. Healthy controls were recruited with poster advertisements at Leeds Teaching Hospitals, poster advertisements at the University of Leeds, social media posts, group emails to staff based at LTHT, and from personal recommendations from participants within the study. In addition, healthy family members of recruited patients were invited to take part as healthy controls. Furthermore, through a collaboration with the Bradford Institute for Health Research, healthy participants over the age of 75 were recruited from the Care 75+ database, which consists of older individuals who had consented to be approached to take part in research.

All participants received a verbal explanation of the study and a participant information sheet which included information about the rationale and design of the study. All participants were screened for MRI safety. All data collected was anonymised and assigned a unique participant identifier. The research visit took approximately two hours. The participant pathway can be seen in Figure 3-1.

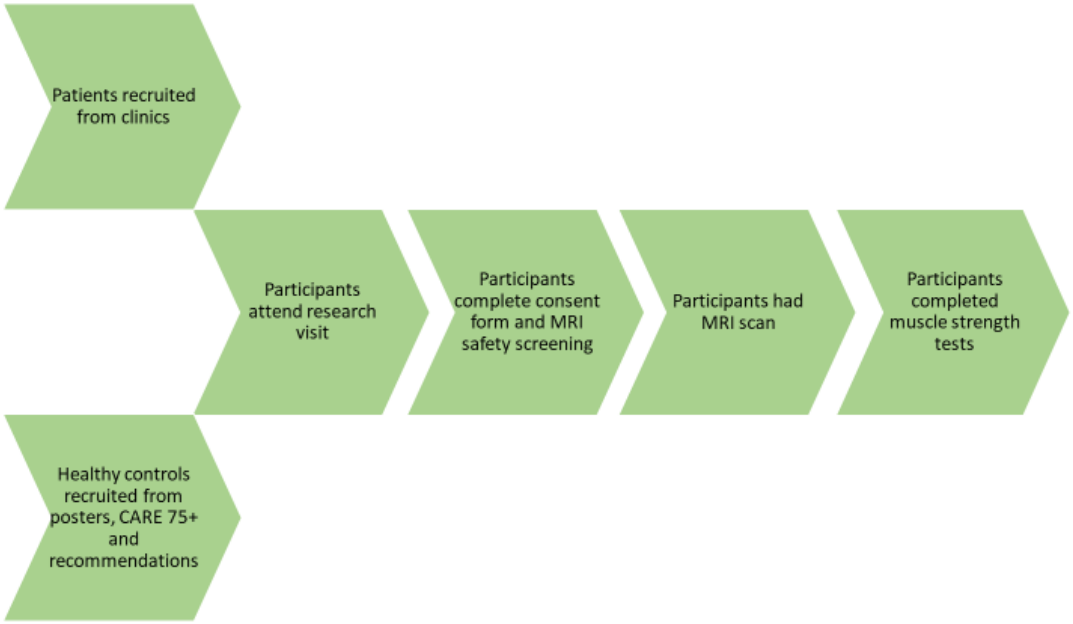

Figure 3-1: Participant pathway

3.4.1 Inclusion criteria

Healthy participants in this thesis were asymptomatic with no history of muscle disease. Eligibility criteria for each disease group are explained in their respective chapters.

3.4.2 Exclusion criteria

Exclusion criteria included: contraindications to MRI, including claustrophobia, possession of cardiac pacemaker, surgical clips within the head, metal fragments in eye or head, and pregnancy. Healthy controls were ineligible to take part in this research study if they had a previous history of muscle disorder or arthritis. Patients

were ineligible to take part in this study if they had a previous history of spinal disease, neuropathy, or overlap connective tissue disease syndrome.

3.5 MRI methodology

3.5.1 MRI protocol

All MRI data were acquired using a MAGNETOM Verio 3T MR scanner (Siemens Healthcare, Erlangen, Germany). Imaging parameters are presented in Table 3-1. Participants were laid supine in the bore of the magnet and placed centrally within the magnet bore. Two small four-channel flex coils were wrapped around the dominant thigh and placed with the distal end of both coils positioned 4cm from the superior edge of the patella. To ensure that the imaging volume was positioned consistently in all participants, the inferior edge of the volumetric interpolated breath-hold examination (VIBE) Dixon volume was located at the insertion point of the distal rectus femoris muscle into the tendon (Figure 3-2).

Diffusion tensor images were acquired using a stimulated echo acquisition mode (STEAM) prototype sequence, with an echo-planar imaging (EPI) readout (229) and SPAIR (spectral attenuated inversion recovery) fat suppression. The STEAM sequence was employed as it allows for a longer mixing time (T_m), which may be beneficial if diffusion measurements are sensitive to restricted diffusion within muscle fibres due to their size and composition. The mixing time, the time between the second and third 90° RF pulses, was 981ms. The diffusion time, the time between the start of two diffusion encoding gradients was 1,000ms. The acquisition time was 6 minutes and 12 seconds. The diffusion and T2 acquisition slices were aligned with the central four slices of the VIBE Dixon volume (slices 19 - 22 of 40).

Figure 3-2: Sagittal MRI localiser

Localiser image of the thigh used in the planning of the VIBE Dixon imaging volume (shown by the yellow box). This volume was located such that its inferior edge was positioned at the insertion of the rectus femoris muscle into its associated tendon.

Table 3-1: MRI parameters

	T1 weighted	T2	Fat quantification	Diffusion
Imaging sequence	Turbo spin-echo (TSE)	Multi-Echo, multi-slice (MESE)	2-point VIBE Dixon	STEAM-EPI
TR: Repetition Time	697	1,500	11	6,300
TE: Echo Time(s) [ms]	9.1	9.6:9.4:153.6 (16 echoes)	2.45 and 3.675	42.4
Field of View [mm]	300*300	300*300	300*300	300*300
Slice thickness [mm]	5	5	5	5
Fat suppression	STIR	SPAIR	N/A	SPAIR
Acquisition Matrix	256*256	256*256	256*256	128*128
Number of slices	60	4	40	4
Number of averages	1	1	1	8
Receiver bandwidth [Hz/pixel]	222	510	510	1502
Flip Angle [degree]	90	15	15	-
Generalized auto calibrating partial parallel	-	-	-	2 (24 reference lines)

acquisition (GRAPPA)				
Partial Fourier	-	-	-	6/8
B values [s/mm^2]	-	-	-	0, 500
Directions	-	-	-	6
Mixing time (T_m)[ms]	-	-	-	981
Diffusion time (Δ) [ms]	-	-	-	1,000
Acquisition Time [min: s]	2:19	2:05	1:47	6:12

3.5.2 Manual contouring of MR images

Regions of interest (ROI) were contoured using OsiriX imaging software (version 4.0; open-source DICOM viewer). ROIs depicting the individual hamstring muscles (semitendinosus, semimembranosus, and biceps femoris) and quadriceps muscles (rectus femoris, vastus lateralis, vastus medialis, and vastus intermedius) were drawn on the middle slice (slice 20) of the in-phase VIBE Dixon volume for each participant, avoiding fascial tissue and subcutaneous fat (Figure 3-3). Slice 20 was chosen to provide consistency across all participants at a similar level of anatomy to decrease variation. Hamstrings and quadriceps were used primarily in this research project, as in pathological muscle, the individual muscles of the medial group can be challenging to demarcate without including fascial tissue and subcutaneous fat (Figure 3-4). In addition, the hamstrings and quadriceps are the most frequently researched muscles of the thigh, and the quadriceps are the most frequently biopsied muscle. The mean signal intensity was taken for each ROI and

used in the subsequent analysis. ROIs were copied to the corresponding T2, fat fraction, and diffusion parameter maps, accounting for differences in image resolution. For muscle groups (quadriceps and hamstrings), the mean of all voxels from all regions of interest belonging to the muscle group was calculated.

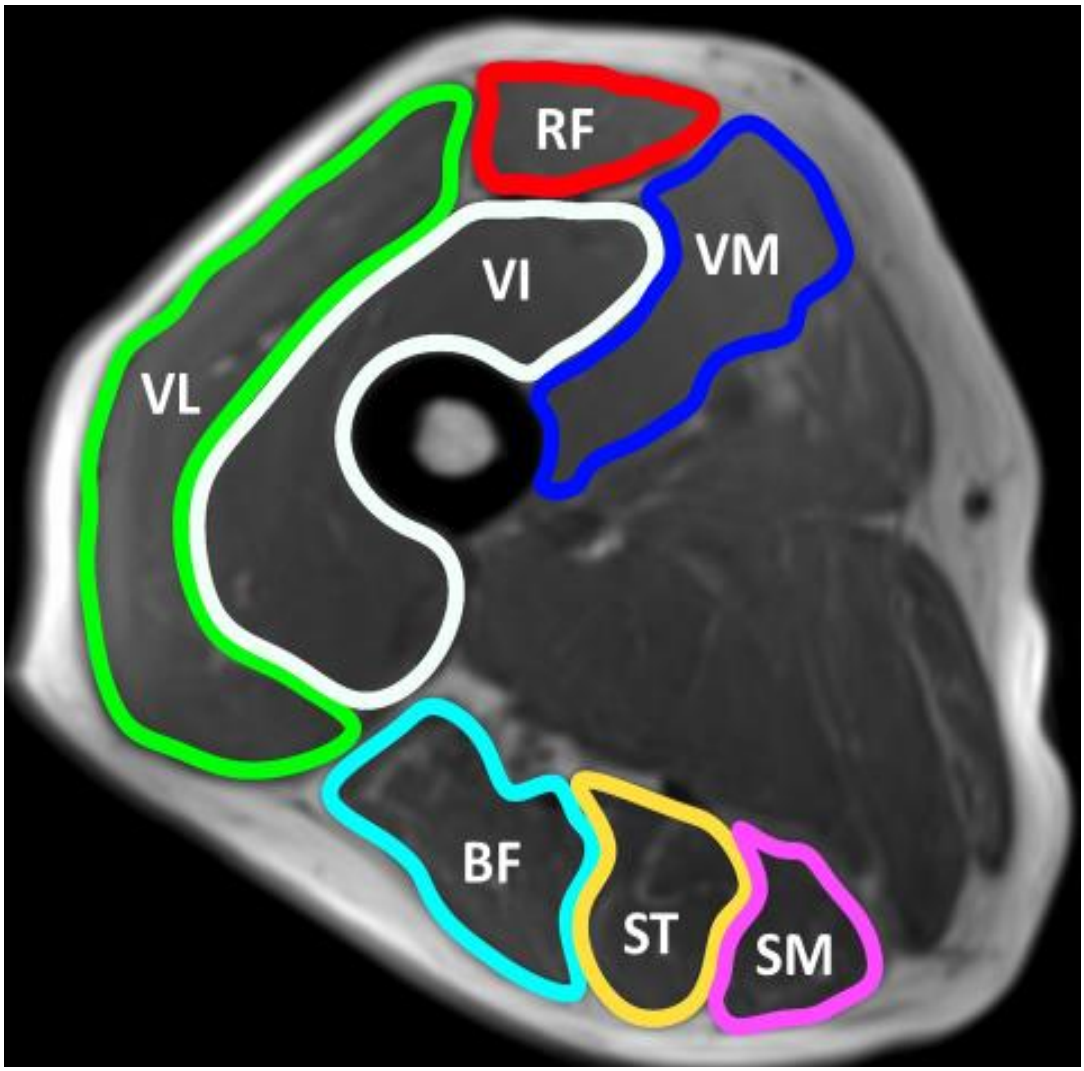

Figure 3-3: Regions of interest

In-phase two-point Dixon MR image of the regions of interest used in this thesis. Quadriceps: RF- rectus femoris. VL- vastus lateralis. VM- vastus medialis. VI- vastus intermedius. Hamstrings: BF- biceps femoris. ST- semitendinosus. SM- semimembranosus.

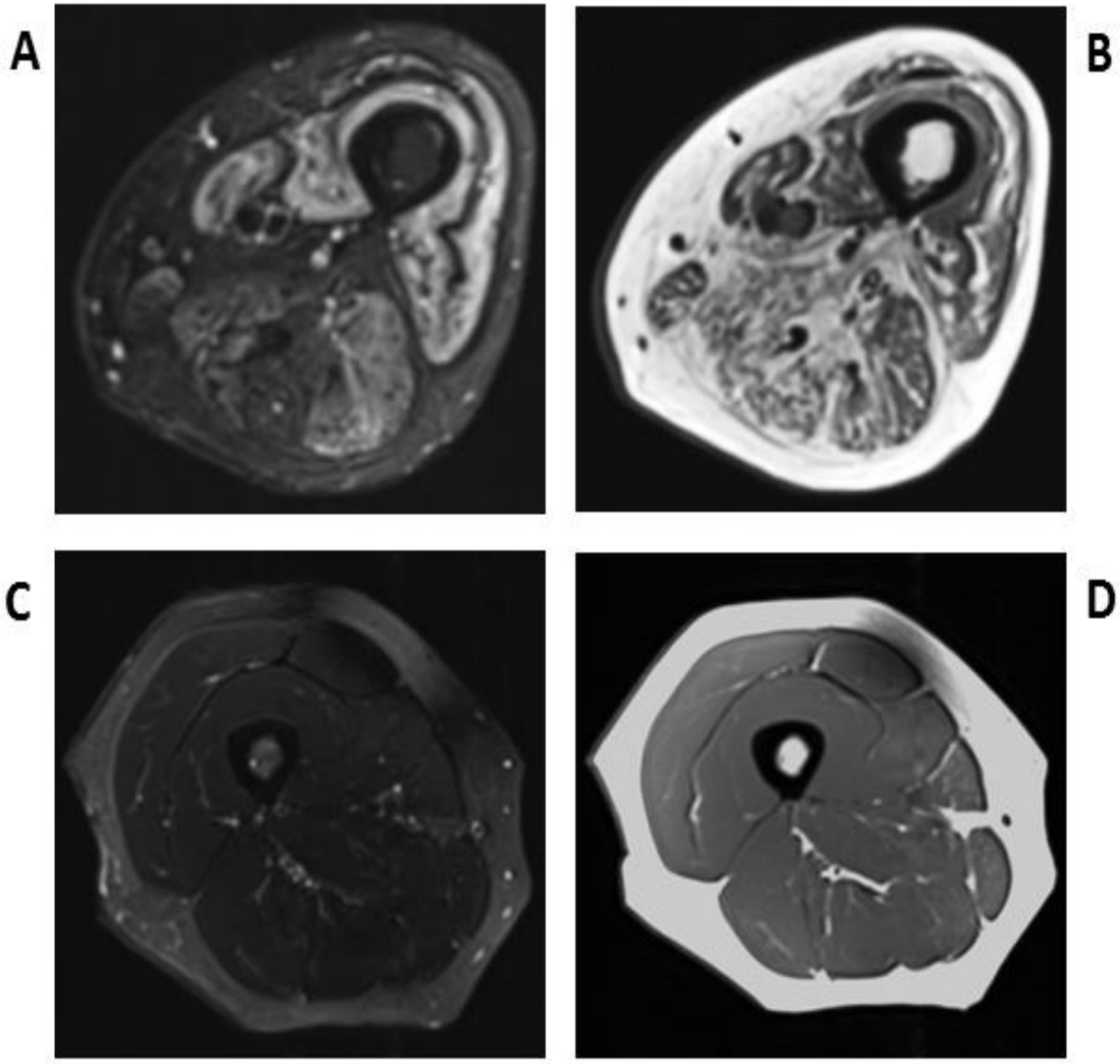

Figure 3-4: Conventional MRI of the right thigh

(A) T2-STIR and (B) T1-weighted images of a myositis patient, compared to (C) T2-STIR and (D) T1-weighted images of a healthy control.

Muscle oedema (T2-STIR) and fat infiltration (T1-weighted) is present in patients with myositis compared to healthy controls. In myositis patients, the medial muscles of the thigh are more difficult to contour regions of interest compared to quadriceps and hamstring muscles without contaminating the region of interest with subcutaneous fat.

3.5.3 Quantitative MRI measurements used in this thesis

3.5.3.1 T2 MRI

For T2 measurements, axial images were obtained using a T2-weighted, multi-echo, spin-echo (MESE) sequence with SPAIR fat suppression, and an echo train length of 16, with echo times (TE) of 9.6, 19.2, 28.8, 38.4, 48.0, 57.6, 67.2, 76.8, 86.4, 96.0, 105.6, 115.2, 124.8, 134.4, 144.0, and 153.6 ms. To calculate T2, signal intensity measurements were obtained from each of these echo times for each muscle. The mean signal intensity for each case was then plotted against the echo times and fitted using a mono-exponential decay equation: ($S=S_0 exp(-TE/T_2)$) (Figure 3-5) (164).

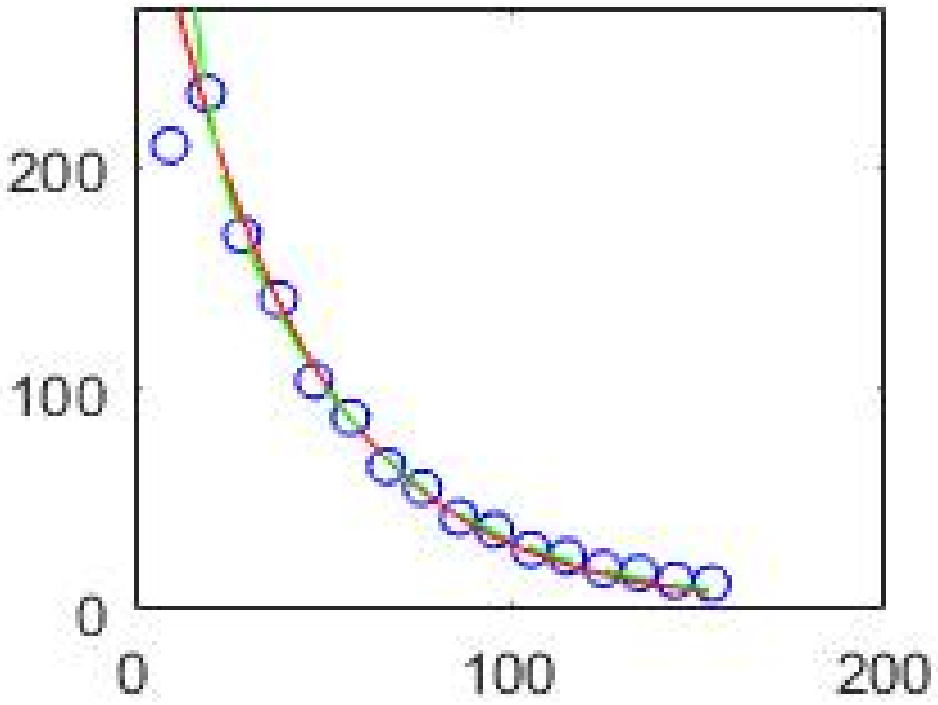

Figure 3-5: T2 mono-exponential decay curve

Measurements were obtained from multiple echo times using a mono-exponential decay equation.

3.5.3.2 Fat fraction

For fat quantitation, a 40-slice, two-point VIBE Dixon sequence (Figure 3-6) was used. A two-point VIBE Dixon sequence was selected because of its wide availability and well documented recent use in the muscle (115, 178, 230-232).

Fat and water images were generated from the acquired in-phase and out-of-phase images using the scanner vendor's post-processing software. B_0 variations due to changes in magnetic susceptibility at tissue interfaces were corrected for using the Jellus phase-correction method (233). The use of a 15° excitation flip-angle generated images with a good signal to noise ratio level but increased T1-weighting. Errors due to the difference in T1 between fat and water were corrected for by employing methods described by Liu et al (234). The proton densities of fat and water (M_f) and (M_w) were derived from the measured signals (S_f and S_w) as follows: $M_w = \frac{S_w\left(1-e^{-TR/T_{1w}}\cos\alpha\right)}{\left(1-e^{-TR/T_{1w}}\sin\alpha\right)}$ and $M_f = \frac{S_f\left(1-e^{-TR/T_{1f}}\cos\alpha\right)}{\left(1-e^{-TR/T_{1f}}\sin\alpha\right)}$. Assumed T1 values for water (T1w = 1,420ms) and fat (T1f = 371ms) were used as reported by Gold et al (235). Fat fraction values were calculated as follows: $fat\ fraction = \frac{M_f}{M_f+M_w} \times 100\%$.

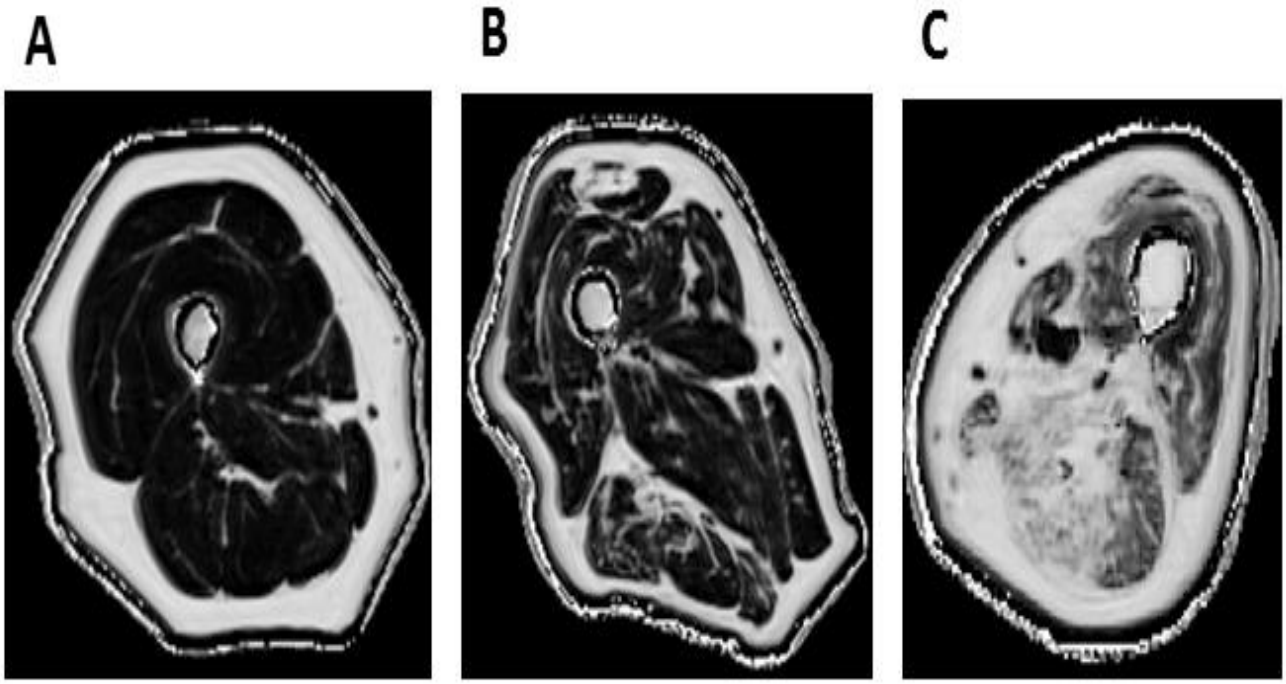

Figure 3-6: Quantitative MRI fat fraction measurement in the quadriceps and hamstrings

(A) 45-year-old healthy female with a fat fraction of 1.9% (quadriceps) and 2.7% (hamstrings) respectively. (B) 83-year-old healthy male presenting with myosteatosis associated with healthy ageing with a fat fraction of 9.6% (quadriceps) and 13.4% (hamstrings) respectively. (C) 60-year-old male with active myositis presenting with myosteatosis with a fat fraction of 19.6% (quadriceps) and 28.5% (hamstrings) respectively.

3.5.3.3 Diffusion tensor imaging

Mean diffusivity and fractional anisotropy maps were generated using the scanner vendor's software (Siemens AG, Healthcare Sector, Erlangen, Germany). The regions of interest were then used to obtain mean values of mean diffusivity and fractional anisotropy (Figure 3-7).

Diffusion data acquired from skeletal muscle is prone to loss of signal artefacts that corrupt measured signal intensities. These signal voids are thought to arise from unintended spontaneous mechanical activity within the musculature (236). To limit the impact of these artefacts on calculated diffusion parameters, the MR images were manually reviewed. If voids were present in more than one individual muscle, that participant would be excluded. No participants had to be excluded in this thesis.

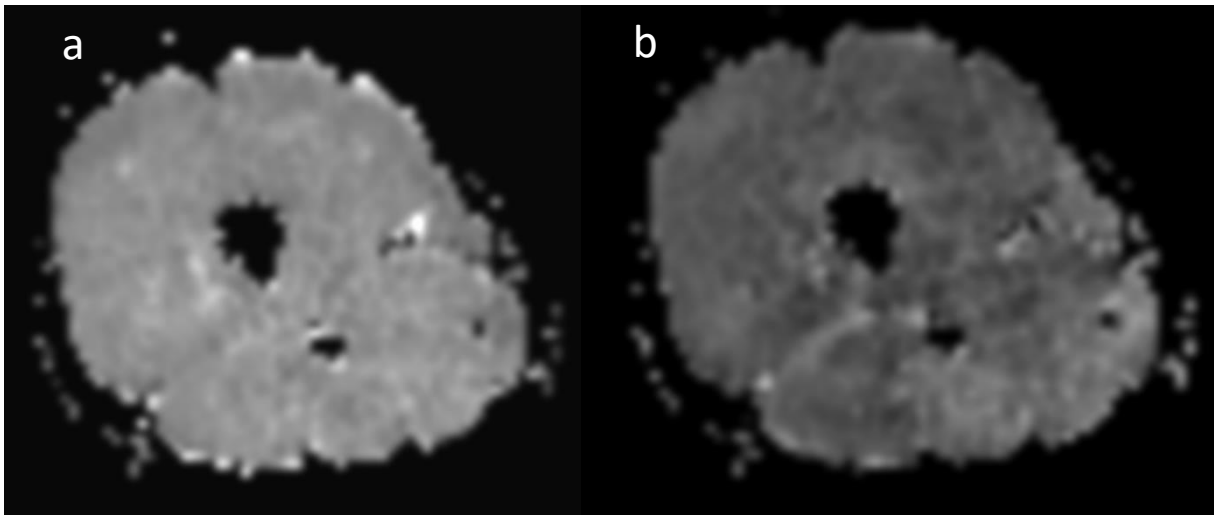

Figure 3-7: Mean diffusivity and fractional anisotropy maps

(a) Mean diffusivity. (b) Fractional anisotropy

3.5.3.4 Muscle volume

Differences in the length of thigh muscles between patients will introduce variation in the muscle volume estimates. This research project attempted to control for these differences by positioning relative to an anatomical reference marker, with the distal end of both coils positioned 4cm from the superior edge of the patella.

Muscle volume estimates were obtained using a semi-automated algorithm that used fat fraction maps generated from the VIBE Dixon volume data. To exclude bone from the image, a seed point was manually placed within the bone on the central slice of the VIBE Dixon volume (Figure 3-8). A 3D connected components algorithm (bwconncomp, MATLAB) was then used to grow a region within the extent of the bone. The in-phase Dixon image was used for this because of the excellent contrast between the bright bone marrow and the dark, surrounding cortical bone. The threshold of <50% fat fraction was chosen as it has been previously used in muscle volume measurements in the lumbar multifidus (237, 238) and erector spinae muscles (239, 240), and no previously used threshold values have been used in the muscles of the thigh. To exclude muscle from the contralateral leg, a bounding box was automatically defined around the imaged leg using a threshold derived from a histogram of the image signal intensities. Finally, a mask defining the muscle was obtained with a fat fraction threshold of 50% (Figure 3-9). Muscle masks were only defined between slices 5 to 35 of the 40-slice volume to avoid errors due to signal drop-off at the outer extremities of the receiver coil. The volume was defined as the number of voxels in the muscle mask multiplied by the voxel size, multiplied by the slice width.

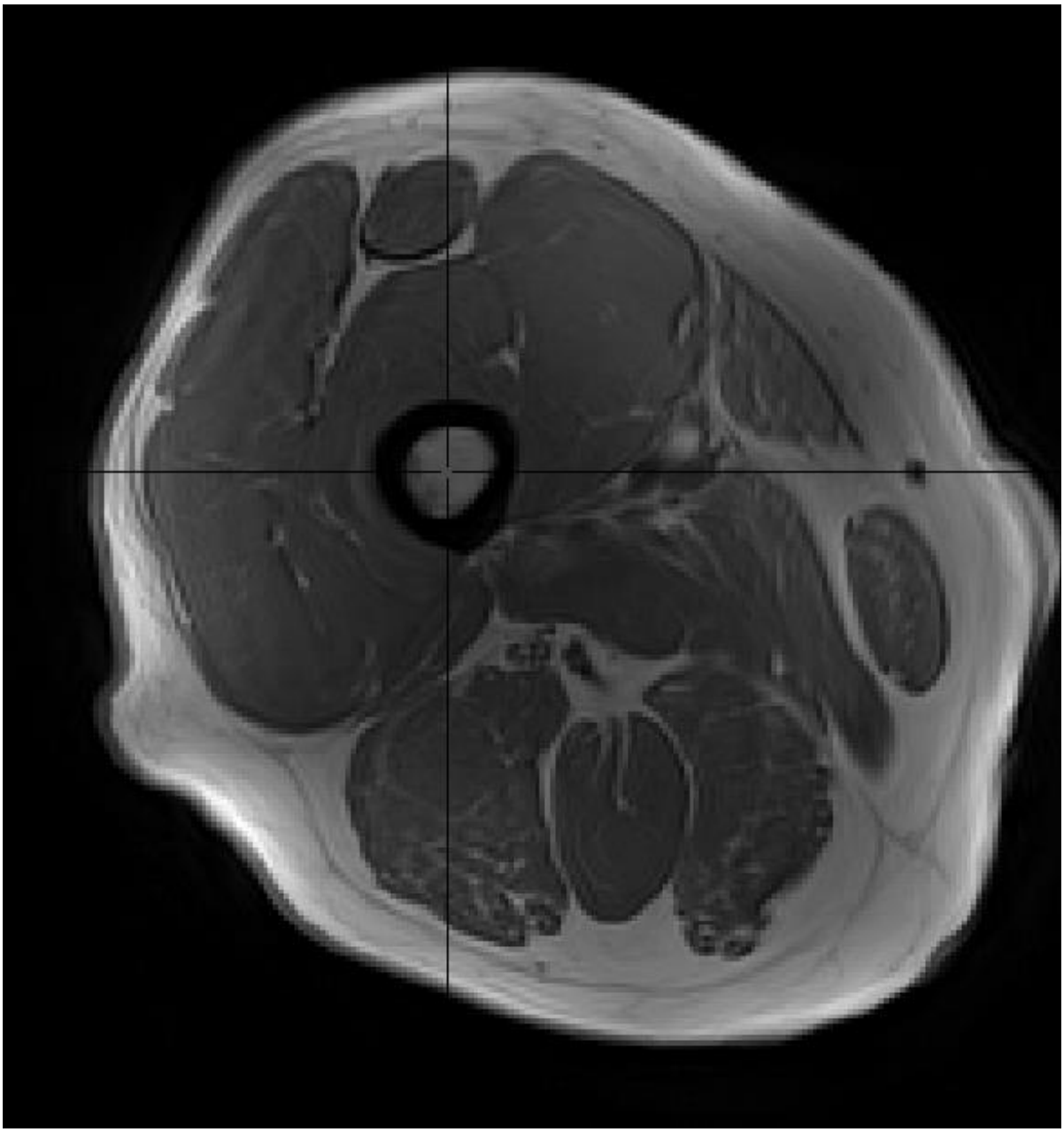

Figure 3-8: Seed point for bone

A seed point was placed in the bone on MatLab in order to generate muscle volume data.

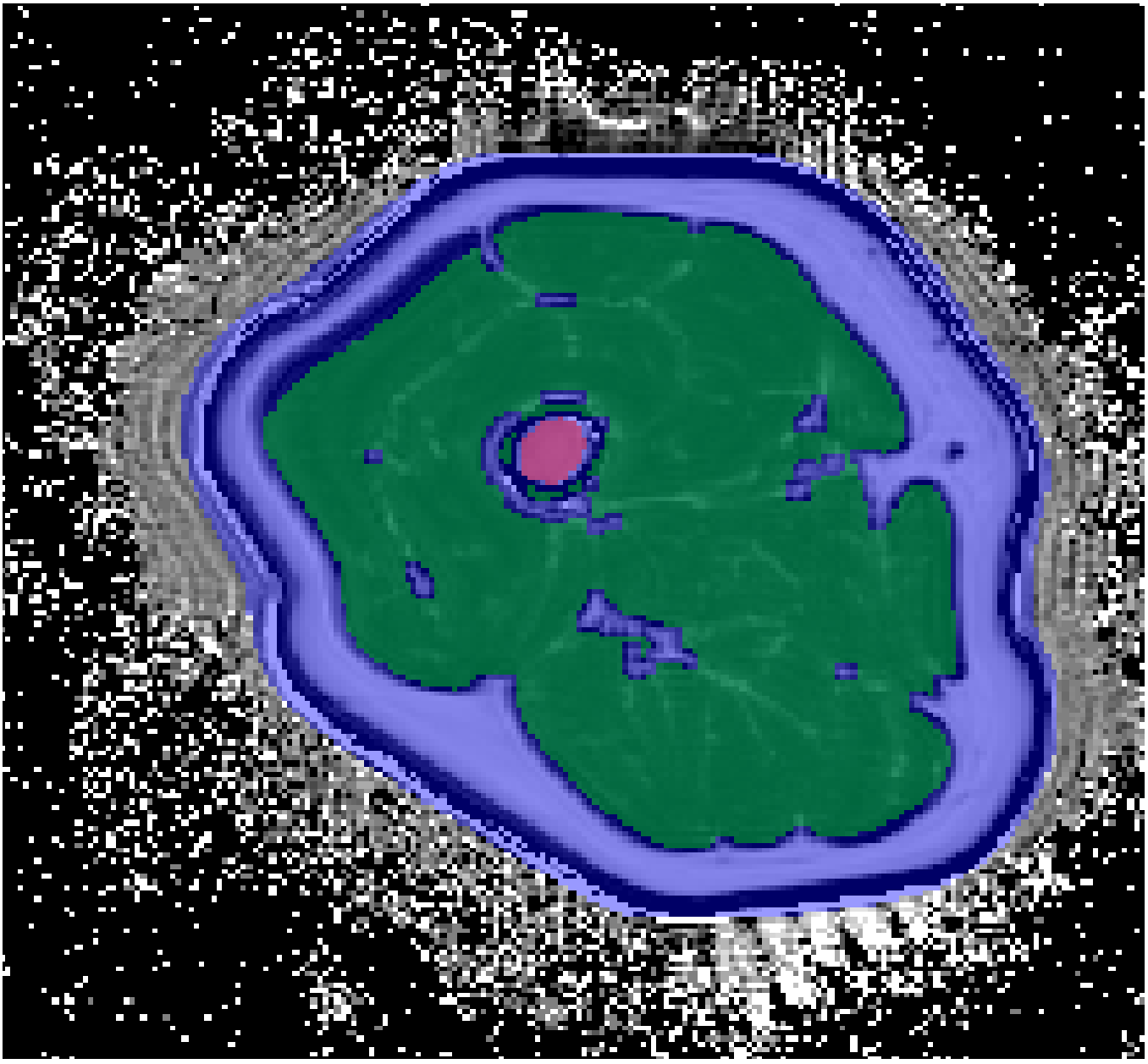

Figure 3-9: Muscle volume image

Automatic definition of muscle, fat, and bone on MatLab used in the assessment of muscle volume.
Green = Muscle, Red = bone, Blue = fat

3.6 Muscle strength assessments

3.6.1 Isokinetic knee extension and flexion strength measurements

Isokinetic knee extension and knee flexion assessment of the same thigh that had an MRI scan was performed following the MRI examination using an isokinetic biodex system four muscle testing and rehabilitation isokinetic dynamometer (IPRS Mediquipe Limited, UK) in a room with a controlled temperature of 20°C. Prior to positioning the participant on the machine, the equipment was calibrated as per manufacturer guidelines. After a standardised warm-up, participants were positioned on the machine according to the manufacturer's instructions. The gravitational correction was performed at 180°. Isokinetic knee extension-flexion (concentric-concentric) at 60°/sec was used to collect data. Participants performed three maximum effort repetitions for three sets, separated by a 30-second rest interval. Participants would apply pressure to extend and flex their knee against a pad positioned on the leg superior to the talus (Figure 3-10). The speed of the attachment would not change regardless of the amount of force applied. Standardised verbal stimuli were provided throughout the evaluation.

Figure 3-10: Participant positioning on isokinetic biodex.

Participant consented for picture to be taken for the Leeds BRC and used for research and advertisement purposes.

3.6.2 Handgrip strength measurements

Handgrip strength of the participant's dominant hand was measured using a Jamar plus isometric dynamometer, which was manufacturer calibrated. The handle was positioned in a comfortable position for the participant. Participants had their grip strength measured in their dominant hand for three sets, and the mean value was recorded. The participant would squeeze the handle as hard as they could (Figure 3-11). This measurement was chosen as handgrip strength is a frequently used tool to measure global muscle function and is simple to use. A score of 20% of body weight has been suggested as a threshold for grip strength for the performance of everyday tasks (241).

Figure 3-11: JAMAR handheld dynamometer

Image available under creative commons licence.

3.7 Statistical analyses:

Offline image analysis was performed using MATLAB software (R2018b, Mathworks, Nattick, MA, USA). Statistical analyses were performed using SPSS (IBM SPSS Statistics for Windows, Version 25.0. Armonk, NY: IBM Corp). The sample sizes for each research study met guidelines of between 12 and 30 participants per group for pilot studies (242, 243). In the research studies within this thesis, multiple inferential statistical tests were performed to elucidate the potential value of the quantitative MRI measurements. Different chapters have used different statistical tests, depending on the research question and the data. The statistical tests used in this thesis include: Bland-Altman plots, intraclass correlation coefficients, t-tests, ANOVAs, ROC curves, effect size measurements, and correlations. P-values have been presented in all chapters to identify potential significant differences between groups which would need to be confirmed in future powered research. In addition, descriptive data has been presented and discussed throughout this thesis. The inferential analysis for each research study is described in more detail within their respective chapters.

3.8 Summary

This research recruited rheumatic patients and healthy controls. Healthy controls were age- and gender-matched with rheumatic patients. Rheumatic patients were recruited as research into inflammatory rheumatic diseases has focussed on the joints, and comparatively, little research exists for the muscles, despite rheumatic diseases presenting with potential muscle involvement. In addition to acting as matched controls, healthy participants were recruited to study the effects of ageing on the muscle. All participants underwent MRI scans to obtain quantitative measurements (T2, fat fraction, diffusion tensor imaging, and muscle volume) and muscle function tests (knee extension, knee flexion, and handgrip strength).

Chapter 4 Normal values and reliability of stimulated-echo diffusion tensor imaging and fat fraction measurements in the muscle

This chapter describes a research study by Matthew Farrow, Andrew Grainger, Ai Lyn Tan, Maya Buch, Paul Emery, John Ridgway, Thorsten Feiweier, Steven Tanner, and John Biglands published in the British Journal of Radiology, 2019 (2).

4.1 Introduction

In the clinical management of patients with muscle pathology, quantitative MRI could be utilised to assess muscle health. The integration of quantitative MRI measurements clinically could improve the management of patients because accurate measurements with high precision may be beneficial in providing high-quality care by providing a more accurate assessment of muscle health. The research described in this chapter aimed to identify normal values and investigate the reliability of quantitative MRI parameters by assessing two measurements: fat fraction and diffusion tensor imaging (mean diffusivity and fractional anisotropy). Fat fraction (FF) was chosen because myosteatosis is regarded as a measure of muscle quality, and two-point Dixon is a widely available technique for measuring fat fraction. Diffusion tensor imaging (DTI) measurements, which is a relatively new technique in muscle, was chosen within this thesis as it might be able to identify changes at the microstructural level. It has been shown to be sensitive to muscle changes due to diabetes mellitus (244), muscle injury (245, 246), and exercise (247-249). Furthermore, no previous study has assessed the reliability of diffusion tensor imaging in muscle using a stimulated echo acquisition mode (STEAM) diffusion sequence.

The majority of previous studies investigating DTI in muscle have used spin-echo (SE) diffusion sequences. There are advantages in using a STEAM approach compared to SE within the muscle. The STEAM preparation stores transverse magnetisation along the longitudinal axis before recovering it after a long mixing time (TM). During the long mixing time, signal decay is governed by T1. A long mixing time allows for a long diffusion time, which may be necessary to ensure sensitivity to restricted diffusion in the muscle as the diameter of muscle fibres is relatively large (~50 μm) (198). Fat is suppressed during the mixing time due to the short T1 of fat, including the olefinic fat peak, whose resonant frequency is close to that of water and is usually not suppressed by chemical-shift-selective fat suppression techniques (250). This is because, in a STEAM sequence, the signal is in the longitudinal direction during the diffusion time. As fat has a shorter T1 than that of water, the use of STEAM with a long diffusion time suppresses fat signal in the final image. This additional fat suppression is particularly crucial in diffusion imaging in muscle, where the fat signal can potentially confound quantitative measurements (163, 251).

4.1.1 Normal values

In order to appreciate changes in muscle due to disease processes, it is crucial to understand what constitutes typical values in people without disease. Furthermore, it is essential to identify whether different muscle groups have different values, potentially due to different lipid levels or microstructural differences between muscles (25, 252, 253), so that these can be accounted for when studying changes due to disease. These differences are essential to consider, because if different muscles have different quantitative MRI values; they should be separated into muscle groups (hamstrings and quadriceps) and not combined (thigh) when investigating disease processes so that the differences between normal muscles do not confound observed differences due to disease.

4.1.2 Reliability

A variety of factors can lead to variations in quantitative imaging measurements, including patient positioning, segmenting of regions of interest, variations in B_0 and B_1 fields, changes in scanning parameters, and post-processing filters. Such errors may confound studies into the effect of disease on the muscle; therefore, it is vital to assess measurement reliability. There have been previous studies into the reliability of quantitative MRI measurements in the muscle, but the existing literature is based on small study sizes for both fat fraction (254-256) and diffusion measurements (254, 257, 258). Furthermore, all previous diffusion reliability studies have utilised a spin-echo sequence, and the reliability of STEAM diffusion sequences is yet to be measured.

4.1.3 Hypothesis

The hypothesis of this study was that diffusion tensor imaging and fat fraction have different values between the hamstrings (semitendinosus, semimembranosus, and biceps femoris) and the quadriceps (rectus femoris, vastus lateralis, vastus medialis, and vastus intermedius) and that they have excellent test-retest, inter-observer, and intra-observer reliability.

4.1.4 Objectives

To assess differences in normal values between the muscles of the hamstrings and quadriceps in the thigh and to measure the reliability of fat fraction, mean diffusivity, and fractional anisotropy in healthy muscle.

4.2 Methods

4.2.1 Participants

This prospective study was conducted at the Leeds Teaching Hospitals Trust between January 2015 and January 2017. Thirty healthy volunteers gave written, informed consent to take part in the study. Out of the 30 participants, 19 agreed to return for a second scan on the same day to assess test-retest reliability, with a randomly selected proportion also undergoing MR spectroscopy (MRS).

4.2.2 MRI protocol

MRI data were acquired using a MAGNETOM Verio 3T MRI scanner, as described in section 3.5.1. Fat quantitation was performed using a 40-slice, volume interpolated breath-hold examination (VIBE), two-point Dixon sequence. Two-point VIBE Dixon was selected because of its wide availability and well documented recent use in the muscle (115, 178, 230-232, 259-261). Diffusion tensor images were acquired using a STEAM prototype sequence, with an echo-planar imaging (EPI) readout (229) and SPAIR fat suppression. All participants had one scan (scan one), and 19 participants returned for a second scan (scan two). The participants who completed both scans left the scanner room for thirty-minutes between scans for a rest. Participants did not undertake any activity in the 24 hours prior to the research visit or during the 30-minute interval to avoid exercise-induced physiological muscle changes. The four slices of the diffusion acquisition were aligned with the central four slices of the VIBE Dixon volume (slices 19-22 of 40).

4.2.3 Spectroscopy analysis

To validate the Dixon fat fraction measurements, a 10×10×10mm^3 single-voxel MR spectra were acquired on a subset of the recruited population (n=12). The voxel was positioned in the vastus lateralis avoiding regions of the vasculature or fascial fat. The acquisition employed a STEAM sequence with TR: 4,000 ms, TE: 20ms, 30ms, 40ms, 50ms 70ms, 1024 data points, bandwidth: 1500Hz and 24 averages.

To obtain fat fraction measurements from the spectroscopy data, the acquired free-induction-decays were zero-filled (times 2) and line-broadened using a Gaussian filter. After Fourier transformation, the resulting spectra were baseline- and phase-corrected. The areas under the fat and water spectral peaks were measured by integrating between the 0.5 to 3.5ppm range for lipid and 3.6 to 5.8ppm range for water. To correct for differences in MRI T2 relaxation times between water and fat, water T2 values were determined using the area under the water peak from spectra acquired with echo times of 20, 30, 40, 50, and 70ms and a mono-exponential fit was used to derive T2. Analogous T2 measurements for fat were unreliable because the fat peaks were too small. Therefore, an assumed T2 for lipids of 59.1ms was used (262). Finally, the fat fraction was determined from the area under the peak values from the fat and water signals in the echo time = 20ms spectrum, corrected for T2 effects. Spectroscopy based fat fraction measurements were compared against the imaging fat fraction measurements taken from the vastus lateralis.

4.2.4 MRI measurements

Fat and water images were generated from the in-phase and out-of-phase images using the scanner vendor's software. Differences in T1 between fat and water were corrected for using assumed values for water (T1w=1,420ms) and fat (T1f=371ms) (235) as described by Liu et al. (234). The fat fraction was then calculated from the adjusted fat (Sf) and water (Sw) signals as follows: $fat\ fraction = \frac{Sf}{Sf+Sw}\ x\ 100\%$. Diffusion images were converted to mean diffusivity (MD), fractional anisotropy (FA), and diffusion eigenvalue (λ1, λ2, λ3) maps using the scanner vendor's software.

4.2.5 Regions of interest

Regions of interest were contoured by two researchers (Andrew Grainger with 20 years of experience; Matthew Farrow with one year of experience), including repeated measurements, using OsiriX imaging software (v. 4.0; open-source DICOM viewer, www.osirix-viewer.com). Regions depicting the individual hamstring muscles (semitendinosus, semimembranosus, biceps femoris) and quadriceps muscles (rectus femoris, vastus lateralis, vastus medialis, and vastus intermedius) were drawn on the middle slice (slice 20) of the in-phase VIBE Dixon volume for each participant, avoiding fascial tissue and subcutaneous fat (Figure 4-1). The medial compartment of the thigh was not included as individual muscles in this compartment can be challenging to discriminate.

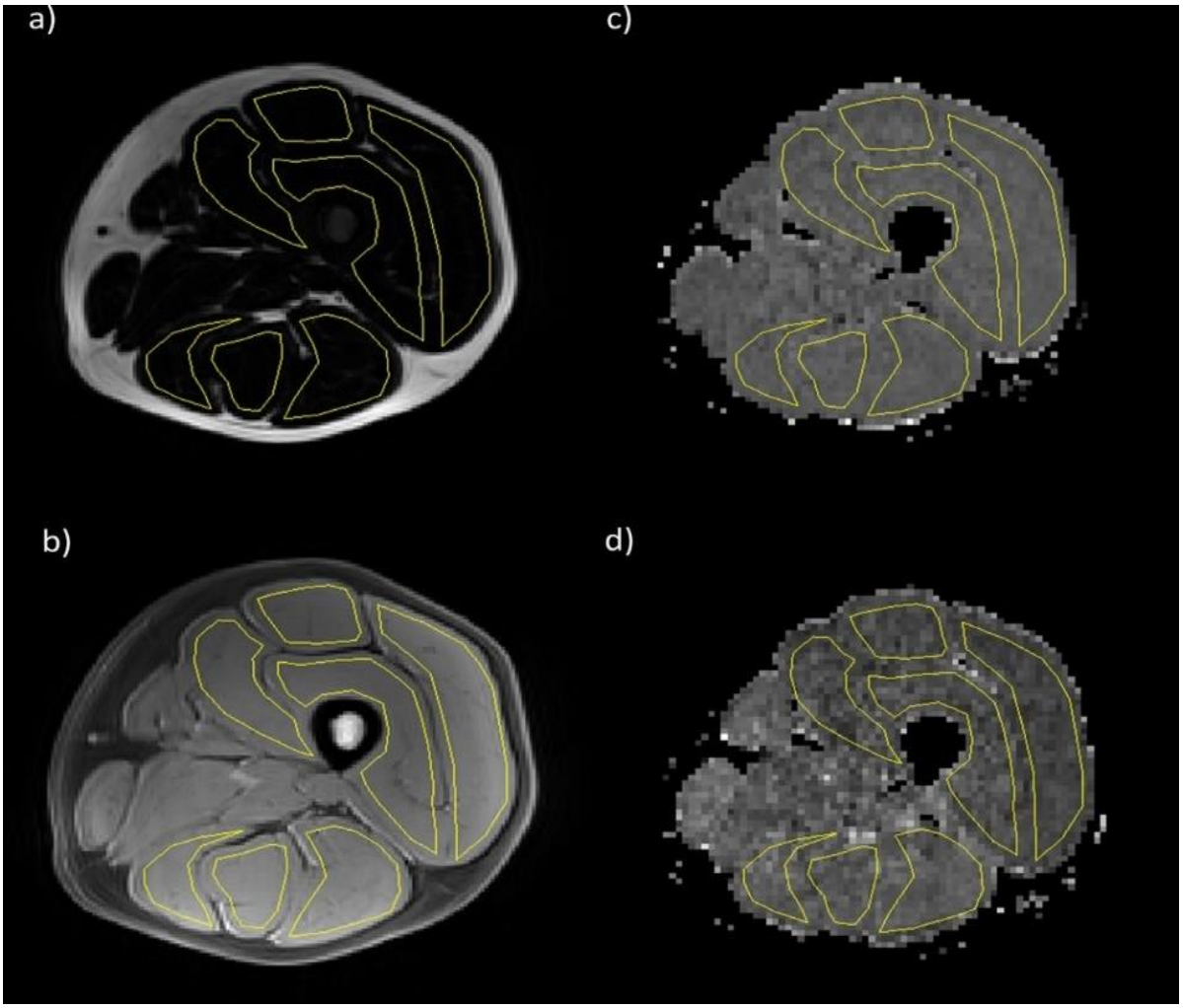

Figure 4-1: Regions of interest in VIBE Dixon and STEAM diffusion maps

Example images from a single healthy volunteer showing VIBE Dixon (a) fat and (b) water images and STEAM diffusion maps (c) MD and (d) FA. Regions of interest (shown in yellow) were drawn corresponding to the individual muscles of the hamstrings and quadriceps.

4.2.6 Reliability

To assess test-retest reliability, scan one and scan two MRI data sets were contoured by the same researcher. To assess inter-rater reliability, two researchers contoured the scan one MRI data sets separately, blinded to each other's regions of interest. To assess intra-rater reliability, the same researcher contoured the scan one MRI data sets, with a 6-month interval between contours. All regions of interest were copied to the corresponding diffusion parameter maps, accounting for differences in image resolution, and the mean value within each region of interest was taken.

4.2.7 Statistical analysis

Statistical analyses were performed using SPSS. Intraclass correlation coefficients (ICC) and Bland–Altman plots were generated in MedCalc (MedCalc Software, Ostend, Belgium; http://www.medcalc.org; 2017). Analysis of variance (ANOVA) was used to evaluate potential significant differences between individual muscles. A Greenhouse–Geisser correction was used in cases where sphericity was violated, and the Bonferroni correction was used in post-hoc analyses. The agreement was measured using Bland–Altman plots. Reliability was assessed using the intraclass correlation coefficient (ICC) using a two-way mixed model with absolute agreement. ICC values above 0.60 were classed as 'good' and values above 0.75 were classed as 'excellent' for reliability between the two measurements (263). All data are presented as: mean (95% confidence interval; p-value) unless stated otherwise.

4.3 Results

4.3.1 Participants

Thirty healthy volunteers were recruited, (mean age 36.5 years, range 20–60 years, 17/30 males). Imaging data from one healthy volunteer was excluded due to misalignment between the fat and diffusion images at acquisition, resulting in a movement artefact. The remaining 29 healthy volunteers had a mean age of 37 years, range 20–60 years, 17/29 males. Nineteen participants (11/19 males) returned for a second scan to assess test-retest reliability. The semimembranosus muscle was not visible on the relevant slice in three participants, so this muscle did not contribute to the hamstring measurement in those participants.

4.3.2 Spectroscopy

The Bland–Altman plot (Figure 4-2) showed that imaging underestimated fat fraction relative to spectroscopy with a mean absolute bias of −0.91% (95% CI= -4.4 to 2.6).

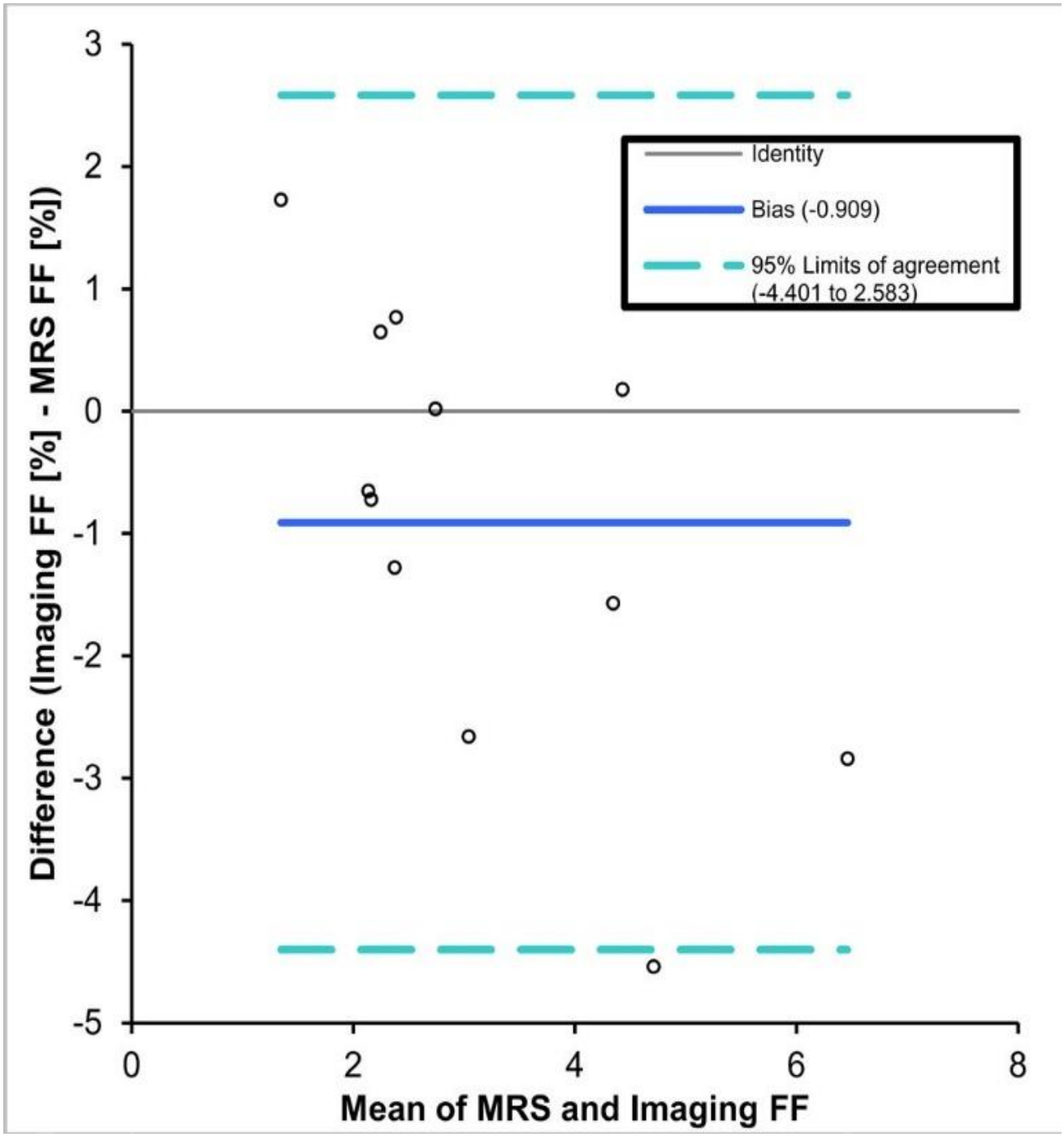

Figure 4-2: MRS and Dixon comparison

Bland-Altman agreement plot showing the comparison of fat fraction values measured by spectroscopic and Dixon imaging techniques. N=12

4.3.3 Differences between muscles

Mean values for fat fraction and diffusion parameters for each muscle are shown in Table 4-1. Boxplots for the hamstrings and quadriceps are shown in Figure 4-3. Fat fraction in the hamstrings was approximately twice that in the quadriceps with a mean difference in fat fraction between the two muscle groups of 1.81% (95% CI= 1.63, 2.00; p< 0.001). Mean diffusivity was lower in the hamstrings than in the quadriceps with a mean difference of $0.26x10^{-3}mm^2s^{-1}$ (95% CI= 0.13, 0.39; p< 0.001). Fractional anisotropy was higher in the hamstrings than the quadriceps with a mean difference of 0.063 (95% CI= 0.05, 0.07; p< 0.001). The diffusion eigenvalues showed that λ1 was higher with a mean difference of $0.076x10^{-3}mm^2s^{-1}$ (95% CI= 0.059, 0.092; p< 0.001), and λ2, and λ3 were lower in the hamstrings relative to the quadriceps with a mean difference of $0.083x10^{-3}mm^2s^{-1}$ (95% CI= 0.064, 1.03; p< 0.001) and $0.068x10^{-3}mm^2s^{-1}$ (95% CI= 0.051, 0.085; p< 0.001), respectively.

Boxplots for the individual muscles measured are shown in Figure 4-4. There were substantive differences in fat fraction, fractional anisotropy, and mean diffusivity between muscles (ANOVA: p< 0.001). Pairwise post-hoc analysis showed that all substantive differences were explained by the differences between the hamstrings and quadriceps groups. That is, any of the individual muscles that make up the hamstrings had a substantively different fat fraction to any of the muscles that make up the quadriceps. However, they were not substantively different from any other muscles within the hamstrings, and vice-versa.

Table 4-1: Normal values of fat fraction and diffusion

Mean ± standard deviation for individual muscles and muscle groups for fat fraction, mean diffusivity (MD), eigenvalue (λ) and fractional anisotropy (FA) measurements.

Muscle	FF (%)	MD ($x10^{-3}mm^2s^{-1}$)	λ1 ($x10^{-3}mm^2s^{-1}$)	λ2 ($x10^{-3}mm^2s^{-1}$)	λ3 ($x10^{-3}mm^2s^{-1}$)	FA (range 0-1)
Semimembranosus	4.02±1.67	1.30±0.06	1.91±0.10	1.09±0.07	0.90±0.07	0.39±0.04
Semitendinosus	4.34±2.26	1.25±0.05	1.92±0.06	1.02±0.08	0.82±0.08	0.44±0.05
Biceps femoris	4.17±1.63	1.29±0.04	1.87±0.06	1.08±0.06	0.91±0.06	0.38±0.04
Hamstrings (Mean of three muscles above)	**4.21±1.85**	**1.28±0.05**	**1.90±0.05**	**1.06±0.06**	**0.87±0.06**	**0.41±0.04**
Vastus medialis	2.07±0.53	1.35±0.06	1.87±0.07	1.22±0.07	0.96±0.05	0.34±0.03
Vastus intermedius	2.43±0.47	1.33±0.06	1.86±0.06	1.17±0.09	0.96±0.07	0.35±0.04
Vastus lateralis	2.53±0.61	1.30±0.06	1.80±0.07	1.12±0.09	0.97±0.07	0.33±0.04
Rectus femoris	1.80±0.66	1.26±0.05	1.77±0.07	1.09±0.06	0.90±0.07	0.35±0.04
Quadriceps (Mean of four muscles above)	**2.21±0.48**	**1.31±0.05**	**1.83±0.07**	**1.15±0.08**	**0.95±0.06**	**0.34±0.03**

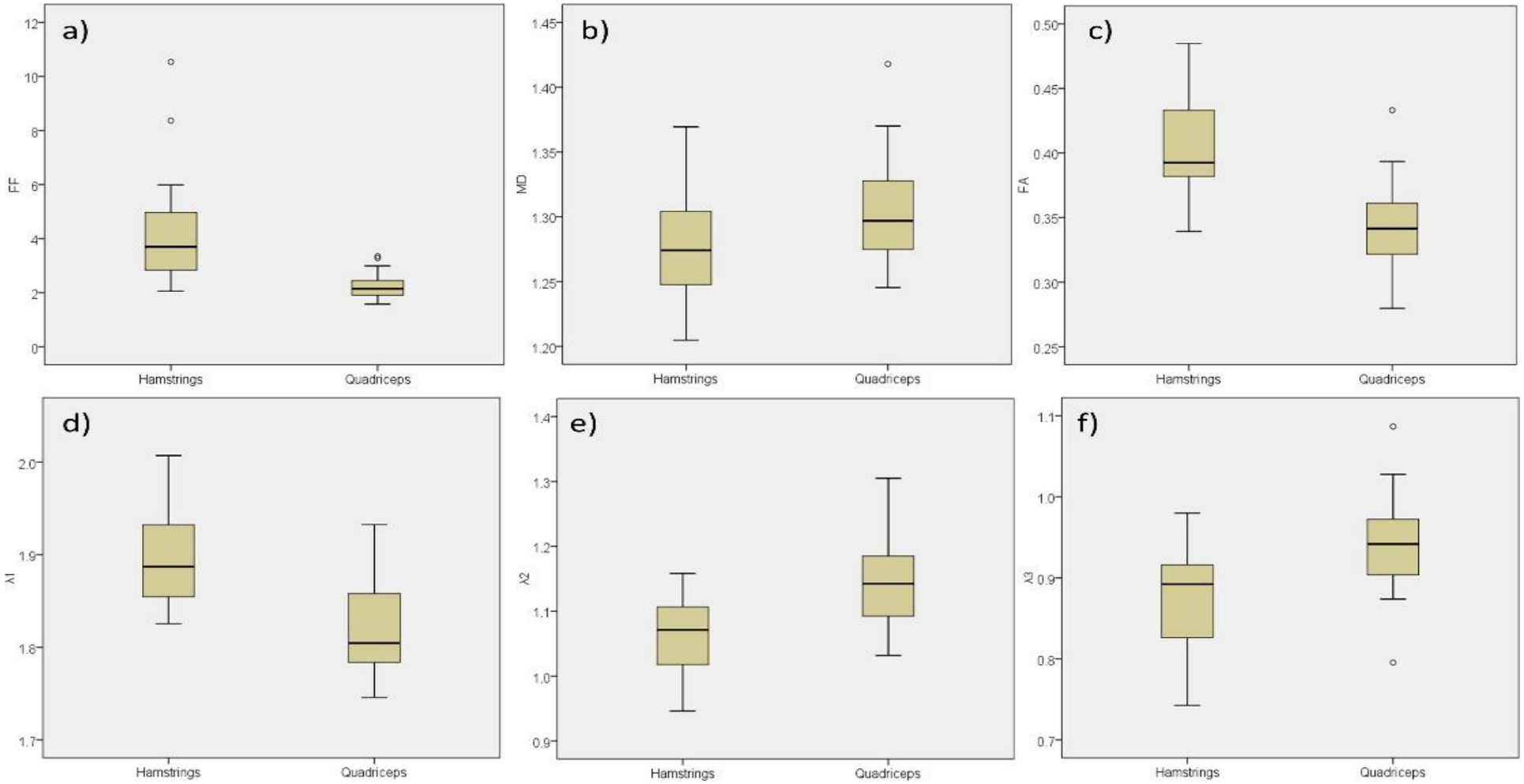

Figure 4-3: Differences in fat fraction and diffusion measurements between hamstrings and quadriceps

(a) Fat fraction [%], (b) Mean diffusivity [x10^{-3}mm^{2}s^{-1}], (c) Fractional anisotropy, (d) λ1 [x10^{-3}mm^{2}s^{-1}], (e) λ2 [x10^{-3}mm^{2}s^{-1}], (f) λ3 [x10^{-3}mm^{2}s^{-1}].

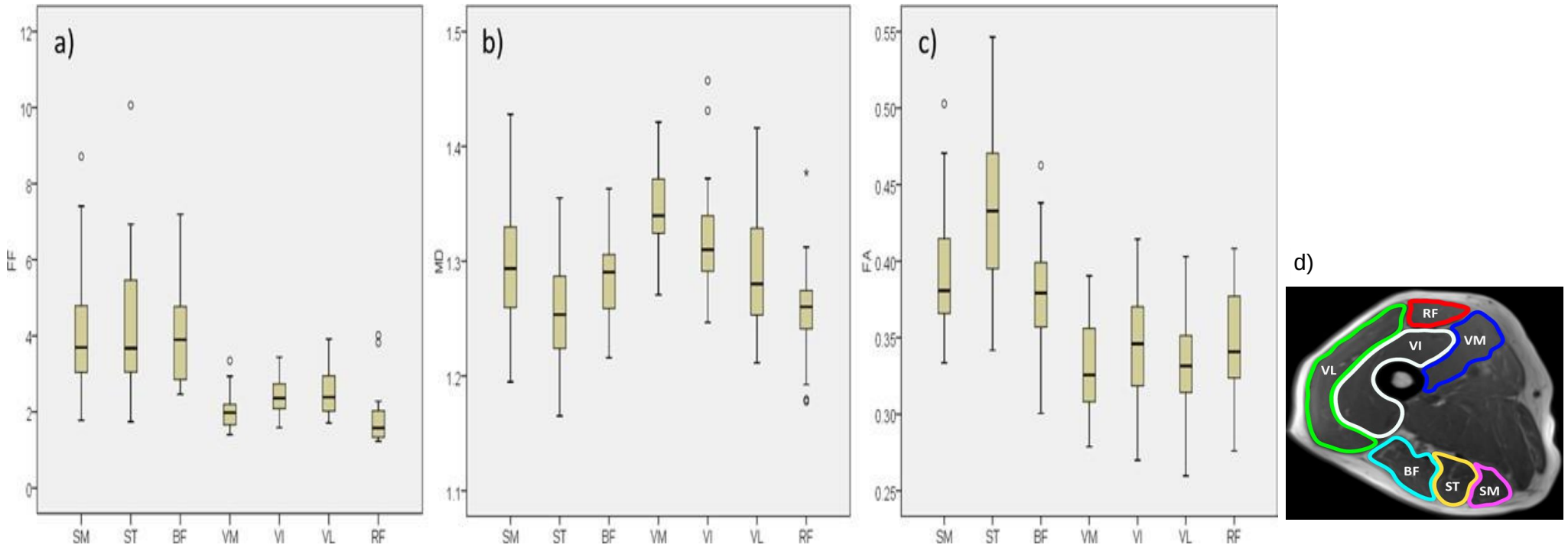

Figure 4-4: Distribution of values for individual muscles

Boxplots showing distribution of values for each individual muscle for (a) Fat fraction [%], (b) Mean diffusivity [x10^{-3}mm^{2}s^{-1}], (c) Fractional anisotropy, for the RF, rectus femoris; SM, semimembranosus, ST, semitendinosus; BF, biceps femoris; VM, vastus medialis; VI, vastus intermedius and VL, vastus lateralis. d) Axial image of muscles of thigh.

4.3.4 Reliability

Figure 4-5 depicts the test-retest Bland–Altman agreement plots with excellent reliability between scans with the same region of interest drawer: Fat fraction ICCs of 0.99 (range= 0.98, 1), mean bias= 0.07% (95% CI= -0.24, 0.38), p< 0.05. Mean diffusivity ICCs of 0.94 (range= 0.84, 0.97), mean bias= $0.02x10^{-3}mm^2s^{-1}$ (95% CI= -0.023, 0.026), p< 0.05. Fractional anisotropy ICCs of 0.89 (range= 0.74, 0.96), mean bias= 0.02 (95% CI= -0.020, 0.025) p< 0.05.

Figure 4-6 depicts the inter-rater Bland–Altman agreement plots with excellent reliability between two different region of interest drawers: Fat fraction ICCs of 0.97 (range= 0.93, 0.99), mean bias= −0.09% (95% CI= -0.60, 0.42), p< 0.05. Mean diffusivity ICCs of 0.99 (range= 0.97, 1), mean bias= $-0.013x10^{-3}mm^2s^{-1}$ (95% CI= -0.017, 0.009), p< 0.05. Fractional anisotropy ICCs of 0.99 (range= 0.98, 1), mean bias= −0.001 (95% CI= -0.010, 0.007), p< 0.05.

Figure 4-7 depicts the intra-rater Bland–Altman agreement plots with excellent reliability between the same researcher who drew the regions of interest twice with a 6-month interval between drawing: Fat fraction ICCs of 0.99 (range= 0.96, 1), mean bias= 0.10% (95% CI= -0.17, 0.36), p< 0.05. Mean diffusivity ICCs of 0.93 (range= 0.85, 0.97), mean bias= $-0.003x10^{-3}mm^2s^{-1}$ (95% CI= -0.035, 0.029), p< 0.05. Fractional anisotropy with ICCs of 0.99 (range= 0.97, 0.99), mean bias= −0.001 (95% CI= -0.012, 0.009), p< 0.05.

Table 4-2: Reliability of ICC values for hamstrings, quadriceps, and combined measures

ICC (ranges) for hamstrings, quadriceps and thigh. Thigh consists of hamstrings and quadriceps combined. Mean bias describes the mean difference (and range) between 95% confidence intervals.

Test-retest	FF	MD	FA	λ1	λ2	λ3
Hamstrings ICC (range)	0.99 (0.96, 1)	0.92 (0.8, 0.97)	0.84 (0.63, 0.94)	0.72 (0.39, 0.89)	0.93 (0.83, 0.97)	0.85 (0.64, 0.94)
Quadriceps ICC (range)	0.98 (0.94, 0.99)	0.88 (0.70, 0.95)	0.73 (0.40, 0.89)	0.73 (0.40, 0.89)	0.94 (0.84, 0.98)	0.85 (0.64, 0.94)
Thigh (both) ICC (range)	**0.99 (0.98, 1)**	**0.94 (0.84, 0.97)**	**0.89 (0.74, 0.96)**	**0.85 (0.64, 0.94)**	**0.96 (0.89, 0.98)**	**0.88 (0.71, 0.95)**
Mean bias (Mean difference and range between 95% CI for thigh)	0.07 (-0.24, 0.38)	0.02 (-0.023, 0.026)	0.02 (-0.02, 0.025)	0.007 (-0.03, 0.04)	0.00 (-0.003, 0.03)	-0.02 (-0.04, 0.04)
Inter-rater						
Hamstrings ICC (range)	0.96 (0.91, 0.99)	0.96 (0.90, 0.98)	0.98 (0.96, 1)	0.90 (0.76, 0.96)	0.99 (0.97, 1)	1 (0.98, 1)
Quadriceps ICC (range)	0.99 (0.98, 1)	1 (0.99, 1)	0.99 (0.98, 1)	1 (0.99, 1)	1 (0.99, 1)	0.98 (0.96, 0.99)
Thigh (both) ICC (range)	**0.97 (0.93, 0.99)**	**0.99 (0.97, 1)**	**0.99 (0.98, 1)**	**0.98 (0.95, 0.99)**	**1 (0.99, 1)**	**0.99 (0.98, 1)**
Mean bias	-0.09	-0.013	-0.001	-0.005	-0.001	0.00

(Mean difference and range between 95% CI for thigh)	(-0.60, 0.42)	(-0.010, 0.007)	(-0.010, 0.007)	(-0.03, 0.02)	(-0.01, 0.01)	(-0.01, 0.01)
Intra-rater						
Hamstrings ICC (range)	0.99 (0.94, 1)	0.94 (0.84, 0.98)	0.99 (0.98, 1)	0.90 (0.76, 0.96)	0.98 (0.95, 0.99)	0.98 (0.95, 0.99)
Quadriceps ICC (range)	0.99 (0.98, 1)	0.88 (0.72, 0.96)	0.96 (0.90, 0.98)	0.90 (0.76, 0.96)	0.96 (0.90, 0.98)	0.98 (0.95, 0.99)
Thigh (both) ICC (range)	**0.99 (0.96, 1)**	**0.93 (0.85, 0.97)**	**0.99 (0.97, 0.99)**	**0.64 (0.29, 0.84)**	**0.98 (0.96, 0.99)**	**0.99 (0.98, 1)**
Mean bias (Mean difference and range between 95% CI for thigh)	0.10 (-0.17, 0.36)	-0.003 (-0.035, 0.029)	-0.001 (-0.012, 0.009)	0.01 (-0.16, 0.18)	-0.001 (-0.02, 0.02)	-0.001 (-0.01, 0.01)

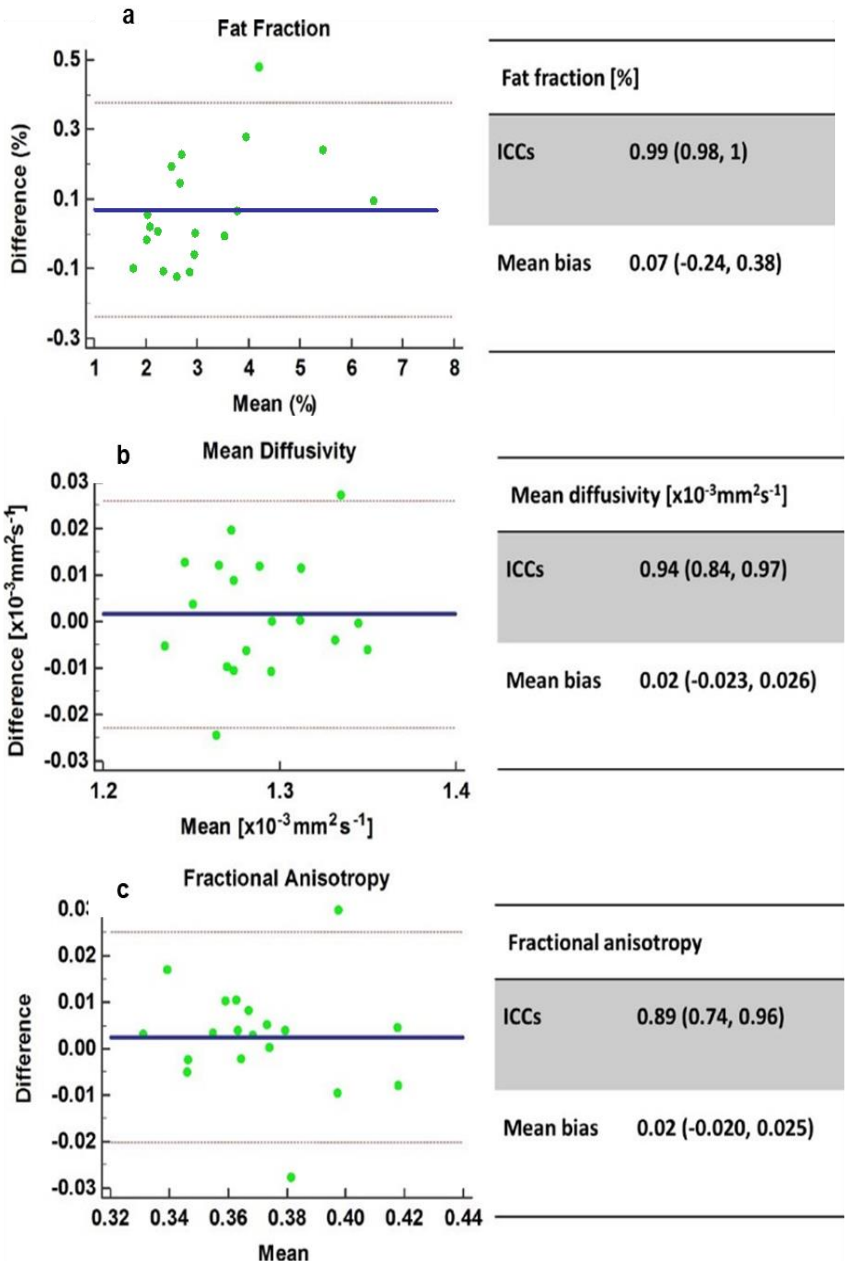

Figure 4-5: Test retest reliability of thigh

Thigh (hamstrings and quadriceps) test–retest reliability Bland–Altman agreement plots for a) fat fraction, b) mean diffusivity, and c) fractional anisotropy. N=19.

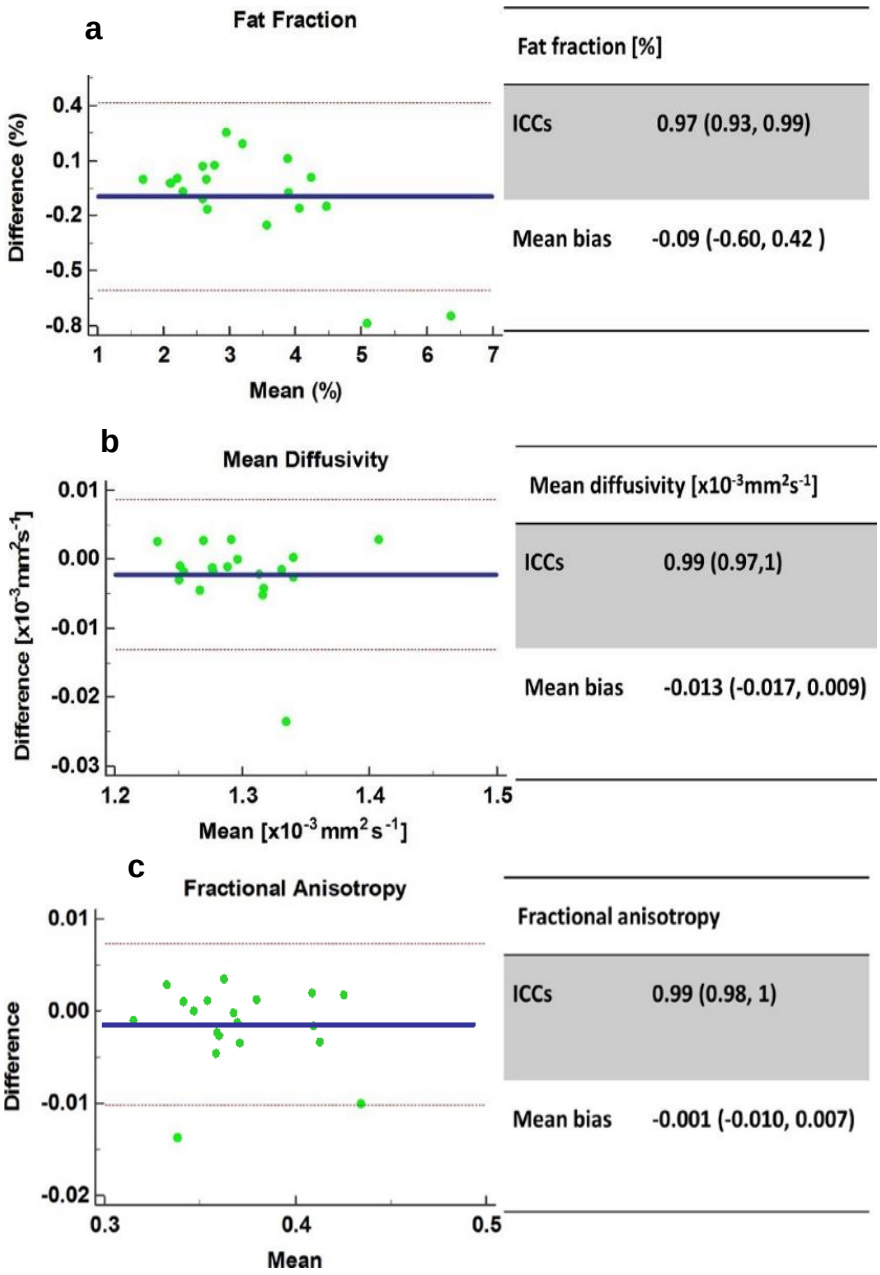

Figure 4-6: Inter-rater reliability of thigh

Thigh (hamstrings and quadriceps) inter-rater reliability Bland–Altman agreement plots for a) fat fraction, b) mean diffusivity, and c) fractional anisotropy. N=19.

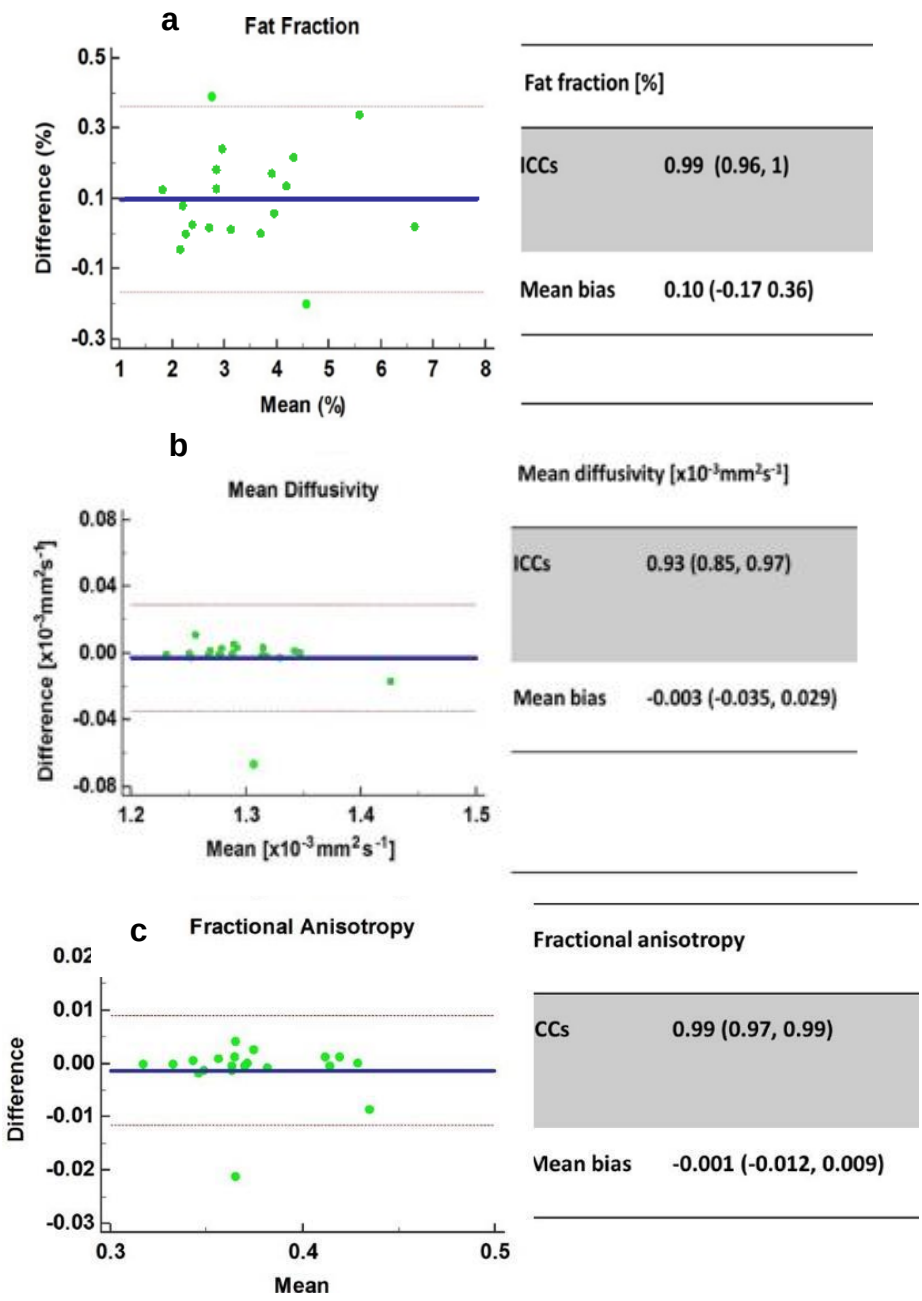

Figure 4-7: Intra-rater reliability of thigh

Thigh (hamstrings and quadriceps) intra-rater reliability Bland–Altman agreement plots for a) fat fraction, b) mean diffusivity, and c) fractional anisotropy. N=19.

4.4 Discussion

This chapter aimed to identify the differences in normal values between muscles in the thigh and to assess the reliability of fat fraction and diffusion measurements in healthy muscle. This study successfully met its aims and demonstrated that the hamstrings and quadriceps present with substantively different fat fraction and diffusion measurements, and that there is high reliability for test-retest, intra-rater, and inter-rater contouring of regions of interest.

4.4.1 Spectroscopy

Imaging slightly underestimated fat fraction with a mean bias of 0.9% absolute fat fraction, which was likely to be due to noise bias and the use of only a single spectral peak when quantifying the fat (168, 260, 264). There was good agreement between measured fat fraction values obtained using imaging and spectroscopy, which has been observed previously (178, 262). This outcome suggests that the fat fraction measurements used within this study are valid.

4.4.2 Differences between muscle groups

The study shows substantive differences in fat fraction and diffusion tensor imaging measurements between the hamstrings and quadriceps muscles. Mean values agreed well with previous studies using similar techniques to measure fat fraction (178, 259) and diffusion tensor imaging values (265).

The data in this study showed that, in healthy volunteers, the fat fraction was higher in the hamstrings relative to the quadriceps, which is consistent with previous research (266). This higher fat fraction could be because the hamstrings have a greater number of Type I (slow-twitch) muscle fibres (252), which have a higher lipid content than Type II (fast-twitch) muscle fibres (267). This study has also shown substantive differences in measured diffusion parameters between the hamstrings and quadriceps. The differences in diffusion parameters observed here are consistent with previous studies (254). The higher mean diffusivity in the quadriceps could be due to greater relative hydration (extracellular water) in these muscles (268), whilst differences in fractional anisotropy could be due to differences in the uniformity of fibre tracks (269). Alternatively, anatomical studies report a higher density of Type I fibres in the hamstrings than the quadriceps (252). Therefore, the reduced λ2 and λ3, and increased fractional anisotropy values that this study observed in the hamstrings could reflect the denser microstructure in type I fibres (25).

The presence of fat is known to decrease mean diffusivity measurements. However, this is unlikely to be the reason that this study observed reduced mean diffusivity in the hamstrings as the fat fraction required to induce inaccuracies in diffusion measurements are estimated to be around 24% (251) whilst the muscle fat fraction in this study were below this (<10%). Furthermore, the use of STEAM sequences with a long mixing time provides additional suppression of the olefinic fat peak.

Clinically, the fact that both fat fraction and diffusion measurements differ between the hamstrings and quadriceps is important. Firstly, it highlights the fact that these measures are sensitive to subtle differences between muscles that are not detectable visually from conventional MR images. These differences may be of interest in studying healthy and diseased muscles. Secondly, researchers using these measures to investigate muscle disease should take these differences into

account in their measurements so that normal differences between muscles do not bias their findings.

4.4.3 Reliability

This study showed excellent reliability for fat fraction and diffusion measurements which compared favourably with previous work (256). For fat fraction, the test-retest reliability within this study was 0.99. However, Figure 4-5 (a) appears to show lower test-retest differences at low-fat fraction values and larger differences at higher fat fraction values in healthy controls. This finding demonstrates a potential systematic error where larger fat fraction measurements have lower test-retest reliability compared to lower fat fraction measurements. Whilst in this study, in healthy controls, the test-retest difference in fat fraction was below 0.4%, the decrease in reliability as fat fraction increases may be problematic in patients with muscle disease who could present with increased fat infiltration. This result could be due to the two-point Dixon sequences used in this thesis, which was demonstrated in Figure 4-2 to be less accurate with larger fat fraction values. Future research should investigate whether patients with increased fat infiltration have lower reliability of fat fraction measures using two-point Dixon and whether more advanced techniques to assess fat fraction have the same systematic error. The test-retest reliability scores for diffusion tensor imaging values within this study were excellent with ICC values of 0.94 & 0.89 for mean diffusivity and fractional anisotropy, respectively. In smaller studies using spin-echo diffusion tensor imaging, Ponrartana et al. reported ICCs of 0.88 for mean diffusivity and 0.75 for fractional anisotropy in the lower leg (270), and Froeling et al. reported ICCs of 0.89 for mean diffusivity and 0.60 for fractional anisotropy in the forearm (258). The superior reliability scores within this study may be due to the shorter interval between visits (30 minutes) compared to 1–2 weeks in previous studies (256, 258). Short-term factors such as exercise are known to affect fat fraction (230) and

diffusion tensor imaging (247, 248), so the increased reliability in these studies better reflect what would be expected in longitudinal studies. However, the choice of a short between scan interval minimises changes due to physiological variations between tests providing a measure of the reliability of the system alone. Researchers undertaking longitudinal studies should expect inferior reliability in the measurements than those presented here due to physiological variation.

Mean biases and confidence intervals for test-retest reliability in this study were small; fat fraction: 0.07% (95% CI= -0.24, 0.38), mean diffusivity: $0.02x10^{-3}mm^2s^{-1}$ (95% CI= −0.023, 0.026), and fractional anisotropy: 0.02 (95% CI= -0.020, 0.025). In addition, inter-rater and intra-rater reliability were also excellent. Demonstrating that the selection of regions of interest by different raters does not influence the results, enhancing the usability of quantitative MRI measurements.

These results suggest that measured differences greater than a fat fraction of 0.4%, mean diffusivity of $0.03x10^{-3}mm^2s^{-1}$, and fractional anisotropy of 0.03 should be detectable above reliability errors. These results are an essential early step in the validation of these measurements in muscle disease as potential biomarkers for assessing muscle disease.

4.4.4 Limitations

This study was subject to a number of limitations. This research did not assess the reliability of MRI T2 and muscle volume used within this thesis, due to those two measurements being included in the thesis following the completion of this study. Future research would need to confirm whether T2 and muscle volume also have excellent reliability. As this study only used healthy controls, it has a limited range of values. The range of values could be increased by repeating studies in

pathological cases. Furthermore, future work should also assess test-retest reliability with a longer duration between the first and second scan, to simulate longitudinal studies. Further research should identify if reliability is compromised in smaller muscles which are harder to identify accurately, such as muscles of the hand, which would be of interest in the study of rheumatic diseases as the joints of the hands are often scanned clinically.

4.5 Conclusion

This study has demonstrated substantive differences between the hamstrings and quadriceps with quantitative MRI measures in the healthy thigh. These results suggest that hamstrings and quadriceps should be considered separately in future studies; however, it is not necessary to separate further into the individual muscles that make up the hamstrings (semitendinosus, semimembranosus, and biceps femoris) and quadriceps (rectus femoris, vastus lateralis, vastus medialis, and vastus intermedius). In addition, this study has shown excellent reliability in MR-based fat fraction and STEAM-based diffusion measurements, suggesting that quantitative MRI measurements have high enough reliability to be of use clinically. However, the results in this study suggest that the reliability of fat fraction may decrease as fat infiltration increases. However, the differences are still small, so it does not significantly detract from the potential advantages of using two-point Dixon MRI to assess fat fraction.

4.6 Key messages

- There are substantive differences in fat fraction and diffusion measurements between the hamstrings and quadriceps in the healthy muscle.
- Test-retest reliability is excellent for two-point Dixon based fat fraction and STEAM-EPI diffusion measurements in healthy muscle, suggesting measurements could be used clinically.
- Inter-rater and intra-rater reliability were excellent for the region of interest placement for two-point Dixon based fat fraction and STEAM-EPI diffusion measurements in the healthy muscle, suggesting the selection of the region of interest is not operator dependent.

Chapter 5 The effects of ageing on skeletal muscle as assessed by quantitative MR imaging: An association with frailty and muscle strength

This chapter describes a research study by Matthew Farrow, John Biglands, Steven Tanner, Andrew Clegg, Lesley Brown, Elizabeth Hensor, Philip O'Connor, Paul Emery, and Ai Lyn Tan published in Aging Clinical and Experimental Research, 2020 (3).

5.1 Introduction

The proportion of older people in the population is increasing, from 461 million individuals above the age of 65 in 2004 to an approximate 2 billion individuals by the year 2050 (271). This increase in age can have a substantial impact on the health of individuals, including decreases in muscle health. This is important to consider as decreased muscle health is a well-known factor of impaired functional status and increased falls (272-278) and can have a significant impact on quality of life. This decrease in muscle health in the older population is often referred to as sarcopenia, as discussed in section 2.3.1.1. The primary area of research in sarcopenia has been the loss of muscle function due to a decrease in muscle mass. It is known that the loss of muscle mass starts between the ages of 30 and 40, and accelerates with age (37, 71, 99, 279-284). This rate of muscle mass atrophy can be up to 2% per year (91, 285, 286). The majority of this muscle atrophy is from the lower limb (37), demonstrating the importance of investigating muscle health within the thigh.

Sarcopenia has rapidly become a common term in geriatrics and academic research. The term sarcopenia is used to describe the progressive decrease in muscle mass, muscle quality, physical function, and muscle strength with

advancing age. Muscle quality, as discussed in section 2.3.1.1, refers to muscle function and, within this thesis, is defined as the microscopic and macroscopic properties of muscle, such as inflammation, myosteatosis, muscle microstructure milieu, and muscle quantity. These variables in muscle quality are independent of each other; however, can occur in unison due to disease or disuse. Muscle quantity, as discussed in section 2.4.3.4, is defined as a measure of the total muscle mass. There are several classification criteria for sarcopenia, with different cut off values and required measurements. Within the literature, the prevalence of sarcopenia in 60-70-year-olds is approximately 13% (287, 288) and increases to 50% for the population aged above 80 (287). However, these figures are dependent on what classification is being used. Historically, the most commonly used classification is the 2010 European Working Group on Sarcopenia in Older People (EWGSOP) (71). The EWGSOP criterion for sarcopenia includes: 1) Low muscle mass; 2) Low physical function (such as gait speed); 3) Low muscle strength (such as grip strength) (Table 2-2). A diagnosis depended on low muscle mass, in addition to either low muscle strength or physical performance. However, the EWGSOP updated its classification of sarcopenia in 2019 (99). This new criterion by the EWGSOP includes: 1) Low muscle strength; 2) Low muscle quantity or quality; 3) Low physical performance (Table 2-3). With the new EWGSOP guidelines, individuals are classified as having probable sarcopenia if they have low muscle strength, definite sarcopenia if they have low muscle strength and low muscle quality or quantity, and severe sarcopenia if all three are met.

Despite it being known that decreased muscle mass is a factor in age-related loss of physical function, muscle mass by itself is a weak predictor of physical performance (272, 275, 285, 289-291). In addition to muscle atrophy, there is also a decrease in muscle quality which has historically not been considered to the same extent as muscle mass (292); however, this appears to be changing with the new 2019 EWGSOP diagnostic criterion.

Possible explanations for decreases in muscle quality due to ageing include: 1) Infiltration of fat into muscle, known as myosteatosis (272); 2) Infiltration of collagen and other non-contractile tissue into the muscle (293); 3) Muscle inflammation; 4) Progressive atrophy and loss of individual muscle fibres (81, 294), including a decrease in the proportion of type II (fast-twitch) muscle fibres (295-301), which is associated with a decrease in physical performance (302). In support of this, imaging studies have found increased amounts of interstitial fat, fluid, and other non-muscle contractile tissue in older individuals compared to young individuals (303, 304).

Therefore, the reduction in muscle mass accounts for an even more significant loss of contractile material than is accounted for using muscle mass alone, with fat infiltration and increased fluid within the muscle, possibly mediated through macrophage released inflammatory cytokines (305, 306). In addition, ageing is associated with increased levels of circulating inflammatory components, including an elevated concentration of cytokines (307). These proinflammatory cytokines promote muscle wasting by increasing myofibrillar protein degradation (308) and decreasing protein synthesis (309). It is known that increased fat within the muscle (myosteatosis), which is known to occur with ageing, participates in metabolic regulation, releasing protein factors termed adipokines. Several adipokines are linked to the inflammatory response, resulting in those with high quantities of fat having a higher quantity of cytokines that can cause catabolic consequences on muscle, including muscle oedema. Therefore, fat fraction and T2 within the muscle may be suitable measures for monitoring this infiltration of fat and fluid.

In addition to a reduction in the total number of muscle fibres due to ageing, older individuals often live a more sedentary lifestyle which results in muscle atrophy due to disuse. This disuse atrophy presents with a decrease in muscle fibre size but not a decrease in the total number of muscle fibres (310). Therefore, diffusion measurements may be suitable for identifying these changes in muscle fibres.

This decline in muscle quality is essential to consider as muscle mass and physical function do not decline in a parallel manner (282, 311). A longitudinal study of 1,880 older participants showed that muscle power declined with age at 4% a year whilst muscle mass declined at 1% (285). Furthermore, there is also a substantial difference in decline between power (work done per unit of time) and strength (maximal force) (71). In a study of 100 older participants, muscle power was found to decline with age at 4% per year whilst muscle strength was found to decline at 2% per year (311). This prior research suggests that peak strength, while affected by age, does not deteriorate as quickly as muscle power which is required to complete tasks such as walking. Therefore, the measurement of muscle power is of more importance in the study of sarcopenia than the more frequently used measurement of muscle strength.

Opposing views have suggested that ‘dynapenia’ (loss of muscle strength) and ‘sarcopenia’ (loss of muscle mass) should not be used interchangeably, and instead propose that sarcopenia and dynapenia should be used to describe the age-related loss of muscle mass and muscle strength separately (310). However, as sarcopenia includes loss of muscle mass, decrease in muscle quality, loss of muscle strength, and impaired physical function (292), for this thesis, the term ‘sarcopenia’ will be used to encompass all aspects of a decrease in muscle health as a result of ageing.

Frailty is gaining increasing prominence as a critical healthcare policy issue, and there is growing recognition that healthcare systems need to adapt to meet the needs of older people living with the condition of frailty (312). Frailty is defined as the consequence of age-related decline across physiological systems and encompasses physical, psychological, and social aspects. Frailty results in an increased vulnerability to adverse health conditions, such as falls, hospitalisation, and mortality (313). The conditions of sarcopenia and frailty can overlap, with frail people exhibiting decreased muscle mass and muscle strength (314). Up to 50% of individuals older than 85 years are estimated to be frail, and these people have a

significantly increased risk of disability and a lower quality of life (315, 316). Reducing the prevalence or the severity of frailty is likely to have considerable benefits for individuals and society (317). Current models of frailty are primarily based on the phenotype or deficit model of frailty. Whilst these models are robust and useful to identify and grade frailty, they do not consider muscle health as a separate entity. In the search for interventions to reduce frailty, the identification of sub-clinical muscular features using quantitative MRI has the potential to improve clinical interventions based on well-defined quantitative measures that are associated with frailty (99, 318, 319). This could include predicting those at risk of developing frailty and monitoring interventions, such as exercise, to identify the optimum management.

Quantitative MRI measurements show exciting potential in detecting microscopic and macroscopic muscle changes. Quantitative MRI measurements show promising results for assessing skeletal muscles as it provides a more objective measure compared to the visual assessment based on changes of signal intensity with conventional MRI. The quantitative measurements used in this thesis are discussed in section 2.4.3. Diffusion measurements have previously been shown to be sensitive to changes due to age (320), and fat fraction and muscle volume measurements are known to be sensitive to myosteatosis and muscle atrophy, which occurs with ageing. However, there is a lack of literature investigating whether T2 measurements have a role in assessing the effects of ageing on the muscle. Previously, quantitative MRI measurements have not been compared with formal independent measurements of frailty or with muscle power, gait speed, or handgrip strength measurements, resulting in a lack of understanding between quantitative MRI in the muscle with muscle strength, physical function, and frailty.

In order for quantitative MRI measurements to be used clinically as a diagnostic tool to aid in the monitoring of properties associated with frailty and sarcopenia, it must be investigated whether these measurements can accurately identify

differences within the muscle and elucidate whether these pathological features are associated with frailty, gait speed, and muscle function.

5.1.1 Hypothesis

The effects of ageing on the muscles can be detected using quantitative MRI (T2, two-point Dixon fat fraction, diffusion tensor imaging, and muscle volume) between young, middle-aged, and older people.

5.1.2 Objectives

The aim of this study was to investigate whether quantitative MRI techniques (T2, two-point Dixon fat fraction, diffusion tensor imaging, and muscle volume) are sufficiently sensitive to detect differences in muscle properties between young, middle-aged, and older participants and to show how quantitative MRI parameters relate to muscle function and frailty.

5.2 Methods

5.2.1 Study design

This study was conducted using a cross-sectional design and delivered at the Leeds Teaching Hospitals NHS Trust (LTHT). It was approved by the local research ethics committee, and all participants provided written informed consent. Recruitment began in May 2017 and ended in December 2018. 1:1 matching for gender was used. Participants were recruited into three age groups: ‘young’ (18-30 years), ‘middle-aged’ (31-68 years), and ‘older’ (≥69 years). The age classifications for the young and older participant groups were chosen based on the European

MyoAge study (321). Healthy controls were obtained from the pool of healthy controls recruited for the MUSCLE study. The older participants included participants from a longitudinal research cohort [the Community Ageing Research 75+ (CARE-75+) study] (Trial registration number ISRCTN16588124) (322) who also provided the English Longitudinal Study of Ageing (ELSA) frailty index (FI) scores for each of the individuals. The ELSA frailty index scores (0 - 10 = very fit, 11 – 14 = well, 15 – 24 = vulnerable, 25+ = frail) (323) were utilised for the older participants for a sub-study analysis to investigate if there was a correlation between MRI and muscle function measurements with frailty index in older individuals. All participants had an ELSA frailty index score of ≤14 (‘very fit’ or ‘well’) to ensure they were healthy enough to take part in the research study. Osteoarthritis was not an exclusion criterion for the older participants within this study due to its high prevalence in the older population.

As only participants in the older group were scored with the English Longitudinal Study of Ageing (ELSA) frailty index (324), a separate sub-study was conducted to investigate how MRI and muscle function parameters are associated with the ELSA frailty index.

5.2.2 MRI and physical function measurements

MRI measurements collected include T2, fat fraction, diffusion tensor imaging, and muscle volume. Muscle function measurements collected include knee extension and knee flexion power and handgrip strength. Gait speed was measured with a 4m walk test (99). This methodology has been described in section 3.6.

5.2.3 Statistical analyses

Statistical analyses were performed using SPSS. One-Way ANOVA with Bonferroni post-hoc analysis was used to test for potential significant differences in quantitative MRI, handgrip strength, and muscle power measurements between all groups.

Spearman's rank correlation was used to measure correlation. This study utilised r_s values ≥0.4 as indicative of a correlation. Correlations between participants with gait speed and frailty were only calculated in older participants who had undergone a gait speed test and the ELSA frailty index assessment.

5.3 Results

18 young (18 - 30 years, mean age 26 ± 8), 18 middle-aged (31 - 68 years, mean age 49 ± 19), and 18 older (≥ 69 years, mean age 79 ± 5, mean ELSA frailty index score 10 ± 5) participants took part in this study. Each group consisted of nine males and nine females. Participants were obtained from the pool of healthy controls recruited for the MUSCLE study. There were substantive differences in quantitative MRI and muscle strength measurements between all age groups. Descriptive data for quantitative MRI and muscle power/volume measurements are shown in Table 5-1 and Table 5-2.

Table 5-1:Quantitative MRI measurements with ANOVA to determine significance between young, middle-aged, and older participants

	T2 (ms)			Fat fraction (%)			Mean diffusivity ($x10^{-3}mm^2s^{-1}$)			Fractional anisotropy (0-1)		
	Mean (SD)	95% CI	p-value	Mean (SD)	95% CI	p-value	Mean (SD)	95% CI	p-value	Mean (SD)	95% CI	p-value
Hamstrings												
Young (n=18)	39.3 (1.8)	38.5, 40.3	<0.001	3.4 (1.6)	2.7, 4.3	<0.001	1.26 (0.1)	1.23, 1.29	<0.001	0.42 (0.04)	0.40, 0.44	0.2
Middle-aged (n=18)	40.8 (1.4)	40.1, 41.6		5.6 (2.2)	4.4, 6.7		1.34 (0.1)	1.28, 1.39		0.40 (0.1)	0.39, 0.41	
Older (n=18)	42.9 (2.9)	41.4, 44.4		9.5 (3.6)	7.6, 11.3		1.40 (0.1)	1.34, 1.45		0.39 (0.04)	0.35, 0.41	
Quadriceps												
Young (n=18)	40.6 (1.4)	40, 41	<0.001	2.2 (0.8)	1.9, 2.6	<0.001	1.30 (0.1)	1.26, 1.33	<0.001	0.35 (0.05)	0.30, 0.40	0.7
Middle-aged (n=18)	42.8 (2.1)	41.9, 43.9		3.2 (2.3)	2.4, 4.8		1.35 (0.1)	1.29, 1.33		0.34 (0.05)	0.30, 0.40	
Older (n=18)	45.0 (2.4)	43.8, 46.2		6.4 (1.9)	5.2, 7.1		1.41 (0.1)	1.29, 1.41		0.33 (0.06)	1.3, 0.4	

Table 5-2: Muscle volume, knee extension, knee flexion, and handgrip strength measurements with ANOVA to determine significance between young, middle-aged, and older participants

	Muscle volume (cm3)			Flexion power (w)			Extension power (w)			Handgrip strength (kg)		
	Mean (SD)	95% CI	p-value	Mean (SD)	95% CI	p-value	Mean (SD)	95% CI	p-value	Mean (SD)	95% CI	p-value
Young (n=18)	1563 (412)	1357.6, 1768.3	0.002	45 (22.0)	34, 55	<0.001	84 (43.2)	63, 106	<0.001	36.8 (10.7)	31.5, 42.2	<0.001
Middle-aged (n=18)	1365 (362)	1195.6, 1534.8		33 (11.1)	26, 37		51 (20.4)	39, 60		31.5 (5.1)	28.9, 34.2	
Older (n=18)	1151 (327)	988.7, 1314.4		18 (9.9)	12, 22		28 (18.3)	18, 37		23.1 (9.7)	18.1, 28.1	

5.3.1 T2

Quantitative MRI T2 relaxation times increased with age (Table 5-1). Within the hamstrings, differences between young and old, young and middle-aged, and middle-aged and older participants were 3.6ms (95% CI= 1.8, 5.2; p< 0.001), 1.5ms (95% CI= 0.4, 2.7; p= 0.01), and 2.1ms (95% CI= 0.3, 3.7; p= 0.02) respectively. Within the quadriceps these differences were 4.4ms (95% CI= 2.8, 5.9; p< 0.001), 2.2ms (95% CI= 1, 3.4; p= 0.001), and 2.2ms (95% CI= 0.6, 3.7; p= 0.005) respectively (Figure 5-1).

5.3.2 Fat fraction

Quantitative MRI fat fraction values substantively increased within each age group increment (Table 5-1). Within the hamstrings, differences between young and old, young and middle-aged, and middle-aged and older participants were 6.1% (95% CI= 4.0, 8.2; p< 0.001), 2.2% (95% CI= 0.8, 3; p= 0.003), and 3.9% (95% CI= 2, 6; p< 0.001) respectively. Within the quadriceps the differences were 4.2% (95% CI= 3, 5; p< 0.001), 1.0% (95% CI= 0.2, 3; p= 0.02), and 3.2% (95% CI= 1, 4; p< 0.001) respectively (Figure 5-1).

5.3.3 Diffusion tensor imaging

5.3.3.1 Mean diffusivity

Mean diffusivity substantively increased with age (Table 5-1). Within the hamstrings differences between young and old, young and middle-aged, and middle-aged and

older participants for mean diffusivity were $0.14x10^{-3}mm^2s^{-1}$ (95% CI= 0.06, 0.21; p< 0.001), $0.08x10^{-3}mm^2s^{-1}$ (95% CI= 0.01, 0.1; p= 0.01), and $0.06x10^{-3}mm^2s^{-1}$ (95% CI= 0.11, 0.13; p= 0.1) respectively. Within the quadriceps the differences were $0.11x10^{-3}mm^2s^{-1}$ (95% CI= 0.03, 0.16; p= 0.002), $0.05x10^{-3}mm^2s^{-1}$ (95% CI= 0.01, 0.1; p= 0.1), and $0.06x10^{-3}mm^2s^{-1}$ (95% CI= 0.03, 0.11; p= 0.2) respectively (Figure 5-1), demonstrating higher mean diffusivity in older individuals.

5.3.3.2 Fractional anisotropy

There were no substantial differences in fractional anisotropy between age groups (Table 5-1). Within the hamstrings, differences between young and old, young and middle-aged, and middle-aged and older participants for fractional anisotropy were 0.03 (95% CI= 0.01, 0.06; p= 0.3), 0.02 (95% CI= 0.01, 0.06; p= 0.3), and 0.01 (95% CI= 0.01, 0.02; p= 0.9) respectively. Within the quadriceps these differences were 0.02 (95% CI= 0.01, 0.03; p= 0.9), 0.01 (95% CI= 0.01, 0.02; p= 0.5), and 0.01 (95% CI= 0.01, 0.03; p= 0.9) respectively (Figure 5-1).

5.3.4 Muscle volume

Muscle volume decreased with age (Table 5-2). There were differences in muscle volume between young and old, young and middle-aged, and middle-aged and older participants of $412cm^3$ (95% CI= 106, 690; p= 0.006), $198cm^3$ (95% CI= 0, 500; p= 0.1), and 214 cm^3 (95% CI= 62, 493; p= 0.1) respectively.

5.3.5 Muscle power and grip strength

Muscle power and grip strength decreased substantively between each age group increment (Table 5-2). There was a substantive difference in knee flexion power between young and old, young and middle-aged, and middle-aged and older participants of 27W (95% CI= 15, 39; p< 0.001), 12W (95% CI= 1, 25; p= 0.03), and 15W (95% CI= 2.2, 27.4; p= 0.01) respectively.

Within the quadriceps there was a substantive difference in knee extension power between young and old, young and middle-aged, and middle-aged and older participants of 56W (95% CI= 33, 79; p< 0.001), 33W (95% CI= 11, 58; p= 0.005), and 23W (95% CI= 1, 45; p= 0.07) respectively, demonstrating lower muscle power in older individuals.

There was a substantive difference in handgrip strength of 13.7kg (95% CI= 6.6, 20.8; p< 0.001) between the young and older participants, a difference of 5.3kg (95% CI= 1, 11; p= 0.07) between young and middle-aged participants, and a difference of 8.4kg (95% CI= 3.1, 13.9; p= 0.003) between the middle-aged and older participants, demonstrating lower muscle strength in the older groups.

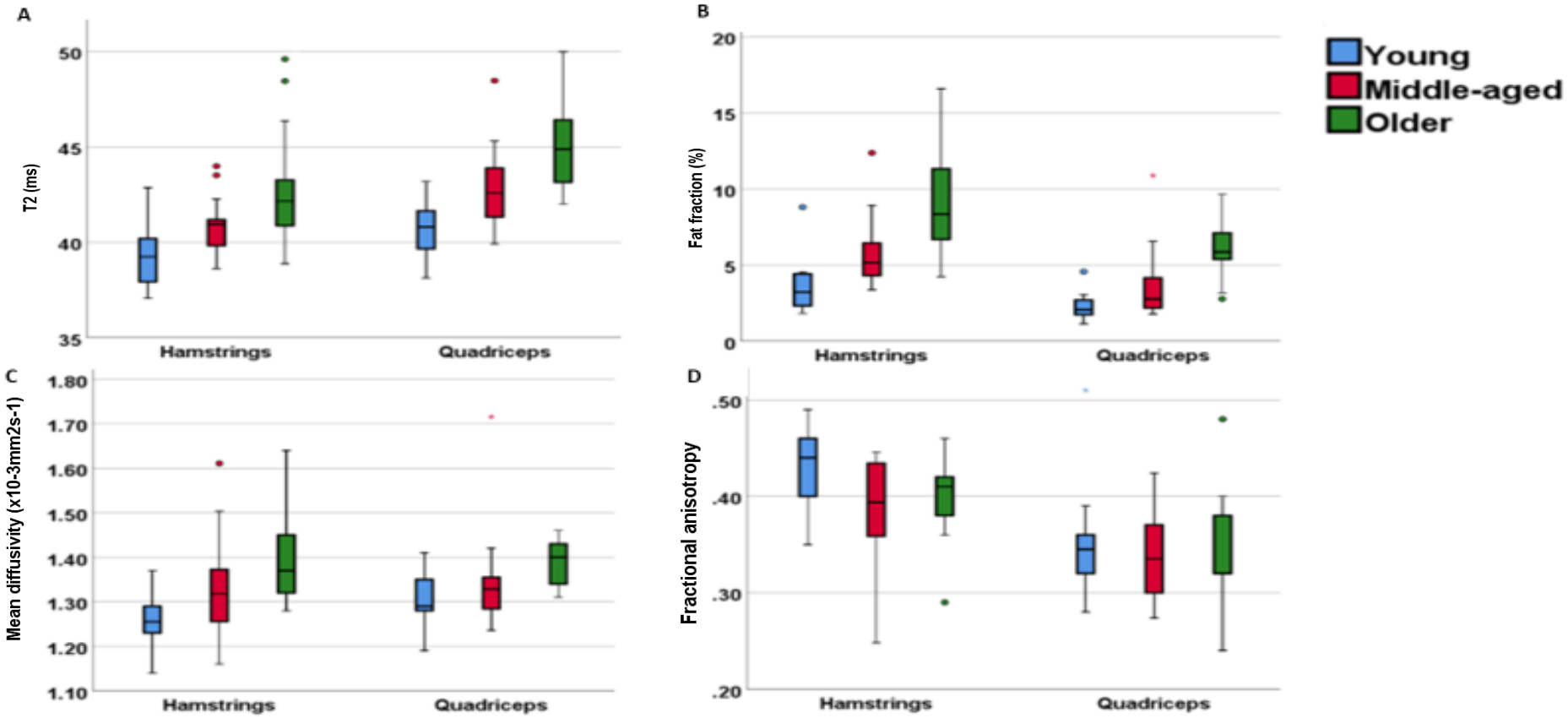

Figure 5-1: Quantitative MRI measurements of young, middle-aged and older participant groups.

A- T2, B- fat fraction, C- mean diffusivity, D- fractional anisotropy.

5.3.6 MRI and muscle function correlations in all participants

When all participants were combined into one group of 54 participants (Figure 5-2 and Figure 5-3), quantitative MRI T2 correlated with knee flexion (r_s= -0.7; p< 0.001), knee extension (r_s= -0.7; p< 0.001), and handgrip strength (r_s= -0.6; p< 0.001). Fat fraction correlated with knee flexion (r_s= -0.6; p< 0.001), knee extension (r_s= -0.7; p< 0.001), and handgrip strength (r_s= -0.6; p< 0.001). Mean diffusivity correlated with knee flexion (r_s= -0.4; p= 0.04), but did not correlate with knee extension (r_s= -0.3; p= 0.05) or handgrip strength (r_s= -0.1; p= 0.9). Fractional anisotropy did not appear to correlate with any of the muscle function tests: knee flexion power (r_s= 0.1; p= 0.9), knee extension power (r_s= -0.1; p= 0.1), and handgrip strength (r_s= 0.01; p= 0.9). Handgrip strength was also found to correlate with knee flexion power (r_s= 0.7; p< 0.001) and knee extension power (r_s= 0.7; p< 0.001).

5.3.7 MRI, muscle function, frailty index, and gait speed correlations in older participants

Quantitative MRI T2, fat fraction, and muscle volume, and quantitative muscle strength for knee flexion and knee extension substantively correlated with frailty index and gait speed in older participants (Figure 5-4). In the hamstrings, T2 correlated with frailty index (r_s= 0.8; p< 0.001), gait speed (r_s= -0.4, p= 0.05), and knee flexion (r_s= -0.7, p= 0.01). In the quadriceps T2 correlated with frailty index (r_s= 0.7, p< 0.001), gait speed (r_s= -0.5; p= 0.007), and knee extension (r_s= -0.6; p< 0.001). In the hamstrings, fat fraction correlated with frailty index (r_s= 0.7, p< 0.001), gait speed (r_s= -0.4; p= 0.02), and knee flexion (r_s= -0.6; p= 0.001). In the quadriceps fat fraction correlated with frailty index (r_s= 0.7; p< 0.001), gait speed (r_s= -0.6, p= 0.001), and knee extension (r_s= -0.7; p< 0.001). In the hamstrings mean diffusivity correlated with knee flexion (r_s= -0.4, p= 0.004), but did not appear

to correlate with frailty index (r_s= 0.3; p= 0.2), or gait speed (r_s= -0.3, p= 0.1). In the quadriceps mean diffusivity correlated with frailty index (r_s= 0.4, p= 0.1), and knee extension (r_s= -0.4; p= 0.007), but did not correlate with gait speed (r_s= -0.3, p= 0.2). Muscle volume (Figure 5-5) correlated with frailty index (r_s= -0.6; p< 0.001), gait speed (r_s= 0.6; p= 0.01), knee flexion (r_s= 0.6; p< 0.001), and knee extension (r_s= 0.6; p< 0.001). Knee flexion (Figure 5-5) correlated with frailty index (r_s= -0.7, p= 0.002), gait speed (r_s= -0.4, p= 0.05), and grip strength (r_s= 0.7; p< 0.001). Knee extension (Figure 5-5) correlated with frailty index (r_s= -0.7; p= 0.001), gait speed (r_s= 0.5; p= 0.01), and grip strength (r_s= 0.7; p< 0.001). Handgrip strength correlated with frailty index (FI) and gait speed (FI r_s= -0.7, p= 0.001, gait speed r_s= 0.5, p= 0.06).

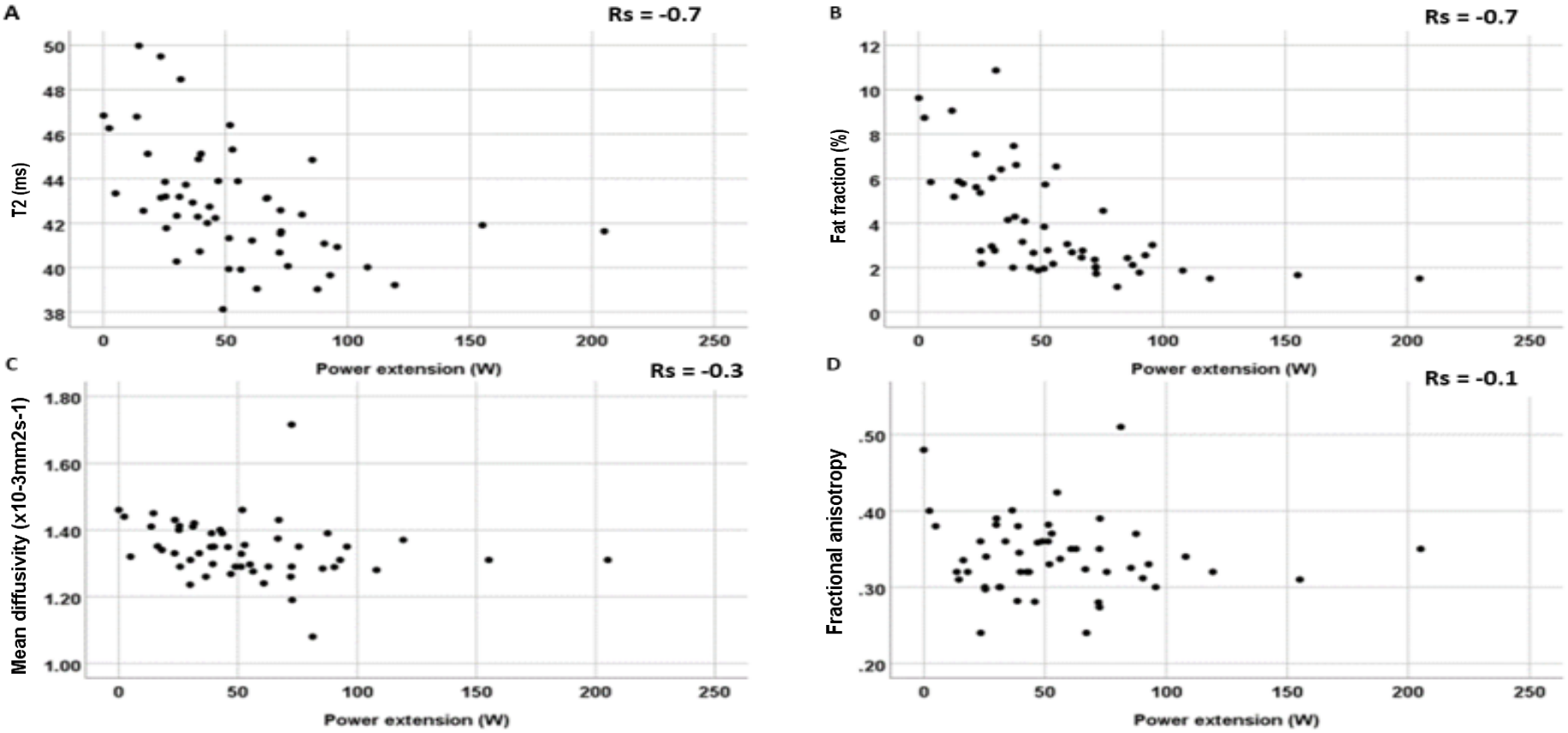

Figure 5-2: Quantitative MRI of the quadriceps and correlation versus power extension for all participants

A- T2, B- fat fraction, C- mean diffusivity, D- fractional anisotropy. (Young, middle-aged, and older participants combined as one).

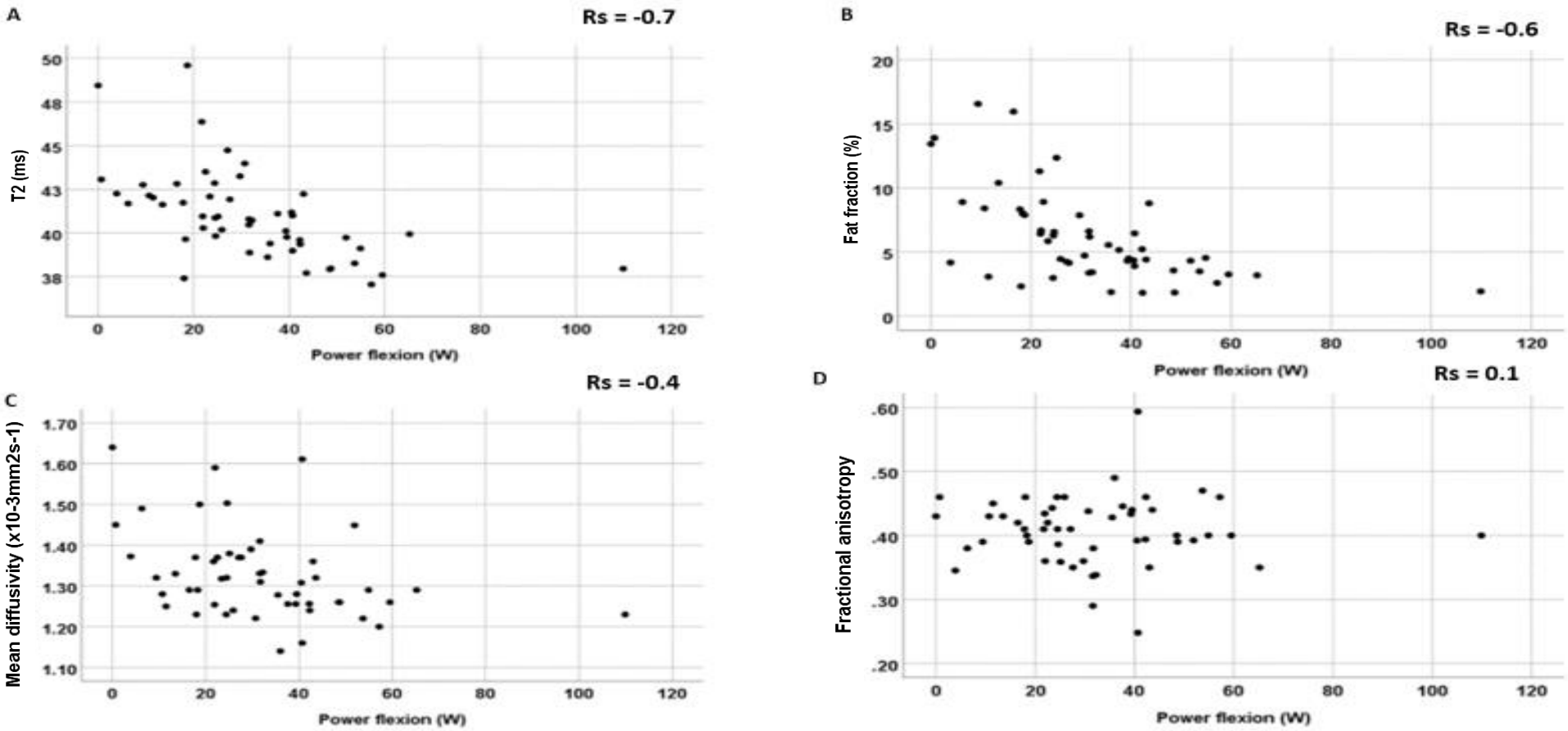

Figure 5-3: Quantitative MRI of the hamstrings and correlation versus power flexion for all participants

A- T2, B- fat fraction, C- mean diffusivity, D- fractional anisotropy. (Young, middle-aged, and older participants combined as one).

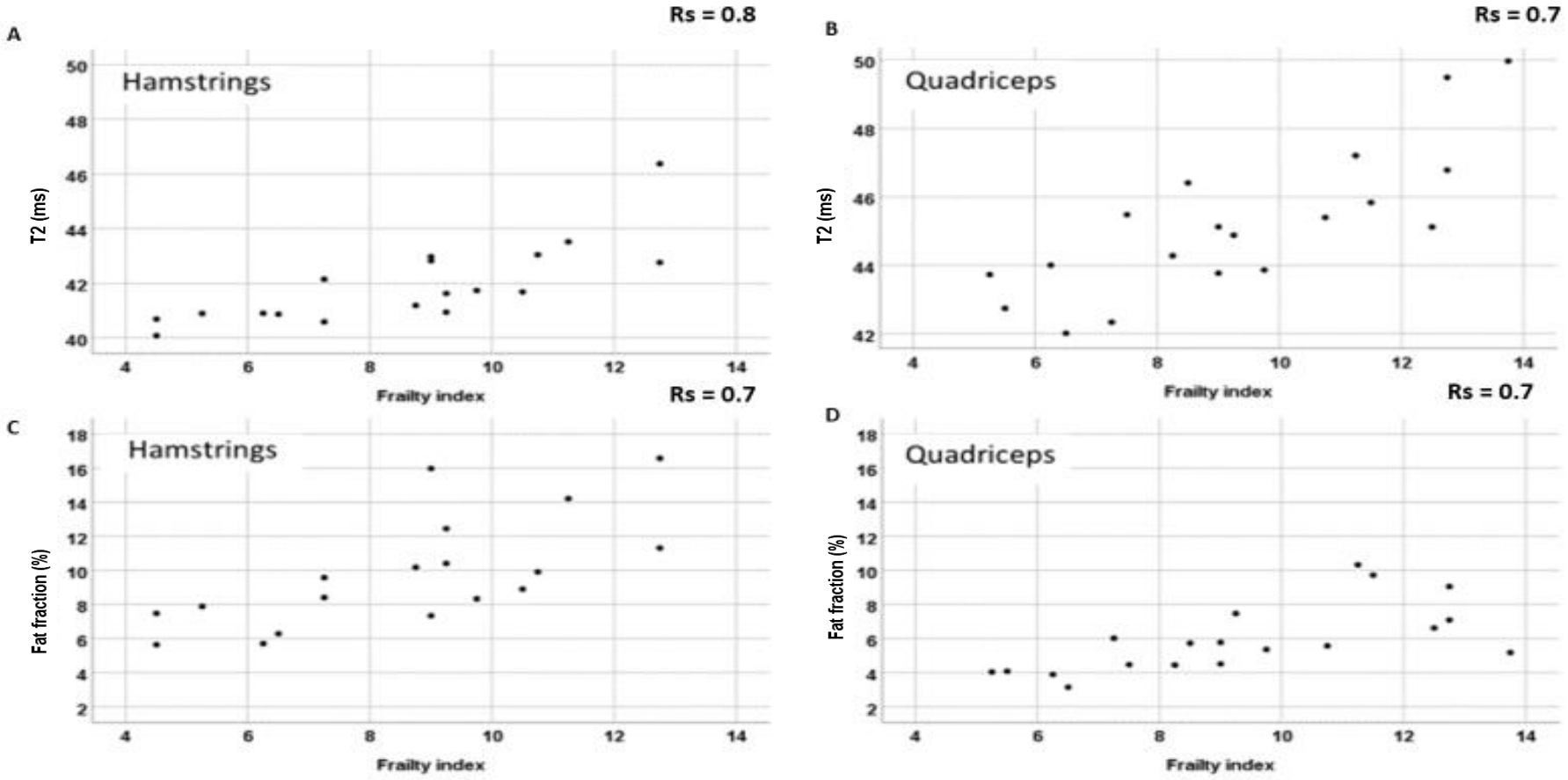

Figure 5-4: Quantitative T2 and FF MRI and frailty index correlation of older participants in the hamstrings and quadriceps.

A- T2 hamstrings, B- T2 quadriceps, C- fat fraction hamstrings, D- fat fraction quadriceps.

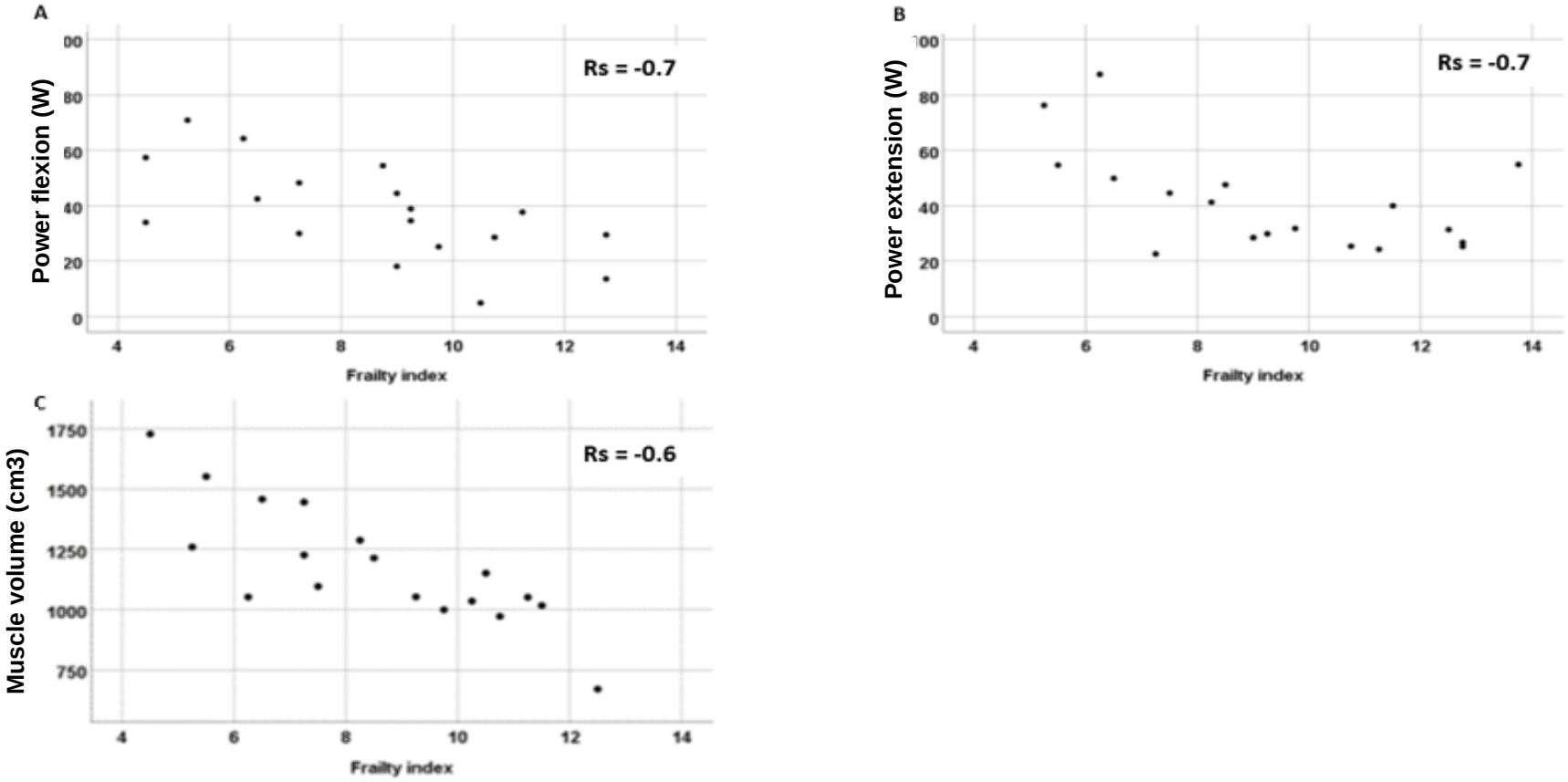

Figure 5-5: Muscle volume and muscle power versus frailty index correlation of older participants.

A- Knee flexion power, B- Knee extension power, C- Muscle volume.

5.4 Discussion

This chapter aimed to investigate whether quantitative MRI measures can detect differences within the muscle between three age groups and assess how these measures compare with frailty index, gait speed, and muscle power.

This study has shown substantive differences in T2, fat fraction, mean diffusivity, and muscle volume associated with ageing. However, this study did not show substantial differences in fractional anisotropy. The results from this study suggest that not only is quantitative MRI an independent measure of muscle function, but also shows potential as a quantitative adjunct assessment of frailty. The study demonstrates the potential of these quantitative measures to assess muscle status during ageing to detect sarcopenia, frailty, and to monitor muscle health. A strength of this study is that the measurements are useful not only for sarcopenia but also for frailty. Furthermore, this research matched for gender between the different age groups, which has not been done in previous research studies. In addition, for the first time, this study has gone further than previous studies by showing that these measurements also correlate with an independent measure of frailty (ELSA frailty index) and with quantitative muscle strength measurements (knee flexion, knee extension, and handgrip strength) and physical function (gait speed). In addition to being components of frailty, many of these measures are critical components in the diagnosis of sarcopenia (99). This study has also shown that grip strength substantively correlates with lower limb function and frailty index and therefore could be used as a convenient tool to measure an overall muscle function status.

Quantitative T2 measurements, as described in section 2.4.3, increased substantively with age, supporting previous work (325-328). Ageing is known to be associated with increased systemic inflammatory markers, such as CRP, IL-1RA, and IL-1 (329, 330). As previously mentioned in section 2.4.3, there is evidence to suggest that quantitative T2 MRI can identify muscle inflammation (26). However,

the increase in T2 relaxation time measurements in this study may also be due to the contribution of fat inadequately suppressed by the SPAIR fat suppression in the MRI acquisition (163, 167). This is important to consider due to the known fat infiltration in muscle due to ageing.

The fat fraction was found to be substantively higher in older participants in this study, which agrees with other studies investigating ageing in the muscle (255), suggesting its capability to identify myosteatosis using two-point Dixon MRI sequences. Myosteatosis results in a decrease in contractile properties of type II (fast-twitch) muscle fibres which have lower resilience to the increases in lipid content. This increase in lipid content results in dysregulated homeostasis (331, 332), decreased muscle quality, decreased muscle mass, and impaired physical function.

Mean diffusivity was substantively higher with age, and there were minor differences in fractional anisotropy, with lower measurements of fractional anisotropy in older participants. The findings found in this study are consistent with what is observed following muscle injury and exercise-induced trauma (26, 333-335). These diffusion differences could be due to interstitial oedema, or changes to the microstructure of tissue. The observed trend of higher mean diffusivity in older participants in this study supports a previous study (319). This previous study interpreted diffusion changes as an age-related increase in the amount of intramuscular fluid (319), which is consistent with Azzabou's interpretation of increased T2 relaxation time values (327).

Muscle volume substantively correlated with muscle power, and there were substantive differences in muscle volume between the age groups. This correlation is also seen in previous studies where muscle loss, which is well known to occur due to: decreased physical activity (336), declining androgen concentrations (337), nutritional deficiencies (338), and chronic inflammation (329, 330, 339), can reduce

function (99). As muscle mass is a primary component in the diagnosis of sarcopenia, the more accurate muscle volume measurements available with quantitative MRI may be useful in the diagnosis of sarcopenia.

This study also compared quantitative MRI of the thigh with forearm strength, measured by the handgrip test, which is frequently measured as a proxy for global muscle strength (340). Handgrip strength was reduced in older participants and correlated with lower limb function and frailty. This research project is the first study to demonstrate an association of handgrip strength with quantitative MRI. Whilst it is not correct to equate forearm strength with muscle parameters of the thigh, as handgrip strength is a frequently used assessment of frailty and sarcopenia [72, 80], and due to its simplicity and its frequent use, it was therefore deemed to be a useful addition to this study.

This study successfully met its aims and demonstrated that quantitative MRI can detect substantive differences between young, middle-aged, and older participants and that these measures correlate with frailty index, gait speed, and muscle power.

5.4.1 Limitations

This study is subject to some limitations. This study only recruited older participants who were assessed as ‘fit’ and ‘well’ according to the ELSA frailty index. Therefore, while this study has shown a strong association between quantitative MRI measures and frailty index, this study did not investigate this association in patients who have been classified as being vulnerable or frail. Further research should investigate whether this trajectory continues in vulnerable and older people with frailty. Furthermore, this study did not consider the fact that the ELSA frailty index score considers 44 deficits in total, including functional, sensory, and cognitive

function, which are all crucial aspects of frailty. However, despite this, the measurements of the muscle utilising quantitative MRI within this study still correlate with the frailty index scores, demonstrating its strength in identifying frailty.

5.5 Conclusion

Ageing is associated with longer T2, higher fat fraction and mean diffusivity, and lower muscle volume, grip strength, and muscle power. Quantitative MRI parameters correlated with grip strength, muscle power, and the ELSA frailty index, which is a research standard frailty index. This study demonstrates that quantitative MRI measurements have the potential to be useful markers of age and muscle health and could be useful in the management of sarcopenia and frailty.

5.6 Key messages

- There are substantive differences in T2, fat fraction, mean diffusivity, and muscle volume between age groups.
- Quantitative MRI correlates with the ELSA frailty index, gait speed, grip strength, and muscle function.
- Quantitative MRI shows promise in identifying the changes within the muscle due to ageing.

Chapter 6 Quantitative MRI in myositis patients: A comparison with healthy volunteers and radiological visual assessment

This chapter describes a research study by Matthew Farrow, John Biglands, Andrew Grainger, Philip O'Connor, Elizabeth Hensor, Andreas Ladas, Steven Tanner, Paul Emery, and Ai Lyn Tan published in Clinical Radiology, 2020 (4).

6.1 Introduction

Idiopathic inflammatory myopathies (IIM), representing forms of myositis, are a heterogeneous group of diseases affecting approximately 5,000 – 6,000 people in the UK. IIM predominantly manifests in skeletal muscle, with features of inflammation, myosteatosis, muscle atrophy, and alterations in muscle microstructure. Dermatomyositis (DM) and polymyositis (PM) are two common types of myositis. They are characterised by muscle pain and weakness, with overlapping features and often present with the same autoantibodies (341). The symptoms of myositis often result in severe impairment in quality of life (342, 343), and are associated with increased mortality (344).

The Bohan and Peter criterion is the most widely used criterion and remains one of the preferred criteria in clinical studies and trials worldwide. Others have been proposed, such as the criteria by Dalakas (345), Dalakas and Hohlfield (346) and, more recently, the 2017 EULAR/ACR criteria (347). The diagnosis and monitoring of myositis is reliant on clinical examination, invasive muscle biopsies, blood tests, and conventional MRI (127).

Proximal muscle weakness is one of the most common clinical manifestations of myositis and is a significant contributor for the loss of physical function and the decrease in quality of life in patients. This weakness often develops insidiously over several months, with a decline estimated at 3.5-5.4% per year (348-351). As such, muscle strength is frequently measured as part of a physical examination, with manual muscle testing widely used in clinical studies as a primary endpoint (352, 353). Manual muscle testing (MMT) is reported as a summary score of a total number of 26 proximal, distal, and axial muscle groups from the upper and lower extremities (352, 354). Grades between 0-3 indicate severe weakness; grades 4-6 indicates moderate weakness, grades 7-9 indicate mild weakness and grade 10 indicates no detectable weakness (355, 356). However, whilst MMT is widely used, it is limited as it is subjective and has low sensitivity (354, 357-360).

Muscle biopsies are frequently used in the diagnosis of myositis, with the vastus lateralis usually being selected for biopsy. Unfortunately, muscle biopsy results can be diagnostically inconclusive in up to 45% of cases, due to sampling error caused by the variable distribution muscle pathology (361).

Medical imaging is frequently used to aid in the diagnosis and monitoring of myositis (108), with MRI visual scoring playing a pivotal role in the assessment of muscle oedema, myosteatosis, and muscle atrophy (362). An important role of imaging is the identification of sites of muscle inflammation which can then be targeted for muscle biopsy (363). Currently, this is usually done by subjective visual assessment of the muscle, a technique which may be insensitive to systemic muscle changes. As an alternative to conventional MRI, there is a range of quantitative MRI techniques that may be able to detect subtle muscle changes due to disease and may have a role in the future clinical management of myositis, including the monitoring of response to treatment (26, 115, 364).

Quantitative T2 measurements are sensitive to fluid changes within the body, which can relate to physiological or pathological changes at the macromolecular level (162). T2 measurements may have a role in the long term follow up of muscle oedema and inflammation (160). MR-based fat fraction (FF) measurements in the muscle are useful for identifying fat infiltration (255, 365). Recently, interest has grown regarding diffusion tensor imaging (DTI) techniques in the muscle, which are sensitive to changes in muscle microstructure (26, 366). These measurements are discussed in greater detail in section 2.4.3. There are few published studies that have investigated quantitative MRI measurements in myositis, and this is the first study to compare these MRI techniques with semi-quantitative radiologist scoring and quantitative muscle strength.

This study aimed to compare quantitative T2, fat fraction, diffusion tensor imaging, and muscle volume measurements in the muscle between patients with myositis and a directly matched healthy population, and to compare the quantitative MRI measurements with semi-quantitative radiologist scores and muscle strength.

6.1.1 Imaging of skeletal muscle in myositis

6.1.1.1 Ultrasonography

Ultrasound can be used in the management of myositis, including for guiding muscle biopsies; however, its sensitivity ranges from 2-82% for detecting myositis (367). A benefit of ultrasound-guided muscle biopsies includes the fact that they can be done simultaneously. Ultrasound can demonstrate muscle atrophy, fat replacement, and oedema, which manifests as increased echogenicity; however, MRI is more accurate to grade the loss in muscle bulk and fat infiltration (160, 368). Therefore, MRI is used more frequently in the diagnosis of myositis.

6.1.1.2 Magnetic resonance imaging

Oedema, fat replacement and muscle atrophy are frequently seen features in patients with myositis. Therefore, MRI is frequently used in the management of myositis due to its excellent ability to detect these features (369).

Muscle oedema, which represents inflammation (370), is found in approximately 80% of active myositis patients (369, 371). Oedema can be visually observed on both T2 and short tau inversion recovery (STIR) sequences as a bright signal located within the affected muscles providing a qualitative measurement. MRI can also be used to guide muscle biopsies by targeting an area of inflammation. Using MRI to guide biopsies is beneficial as blind muscle biopsies may be false-negative in up to 45% of cases (361). Whereas, muscle biopsies guided by MRI show a significantly higher number of inflammatory cells in comparison to non-guided MRI biopsies, demonstrating an increase in the yield of a histological diagnosis after MRI-guided biopsy (368). It could be speculated that quantitative T2 may have a valuable role in clinical practice for myositis diagnosis and management, including the guidance of muscle biopsies in muscles which do not demonstrate inflammation visually. Unfortunately, very few studies have investigated the utility of quantitative T2 in myositis.

Myosteatosis and muscle atrophy are notable features of myositis. Surprisingly, few studies have utilised quantitative fat fraction imaging in myositis patients. The few that have been published have demonstrated that quantitative fat fraction can be used to assess damage in myositis patients and that there are substantive differences between patients and healthy controls (369, 372, 373), demonstrating the potential for MR fat fraction imaging to act as a biomarker in observing disease.

Few studies have investigated the possible diagnostic value of diffusion tensor imaging in myositis (26, 366). These studies have returned mixed results. One study showed that mean diffusivity values decrease in patients with myositis compared to healthy controls (374). In contrast, two studies identified a higher mean diffusivity within the affected muscles of myositis patients compared to non-affected myositis patient muscles and healthy controls (26, 366). These differences in results could have been due to the different methods to create the regions of interest. As some studies have drawn the regions of interest around the entire muscle, whilst others utilised small circular regions of interest in a location chosen for its clinical significance (affected or unaffected). It could be believed that the presence of oedema and fat infiltration is the reason behind the conflicting data. In these studies, the muscles of the patients with myositis that visually appeared normal on T1 and T2 weighted images showed no difference in mean diffusivity compared to healthy controls, whilst the muscles of the patients with inflammation showed increases of 15% in mean diffusivity values compared to healthy controls. This increase in mean diffusivity may have been due to infiltration of fluid, resulting in greater unrestricted movement of molecules, suggesting that muscle oedema is associated with increased diffusion values.

In contrast, it was also found that in patients with myositis, fat infiltrated muscles showed lower mean diffusivity values (26), suggesting restricted diffusion. These results agree with studies showing that the typical pathological changes in myositis patients can result in progressive muscle damage and infiltration of fat and fibrous tissue, which can restrict diffusion, suggesting that greater fat infiltration is associated with lower diffusion values (122, 375). Unfortunately, no previous study has investigated both large ROIs taking into account the entire muscle, and small ROIs based on clinical features. Evidently, further research is still required to elucidate diffusion tensor imaging in myositis, in particular the effect of myosteatosis and oedema on mean diffusivity.

6.1.2 Hypothesis

Quantitative MRI can detect differences in muscle properties in patients with myositis compared to age- and gender-matched healthy controls.

6.1.3 Objectives

To assess whether quantitative MRI can detect differences between the muscles of patients with myositis and healthy controls and to assess how this compares to radiologist scoring.

6.2 Methods

6.2.1 Study design

This observational, case-control study was approved by the local research ethics committee. Recruitment started in May 2017 and finished in July 2018. 1:1 matching was used (matching the patient with a healthy control of the same gender within a 5-year age range). Healthy controls were obtained from the pool of healthy controls recruited for the MUSCLE study. The inclusion criteria for patients was based on the Bohan and Peter criteria for myositis (376). Patients also fulfilled the 2017 EULAR/ACR criteria for dermatomyositis or polymyositis, which was published after the commencement of the study (347). Myositis patients were included in the study if they were clinically suspected of being active at the time of recruitment by a clinician, based on muscle weakness and elevated creatinine kinase (CK) (above 200 IU/L in females and 320 IU/L in males), or had clinically diagnosed muscle weakness, antibody positive, on treatment for myositis, or had a

patient global visual analogue score (VAS) of more than 20mm/100mm. Clinical information was collected, including creatine kinase, antibody status, and medication. Healthy controls were included if they were asymptomatic with no history of muscle disease.

6.2.2 MRI and muscle strength measurements

MRI measurements collected include T2, fat fraction, diffusion tensor imaging, and muscle volume. Muscle function measurements collected include knee extension, knee flexion, and handgrip strength. This methodology has been described in section 3.6.

As ROIs depicting the whole muscle cross-section were used in this study, both fat infiltration and oedema may be present within the same region of interest. As previously discussed, these two pathologies may have opposite influences on mean diffusivity measurements so that if both oedema and fat are present in the same region of interest, the effects can oppose each other and reduce the sensitivity of the diffusion measurements to disease (26). Therefore, in a subgroup analysis, nine patients were identified: 3 with fat infiltrated regions, 3 with oedematous regions and 3 with unaffected regions. One identical circular ROI was placed within either a fat infiltrated, oedematous or unaffected muscle region, respectively (Figure 6-1). Mean diffusivity measurements in these three separate regions were then compared.

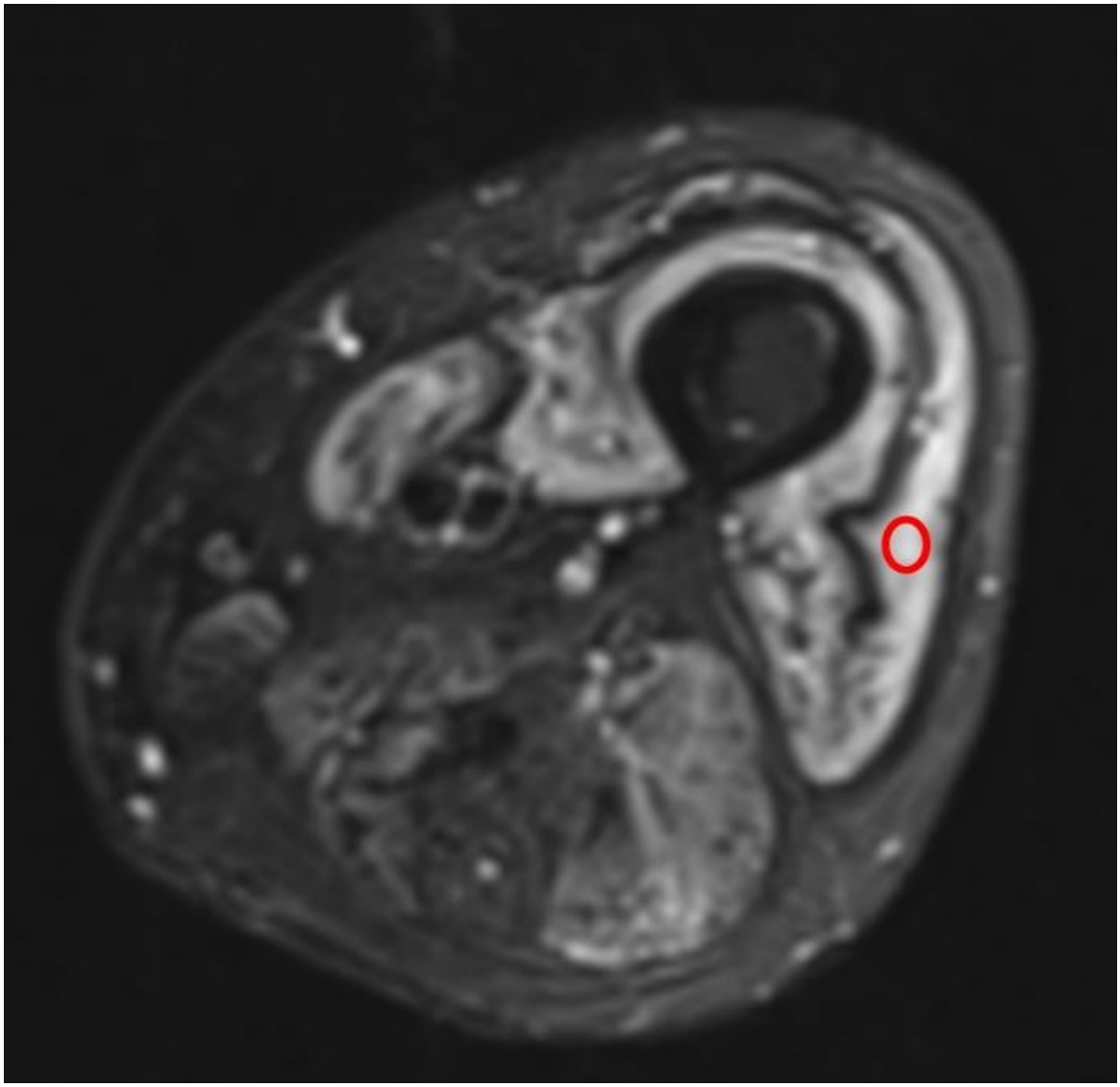

Figure 6-1: Small region of interest in quadriceps (vastus lateralis) in case of severe oedema on T2-weighted STIR sequence.

6.2.3 Radiologist semi-quantitative scoring

To compare with semi-quantitative radiologist scoring, the muscles of the hamstrings and quadriceps were scored on a 4-point visual scale as either unaffected (0), mild (1): up to 1/3 of muscle involved, moderate (2): 1/3 - 2/3 of muscle involved, or severe (3): greater than 2/3 of muscle involved. Two radiologists scored the individual muscles of the hamstrings and quadriceps using T2-weighted STIR images (TA-3:18, 6,550ms, TE-87ms) to identify muscle oedema and T1-weighted images (TA- 1:21, TR- 658ms, TE-8.8ms) to identify fat infiltration (Figure 6-2). If there was disagreement between scores, these were resolved on consensus following joint review.

Hamstrings and quadriceps scores were derived from the mean value of the individual muscle scores and rounded to the nearest integer. The radiologists were blinded to other clinical, laboratory, quantitative MRI, and muscle function results. Radiologists scored all patients on STIR and T1 weighted images to assess muscle oedema and fat infiltration. Eight patients were scored as having unaffected muscle by two radiologists on STIR and T1-weighted MRI sequences. These eight patients were compared in a separate matched sub-study with age-and-gender matched healthy controls (n=8) to investigate whether quantitative T2 and two-point Dixon could identify differences that currently go undetected by conventional radiologist scoring.

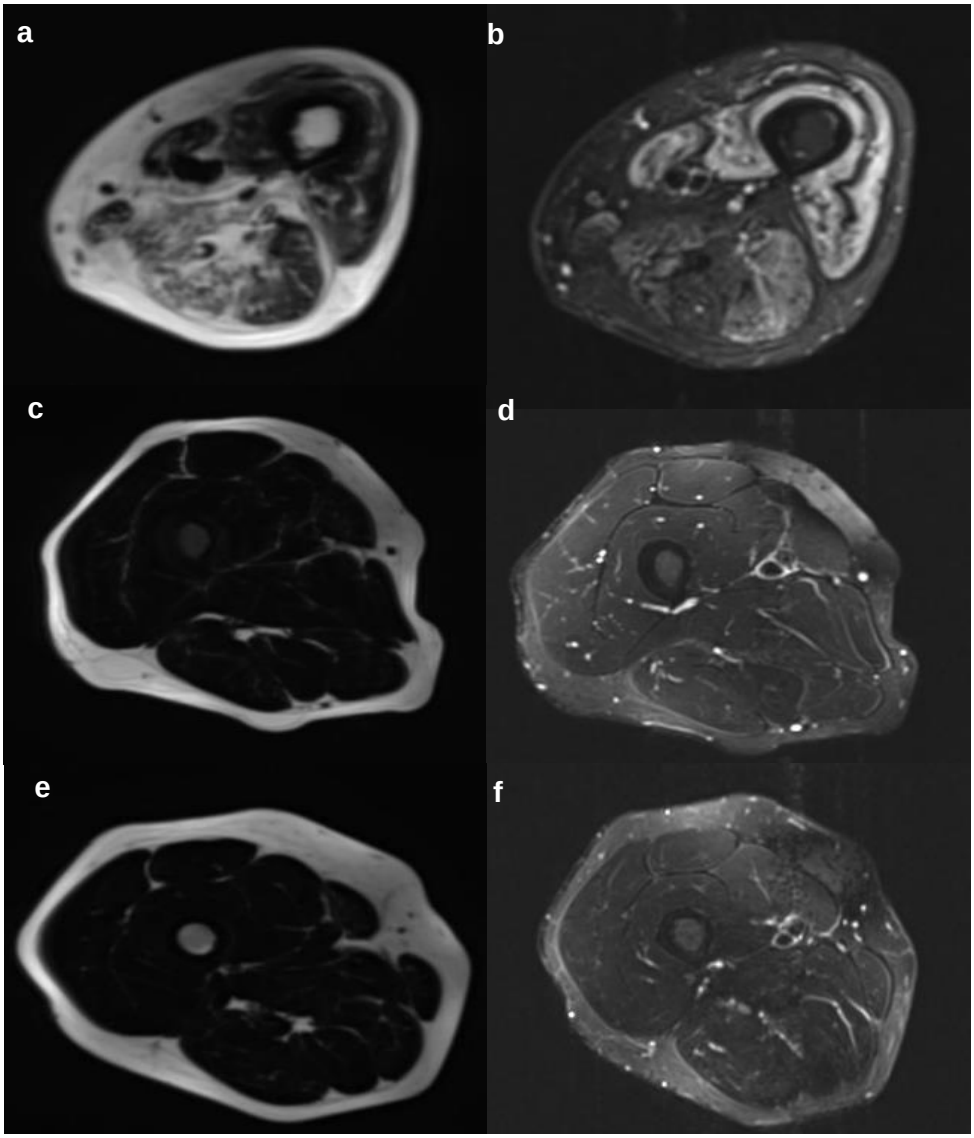

Figure 6-2: MRI images as reported by radiologists and region of interest

Images of myositis patient with affected muscle (left thigh) a) Dixon fat fraction b) T2-STIR.
Images of myositis patient with scored unaffected muscle (but elevated quantitative T2) (right thigh) c) Dixon fat fraction d) T2-STIR.
Images of healthy control (right thigh) e) Dixon fat fraction. f) T2-STIR.

6.2.4 Statistical analyses

Statistical analyses were performed using SPSS. Paired samples t-tests were used to test for potential significant differences in MRI measurements between patients and healthy controls. Spearman's rank correlation was used to measure correlation; r_s values ≥0.4 were considered indicative of potential correlation, and p-values have been reported to identify potential significance. Receiver operator characteristic (ROC) curves were generated to assess diagnostic performance. Cohen's delta (d) has been provided for key comparisons, with effect sizes interpreted as small (d=0.2), medium (d=0.5), or large (d=0.8). A d of 1 indicates the two groups differ by one standard deviation. The standard deviation is a measure of the dispersion of data. The formula for Cohen's delta is $d = \frac{mean\ of\ group\ 1 - mean\ of\ group\ 2}{Pooled\ standard\ deviation}$. The Pooled standard deviation is an average of standard deviations of two or more groups: $Pooled\ standard\ deviation = \sqrt{\frac{Standard\ deviation\ for\ group\ 1 + standard\ deviation\ for\ group\ 2}{2}}$.

6.3 Results

Sixteen myositis patients were recruited (10/16 female, ten polymyositis, six dermatomyositis, mean age 50 ± 26, mean height 165cm ± 10cm, mean weight 77.1kg ± 8kg, mean BMI 25 ± 4), median CK of 1,000IU/L (range 70 – 12,802). The mean disease duration for the myositis patients was five years (range one month – 22 years). 5/16 (31%) of the myositis patients were positive for the anti-Jo-1 antibody. The following myositis associated antibodies were recorded as anti-PM-Scl 75 (2/16, 13%), anti-PM-Scl 100 (2/16, 13%), and anti-PL 12 (1/16, 6%). Other connective tissue disease-associated antibodies included anti-Ro (5/16, 31%), anti-La (1/16, 6%), anti-Sm/RNP (3/16, 19%), anti-chromatin (3/16, 19%), and anti-

centromere (1/16, 6%). Four patients tested negative for antibodies. At the time of the study, the patients were on the following therapies: prednisolone - 9/16 (56%), hydroxychloroquine - 4/16 (25%), methotrexate - 3/16 (19%), rituximab - 2/16 (13%), intravenous immunoglobulins – 2/16 (13%), cyclophosphamide – 2/16 (13%), mycophenolate mofetil – 2/16 (13%), and azathioprine - 1/16 (6%). Most of the patients were receiving therapy for the entire duration of their disease in accordance with the British Society of Rheumatology management guidelines (129). One patient was newly diagnosed and yet to receive any therapy at the time of the MRI. Sixteen age- and gender-matched healthy controls were recruited (mean height 167cm ± 9cm, mean weight 74kg ± 11kg, mean BMI 26 ± 2).

Within the hamstrings, the mean peak torque in the myositis patients was lower than healthy controls by -24.4Nm (95% CI= -42.4Nm, 6.4Nm; p= 0.01). Within the quadriceps, the mean peak torque in the patients was lower by -48.2Nm (95% CI= -79.9Nm, -22.2Nm; p< 0.001). Descriptive data for quantitative MRI and muscle strength is reported in Table 6-1 and Table 6-2. The receiver operator characteristic (ROC) curves and area under the curve (AUC) values for the quantitative measures are shown in Figure 6-3.

Table 6-1: Quantitative MRI and strength measurements for healthy controls and myositis patients

		Mean (SD)	
		Hamstrings	**Quadriceps**
T2 (ms)	**Myositis**	47.8 (7.7)	53.8 (12.1)
	Healthy	39.9 (1.5)	42.1 (2.1)
Fat fraction (%)	**Myositis**	10.7 (9.4)	11.1 (13.1)
	Healthy	4.1 (1.2)	2.7 (1.1)
Muscle volume (cm^3)	**Myositis**	1,152 (594)	
	Healthy	1,468 (331.4)	
Mean diffusivity (x10-3mm2s^{-1})	**Myositis**	1.29 (0.1)	1.31 (0.1)
	Healthy	1.32 (0.1)	1.34 (0.1)
Fractional anisotropy	**Myositis**	0.41 (0.004)	0.36 (0.03)
	Healthy	0.39 (0.1)	0.34 (0.1)
Peak torque flexion (Nm)	**Myositis**	32.8 (23)	N/A
	Healthy	57.2 (26)	N/A
Peak torque extension (Nm)	**Myositis**	N/A	53.4 (46)
	Healthy	N/A	101.6 (45)

a

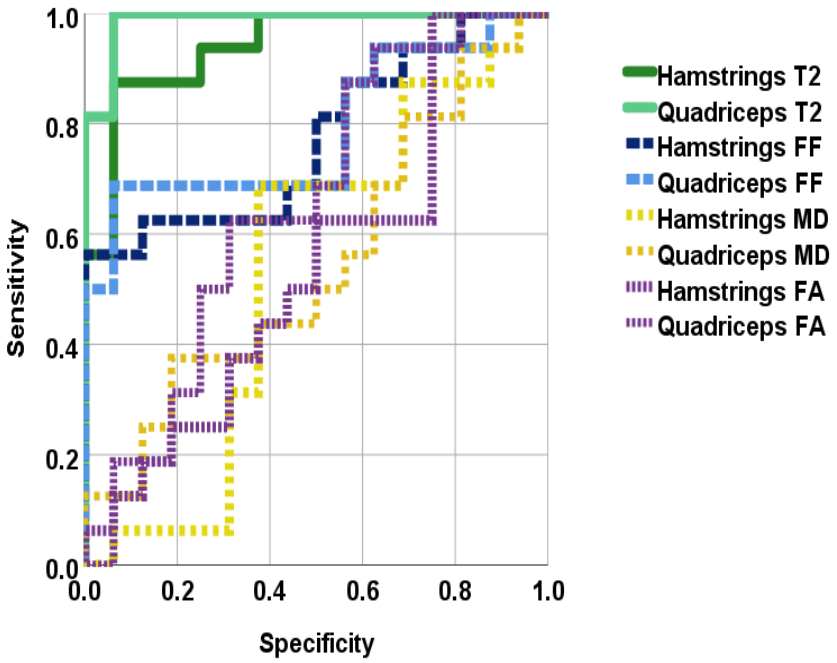

b

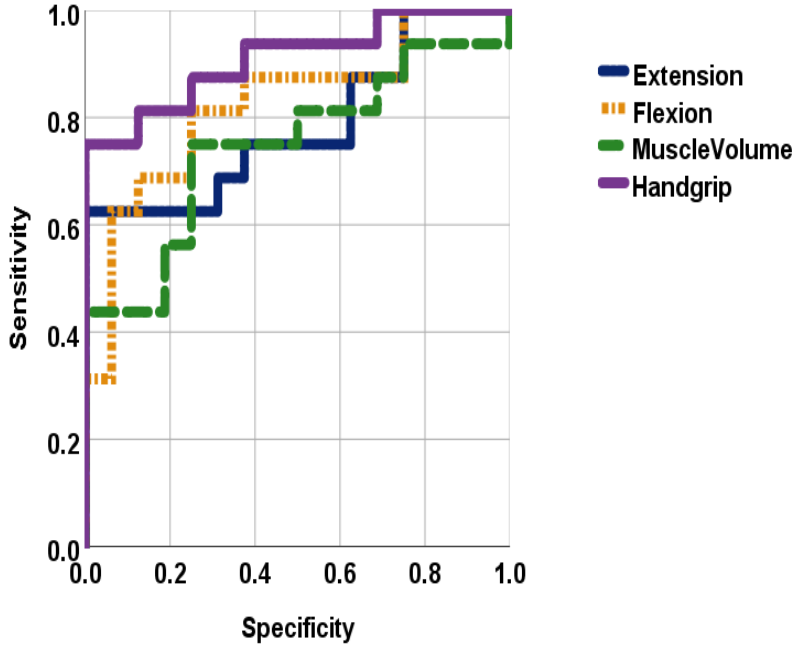

Figure 6-3: Receiver operator characteristic curve in patients with myositis

Quantitative MRI performance in discriminating myositis and healthy muscle. a) AUC hamstrings AUC: T2 = 0.941, MD = 0.535, FF = 0.773; FA = 0.543 Quadriceps: T2 = 0.84, MD = 0.547, FF = 0.789; FA = 0.652. b) Receiver operator characteristic curve for muscle volume and muscle strength performance in discriminating myositis and healthy muscle. AUC: Knee extension=0.785; Knee flexion = 0.824; Muscle volume = 0.746; Handgrip strength = 0.910.

Table 6-2: Differences between individual muscles of hamstrings and quadriceps.

		Mean (SD)						
		Semitendinosus	**Semimembranosus**	**Biceps femoris**	**Vastus lateralis**	**Vastus medialis**	**Vastus intermedius**	**Rectus femoris**
T2 (ms)	**Myositis**	49.2 (7.9)	47.6 (11.2)	45.4 (9.0)	53.9 (13.5)	58. 1 (13.7)	46.2 (12.5)	52.4 (26.2)
	Healthy	38.8 (2.6)	41.8 (3.2)	40.0 (2.0)	40.0 (2.0)	45.8 (3.8)	41.3 (2.0)	47.0 (6.4)
Fat fraction (%)	**Myositis**	13.3 (16.8)	11.9 (11.8)	9.1 (7.1)	12.4 (14.9)	9.3 (11.9)	11.5 (12.2)	10.4 (15.5)
	Healthy	4.1 (1.6)	4.2 (1.9)	4.0 (1.1)	2.8 (1.1)	2.3 (1.1)	2.8 (1.3)	1.8 (1.0)
Mean diffusivity (x10-3mm2s^{-1})	**Myositis**	1.31 (1.5)	1.28 (0.1)	1.31 (0.6)	1.29 (0.1)	1.35 (0.1)	1.32 (0.06)	1.27 (0.1)
	Healthy	1.31 (1.3)	1.34 (0.1)	1.31 (0.1)	1.29 (0.1)	1.35 (0.1)	1.37 (0.1)	1.25 (0.1)
Fractional anisotropy	**Myositis**	0.46 (0.04)	0.36 (0.04)	0.38 (0.04)	0.34 (0.03)	0.35 (0.05)	0.36 (0.03)	0.37 (0.06)
	Healthy	0.43 (0.06)	0.35 (0.05)	0.37 (0.05)	0.34 (0.05)	0.32 (0.05)	0.34 (0.05)	0.36 (0.05)

6.3.1 T2

Within the hamstrings, there was a difference of 7.9ms (95% CI= 3.9ms, 11.9ms; p< 0.001) between the myositis patients and healthy controls, representing a large effect size (Cohen's d= 0.80). Within the quadriceps, there was a difference of 11.7ms (95% CI= 5.4ms, 17.9ms; d= 0.88; p< 0.001) (Figure 6-5).

T2 was inversely correlated with muscle strength measurements in myositis and healthy controls in both the quadriceps and the hamstrings (Figure 6-6).

6.3.2 Fat fraction

Fat fraction (FF) was higher in myositis patients compared to healthy controls with a difference in the hamstrings of 6.6% (95% CI= 1.9%, 11.4%; d= 0.68; p= 0.006) and in quadriceps of 8.4% (95% CI= 1.6%, 15.1%; d= 0.64; p= 0.01), representing medium-to-large effect sizes (Figure 6-5).

Fat fraction correlated with muscle strength in the quadriceps with a correlation coefficient of r_s= -0.5 (p= 0.001) but did not correlate in the hamstrings r_s= 0.3 (p= 0.08).

6.3.3 Diffusion tensor imaging

6.3.3.1 Mean diffusivity

There was no substantive difference in mean diffusivity (MD) between the myositis patients and healthy controls in the hamstrings (Figure 6-5), with a difference of $0.03x10^{-3}mm^2s^{-1}$ (95% CI= -0.05, 0.06; d= 0.17; p= 0.5) or the quadriceps, with a difference of $0.03x10^{-3}mm^2s^{-1}$ (95% CI= -0.09, 0.06; d= 0.14; p= 0.6).

In the small sub-analysis that investigated the contradictory effects of fat and oedema on DTI measurements, diffusion was found to be higher in the oedematous regions and lower in the fat infiltrated regions (Figure 6-4).

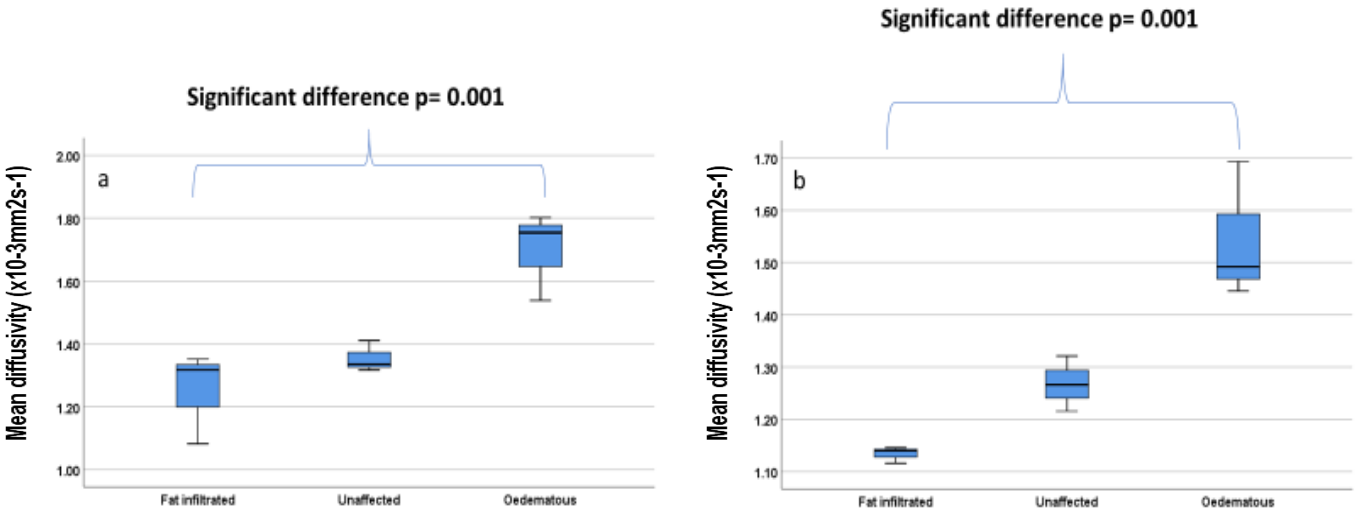

Figure 6-4: Mean diffusivity in patients with myositis with fat infiltrated, unaffected, and oedematous muscle.

a) Mean diffusivity in hamstrings in severe cases b) Mean diffusivity in quadriceps in severe cases.

6.3.3.2 Fractional anisotropy

There were no substantive differences between myositis and healthy controls in fractional anisotropy (FA) in the hamstrings with a difference of 0.02 (95% CI= -0.01, 0.06; d= 0.2; p= 0.2) or quadriceps, with a difference of 0.02 (95% CI= -0.01, 0.06; d= 0.1; p= 0.6).

6.3.4 Muscle volume

Patients had smaller muscle volumes than age- and gender-matched healthy controls (Figure 6-7) with a difference of -316cm^3 (95% CI= -648 cm^3 and -62 cm^3; p= 0.01). Muscle volume correlated with knee flexion torque (r_s= 0.5) and knee extension torque (r_s= 0.6) in patients and healthy controls combined (both p< 0.001).

6.3.5 Comparison with radiologist scoring

Quantitative T2 substantively correlated with the radiologists' oedema scores with r_s= 0.7 in the hamstrings (p< 0.001) and r_s= 0.6 in the quadriceps (p< 0.001), with an upward trend in T2 as radiologist scored visible oedema increased (Figure 6-8). In a separate comparison between the muscles in the myositis patients who had been classified as unaffected by the radiologists' (n= 8), T2 values for patients were still substantively higher than those for the age- and gender-matched healthy controls. In this subgroup analysis, the mean T2 in the hamstrings in patients was 42.2ms while healthy controls had a mean T2 of 38.7ms, a difference of 3.5ms

(95% CI= 1.4, 5.5; p= 0.004). In the quadriceps, the mean T2 in unaffected muscles of the myositis patients (n= 8) was 43.9ms, and healthy controls had a T2 of 40.1ms, a difference of 3.8ms (95% CI= 1.9, 5.6; p= 0.001) (Figure 6-9).

Within both the hamstrings and quadriceps, quantitative fat fraction substantively correlated with radiologists' scores for fat infiltration at r_s= 0.8 in the hamstrings (p< 0.001) and r_s= 0.9 in the quadriceps (p< 0.001), with an upward trend in fat fraction as radiologist scored visible fat infiltration increased (Figure 6-10). Fat fraction values for myositis patients classified as unaffected by the radiologists were not substantively different from those for healthy controls. In this subgroup analysis, the mean fat fraction in the hamstrings in patients was 3.4%, while matched healthy controls had a mean fat fraction of 2.9%, a difference of 0.5% (95% CI= -1.6, 0.9; p= 0.5). In the quadriceps, the mean fat fraction in patients was 2.5% and 2.0% in healthy controls, a difference of 0.5% (95% CI= -0.9, 0.1; p= 0.1).

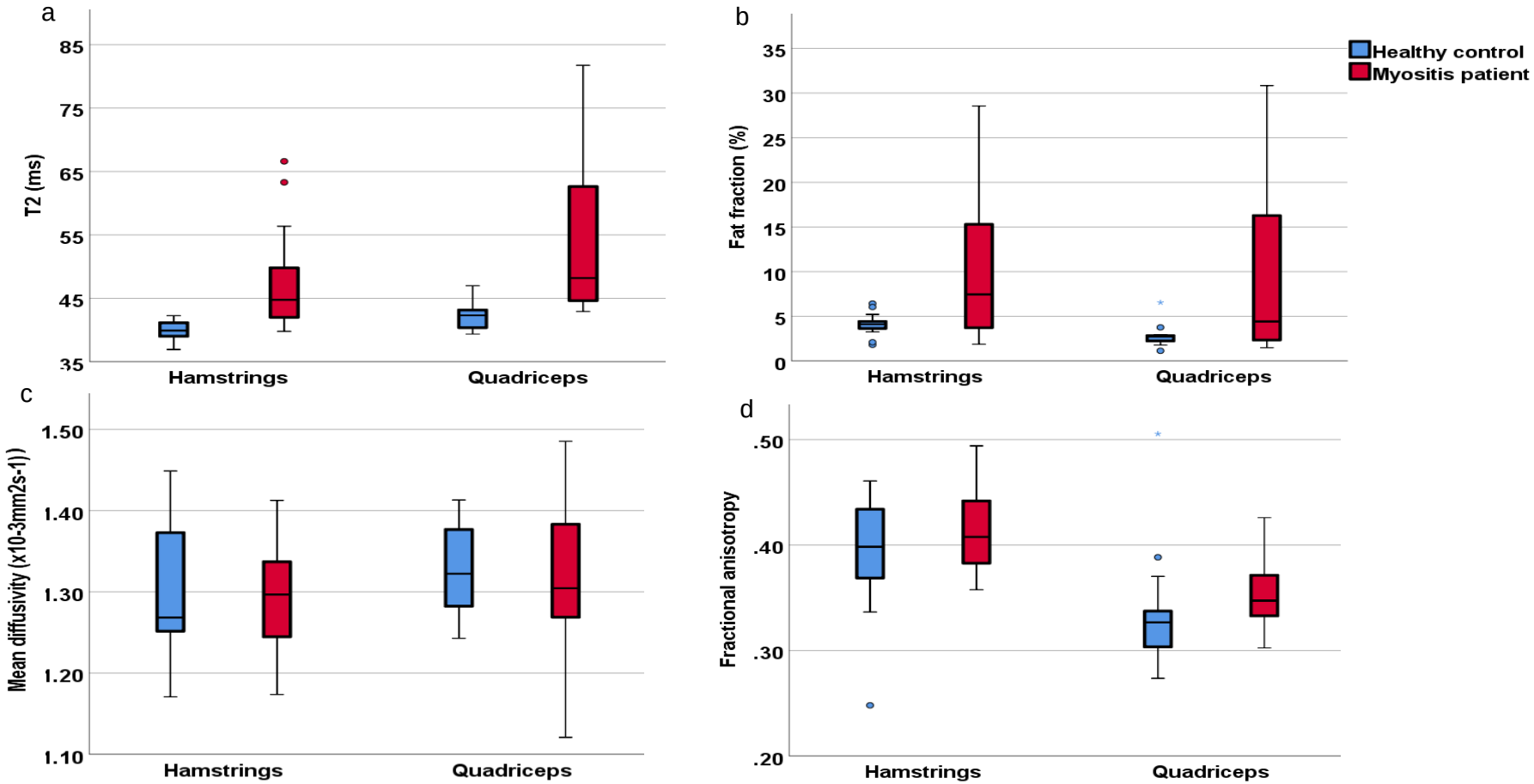

Figure 6-5: Quantitative MRI measurements in 16 patients with myositis compared to 16 healthy controls.

a) Quantitative T2 b) Quantitative fat fraction c) Quantitative mean diffusivity d) Quantitative fractional anisotropy.

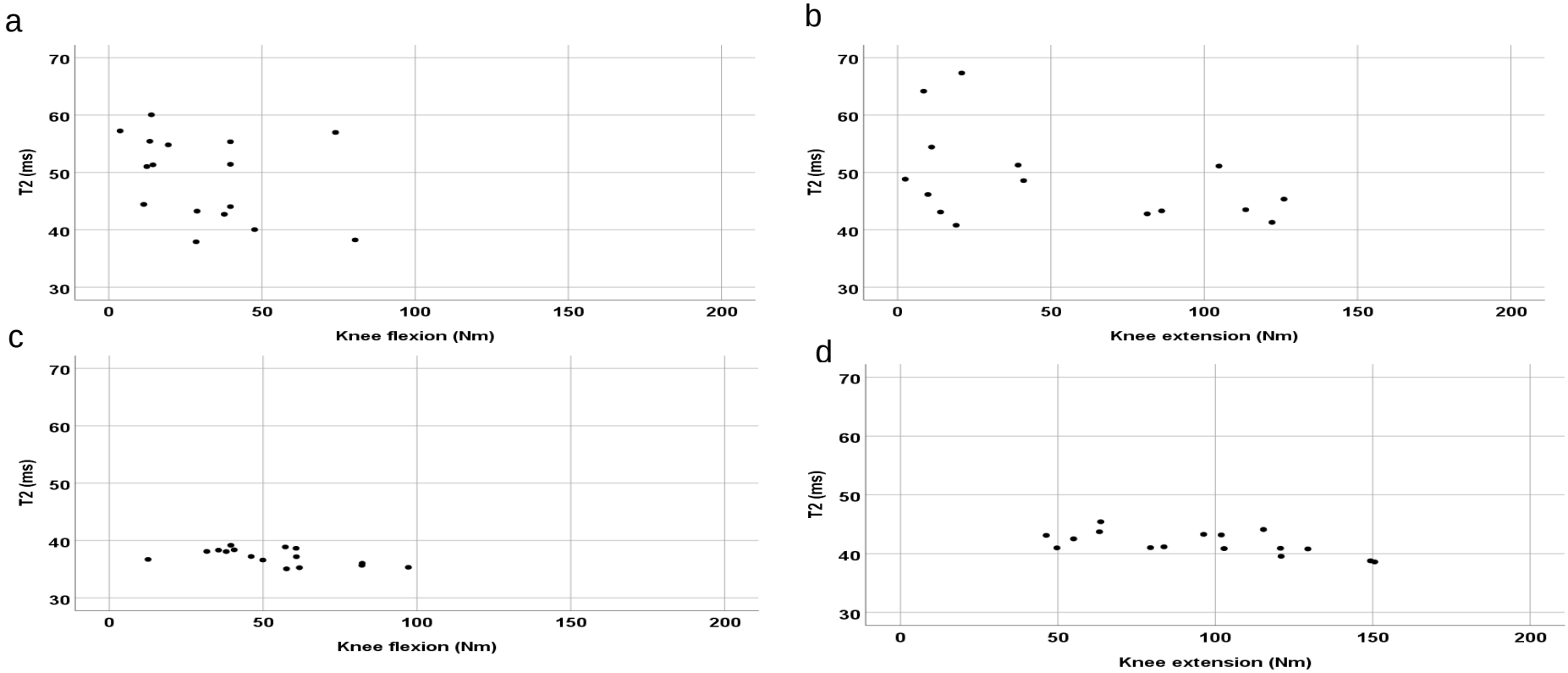

Figure 6-6: Quantitative T2 measurements.

Substantive correlation with peak torque flexion (hamstrings) and extension (quadriceps) in 16 patients with myositis and healthy controls in the a) Myositis patients hamstrings (rs=-0.4; p=0.1) b) Myositis patients quadriceps (rs = -0.7; p = 0.001) c) healthy control hamstrings (rs = -0.9; p<0.001) d) healthy control quadriceps.

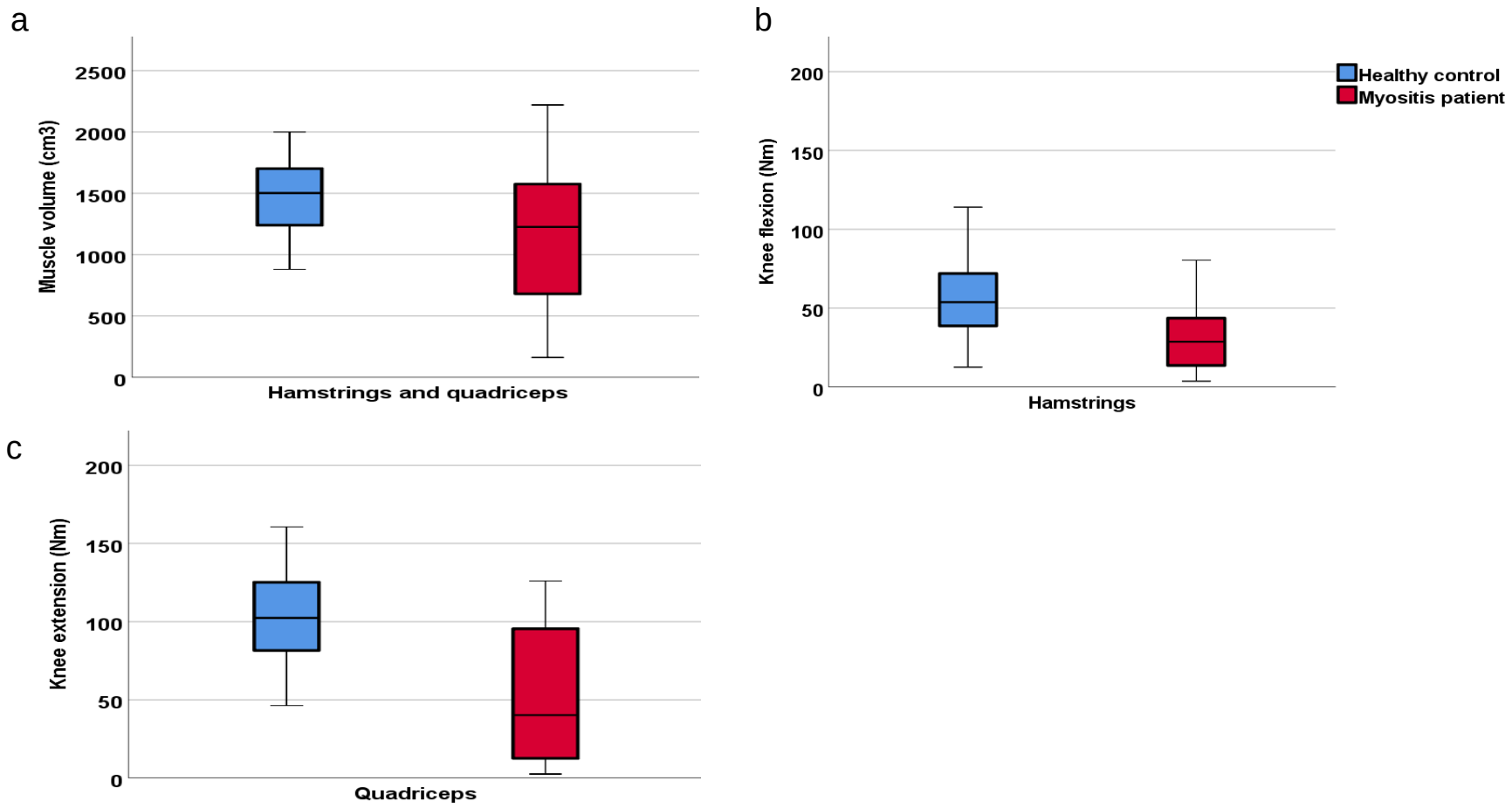

Figure 6-7: Quantitative muscle volume measurements, knee flexion and extension in 16 myositis patients compared to 16 healthy controls.

Muscle volume b) Knee flexion c) Knee extension.

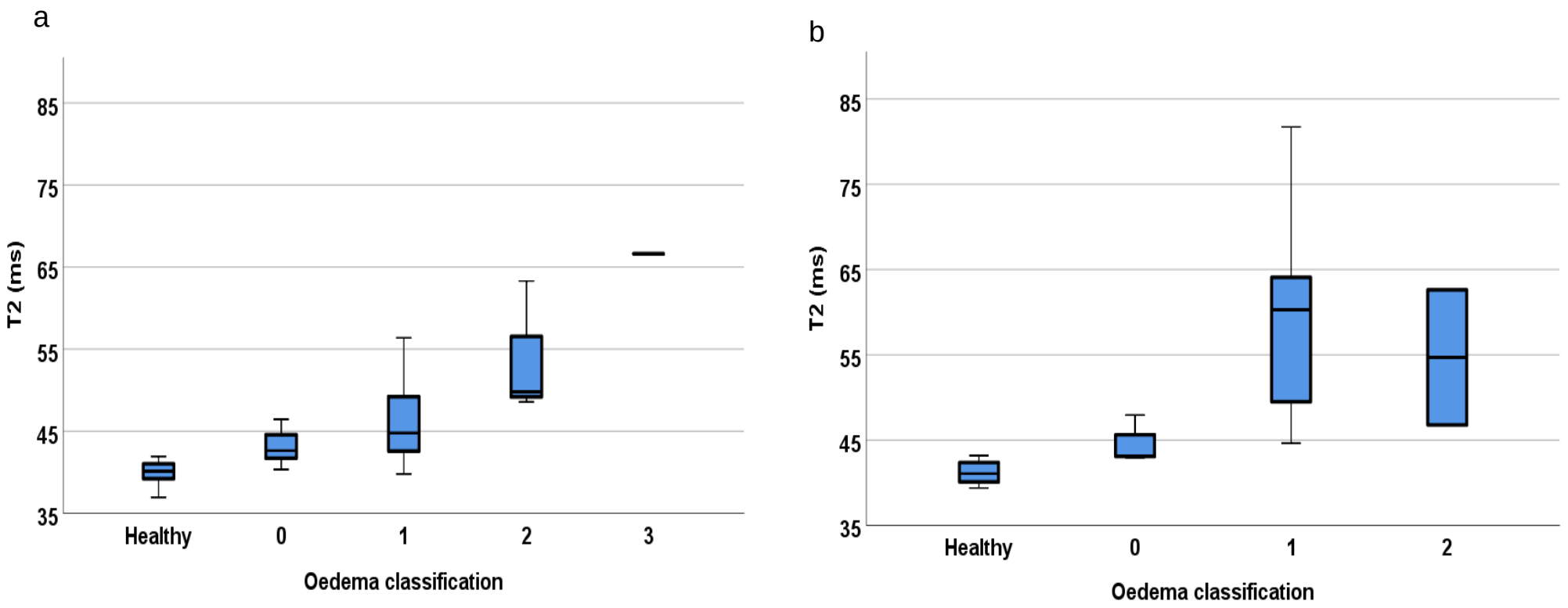

Figure 6-8: T2 values grouped by radiologists' oedema score compared with values in 16 matched healthy controls and 16 patients with myositis.

(0- no oedema, 1- mild oedema, 2- moderate oedema, 3- severe oedema a) hamstrings b) quadriceps. *Quadriceps had no grade 3 (severe oedema) scored.

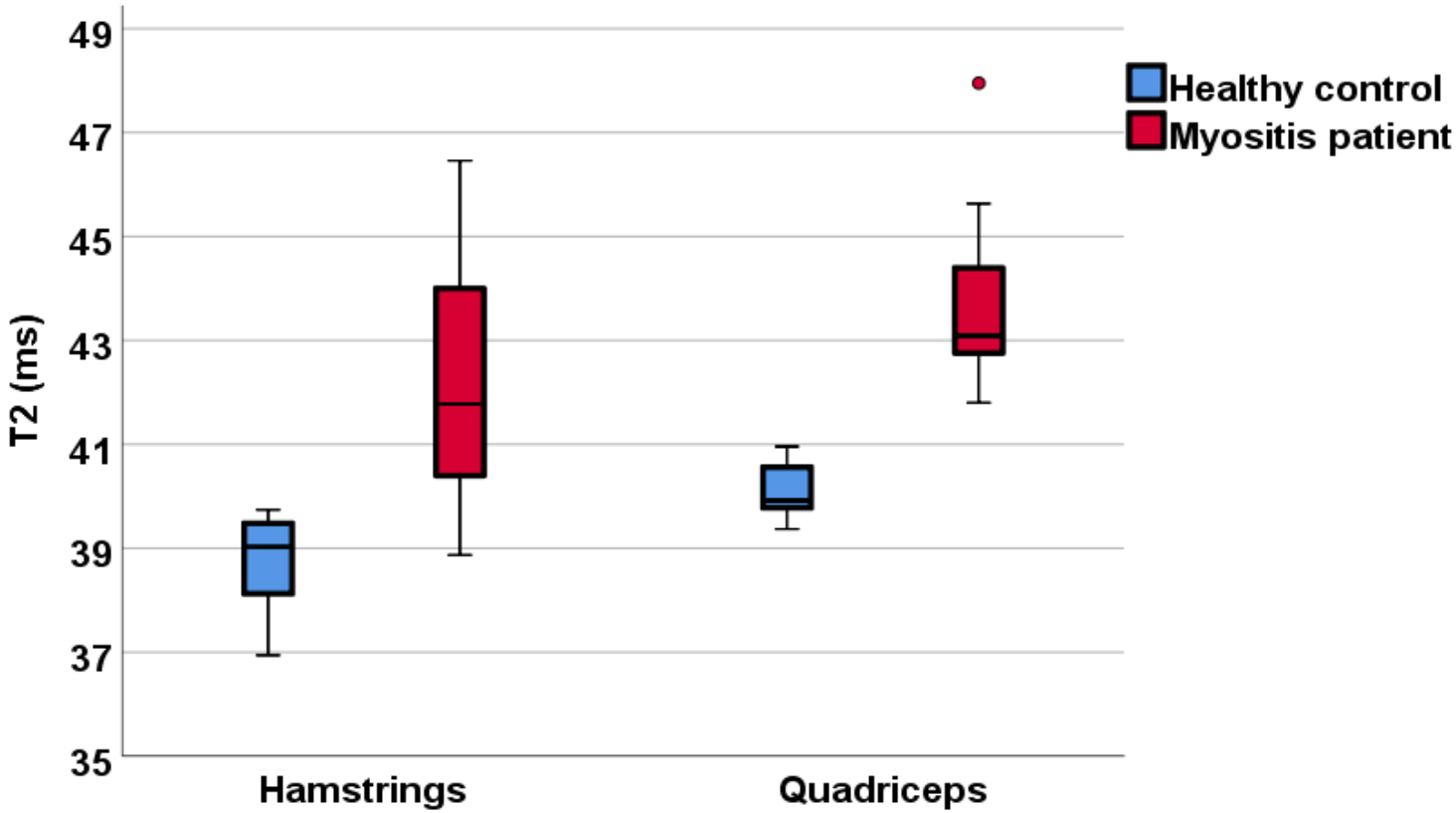

Figure 6-9: T2 values of patients scored as having unaffected muscles matched with age- and gender-matched healthy controls.

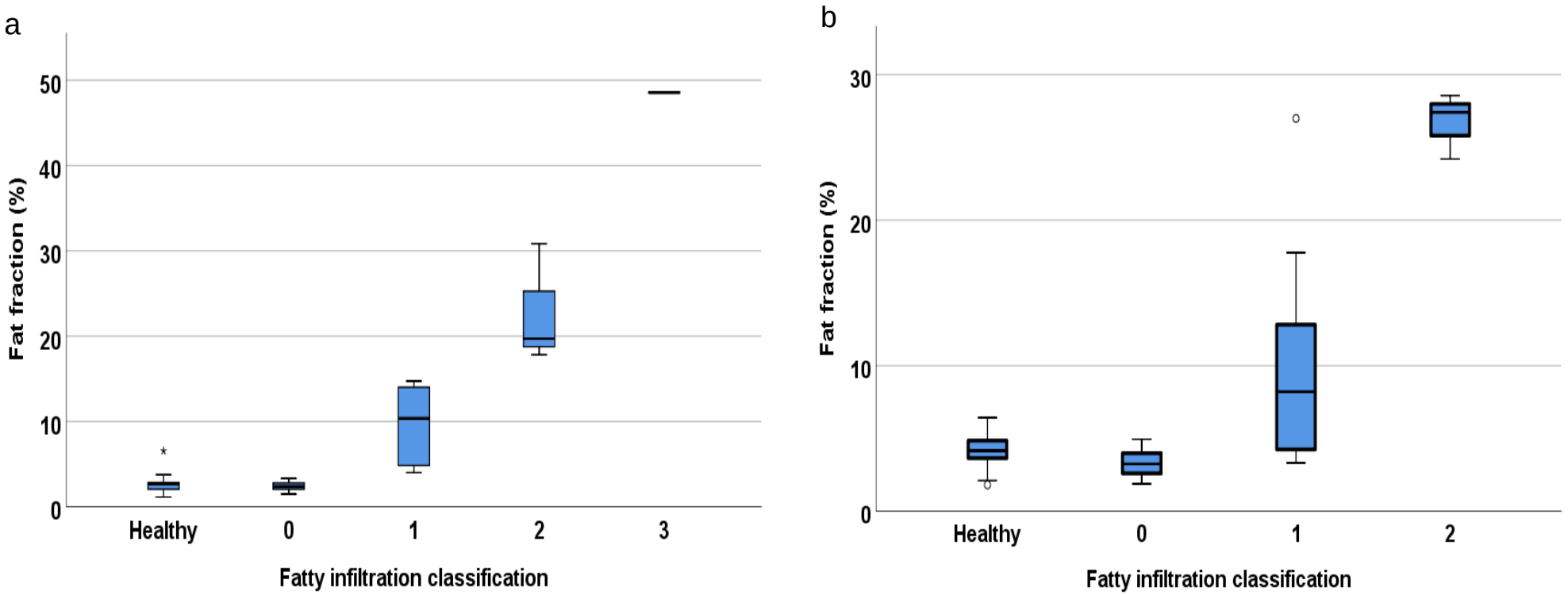

Figure 6-10: Fat fraction values grouped by radiologists' oedema score compared with values in patients with myositis.

(0- no fat infiltration, 1- mild fat infiltration, 2- moderate fat infiltration, 3- severe fat infiltration a) hamstrings b) quadriceps. *Quadriceps had no grade 3 (severe fat infiltration) scored.

6.4 Discussion

This chapter aimed to assess whether quantitative MRI can detect differences between the muscles of patients with myositis and age-and-gender matched healthy controls, and to assess how T2 and fat fraction compares to radiologist scoring for muscle oedema and fat infiltration.

In this study, the utility of quantitative MRI as an indicator of active disease and muscle damage in dermatomyositis and polymyositis patients compared with healthy controls was investigated. As expected, there were substantive differences in T2, fat fraction, and muscle volume between patients with myositis and matched healthy controls. However, this study advanced knowledge by demonstrating that differences in quantitative T2 remained substantial even when myositis patients who had been classified as ‘unaffected’ by radiologists’ on STIR and T1-weighted sequences were compared with matched healthy controls. Following the results from this study, it could be speculated that these measures may be a useful non-invasive measure in the diagnosis and monitoring of myositis. The receiver operator characteristic analysis corroborates this hypothesis which demonstrates that T2 and fat fraction measurements could be useful in the diagnosis of myositis.

T2 was substantively higher in patients with myositis compared to healthy controls, which is consistent with previous studies (115, 377). This increase in T2 measured by quantitative MRI may be due to the combined effects of increased fat [10,43], inadequately suppressed by the SPAIR fat suppression, and increased fluid due to inflammation (364). Although most papers, using fat corrected T2 measurements, show increased T2 in myositis (115, 378). Schlaeger et al. found that T2 can decrease in neuromuscular disease patients (379). However, their study sample was heterogeneous, including a range of muscular diseases along with myositis.

In this study, the patient T2 values correlated with radiologists’ visual scoring of muscle pathology, showing, for the first time, that changes in T2 agree with the

radiological assessment of active disease. However, in Figure 6-8, it needs to be considered that only two patients had a score of 2. Therefore, the lack of a systematic effect is explained by the small number of eligible participants**.** The fact that the eight myositis patients, classified as unaffected by radiologists on STIR sequences, showed substantively raised T2 compared to healthy controls suggests that there is a certain threshold of muscle pathology that is required before myositis can be visually detected on conventional MRI STIR sequences. These results suggest that quantitative T2 measurements could be used in conjunction with the visual assessment of muscle to improve diagnostic sensitivity. In particular, it suggests that relying on subjective assessment using STIR sequences may fail to identify low-grade inflammation in the muscle and subtle changes in disease activity. It also suggests that muscles classified as unaffected, but with elevated T2, may be a useful target for muscle biopsy. Indeed, the use of quantitative measures may increase the number of sites available for biopsy and identify sites which are technically less challenging and safer for biopsy.

This study demonstrated, for the first time, that T2 correlates with muscle strength. However, the relationship in this study appears to be bimodal, giving the plots a characteristic ‘L-shape.’ This bimodal relationship suggests that after a certain threshold of T2, muscle strength deteriorates at a substantive rate. Further work is required to characterise this relationship better. In healthy individuals, T2 had a linear correlation with muscle strength, and lower T2 values were associated with increased strength, suggesting that T2 is associated with physical function in both healthy individuals and patients with myositis.

Patients’ fat fraction values were higher in both the hamstrings and the quadriceps compared to healthy controls, which is consistent with the known fat infiltration that occurs due to myositis. This study showed for the first time that fat fraction correlated with muscle strength within the quadriceps and the hamstrings in myositis patients. The results of this study are in agreement with a study that found an inverse relationship between muscle strength and fat infiltration in Duchenne

muscular dystrophy patients (380). The results from this study support the hypothesis that when fat infiltration increases due to myositis, muscle strength decreases, and this can be identified by quantitative MRI fat fraction.

There was a substantive difference in muscle volume between myositis patients and healthy controls, and it was found that, in both patients and healthy controls, muscle volume correlated with muscle strength. These results confirm that muscle volume and muscle strength are related, and that muscle loss is apparent in myositis. The results from this study agree with previous studies that suggest that muscle volume is an important measure in terms of muscle function and that interventions such as exercise to increase muscle mass might be beneficial for function and to improve quality of life in myositis patients (381).

Diffusion tensor imaging measurements showed no meaningful differences in mean diffusivity, fractional anisotropy, or eigenvalues between myositis patients and healthy controls. This finding disagrees with previously published work (382). Given that T2 relaxation times were longer in patients, one might expect to see raised mean diffusivity due to increased fluid. However, increased fat infiltration, which was observed in this study, is known to occur in myositis, has been demonstrated to restrict diffusion (26).

Ai et al. used small regions of interest over diseased areas (382) as opposed to the regions of interest in this study depicting the entire muscle (Figure 6-2). The differences in the results observed in this study could be due to the competing influences of fat and water across the whole muscle in the large regions of interest used in this thesis. In contrast, the measurements by Ai et al. would be dominated by reduced mean diffusivity due to fat in the small regions of interest focussed on the fat infiltrated area of muscle.

The results from the sub-study in this chapter investigating diffusion measurements, which utilised small regions of interest, support this theory (26). This sub-study found an increase in mean diffusivity in oedematous regions and a decrease in mean diffusivity in fat infiltrated regions. This finding suggests that diffusion measurements may be useful in the management of myositis but should be used with small regions of interest due to the competing influence of fat and oedema on the measurements.

This study successfully met its aims and demonstrated that quantitative MRI can detect substantive differences between patients with myositis and matched healthy controls. In addition, this study demonstrated that T2 and fat fraction correlate with radiologist scoring for muscle oedema and fat infiltration. Furthermore, it was demonstrated that quantitative T2 measurements were more sensitive at identifying oedema than conventional radiology using STIR MRI sequences assessed by radiologists. However, fat fraction did not appear to be more sensitive at identifying fat infiltration compared to radiologists using T1 weighted MRI sequences to assess myosteatosis in the muscle on visual inspection.

6.4.1 Limitations

Within this study, patients were on medication that may affect muscle; however, data on the duration of exposure to such treatments were not collected. Therefore, it could be speculated that any changes observed may be due to the effect of medication. This study did not consider BMI or disease duration, which could influence muscle quality. Future research should consider matching for the duration of disease, treatment, and BMI. It was not essential for a patient to have a positive muscle biopsy for myositis to take part in this study. Future research could include only patients with a biopsy confirmed myositis diagnosis to ensure a homogenous cohort.

6.5 Conclusions

In conclusion, this study demonstrated differences in quantitative muscle strength and MRI T2, fat fraction, and muscle volume between patients with myositis and age- and gender-matched healthy controls. The results of this study suggest that these measurements, in particular muscle strength, T2, fat fraction, and muscle volume could be used as an objective method to monitor muscles. Furthermore, this study demonstrated for the first time that T2, fat fraction and muscle volume correlated with muscle function in patients with myositis, potentially identifying a relationship between inflammation, myosteatosis, muscle atrophy, and function in patients with myositis.

The results from the sub-study show that mean diffusivity can identify the changes within the muscle that occur due to myositis, however, due to the opposite influences of oedema and fat infiltration, regions of interest must be selected based on their clinical features.

This study has also shown that quantitative T2 measurements are sensitive to differences that may not be detected by radiologists on T2 weighted STIR sequences, potentially offering an improvement in the ability of MRI to detect changes in disease activity compared to reliance on subjective assessment using STIR MRI sequences. The use of quantitative techniques may also identify additional sites of muscle inflammation as a target for a diagnostic biopsy. This work will inform future efforts to validate quantitative MRI measurements as a diagnostic and management tool in myositis.

6.6 Key messages

- There are substantive differences in T2, fat fraction, and muscle volume between patients with myositis and age- and gender-matched healthy controls.
- Quantitative MRI correlates with muscle function in patients with myositis.
- Quantitative T2 MRI can identify differences in radiologist scored unaffected muscle in patients with myositis compared to age- and gender-matched healthy controls.
- Mean diffusivity increases due to oedema and decreases due to fat infiltration.

Chapter 7 Muscle deterioration due to rheumatoid arthritis: Assessment by quantitative MRI and strength testing

This chapter describes a research study by Matthew Farrow, John Biglands, Steven Tanner, Elizabeth Hensor, Maya Buch, Paul Emery, and Ai Lyn Tan published in Rheumatology, 2020 (5).

7.1 Introduction

Rheumatoid arthritis (RA) is a chronic, progressive, autoimmune, inflammatory disease with a prevalence of 0.8% in the UK (383). It is characterised by a symmetrical polyarticular arthritis and can result in significant disability. RA is a multisystem disease associated with a reduction in life expectancy. The usual presenting symptoms of RA are joint pain, stiffness, and swelling. For the patient's quality of life, it is vital to recognise the disease early and treat it effectively from the beginning. Management of RA aims to achieve clinical disease remission, which is associated with improved physical function and reduced radiographic progression.

As well as joint damage, RA is also associated with altered body composition (384). This altered body composition could be due to: an inactive lifestyle as a result of the disease causing pain or fear of making the disease worse, drug-induced myopathies such as steroid treatment (385, 386), or the activation of the nuclear factor kappa-beta pathway (NF-κB), which triggers metabolic alterations leading to the degradation of muscle tissue (387). Furthermore, the production of tumour necrosis factor-alpha (TNF-α) and other inflammatory cytokines, which are critical to the pathogenesis of RA, are reported to have catabolic effects on skeletal muscle (388). These combined factors can result in rheumatoid cachexia (389, 390).

Rheumatoid cachexia is characterised by increased inflammatory biomarkers in the muscle, muscle atrophy, changes in muscle fibre microstructure, and decreased muscle strength, with the preservation, or increase, of adipose tissue (123). The prevalence of rheumatoid cachexia is not known as there is no consensus on its definition and assessment. However, approximately 40% of patients with active RA suffer from rheumatoid cachexia (124), making it one of the most common complications of RA. Rheumatoid cachexia is associated with increased disease severity and fatigue, reduced quality of life, and can accelerate age-related sarcopenia (391-393). Therefore, muscle health is an important aspect of RA that should be considered. However, it is currently unknown at what stage muscle involvement begins in patients with RA, and if the muscle damage that is caused by the disease is reversed when patients achieve disease remission.

Historically, the gold standard for imaging in RA was conventional radiography (X-ray). However, conventional radiography is not able to assess disease activity (394). Ultrasound has shown great promise in assessing joints for disease activity and pathology, including the detection of synovitis, and is frequently integrated into the clinical management of patients with RA (395, 396). MRI has also been demonstrated to be suitable for identifying pathology in the joints of patients with RA, particularly of the wrist and hand, and is a sensitive measure of synovitis (397, 398). A recent review by Castensen et al. published in 2020 summarises that MRI can detect RA at early stages and predict the course of the disease; however, further research is required (399).

Despite the many causes of muscle involvement in inflammatory arthritis, there are few muscle imaging studies in RA. Medical imaging techniques such as quantitative MRI, discussed in section 2.4.3, can non-invasively measure the imaging biomarkers associated with muscle pathology, which is observed in patients with rheumatoid cachexia. Therefore, quantitative MRI may be able to provide further information regarding muscle health in patients with rheumatoid arthritis and aid in the management of the disease, including assisting in the development of

preventative and therapeutic strategies, such as exercise, medication, and supplements.

The purpose of this study was to estimate, using quantitative MRI, the extent to which muscle state may differ from matched healthy controls in different stages of RA progression.

7.1.1 Hypothesis

Quantitative MRI can detect differences in the muscles of patients with rheumatoid arthritis compared to age- and gender-matched healthy controls.

7.1.2 Objectives

The aim of this study was to obtain and compare preliminary data comparing quantitative MRI measurements between patients with rheumatoid arthritis who were newly diagnosed, those with persistently active disease, and those in clinical remission with age- and gender-matched healthy controls.

7.2 Methods

7.2.1 Study design

This study was a cross-sectional pilot study conducted at the Leeds Teaching Hospitals Trust. Recruitment started in May 2017 and finished in December 2018. Fifty-two participants were recruited into four separate groups of 13 participants

each: (1) New rheumatoid arthritis patients who were treatment naïve; (2) Rheumatoid arthritis patients who had persistent active disease for at least one year; (3) Rheumatoid arthritis patients in sustained remission for at least one year; (4) Healthy controls (HC). The four groups (3 RA and 1 HC) were age- and gender-matched. Healthy controls were obtained from the pool of healthy controls recruited for the MUSCLE study.

The RA patients within this study were recruited from clinics at Chapel Allerton Hospital. New RA patients partook in the study on the same day as their initial diagnosis. Clinical parameters collected included: Body mass index (BMI), Disease Activity Score (DAS28), early morning stiffness, medication, disease duration, patient global assessment of disease activity visual analogue scale (VAS), and inflammatory biomarkers (CRP and ESR).

All RA patients within this study had an established diagnosis of RA based on the 2010 ACR/EULAR classification criteria (400). Patients were classified as (1) ‘New rheumatoid arthritis’ if they were newly diagnosed with rheumatoid arthritis and had not previously taken disease-modifying antirheumatic drugs (DMARDs) or steroids. Patients were classified as (2) ‘Active rheumatoid arthritis’ if they had a clinical diagnosis of active rheumatoid arthritis for more than one year, had a DAS28 higher than 3.2 at the time of recruitment, and had at least two of the following markers of active disease within the past 12 months:

- (2.1) raised inflammatory markers;
- (2.2) requiring steroid therapy;
- (2.3) DAS higher than >3.2 at a second time-point within 12 months;
- (2.4) escalation to or recent changes in biologic medication.

Patients were classified as (3) ‘remission rheumatoid arthritis’ if they had a diagnosis of rheumatoid arthritis for more than one year, were in clinical remission for the past 12 months determined by clinical opinion, a DAS28 lower than 2.6 at

the time of recruitment, and did not have a DAS28 higher than 2.6 in the past 12 months.

7.2.2 MRI and muscle strength measurements

MRI measurements collected include T2, fat fraction, diffusion tensor imaging, and muscle volume. Muscle function measurements collected include knee extension, knee flexion, and handgrip strength. This methodology has been described in section 3.6.

7.2.3 Statistical analysis

Statistical analyses were performed using SPSS. One-Way ANOVA with Dunnett's post-hoc analysis was used to test for potential significant differences in quantitative MRI (T2, FF, DTI, and muscle volume) and muscle strength measurements (knee flexion, knee extension, and handgrip) between the different RA patients' disease stages and healthy controls. Spearman's rank correlation was used to measure correlation. This study utilised r_s values ≥ 0.7 as indicative of a strong correlation and r_s ≥ 0.4 as indicative of a weak correlation (401).

7.3 Results

There were 75 patients recruited into the MUSCLE study who had RA. No patients declined to take part. The patients were categorised into the three groups of RA patients. There were 27 newly diagnosed RA patients, 13 patients with active disease, and 35 patients in clinical remission. To enable age- and gender-matching, all RA groups and healthy controls were matched with the 13 RA patients with active disease. Therefore, this study included 52 participants in total, with 13 patients in each of the three RA groups and 13 participants in the healthy control group for statistical analysis. Each of the four groups consisted of ten females and three males (Table 7-1). At the time of the study, the 26 RA patients with active disease and those in remission were on the following therapies: Prednisolone - 5/26 (19.2%), hydroxychloroquine - 5/26 (19.2%), methotrexate 16/26 (61.5%), rituximab - 4/26 (15.4%), tofacitinib - 1/26 (3.8%), etanercept - 1/26 (3.8%), infliximab - 1/26 (3.8%), and adalimumab 2/26 (7.7%). 11/39 (28%) of the patients were on lipid-lowering therapy (3 new RA: 1 each on simvastatin, atorvastatin and ezetimibe; 3 active RA: 1 simvastatin, and two on atorvastatin; 5 remission RA: 3 simvastatin, and two on atorvastatin). Most of the patients were receiving a combination of some of the above therapies. The patients with RA who were newly diagnosed and the healthy controls were on no treatment. Quantitative MRI and muscle strength results for the healthy controls and patients with RA are presented in Table 7-2 and Table 7-3.

The results of the one-way ANOVA demonstrate substantive differences between the four disease groups in T2, fat fraction, muscle volume, and muscle strength. However, it found no substantive differences in mean diffusivity or fractional anisotropy. The confidence intervals around the differences between the four disease groups excluded 0 and included potentially clinically meaningful differences (402), providing preliminary proof-of-concept of differences between RA patient groups that would merit further investigation.

Knee flexion (KF) and knee extension (KE) substantively correlated with T2 (KF r_s= -0.4, p= 0.05; KE r_s= -0.4, p= 0.04), fat fraction (KF r_s= -0.4, p= 0.05; KE r_s= -0.4, p= 0.04), and muscle volume (KF r_s= 0.7, p< 0.001; KE r_s= 0.7, p< 0.001). There was no evidence for a correlation with mean diffusivity (KF r_s= 0.2, p= 0.1; KE r_s= -0.1, p= 0.4) or fractional anisotropy (KF r_s= -0.3, p= 0.05; r_s= -0.3, p= 0.05).

Table 7-1: RA participant healthy characteristics

	Healthy controls [mean (s.d)]	New diagnosis [mean (s.d)]	Active disease [mean (s.d)]	Remission [mean (s.d)]	Difference (p-value)
Age (years)	64 (10)	63 (15)	65 (10)	67 (19)	0.2
Weight (kg)	71.4 (35)	78.6 (26)	77.5 (25)	68.3 (26)	0.06
Height (cm)	164.5 (20)	160 (22)	164 (27)	166 (14)	0.2
BMI (kg/m^2)	25 (5)	29 (10)	33 (11)	24 (6)	0.03
DAS28	N/A	5.2 (3)	4.8 (3)	1.7 (0.7)	<0.001
Patient visual analogue scale (out of 100)	N/A	39 (30)	45.8 (25)	12 (12)	<0.001
CRP (mg/l)	N/A	17 (11)	31.5 (59)	12.1 (7)	0.1
ESR (mm/h)	N/A	41.1 (31)	16 (29)	10.6 (28)	<0.001
Early morning stiffness (minutes)	N/A	63 (58)	71 (289)	2 (13)	<0.001
Disease duration (months)	N/A	N/A	123 (20)	74 (35)	0.001

Table 7-2: Quantitative MRI measurements with ANOVA to determine the significance

	T2 (ms)		Fat fraction (%)		Mean diffusivity ($x10^{-3}mm^2s^{-1}$)		Fractional anisotropy (Range 0-1)	
	Mean (95% CI)	p-value	Mean (95% CI)	p-value	Mean (95% CI)	p-value	Mean (95% CI)	p-value
Hamstrings								
Healthy control	39.3 (38.7, 39.9)	<0.001	4.7 (2.9, 6.4)	0.02	1.34 (1.28, 1.40)	0.6	0.39 (0.36, 0.44)	0.02
New RA	43.8 (42.2, 45.3)		7.7 (6.3, 9.1)		1.32 (1.27, 1.37)		0.37 (0.34, 0.39)	
Active RA	42.3 (41.1, 43.5)		6.8 (6.8, 11.1)		1.30 (1.27, 1.33)		0.40 (0.38, 0.42)	
Remission RA	43.3 (43.0, 45.5)		8.9 (7.2, 10.6)		1.31 (1.27, 1.34)		0.34 (0.3, 0.38)	
Quadriceps								
Healthy control	39.1 (38.6, 39.7)		4.4 (3.7, 5.2)		1.36 (1.26, 1.44)		0.33 (0.30, 0.36)	
New	41.1		9.1		1.29		0.40	

RA	(39.6, 42.6)	0.02	(7.2, 11.0)	<0.001	(1.27, 1.32)	0.5	(0.36, 0.42)	<0.001
Active RA	42.8 (41.9, 43.8)		7.3 (6.4, 8.1)		1.31 (1.29, 1.34)		0.35 (0.33, 0.37)	
Remission RA	40.6 (39.4, 31.9)		8.9 (7.4, 10.3)		1.32 (1.24, 1.40)		0.39 (0.38, 0.42)	

Table 7-3: Muscle volume, knee extension, knee flexion and handgrip strength measurements with ANOVA to determine the significance

	Muscle volume (cm^3)		Knee flexion strength (Nm)		Knee extension strength (Nm)		Handgrip strength (kg)	
	Mean (95% CI)	p-value	Mean (95% CI)	p-value	Mean (95% CI)	p-value	Mean (95% CI)	p-value
Healthy control	1453.5 (1258.9, 1648.2)	<0.001	51.8 (43.3, 60.1)	0.03	82.1 (66.1, 98.1)	0.5	30.8 (28.9, 32.8)	<0.001
New RA	936.2 (841.2, 1031.3)		33.4 (25.9, 40.8)		71.1 (52.2, 89.9)		12.8 (11.1, 14.15)	
Active RA	1083 (984.2, 1181.8)		41.7 (26.6, 56.9)		62.5 (38.5, 86.6)		17.2 (12.5, 21.8)	
Remission RA	1141.2 (962.2, 1320.4)		38.5 (26.8, 50.2)		76.4 (55.2, 97.5)		28.9 (23.4, 32.7)	

7.3.1 T2

T2 relaxation times were longer in all RA patient groups compared to healthy controls. Longer T2 relaxation times (higher signal) indicates water which suggests possible inflammation, or increased olefinic fat which was not adequately suppressed, due to rheumatoid arthritis. However, a muscle biopsy is required to confirm this inference. Within the hamstrings, differences between healthy controls versus new patients, active patients, and remission patients were 4.5ms (95% CI= 2.5, 6.4; p< 0.001), 3.0ms (95% CI= 1.1, 4.9; p= 0.001), and 5.0ms (95% CI= 3.0, 6.4; p< 0.001) respectively. Within the quadriceps, differences were 2.6ms (95% CI= 0.2, 3.7; p= 0.02), 3.6ms (95% CI= 1.9, 5.4; p< 0.001), and 1.5ms (95% CI= -0.3, 3.3; p= 0.1) respectively (Figure 7-1).

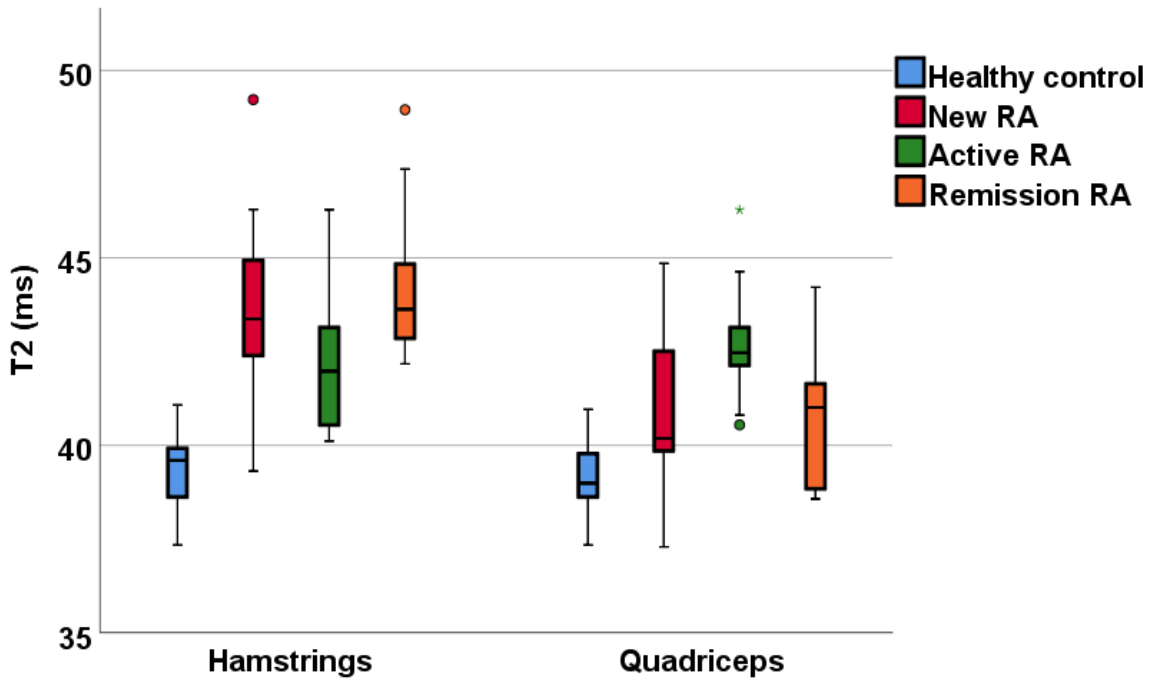

Figure 7-1: Quantitative T2 measurements of patients with RA and healthy controls

7.3.2 Fat fraction

MRI fat fraction measurements within the muscle were substantively higher in all rheumatoid arthritis patient groups compared to age- and gender-matched healthy controls, suggesting fat infiltration into the muscle due to rheumatoid arthritis. Within the hamstrings, differences between healthy controls versus new patients, active patients, and remission patients were 3.0% (95% CI= 0.2, 5.8; p= 0.03), 4.2% (95% CI= 1.6, 6.8; p= 0.002), and 4.2% (95% CI= 1.4, 7.0; p= 0.002) respectively. Within the quadriceps differences were 4.6% (95% CI= 2.7, 6.5; p< 0.001), 2.7% (95% CI= 1.6, 3.9; p< 0.001), and 4.9% (95% CI = 2.8, 5.9; p< 0.001) respectively (Figure 7-2).

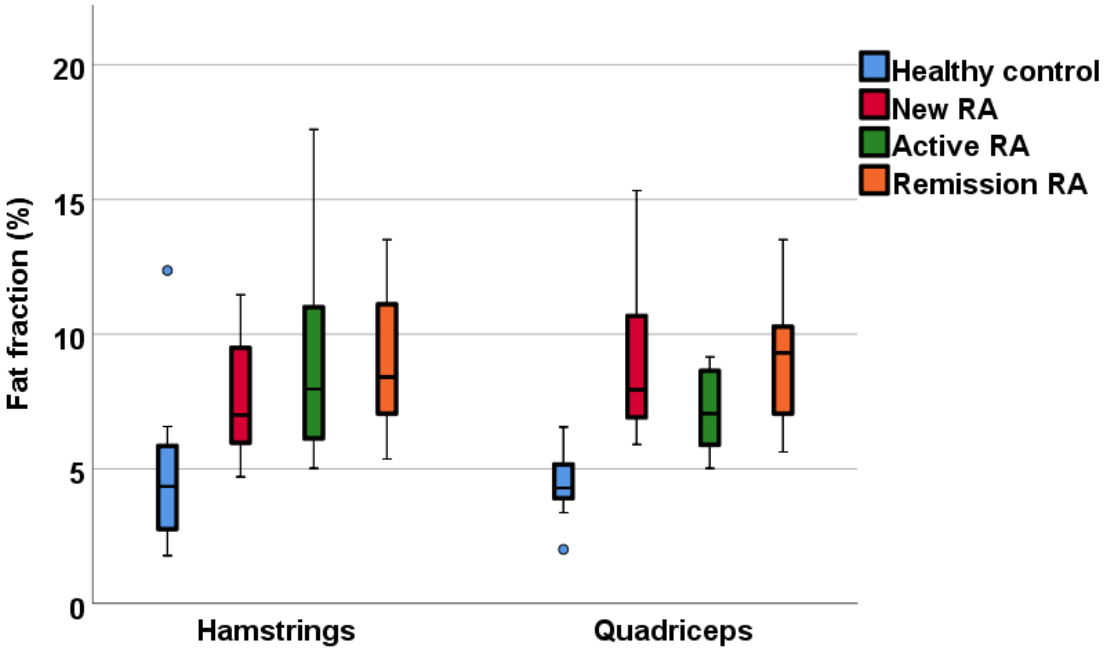

Figure 7-2: Quantitative fat fraction MRI in patients with RA and healthy controls

7.3.3 Diffusion tensor imaging

7.3.3.1 Mean diffusivity

For mean diffusivity, confidence intervals around the differences for all rheumatoid arthritis patient groups compared to healthy controls included 0 and did not include clinically meaningful differences. Within the hamstrings, differences between healthy controls versus new patients, active patients, and remission patients were $0.02x10^{-3}mm^2s^{-1}$ (95% CI= 0, 0.05; p= 0.9), $0.04x10^{-3}mm^2s^{-1}$ (95% CI= -0.1, 0.07; p= 0.4), and $0.03x10^{-3}mm^2s^{-1}$ (95% CI= 0, 0.04; p= 0.6) respectively. Within the quadriceps, differences were $0.07x10^{-3}mm^2s^{-1}$ (95% CI= -0.16, 0.04; p= 0.3), $0.05x10^{-3}mm^2s^{-1}$ (95% CI= -0.14, 0.06; p= 0.6), and $0.04 \times 10^{-3}mm^2s^{-1}$ (95% CI= -0.1, 0.06; p= 0.7) respectively.

7.3.3.2 Fractional anisotropy

There were no clinically meaningful differences in fractional anisotropy between rheumatoid arthritis patients and healthy controls. Within the hamstrings, differences between healthy controls versus new patients, active patients, and remission patients were 0.02 (95% CI= -0.08, 0.02; p= 0.4), 0.01 (95% CI= -0.05, 0.06; p= 0.9), and 0.05 (95% CI= -0.1, 0.004; p= 0.03) respectively. Within the quadriceps differences were 0.07 (95% CI= 0.03, 0.1; p= 0.01), 0.02 (95% CI= -0.02, 0.06; p= 0.6), and 0.06 (95% CI= 0.02, 0.1; p= 0.01) respectively.

7.3.4 Muscle volume

Muscle volume was substantively lower in all rheumatoid arthritis groups compared to healthy controls, suggesting muscle atrophy due to rheumatoid arthritis. Within the thigh, differences between healthy controls versus new patients, active patients, and remission patients were -517.3cm^3 (95% CI= -751, -283; p< 0.001), -370.5cm^3 (95% CI= -605, -136; p= 0.001), and -312.3cm^3 (95% CI= -546. -77; p= 0.006) respectively (Figure 7-3).

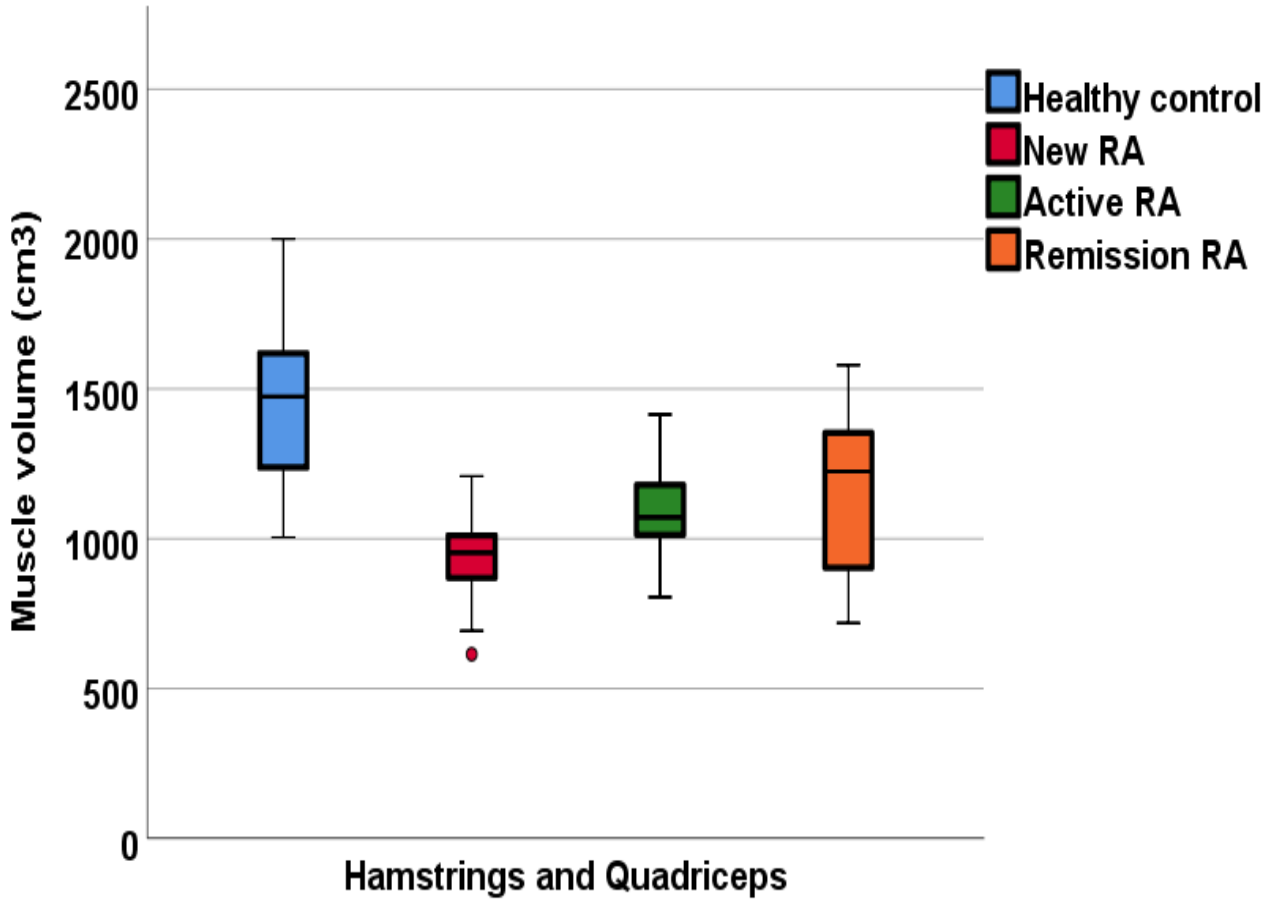

Figure 7-3: Quantitative muscle volume MRI measurements in patients with RA and healthy controls

7.3.5 Muscle strength assessments

Muscle strength was substantively lower in new rheumatoid arthritis patients compared to healthy controls, suggesting a decrease in strength due to rheumatoid arthritis; however, confidence intervals for active and remission patients included 0. Peak flexion (hamstrings) differences between healthy controls versus new patients, active patients, and remission patients were 18.4Nm (95% CI= -35, -1; p= 0.03), 10.1Nm (95% CI= -27, 7; p= 0.3), and 13.3Nm (95% CI= -33, 0; p= 0.1) respectively. Peak extension (quadriceps) differences between healthy controls versus new patients, active patients, and remission patients were 11Nm (95% CI= -45, 22; p= 0.7), 19.6Nm (95% CI= -52.7, 12.5; p= 0.3), and 5.7Nm (95% CI= -40, 28; p= 0.9) respectively. Grip strength differences between healthy controls versus new patients, active patients, and remission patients were 18kg (95% CI= -26, -10; p< 0.001), 13.6kg (95% CI= -22, 05; p< 0.001), and 1.9kg (95% CI= -10, 5; p= 0.8) respectively.

7.4 Discussion

This chapter aimed to explore whether quantitative MRI can detect differences between the thigh muscles of patients with rheumatoid arthritis and healthy controls and to establish whether these measures are sensitive enough to assess the muscle phenotype of different disease stages.

This study suggests that muscle health may be substantively affected in patients with RA from the time of diagnosis compared to age- and gender-matched healthy controls. However, this study did not investigate when decreases in muscle health, including changes in T2, fat fraction, and muscle volume, would have onset within

the natural history of the disease. Future research should investigate the timeline of the appearance of muscle pathology during the disease process. This future research could recruit healthy participants with family members with RA, who are therefore more likely to develop RA, and identify if these quantitative MRI measurements may be able to predict RA, and at what point symptoms may occur.

Within this study, muscle strength was substantively lower in new rheumatoid arthritis patients compared to matched healthy controls. This finding is surprising as it would be expected that decreases in muscle strength would occur later in the disease. It could be speculated that decreases in muscle strength are early features of the disease, potentially due to the decreases in muscle quality observed within this study, with longer T2 relaxation times, increased fat fraction and decreased muscle volume. However, it must be considered that the decreased muscle strength measures for patients with new and active RA may have been due to pain within the joints involved in the examined movement (i.e. quadriceps strength (knee extension), hamstrings strength (knee flexion), and handgrip strength (small joints of the hand)).

This study also provides preliminary evidence that muscle health may not return to normal as determined by quantitative MRI and muscle strength measurements even when patients achieve long term clinical remission. This is an important finding, as it could be speculated that when patients achieve clinical remission, their muscle health, including muscle quality parameters assessed by quantitative MRI (fluid content, myosteatosis, and muscle mass) and muscle strength, would not be substantively different compared to matched healthy controls. However, the data within this study suggests that physical function is still compromised despite achieving clinical remission, which is possibly due to the muscle pathology that is still present and is detectable using quantitative MRI.

This study has provided proof-of-concept that there are differences in quantitative MRI measurements and muscle strength measurements between patients with RA and healthy controls. These differences were detectable in new, active, and remission disease states. The results of this study suggest that clinically important muscle changes may occur in the early stages of RA and persist throughout the disease duration, even in long term clinical remission. These results suggest that current RA treatment, while proven to be effective in controlling the disease, may not be influencing the pathology affecting the muscle and it may be beneficial to include muscle-strengthening interventions in the treatment pathway for RA. If these preliminary results are confirmed, then MRI has the potential to be used as a diagnostic guide and management tool in the assessment of skeletal muscles in patients with RA.

T2 measurements were substantively raised in RA patient groups compared to healthy controls, suggesting the presence of increased inflammation and oedema within the thigh muscles of patients with RA (325). However, it must also be considered that T2 measurements may be identifying myosteatosis as well as oedema, due to the fat suppression not suppressing the olefinic fat. Therefore, it is crucial to interpret quantitative T2 measurements as muscle inflammation, oedema, and myosteatosis. Future work should consider including a spectroscopic assessment of fat to offset the error in the T2 measurements caused by the myosteatosis.

Fat fraction measurements were substantively increased in RA patient groups compared to healthy controls consistent with the known increase in fat mass in patients with RA. These results support previous work using CT scans that determined that skeletal muscle fat accumulation is higher in individuals with RA compared to healthy controls. They also found that patients with RA present with similar fat infiltration as older individuals (403). This decrease in muscle health suggests that RA may mimic a premature ageing process, such as sarcopenia, within the muscle. This decrease in muscle health is important to consider, as

muscles which could be perceived as undergoing normal fat infiltration due to age may be undergoing pathological changes due to the disease and should not be disregarded.

Muscle volume measurements suggested clinically substantive differences between all the RA groups compared to healthy controls. The results from this study agree with Baker et al. who showed that patients with RA have significant skeletal muscle atrophy compared to healthy controls which result in a decrease in strength (119). However, Helliwell and Jackson (404) demonstrated that the reduction in strength occurs at a faster rate than the loss of muscle mass demonstrating the importance of not only assessing muscle mass but also assessing muscle strength and muscle quality. The results in this chapter found that muscle strength was lower in all RA patient groups compared to healthy controls, even in the RA patients who had achieved long term remission. In addition, this study found that muscle volume was lower in all RA patients, including newly diagnosed treatment naïve RA patients. The results in this chapter suggest that the difference in muscle volume is smallest for those in clinical remission for RA compared to age- and gender-matched healthy controls. However, this may still be clinically important to consider, as the muscle volume has still not returned to the same quantity as age- and gender-matched healthy controls.

Interestingly, there were substantive differences in fat fraction and muscle volume in patients with RA, including in treatment naïve patients. This finding is surprising, as it would be expected that fat infiltration and muscle atrophy would occur in later stages of the disease, due to the long-term inflammation and changes in lifestyle. It is unknown why fat infiltration and muscle atrophy occurred so early, however, it could be speculated to be due to deleterious lifestyle habits of patients with disease activity, such as partaking in less physical exercise, or because the pathological changes within the muscle tissue are part of early clinical features of the disease.

This study suggests that interventions should be integrated into the care of patients with RA in clinical remission to return muscle mass levels to that of healthy controls. In addition, for the first time, this research has shown that muscle volume measured with quantitative MRI correlates with muscle strength in patients with RA. This correlation suggests that muscle volume is a promising patient-relevant assessment tool. Therefore, it could be speculated that if efforts were pursued to increase muscle volume in patients with RA, their physical function might improve, which could have significant implications for their wellbeing.

Mean diffusivity and fractional anisotropy did not show substantive differences in patients with RA compared to age- and gender-matched healthy controls. Given that T2 times were longer in RA, one might expect to see raised mean diffusivity due to increased fluid. However, the increased myosteatosis seen in this study could also restrict diffusion and thereby decrease mean diffusivity, as demonstrated within the myositis study conducted as part of this thesis (4). Within this study, diffusion measurements showed no statistical or clinically significant difference. These findings suggest that mean diffusion and fractional anisotropy measurements are not beneficial in the assessment of muscle in patients with rheumatoid arthritis.

Handgrip strength, knee extension, and knee flexion were lower in RA groups compared to healthy controls. This decrease in muscle function could be due to a sedentary lifestyle, joint deformity, pain, or stiffness, which are all factors associated with muscle deconditioning, muscle wasting, and subsequent weakness in RA.

Although the patients in clinical remission had better clinical outcomes than other RA patient groups, their muscle strength and quantitative MRI were not markedly better and were not comparable with healthy controls. These results suggest that although treatment is effective in improving disease activity (DAS28) and increasing

physical function, even those with well-controlled disease, who are in clinical remission, are still substantively weaker, with evident muscle pathology, compared to age- and gender-matched healthy controls. Therefore, future RA therapies should trial strategies such as the use of exercise interventions, medication, and nutritional supplementation to improve the muscle health of patients with RA. Future research could use quantitative MRI to assess other muscles, such as muscles of the hand in patients with RA, to identify if they also show decreases in muscle quality. This future research could be beneficial for clinical care, as patients with RA often undergo MRI scans to assess the joints of the hand. Future research should focus on quantitative MRI T2, fat fraction, and muscle volume, and quantitative muscle strength measurements in patients with RA.

This study successfully met its aims and demonstrated that quantitative MRI and strength testing could detect substantive differences in muscle properties between patients with rheumatoid arthritis and matched healthy controls. However, the measurements did not detect meaningful differences between the different disease stages of rheumatoid arthritis.

7.4.1 Limitations

This study is subject to some limitations. The patients with active drug-resistant RA had a longer disease duration than the patients in clinical remission, which may increase the likelihood of detrimental effects of the disease and medication on the muscles. However, there was no correlation between any quantitative MRI parameters and disease duration (T2: r_s= 0.04; p= 0.7, fat fraction: r_s= 0.01; p= 0.09, mean diffusivity: r_s= 0.09; p= 0.5, fractional anisotropy; r_s= -0.1; p= 0.1, muscle volume: r_s= 0.1; p= 0.4), suggesting that disease duration did not impact on results.

Of note is, while RA patients showed no substantive difference in BMI compared to healthy controls, the MRI measurements could still detect differences in fat fraction and muscle volume between healthy controls and RA patients. These results suggest that quantitative MRI measurements are more sensitive at identifying changes to body composition than BMI. The duration of prednisolone and statin treatment could be an influence on myopathy (405, 406). However, this study did not control for the duration of glucocorticoid exposure or statin treatment. Future research should consider matching for the duration of treatment.

7.5 Conclusion

In conclusion, this study demonstrates evidence that muscle pathology occurs in patients with RA, irrespective of disease phenotype, and that quantitative MRI is sensitive enough to identify these pathological changes within the muscle. These muscle changes are apparent even in early RA patients who are treatment naïve. In addition, this study demonstrates that muscles do not recover substantially, even in sustained clinical remission, suggesting that RA induces long term muscle damage which is currently not being treated effectively. This muscle deterioration is measurable by quantitative MRI T2, fat fraction, muscle volume, and muscle strength. There is evidence that physical activity and partaking in exercise helps maintain muscle health and has a role in RA disease management (407). Therefore, with further research, these quantitative MRI and strength measures could be useful in monitoring muscle change in patients with RA. In addition, it could be speculated that quantitative MRI and strength measurements could be used to assess exercise interventions which may be beneficial to improve muscle health in patients with RA. Following on from the results of this study, future research should investigate how quantitative MRI can be used to understand muscle changes in RA in relation to developing interventions, such as exercise, to restore muscle quality.

7.6 Key messages

- There are substantive differences in the muscle assessed by quantitative MRI and muscle strength between rheumatoid arthritis patients and matched healthy controls, including in newly diagnosed and treatment naïve patients.
- Muscle involvement may be among the earliest clinical features of rheumatoid arthritis.
- The muscle, assessed by quantitative MRI and muscle strength, still shows signs of pathology, even in long term clinical remission.

Chapter 8 Muscle differences in patients with giant cell arteritis on glucocorticoids as assessed by quantitative MRI

This chapter describes a research study by Matthew Farrow, John Biglands, Elizabeth Hensor, Steven Tanner, Sarah Mackie, Paul Emery, and Ai Lyn Tan. The manuscript is currently in preparation.

8.1 Introduction

Giant cell arteritis (GCA) is a systemic inflammatory vasculitis that typically affects medium and large arteries (408) and can have a substantial impact on the quality of life for the patient (409). Vasculitis in GCA can lead to ischemic optic neuropathy, which results in loss of vision in up to 15% of patients (410, 411). GCA is, therefore, a medical emergency. A single GCA patient case-study utilising MRI (114) presented a patient with a high-intensity signal in the limb-girdle muscles with myositis-like images showing muscle oedema, atrophy, and fat infiltration. This case study suggests that it may be beneficial to study the muscle in patients with GCA using quantitative MRI. Furthermore, 50% of patients with GCA develop polymyalgia rheumatica (PMR). Polymyalgia rheumatica, as the name suggests, includes myalgia (134), but the cause of this myalgia is insufficiently defined.

GCA is treated with long-term glucocorticoids to control inflammation. Typical starting doses are 40-60mg prednisolone daily for GCA. This steroid dose is tapered down gradually until treatment can be stopped. Unfortunately, systemic steroid treatment is associated with considerable morbidity in patients with GCA, including: osteoporosis, fractures, hypertension, and glucocorticoid-induced myopathy (GIM). GIM is a non-inflammatory condition which causes muscle atrophy, alters the microstructure of the muscles, and can affect daily tasks and

ambulatory function (130). GIM can be evaluated by clinical assessment, EMG, and histological studies (412-414). For prolonged high dose glucocorticoid exposure, the reported prevalence of GIM is variable, ranging from 2% to 60% (415-417). As decreases in muscle mass and atrophy of type II muscle fibres are known to occur with glucocorticoid-induced myopathy (26, 366), muscle volume and diffusion tensor imaging, which is sensitive to changes in muscle microstructure, could be a valuable measurement in patients to monitor for these changes (130, 418).

The muscles in GCA can, therefore, be affected by the concurrent inflammation of the disease, myalgia from PMR, and by potential glucocorticoid-induced myopathy following treatment with prednisolone, resulting in decreased muscle health. Decreased muscle health is known to affect the quality of life in patients (419), contributing to fatigue and increased duration of hospitalisation, morbidity, and mortality (420). However, no previous studies have used quantitative MRI to measure muscle health in patients with GCA.

The excellent performance of quantitative MRI in characterising muscle changes, coupled with case-study evidence demonstrating that muscle changes are noticeable on conventional MRI [22], suggests that a quantitative MRI study in patients with GCA on glucocorticoids could provide valuable information on the nature and degree of muscle changes in these patients.

This pilot study aimed to investigate the potential differences in muscle properties between patients with GCA at the start of treatment and age- and gender-matched healthy controls assessed by quantitative MRI. A secondary aim was to identify any potential longitudinal muscle changes in patients with GCA on glucocorticoid therapy.

8.1.1 Hypothesis

Quantitative MRI can detect differences in muscle properties in patients with giant cell arteritis compared to age- and gender-matched healthy controls.

8.1.2 Objectives

To identify whether quantitative MRI can:

1. Detect differences within the muscle between newly diagnosed giant cell arteritis patients and healthy controls.
2. Identify whether these measures can detect changes in muscle properties in giant cell arteritis patients on glucocorticoid therapy.

8.2 Methods

8.2.1 Study design

This observational pilot study was conducted at Leeds Teaching Hospitals Trust in the UK between May 2017 and October 2018. The study was approved by the Nottingham UK research ethics committee and written informed consent was obtained from all participants. Patients with GCA had their baseline research visit <14 days after starting treatment and were followed up after 3 and 6 months. These time-points were based on the expected onset of early signs of myopathy (405). Patients were compared at baseline to age (±5 years) and gender-matched healthy controls. Healthy controls were obtained from the pool of healthy controls recruited for the MUSCLE study.

Inclusion criteria were: 1) Fulfilling the 2016 revised American College of Rheumatology (ACR) criteria for GCA (421). 2) <14 days on prednisolone (≥40 mg/per day).

Exclusion criteria were: 1) History of muscle condition. 2) Glucocorticoid treatment >5 mg/per day for more than three months in the past five years prior to the diagnosis of GCA. Healthy controls were eligible if they were asymptomatic, had not been treated with glucocorticoids at any dose in the past five years, and did not have a history of any muscle condition or inflammatory arthritis.

8.2.2 MRI and muscle strength measurements

MRI measurements collected include T2, fat fraction, diffusion tensor imaging, and muscle volume. Muscle function measurements collected include knee extension, knee flexion, and handgrip strength. This methodology has been described in section 3.6.

8.2.3 Statistical analyses:

Statistical analyses were performed using SPSS. On an exploratory basis, two-sided tests at the 5% level of significance were performed. Paired Student's t-tests compared GCA patients at baseline to their matched healthy controls, and baseline to 3 months within GCA patients. To inform the sample size calculation for a powered trial, Pearson's correlation coefficients (r) have been provided for repeated measurements. To aid interpretation of provisional effect size estimates, this study presented Hedges g for repeated measures, which expresses the difference in units of standard deviation (422), and the common-language effect size (CLES), the probability that the measurements from one out of a randomly selected pair will exceed the other (423). Hedges g is a measure of effect size, which provides information on how much one group differs from another: $Hedges'g =$

$\frac{mean\ of\ group\ 1 - mean\ of\ group\ 2}{Pooled\ weighted\ standard\ deviation}$. The Pooled weighted standard deviation is a weighted average of standard deviations of two or more groups. This study, as per the study protocol, also provide sample size estimates for a future confirmatory study.

8.3 Results

Twenty patients starting glucocorticoids for suspected GCA were recruited into this study. Five patients were diagnosed to not have GCA due to a negative temporal artery biopsy result and inadequate GCA clinical features. These five patients were withdrawn from steroid treatment and were, therefore, not included in this study. One participant was initially diagnosed and treated as GCA but later changed to a diagnosis of polymyalgia rheumatica following the completion of the study, and subsequently remained on glucocorticoids, at a lower dose, and has therefore been included in this analysis. The mean age of the GCA cohort was 68.2 years ± 8.3 years, with 11/15 patients being female. Patients started prednisolone 40 – 60mg per day in accordance with the British Society for Rheumatology guidelines (129). The mean time between starting glucocorticoids and undergoing an MRI scan was eight days: range 2 - 14 days. All participants who continued throughout the study remained on glucocorticoid therapy. Fifteen patients returned for their 3-month follow up visit, however, one patient did not complete the MRI scan, and therefore only 14 datasets are available at 3-months. 2/14 patients attended at four months as opposed to three months due to patient availability. Eight patients returned for their 6-month visit, four patients declined to attend, and two participants did not respond to contact from the research team (Figure 8-1).

At baseline, median CRP was 12.6mg/L (range <5 – 445; reference range <10mg/L) and median ESR was 31mm/h (range 6 – 108; reference range

<15mm/h). Four patients had a CRP of <5mg/L but were diagnosed as having GCA based on clinical features, including a positive temporal artery biopsy, jaw claudication, and a new headache. 8/15 patients had a negative temporal artery biopsy but met the 2016 criteria for GCA and were administered glucocorticoid treatment and were, therefore, in the same group within this research. The median (IQR) prednisolone dose per day at baseline in fifteen GCA patients was 40mg. The median cumulative prednisolone dose was a total of 2,701mg over three months in fourteen patients and 4,422mg over six months in eight patients. The median body mass index (BMI) at baseline was 27 (range 21 - 32) for patients with GCA and 25 (range 21 - 30) for healthy controls.

Descriptive data for quantitative MRI and muscle strength measurements are shown in Table 8-1 and Table 8-2. Results of exploratory inferential analyses, which were not pre-specified, are presented in Table 8-2. In this emerging field, as it is not yet known what constitutes a clinically meaningful difference between groups, this study has considered potential differences equivalent to Hedges g of at least 0.2, a benchmark for a small effect size, to be of interest. Confidence intervals (CI) that both excluded 0 and included a potential difference of interest were obtained for several of the quantitative MRI and muscle strength/volume measurements, giving some confidence that substantive differences might be found in a confirmatory study.

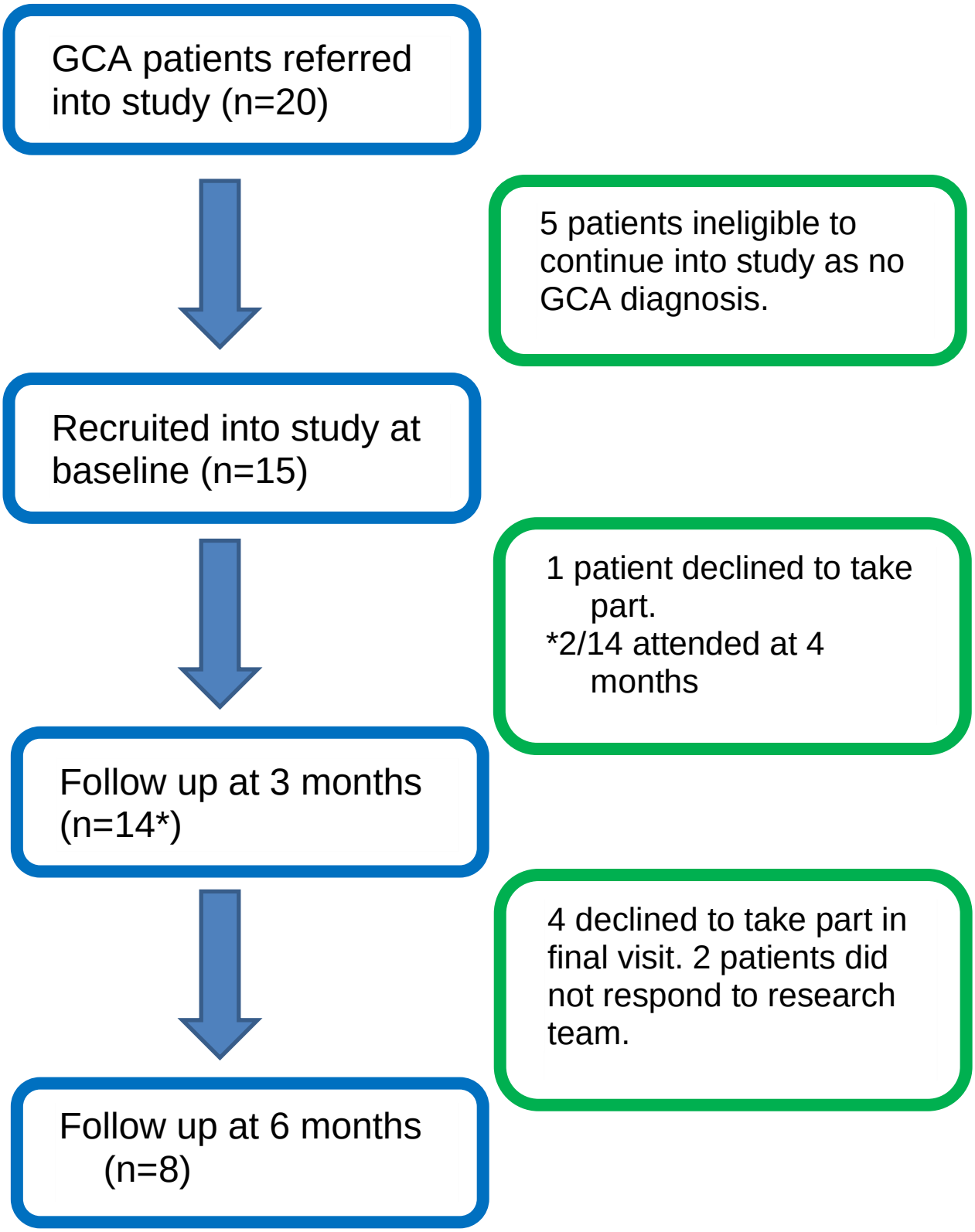

Figure 8-1: Flowchart of GCA patient screening, recruitment and follow up

8.3.1 MRI and muscle strength at baseline

8.3.1.1 T2

Quantitative MRI T2 relaxation times were substantively longer in GCA patients compared to healthy controls, suggesting muscle inflammation (Figure 8-2). Within the hamstrings, the mean difference between healthy controls versus newly diagnosed GCA patients was 2.78ms (95% CI= 1.39, 4.17; p= 0.001; SD= 0.6 – 2.1). Within the quadriceps, mean differences were 5.15ms (95% CI= 3.04, 7.27; p < 0.001; SD= 0.9 – 2.4). The probability that T2 relaxation times would be longer in patients with GCA for a randomly selected pair of measurements was approximately 90%.

8.3.1.2 Fat fraction

MRI fat fraction measurements within the muscle were substantively higher in patients with GCA compared to age- and gender-matched healthy controls, suggesting myosteatosis due to GCA (Figure 8-2). Within the hamstrings, the mean difference between healthy controls versus newly diagnosed patients with GCA was 4.08% (95% CI= 2.10, 6.06; p= 0.001; SD= 0.8 – 2.4). The probability that fat fraction would be higher in patients with GCA for a randomly selected pair in the hamstrings was 87%. However, fat fraction results for quadriceps were less clear as the CI included 0 and indicated the potential for substantive differences in either direction, with a mean difference of 0.63% (95% CI= -0.41, 1.67; p= 0.22). The probability that fat fraction would be higher in patients with GCA for a randomly selected pair in the quadriceps was 63%.

8.3.1.3 Diffusion tensor imaging

Preliminary effect size estimates for mean diffusivity and fractional anisotropy, in both muscle groups, were also unclear due to CIs overlapping zero, and CLES being around 50% (Figure 8-2).

8.3.1.3.1 Mean diffusivity

Within the hamstrings, the mean difference between healthy controls versus newly diagnosed GCA patients was $-0.03 \times 10^{-3} mm^2 s^{-1}$ (95% CI= -0.11, 0.05; p= 0.39). Within the quadriceps, the mean difference between healthy controls versus newly diagnosed GCA patients was $-0.01 \times 10^{-3} mm^2 s^{-1}$ (95% CI= -0.11, 0.09; p= 0.83).

8.3.1.3.2 Fractional anisotropy

Within the hamstrings, the mean difference between healthy controls versus newly diagnosed GCA patients was 0.04 (95% CI= -0.01, 0.09; p= 0.14). Within the quadriceps, the mean difference between healthy controls versus newly diagnosed GCA patients was -0.02 (95% CI= -0.07, 0.04; p= 0.54).

8.3.1.4 Muscle volume

Muscle volume was substantively lower in patients with GCA compared to healthy controls, demonstrating muscle atrophy (Figure 8-3). Within the thigh, the mean difference between healthy controls versus new patients was -459.3cm^3 (95% CI= -730.5, -188.2; p= 0.003; SD= 0.4 – 1.9). There was approximately 80% probability that muscle volume in a randomly selected pair would be greater within a healthy control than a patient with GCA.

8.3.1.5 Muscle strength assessments

Muscle strength was substantively lower in newly diagnosed GCA patients compared to healthy controls, suggesting a decrease in strength due to GCA (Table 8-1 and Figure 8-3). There was approximately 80% probability that the strength in a randomly selected pair would be greater within a healthy control than within a patient with GCA. Peak flexion (hamstrings) differences between healthy controls versus newly diagnosed GCA patients was -21.13 Nm (95% CI= -35.42, -6.84; p= 0.007). Peak extension (quadriceps) differences between healthy controls versus newly diagnosed patients was -31.54Nm (95% CI= -35.42, -6.84; p= 0.007). Grip strength differences between healthy controls versus newly diagnosed patients was -9.63kg (95% CI= -17.51, -1.75; p= 0.02).

Table 8-1: Mean quantitative MRI, muscle volume, knee flexion, knee extension, and handgrip strength measurements in healthy controls and GCA patients at baseline, 3, and 6 months

Muscle measurement: Mean ± SD (95% CI)	Healthy control n=15	GCA patients: baseline n=15	GCA patients: 3 months n=14	GCA patients: 6 months n=8
Quantitative MRI - Hamstrings				
T2 (ms)	39.14 ± 1.08 (38.54, 39.74)	41.92 ± 2.55 (40.51, 43.33)	41.87 ± 2.88 (40.20, 43.53)	43.07 ± 6.57 (37.58, 48.56)
Fat fraction (%)	4.28 ± 2.79 (2.74, 5.83)	8.37 ± 2.15 (7.17, 9.56)	8.55 ± 2.93 (6.86, 10.24)	7.97 ± 1.50 (6.71, 9.23)
Mean diffusivity ($x10^{-3}mm^2s^{-1}$)	1.33 ± 0.14 (1.25, 1.40)	1.29 ± 0.09 (1.25, 1.34)	1.33 ± 0.10 (1.27, 1.38)	1.34 ± 0.11 (1.25, 1.43)
Fractional anisotropy	0.39 ± 0.08 (0.34, 0.43)	0.42 ± 0.05 (0.40, 0.45)	0.40 ± 0.06 (0.36, 0.44)	0.41 ± 0.02 (0.39, 0.42)
Quantitative MRI - Quadriceps				
T2 (ms)	39.54 ± 1.44 (38.74, 40.33)	44.69 ± 3.85 (42.56, 46.82)	43.47 ± 3.18 (41.63, 45.30)	43.04 ± 3.56 (40.06, 46.02)
Fat fraction (%)	3.96 ± 1.66 (3.04, 4.88)	4.59 ± 1.11 (3.97, 5.20)	4.88 ± 1.11 (4.23, 5.52)	4.29 ± 1.33 (3.18, 5.41)
Mean diffusivity ($x10^{-3}mm^2s^{-1}$)	1.32 ± 0.11 (1.26, 1.38)	1.31 ± 0.10 (1.25, 1.37)	1.34 ± 0.07 (1.30, 1.38)	1.33 ± 0.07 (1.27, 1.38)
Fractional anisotropy	0.37 ± 0.06 (0.34, 0.41)	0.36 ± 0.06 (0.33, 0.39)	0.34 ± 0.05 (0.31, 0.38)	0.35 ± 0.03 (0.32, 0.37)
Quantitative MRI - Thigh				

Muscle volume (cm^3)	1584.53 ± 437.15 (1342.45, 1826.62)	1125.22 ± 321.32 (947.28, 1303.16)	1121.83 ± 340.48 (925.24, 1318.42)	1147.60 ± 293.87 (901.92, 1393.29)
Muscle assessments				
Flexion strength (Nm)	62.03 ± 18.12 (52.00, 72.07)	40.91 ± 18.34 (30.75, 51.06)	47.24 ± 23.70 (33.55, 60.92)	43.79 ± 18.53 (28.30, 59.28)
Extension strength (Nm)	108.94 ± 45.86 (83.54, 134.34)	77.40 ± 34.28 (58.41, 96.39)	81.86 ± 40.43 (58.51, 105.20)	77.04 ± 37.95 (45.31, 108.76)
Handgrip strength (kg)	34.87 ± 10.13 (29.26, 40.48)	25.24 ± 13.00 (18.04, 32.44)	26.44 ± 13.17 (18.83, 34.04)	26.18 ± 11.88 (16.25, 36.12)

8.3.2 Longitudinal MRI and muscle strength measurements in giant cell arteritis patients

There were no substantial changes in any of the measurements at the 3-month time point (n = 14) compared to baseline (Table 8-1 and Table 8-2). Due to the level of attrition, this study has not provided provisional estimates of effect size at six months, as the sample size was too small to yield reliable estimates of reliability.

The confidence intervals around the changes at three months were all relatively wide, and most were consistent with a potentially substantive difference in either direction (increases or decreases). Individual trajectories over time, including 6-month data when available, is shown in Figure 8-4 and Figure 8-5. There was no clear pattern in the individual 14 patient trajectories for MRI or muscle strength, with some patients with GCA showing increases over time, others decreasing over time and others showing no substantial change.

Table 8-2: Differences in muscle measurements between paired healthy controls and GCA patients at baseline, and between baseline and three months in GCA patients, and correlations between repeated measures.

Muscle measurement	GCA baseline - HC n=15 paired measurements				GCA 3 months - GCA baseline n=14 paired measurements			
	Difference ± SD (95% CI), P value	*G*, 95% CI	CLES	r	Difference ± SD (95% CI), P value	*G*, 95% CI	CLES	r
Quantitative MRI - Hamstrings								
T2 (ms)	2.78 ± 2.51 (1.39, 4.17), p=0.001	0.6, 2.1	87%	0.24	-0.17 ± 3.27 (-2.05, 1.72), p=0.85	-0.7, 0.5	48%	0.29
Fat fraction (%)	4.08 ± 3.57 (2.10, 6.06), p=0.001	0.8, 2.4	87%	-0.03	0.49 ± 2.33 (-0.85, 1.84), p=0.44	-0.3, 0.6	58%	0.61
Mean diffusivity ($x10^{-3}mm^2s^{-1}$)	-0.03 ± 0.14 (-0.11, 0.05), p=0.39	-0.9, 0.3	41%	0.25	0.03 ± 0.10 (-0.03, 0.08), p=0.35	-0.3, 0.8	60%	0.44
Fractional anisotropy	0.04 ± 0.09 (-0.01, 0.09), p=0.14	-0.1, 1.2	66%	0.15	-0.02 ± 0.05 (-0.05, 0.01), p=0.12	-0.8, 0.1	33%	0.66
Quantitative MRI - Quadriceps								
T2 (ms)	5.15 ± 3.82 (3.04, 7.27), p<0.001	0.9, 2.4	91%	0.21	-1.04 ± 4.42 (-3.59, 1.51), p=0.39	-0.9, 0.4	41%	0.24
Fat fraction (%)	0.63 ± 1.88 (-0.41, 1.67), p=0.22	-0.2, 1.1	63%	0.12	0.36 ± 1.06 (-0.25,0.97), p=0.23	-0.2, 0.8	63%	0.55
Mean diffusivity ($x10^{-3}mm^2s^{-1}$)	-0.01 ± 0.18 (-0.11, 0.09), p=0.83	-0.9, 0.7	48%	-0.45	0.03 ± 0.06 (-0.01, 0.07), p=0.11	-0.1, 0.7	68%	0.80
Fractional anisotropy	-0.02 ± 0.10 (-0.07, 0.04), p=0.54	-1.0, 0.5	44%	-0.26	-0.01 ± 0.03 (-0.03, 0.01), p=0.28	-0.5, 0.2	38%	0.81
Quantitative MRI - Thigh								

Muscle volume (cm^3)	-459.3 ± 489.6 (-730.5, -188.2), p=0.003	-1.9, 0.4	83%	0.19	-19.4 ± 88.2 (-70.4, 31.5), p=0.42	-0.2, 0.1	41%	0.97
Muscle assessments								
Flexion strength (Nm)	-21.13 ± 25.80 (-35.42, -6.84), p=0.007	-1.9, 0.4	79%	0.00	6.04 ± 15.08 (-2.66, 14.75), p=0.16	-0.1, 0.6	66%	0.77
Extension strength (Nm)	-31.54 ± 42.27 (-54.95, -8.13), p=0.01	-1.3, 0.2	77%	0.47	4.04 ± 26.05 (-11.00, 19.08), p=0.57	-0.2, 0.4	56%	0.77
Handgrip strength (kg)	-9.63 ± 14.23 (-17.51, -1.75), p=0.02	-1.4, 0.2	75%	0.26	0.83 ± 3.76 (-1.34, 3.00), p=0.42	-0.1, 0.2	59%	0.96

CLES=Common-language effect size; g = Hedges g; HC = matched healthy control; r= Pearson's correlation coefficient between baseline and 3-month measurements in patients with GCA

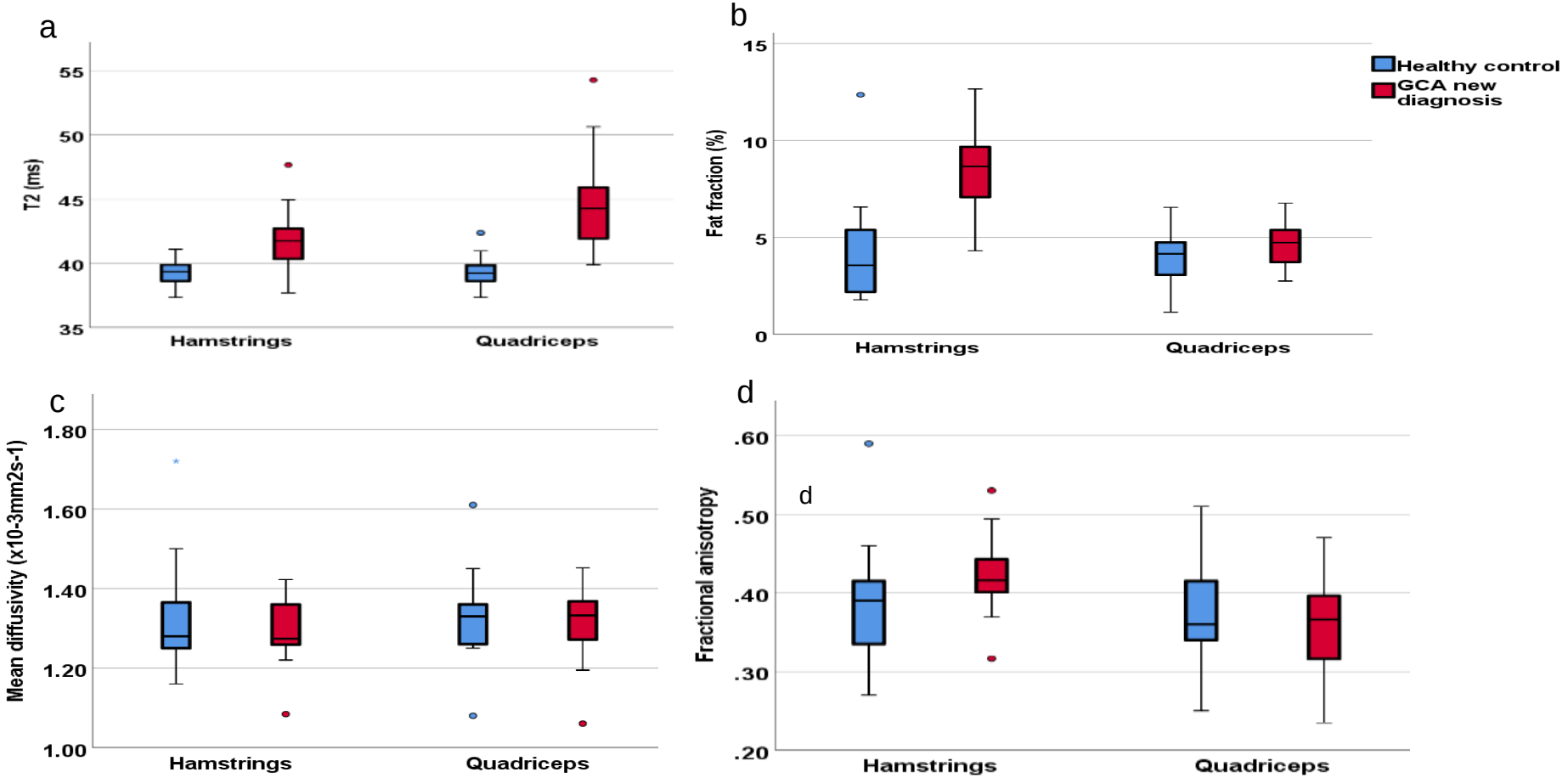

Figure 8-2: Quantitative MRI measurements of 15 newly diagnosed GCA patients and 15 age- and gender-matched healthy controls

a) T2 hamstrings, T2 quadriceps b) FF hamstrings, FF quadriceps c) MD hamstrings, MD quadriceps d) FA hamstrings, FA quadriceps

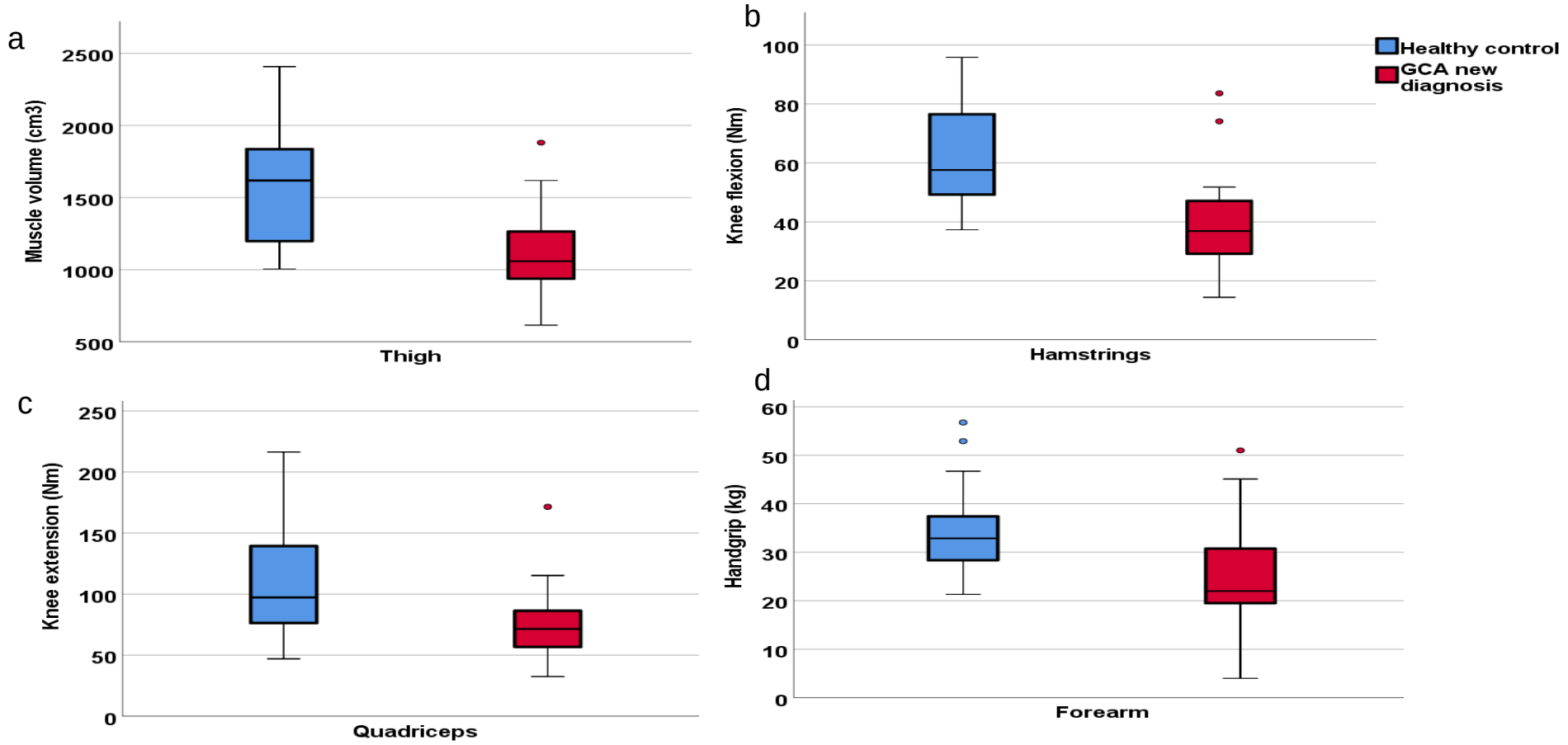

Figure 8-3: Quantitative muscle volume and muscle strength measurements of 15 newly diagnosed GCA patients and 15 age- and gender-matched healthy controls

a) Differences between GCA patients and healthy controls in a) muscle volume b) knee flexion c) knee extension d) handgrip

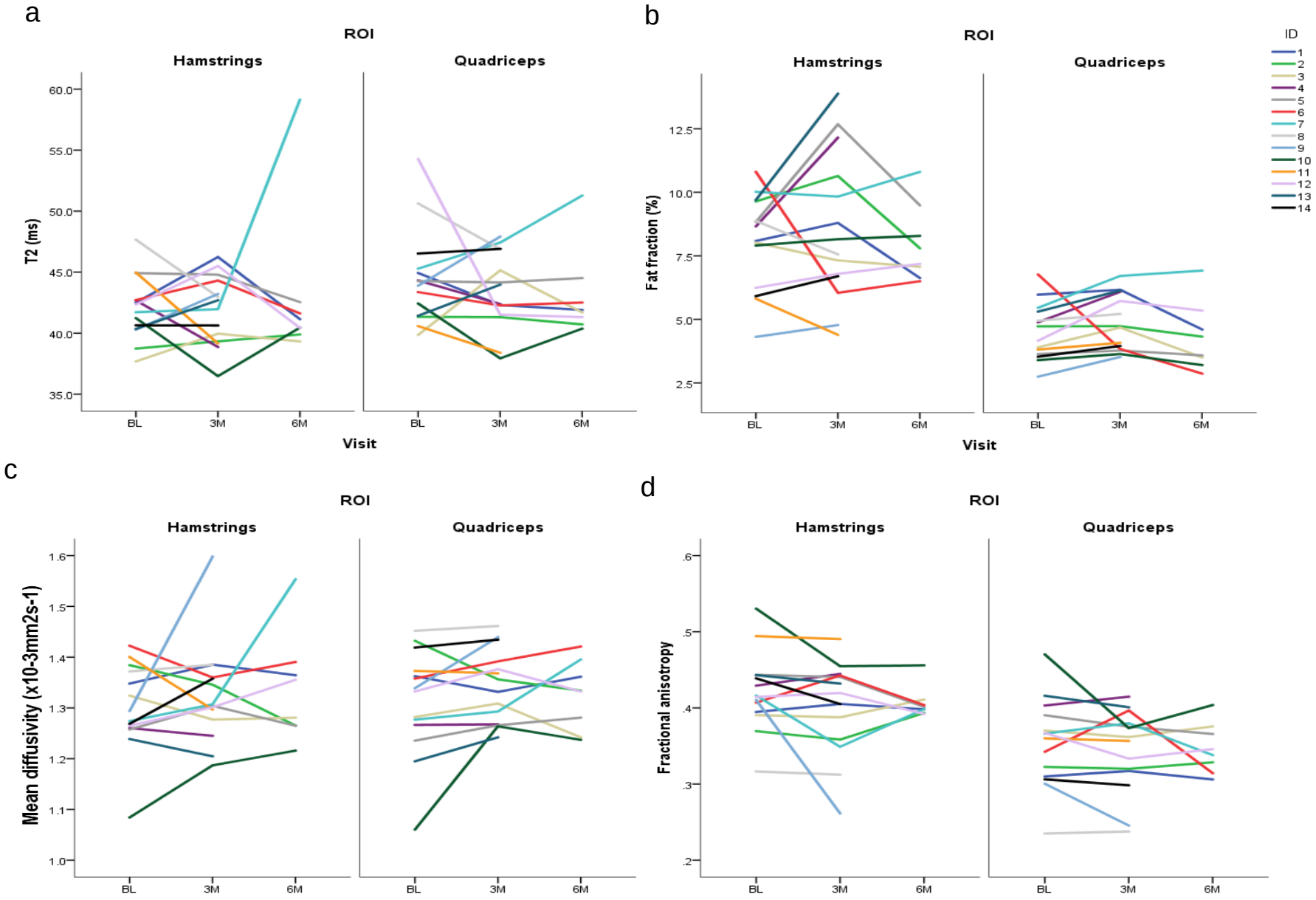

Figure 8-4: Quantitative MRI measurements of 14 GCA patients on long term therapy at baseline, 3 months, and 6 months

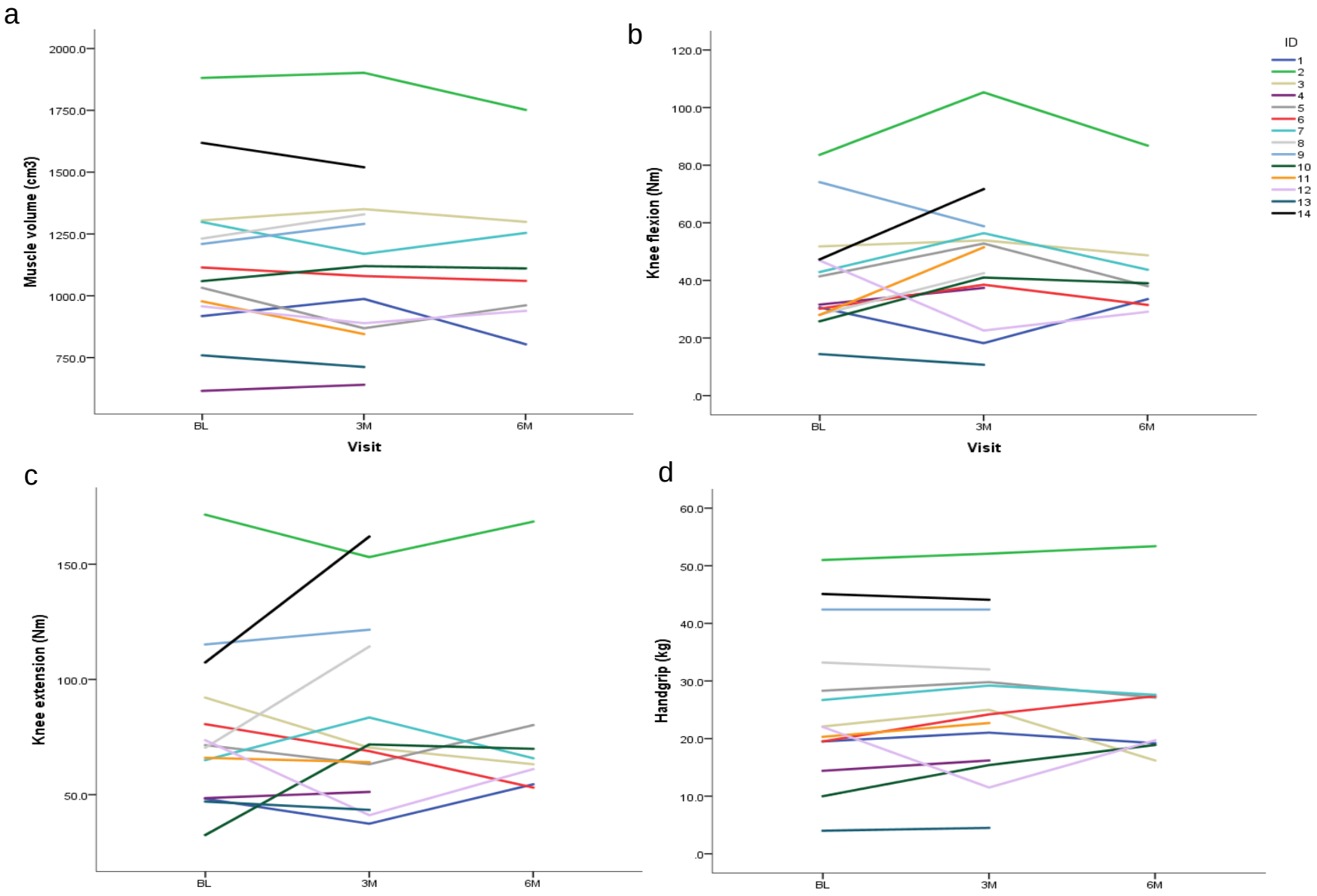

Figure 8-5: Quantitative muscle volume and muscle strength measurements of 14 GCA patients on long term therapy at baseline, 3 months, and 6 months

8.3.3 Sample sizes for a confirmatory study

To confirm that T2 relaxation times are longer in newly diagnosed GCA patients compared to matched healthy controls, future work should aim to detect a difference of at least 5% relative to the mean observed in controls. For the hamstrings, this would equate to a difference of at least 1.9ms. The SD of the differences in T2 was 2.5. At the 5% level of significance, with 90% power, this would require 19 matched pairs.

At the same significance and power, using a paired t-test to detect a change in hamstrings T2 at three months within patients with GCA alone of at least 5% relative to baseline (2.1ms, based on the baseline mean obtained in hamstrings in this sample), assuming SD of differences = 3.3, accounting for 10% drop-out, would require 29 matched pairs.

To show that change in hamstring T2 at three months differed between matched GCA patients and healthy controls, using a general linear mixed model, assuming change = 0 in controls and change = 2.1ms in GCA, SD = 1.4 in healthy controls, SD = 2.7 in GCA, no change in SD over time, the correlation between paired measurements - baseline: 3M = 0.29, healthy control: GCA = 0.24, and accounting for 10% drop-out, would require 114 matched pairs.

8.4 Discussion

This chapter aimed to identify whether quantitative MRI measurements can detect differences within the muscle between newly diagnosed patients with giant cell arteritis and healthy controls, and to show whether these measurements can detect

changes in muscle properties in giant cell arteritis patients on glucocorticoid therapy.

This study suggests that muscle health may be adversely affected in patients with GCA from the time of diagnosis compared to age- and gender-matched healthy controls. However, in this study, when patients were on steroid medication for three and six months, their muscle health neither improved nor decreased. These results provide proof-of-concept that there may be early changes to muscle in patients with GCA on steroid therapy which can be assessed by quantitative MRI and muscle strength measurements, but future work is needed to elucidate the effects of steroids on the muscle longitudinally. This study has identified, for the first time, differences in T2, fat fraction, muscle volume, and muscle strength in patients with GCA compared to age- and gender-matched healthy controls, which merits further investigation. This decrease in muscle health demonstrates that newly diagnosed GCA patients may present with chronic muscle inflammation, myosteatosis, muscle atrophy, and muscle weakness (114, 130). If these findings are confirmed, then these could be useful outcome measures to assess interventions for myopathy in GCA, such as exercise, which might be valuable in the early stages of the disease to prevent muscle pathology and improve quality of life.

The longer T2 relaxation times in patients with GCA at the start of therapy compared to healthy controls suggests the presence of muscle oedema and inflammation occurring early with the disease (115, 377). The higher fat fraction in patients with GCA in this study demonstrates myosteatosis, a measure of muscle quality. Muscle volume measurements demonstrated substantive differences between patients and healthy controls. The observed lower muscle volume in patients with GCA relative to controls is consistent with muscle atrophy, which is associated with decreased muscle function in both young (281) and older people (424). This decrease in muscle health at baseline suggests that GCA, similar to rheumatoid arthritis (as discussed in Chapter 7), may mimic a premature ageing process (as discussed in Chapter 5), within the muscle (sarcopenia), which may be

one of the earliest clinical features of the disease. This decrease in muscle health that is similar to the ageing process is vital to consider, as GCA patients are often at risk of age-related decreases in muscle health, due to the typical age of GCA patients. Therefore, muscles which could be perceived as undergoing normal fat infiltration and atrophy due to age may be undergoing pathological changes due to the disease and should not be disregarded.

Diffusion measurements did not appear to show substantive differences between patients with GCA and healthy controls. This finding could be due to negligible induced changes in muscle structure, or that diffusion measurements are not sensitive to the change. Alternatively, as previously discussed, the presence of oedema and fat infiltration, which this study suggests is present in GCA, can affect diffusion measurements which may explain the small differences seen in this research. However, this study was not a powered confirmatory trial, and the confidence intervals are wide. Therefore, further research is required to confirm these findings.

Studies have shown that GIM can occur within six months (405); therefore, it could have been expected that the preliminary longitudinal measurements in this study might have shown a reduction in both T2 and muscle volume and an increase in fat fraction, due to steroids decreasing inflammation, but GIM causing muscle atrophy and myosteatosis. The maintained increased T2 measurements seen in this longitudinal study could reflect continuing inflammation within the muscle, despite the established glucocorticoid treatment. However, inflammatory biomarkers were not assessed at the 3- and 6-month time points so this cannot be corroborated with ESR or CRP measurements. Similarly, fat fraction and muscle volume measurements did not change over time, suggesting that either the treatment did not substantively change the muscle properties, or that the changes were too subtle to be detectable over this period in this pilot study.

The results from this study suggest a wide variation in the response profile over time, with some patients showing increases, others showing decreases, and others showing a negligible change. It is possible that there was a reduction in systemic inflammation due to therapy, but that the detrimental effect of glucocorticoid-induced myopathy cancelled this out. This hypothesis could explain why the MRI measurements in this study detected no change in muscle properties over time.

Whilst this study found substantive differences in muscle strength between patients with GCA and age- and gender-matched healthy controls at baseline, suggesting muscle weakness occurs early in patients with GCA, there was no clear trend within the longitudinal data. Previous studies have reported decreases in muscle strength at one month of starting glucocorticoid therapy, whilst other studies have indicated that the median time required for a response is two years (425). Evidently, there is uncertainty about the expected time before changes are seen, and this study may have been too short to see detrimental muscle changes in response to therapy.

Despite the limited change over time, the differences at baseline between healthy controls and patients with GCA for both MRI and strength measures, despite only two weeks of glucocorticoids, suggests that the observed differences may have preceded the steroid therapy. Whilst this could be due to GCA/PMR-related systemic muscle changes, it could also be due to decreased levels of physical activity prior to the GCA diagnosis. It is also possible that the inflammatory process within muscle represents a subclinical process that predates patient-presented clinical features of GCA. This early inflammatory process within the muscle due to rheumatic disease was demonstrated in a previous chapter within this thesis that showed that treatment-naïve RA patients also have weaker muscles (5).

This study successfully met its aims and demonstrated that quantitative MRI measures can detect substantive differences within the muscle between newly diagnosed patients with giant cell arteritis and matched healthy controls but did not

detect changes in muscle properties in patients with giant cell arteritis on glucocorticoid therapy.

8.4.1 Limitations

There were limitations to this study. It was not feasible to study the newly diagnosed patients before commencing treatment as management guidelines recommend the immediate start of high dose glucocorticoids at the suspicion of GCA (129). Therefore, patients with GCA at baseline had been taking a high dose of glucocorticoids for a mean of 8 days before their baseline visit, which may have contributed to the potential differences at baseline. However, no evidence has been published which states that muscle changes in response to glucocorticoids happen that quickly. This study did not collect data on statin use in participants, which is known to cause muscle pathology. One patient was initially diagnosed as GCA based on clinical features, but the diagnosis was changed to PMR following the completion of the study. However, as this was an exploratory pilot study to identify if there are any differences between GCA patients and matched healthy controls and the effects of steroid treatment, and GCA can concurrently present with PMR, the data was kept within the analysis. Future research should consider only using patients with a confirmed temporal artery biopsy for GCA. Future studies should collect information longitudinally regarding clinical disease activity, such as CRP and ESR measurements, to identify inflammatory changes happening in response to therapy and how this correlates with MRI measures longitudinally. It is plausible that the MRI outcomes might require a longer duration of treatment to show a more significant effect. One of the potential negatives for more prolonged treatment duration, however, could be its deleterious effect on adherence (426) and the increase in resources (staff, costs, and time).

All but one patient, who did not complete the MRI scan, were re-scanned at three months (two attended at four months instead of three months). However, only eight

attended at six months. In the future, to improve patient retention long-term, study visits could be incorporated with clinical visits. It is particularly important to improve participant retention to study muscle changes over six months or longer, which is required to study the effects of glucocorticoids, as patients with GCA are generally on steroid treatment for 1-2 years or longer (129).

8.5 Conclusion

In conclusion, this study demonstrates evidence that muscle damage occurs at the early stages of GCA and that quantitative MRI and muscle strength measurements are sensitive enough to identify these pathological changes within the muscle. Differences in muscle between patients with GCA and matched healthy controls were measurable by quantitative MRI T2, fat fraction, muscle volume, and quantitative muscle strength. However, the results of the longitudinal aspect of this study showed that the muscle health of patients with GCA on steroid medication showed no change. Therefore, muscle pathology was still present in patients with GCA on treatment longitudinally. Further work is essential to understand the combined effect of the disease and medication in patients with GCA longitudinally. This work can inform the design of a fully powered trial to confirm if there are clinically meaningful differences and the potential implications that these might have on GCA patient management. This study suggests that the development of muscle-related interventions for patients with GCA may be beneficial in restoring muscle quality and improving disease management and that these quantitative MRI measures could be useful in monitoring the muscle change associated with these interventions.

8.6 Key messages

- There are substantive differences in T2, fat fraction, muscle volume, and muscle strength between patients with giant cell arteritis and age- and gender-matched healthy controls.
- A decrease in muscle quality occurs at the early stages of GCA.
- Quantitative MRI and muscle strength did not change substantively following treatment at 3- and 6-month time points, suggesting that muscle health is not improving with current treatment.

Chapter 9 Discussion

This chapter summarises and discusses the main research findings of this thesis and highlights potential future directions. This chapter includes published work by Matthew Farrow, John Biglands, Abdulrahman Alfuraih, Richard Wakefield, and Ai Lyn Tan. "Novel muscle imaging in inflammatory rheumatic diseases" published in Frontiers in Medicine, 2020 (1).

9.1 Overview of thesis

The central overarching hypothesis of this thesis is: 'Quantitative MRI can identify differences in muscle properties assessed by T2, fat fraction, diffusion tensor imaging (DTI), and muscle volume due to ageing and rheumatic disease.' This PhD thesis consists of multiple research studies designed to examine and address the gaps within the current literature, which may be used in the development of future clinical trials. This hypothesis emerged as there has been interest in body composition and its role in physical function in patients with rheumatic disease, and concurrently there has been recent interest in utilising quantitative MRI in the assessment of muscle properties, such as myosteatosis, fluid, and changes to tissue microstructure.

Overall, the results from this research project support the central hypothesis in that the quantitative MRI measurements of T2, fat fraction, and muscle volume could be useful in the assessment of muscle health due to ageing, myositis, rheumatoid arthritis, and giant cell arteritis. Diffusion tensor imaging, a fourth quantitative MRI measurement examined within this thesis, however, was found to yield no clinically significant results. The main concepts and themes that appeared during this research project are discussed within sections below:

9.2 Discussion of main concepts and themes

This thesis has demonstrated that quantitative MRI and muscle strength measurements can provide information that helps further understand the pathogenesis of muscle pathology and could be helpful as an adjunct in the diagnosis and monitoring of muscle health due to ageing and rheumatic disease (2-6).

9.2.1 Reliability of quantitative MRI measures for clinical practice

In the initial stage of this research project, the reliability of quantitative MRI was measured, which established that fat fraction and STEAM DTI have excellent reliability. Based on the results of this thesis, differences greater than a fat fraction of 0.4%, mean diffusivity of $0.03x10^{-3}mm^2s^{-1}$, and fractional anisotropy of 0.03 should be detectable above reliability errors. In this thesis, across all research studies, differences in fat fraction between rheumatic patients and healthy controls ranged from 1.0% to 8.4%. These results agree with a previous research study investigating fat fraction in the muscle of patients with osteoarthritis (266). Supporting the results from this thesis, a recent study published, following the completion of this PhD, by Nagy et al. demonstrated that quantitative MRI fat fraction in muscle is a sensitive and powerful marker of disease progression with excellent reliability over one year (427). Within this thesis, mean diffusivity differences between rheumatic patients and healthy controls ranged from 0.02 to $0.05x10^{-3}mm^2s^{-1}$, and fractional anisotropy differences between rheumatic patients and healthy controls ranged from 0.01 to 0.06. As this thesis is the only study to investigate STEAM DTI in rheumatic disease, it is not possible to compare the results in this thesis with any current literature.

The results of this thesis demonstrate that quantitative Dixon fat fraction MRI measurements are suitable for detecting changes within the muscle due to pathology, as the differences seen with disease in this thesis are larger than the reliability measures observed within Chapter 4. However, the results of this thesis suggest that changes in diffusion may be obscured by measurement reliability as some of the differences seen in the subsequent research studies within this thesis were smaller than the differences seen within Chapter 4. Furthermore, this research project suggests that diffusion measurements can be influenced by myosteatosis and inflammation, which, in this thesis, was demonstrated to be present due to ageing and rheumatic disease (3-5), which further decreases the reliability of the diffusion measurements.

Overall, based on the findings of this PhD, Dixon fat fraction measurements should be considered for future clinical trials and incorporated more routinely into clinical practice as it has been demonstrated to have excellent reliability (Chapter 4) and is able to identify substantive differences due to age (Chapter 5) and rheumatic disease (Chapter 6, Chapter 7, and Chapter 8). In comparison, the results of this PhD do not support the use of STEAM DTI for future research or clinical practice as substantive differences were not found between patients with rheumatic disease and matched healthy controls.

Whilst Chapter 6, Chapter 7, and Chapter 8 would recommend the use of quantitatively assessing T2, muscle volume, and muscle strength, the reliability of these measures were not assessed within this thesis. Therefore, a gap in the literature still exits, which needs to be addressed in future reliability studies.

9.2.2 Quantitative MRI in the assessment of muscle health due to age and rheumatic disease

The main component of this research project examined whether quantitative MRI measurements and physical function measurements could identify differences in muscle properties caused by ageing or rheumatic disease. This research demonstrated that T2 relaxation times were longer, fat fraction was higher, and muscle volume and muscle function were lower with increased age and in patients with rheumatic disease. Within this thesis, diffusion measurements did not show any meaningful differences between patients and healthy controls.

9.2.2.1 Myosteatosis and muscle atrophy

Within this thesis, increased fat fraction and decreased muscle volume were observed due to ageing, myositis, rheumatoid arthritis, and giant cell arteritis. Myosteatosis and muscle atrophy are often regarded as a measure of muscle quality and are known to impair physical function and cause musculoskeletal pain (428). The results of this thesis agree with previous literature, which states that myosteatosis increases and muscle atrophy decreases in patients with rheumatic disease, and both are associated with a reduction in physical capability (118, 403, 429, 430). In a recent research study by Lassche et al. histopathology, following muscle biopsy, significantly correlated with quantitative MRI assessment of fat infiltration (431). This finding confirms the idea that quantitative MRI fat fraction may accurately identify myosteatosis, as suggested within this thesis. Surprisingly, within this thesis, increased myosteatosis and decreased muscle volume was present in newly diagnosed patients with RA and GCA. This is an important finding, as it would be expected that increased myosteatosis and muscle atrophy would take a period of time to manifest.

In addition, given the presence of myosteatosis within patients with rheumatic disease, it should be recognised that muscle volume measurements may be affected by fat-infiltrated muscle. Therefore, the loss of muscle volume may be expected to be more severe than reported within this thesis, as the results in this thesis will include muscle compromised by fat infiltration. The finding of increased myosteatosis and decreased muscle volume in newly diagnosed patients with RA and GCA suggests that muscle pathology may be one of the earliest clinical features of inflammatory rheumatic disease which warrants further study. It would be interesting to know at what point fat infiltration and muscle atrophy occur within the natural history of rheumatic disease, why it occurs, and if it is present at the pre-clinical stage. However, there is no literature currently available on this subject matter in patients with rheumatic disease, or why this is so, highlighting a significant gap in the literature and an area of research need.

Furthermore, in patients with long-term RA in clinical remission, increased fat infiltration and decreased muscle volume appeared to remain present. This finding suggests that despite effective treatment, the muscles of patients with rheumatic disease are still compromised. It is unclear why this is so. It could be due to long-standing disease causing irreversible damage; subclinical low-level inflammation which may go unnoticed (as suggested in Chapter 6, Chapter 7 and Chapter 8); or a change in lifestyle, such as decreased physical activity. Interestingly, previous research has suggested that a decrease in myosteatosis and an increase in muscle volume may be achieved through resistance exercise (432). In addition, a recent study by Heskamp et al. demonstrated that in patients with myotonic dystrophy, a behavioural intervention targeting physical activity increased lower extremity muscle volume and decreased fat infiltration (433), which improved physical function. Despite these findings, there remains a gap in the literature regarding which type of exercise is most effective at reducing myosteatosis and increasing muscle mass to improve physical function, demonstrating a need for further research.

9.2.2.2 Muscle inflammation

Within this thesis, longer T2 relaxation times were observed due to ageing, myositis, rheumatoid arthritis, and giant cell arteritis. Longer T2 relaxation times can occur due to increased water content. This increase in water content could be due to inflammation or oedema, which is known to occur due to increased levels of pro-inflammatory cytokines. An increase in pro-inflammatory cytokines - such as interleukin-6 which can be present due to ageing and rheumatic disease (434) - is associated with increased risk of disease activity, decreased physical function, muscle atrophy, and increased mortality (435, 436). Previous research has suggested that inflammation can be attenuated through physical activity (437). Therefore, physical activity could be beneficial in reducing systemic inflammation, which in turn could decrease inflammation within the muscle and improve physical function. However, other research suggests that exercise can cause an inflammatory response, in particular in the case of unaccustomed exercise (438). This phenomenon has been demonstrated by the observation of a rise in serum interleukin-6 levels immediately following acute exercise (439).

In a recent study by Fu et al., T2 relaxation time was longer in skeletal muscle following eccentric exercise but showed signs of repair after two days with the T2 relaxation time subsequently decreasing (440). However, the values remained higher than the control group for seven days. Unfortunately, this research did not compare different types of exercise, as it is known that eccentric contractions are more damaging to the muscle compared to concentric and isometric contractions, and aerobic exercise (441). Furthermore, this research by Fu et al. has demonstrated that quantitative T2 measurements accurately reflect the histopathological changes of inflammation occurring within the muscle as confirmed on muscle biopsy (440). This finding suggests that the compromised T2 measurements seen within this thesis due to ageing and rheumatic disease were likely due to muscle inflammation. Evidently, there is still uncertainty about the role

of exercise in relation to muscle inflammation which highlights an area of research need.

9.2.2.3 Identifying low-level inflammation

Within this PhD, it appeared that quantitative MRI T2 measurements could identify low-level inflammation which currently goes undetected by conventional radiology. This phenomenon was demonstrated in Chapter 6, in which patients with myositis who had been diagnosed as having unaffected muscle on STIR and T1-weighted MRI sequences had substantively longer T2 relaxation times compared to matched healthy controls. In addition, it was demonstrated that patients with RA (Chapter 7) and GCA (Chapter 8) present with longer T2 relaxation times at disease onset. These findings suggest that muscle inflammation may be an early clinical feature of inflammatory rheumatic disease, which currently goes unnoticed, and warrants further consideration. Furthermore, T2 remained compromised in GCA patients on glucocorticoid treatment, and when patients with RA achieved remission. Together, these findings suggest that muscle inflammation is present despite the prescription of immunosuppression to reduce inflammation and may persist when patients achieve remission. This is an important finding as it could be speculated that muscle inflammation may have a prolonged impact on physical function, muscle quality, and may cause malaise in patients. Therefore, future research is warranted to investigate the presence of subclinical and low-level inflammation in patients with rheumatic disease and to develop interventions to reduce this inflammation.

9.2.2.4 Correlation with physical function

This thesis was the first study to demonstrate that quantitative MRI measurements of T2, fat fraction, and muscle volume correlate with knee extension, knee flexion, gait speed, frailty, and handgrip strength. These findings suggest that these MRI properties may be able to identify differences within the muscle that are directly associated with physical function. If these findings can be confirmed in larger studies, the physical function of patients could be improved by effectively targeting the pathological changes within the muscle that are being measured by these quantitative MRI sequences. The findings from this thesis have been supported in multiple recent reviews by other authors demonstrating that quantitative MRI measurements of the muscle can be used as biomarkers of disease severity in patients with muscle disease and can correlate with physical function (442-444). Furthermore, the results from this thesis support a recent study by Naarding et al. that found that quantitative MRI measurements of the quadriceps may predict a decline in ambulation in patients with Duchenne muscular dystrophy (445). Therefore, the use of quantitative MRI in identifying those at risk of developing frailty and decreased physical function, including a decrease in ambulation, should be investigated in future clinical trials.

9.3 Research considerations

This thesis investigated the use of T2, fat fraction, diffusion tensor imaging, and muscle volume as quantitative MRI techniques to assess muscle health in healthy controls and in patients with: myositis, rheumatoid arthritis, and giant cell arteritis. However, many MRI sequences can provide a quantitative measurement of physiological properties, such as extracellular volume (446), and numerous diseases could be investigated. Regardless of the sequences or the disease group, the same limitations presented throughout this thesis should be addressed.

Limitations that impact all studies within this thesis will now be discussed. This research was conducted at a single site on a single platform (MAGNETOM Verio 3T Siemens). Future research should identify if the data within this thesis is comparable across different MRI machine models and protocols. Potentially, different cut off values may be required depending on the sequences used and the make and model of the MRI machine. The analysis of the T2, fat fraction, and diffusion data was conducted on a single slice, raising the possibility of sampling variation if the muscle were inhomogeneous (447). As the assumption that one slice can represent an entire muscle is incorrect, it would be beneficial to obtain measurements from the entire muscle using multiple slices. This approach, however, may be time-consuming for the individual contouring the images manually and inconvenient for research timelines. This thesis did not match for body mass index (BMI) or account for dyslipidemia, diabetes, medication, or physical activity levels of participants. This lack of matching may have affected results, as it would be expected that those with higher fat mass, diabetes, on statin or glucocorticoid medication, or with high cholesterol may have a lower muscle quality compared to healthy individuals who partake in regular physical activity or are of a healthy weight. Future research should consider controlling for duration of exposure to glucocorticoid therapy and statins, cholesterol, BMI and physical activity levels. A useful method for stratifying physical activity levels could be the international physical activity questionnaire (IPAC) score (448).

9.4 Future directions

As the application of quantitative MRI in muscle is a relatively recent imaging advancement, the capabilities of quantitative MRI in muscle must continue to be investigated to understand the significance of the observations within this thesis.

This study has demonstrated that these measures may be beneficial in the assessment of muscle health. However, it only utilised a single 3T scanner at a

single site. Future research is required to confirm whether the results from this research project can be replicated across a multi-vendor, multiplatform clinical setting, including at varying Tesla. However, as the results of this research project did not demonstrate substantive differences assessed by diffusion imaging, future work should focus on T2, fat fraction, and muscle volume. This future work could potentially be performed using MR fingerprinting, which can quickly generate quantitative multi-parametric maps simultaneously (449).

The findings from this thesis are in agreement with previously published work, suggesting that quantitative MRI could have a valuable role in the management of muscle health (450). However, these results would need to be validated in a powered diagnostic accuracy study to confirm whether quantitative MRI could be used in the management of muscle pathology. Therefore, the future potential of this research is promising, as MRI is used routinely in the management of muscle disease, such as in the diagnosis of myositis, and therefore, quantitative MRI measurements could be easily integrated into clinical care.

9.4.1 Segmenting of muscles for quantitative MRI

Measurements obtained with quantitative MRI are often achieved from contouring a region of interest which permits the calculation of the mean value from the selected region. In addition, segmenting of muscles can be difficult if the regions of interest are small or have complex anatomy. Furthermore, due to the heterogeneous nature of muscle pathology, it would be beneficial to select regions of interest across the entire muscle. Future research should investigate the possibility of automating the segmentation of muscle to enable the analysis of large MRI datasets and to increase its usability in the clinical setting. Due to the limited available time in a healthcare setting or in confirmatory research studies, such as in a large multi-site clinical trial which use a large quantity of participants, automated methods, such as

artificial intelligence for segmentation of the desired tissues, would offer a significant advantage.

9.4.2 Artificial intelligence in rheumatology

The application of artificial intelligence in medical imaging within rheumatology has enhanced the efficacy and efficiency of image interpretation (451). Unsurprisingly, artificial intelligence in rheumatology is currently confined to assessing common joint pathologies such as joint synovitis, tenosynovitis, bone erosions, and cartilage loss, and there has been little development in the use of artificial intelligence in muscle imaging. Therefore, deep learning involving quantitative MRI may accelerate the knowledge and application of these imaging techniques.

9.5 Conclusions

Whilst medical imaging has improved our knowledge of joint pathology, it is now time for a more comprehensive approach to understanding the pathogenesis of rheumatic diseases, with due attention to the muscle, and consideration towards potential interventions for preserving muscle function. Such an approach is important because skeletal muscles are vital for daily activities, and a decrease in muscle health can significantly impact quality of life (452). Quantitative MRI shows potential to improve the understanding of how muscle is compromised due to ageing and rheumatic disease. Quantitative MRI could also be used to diagnose and monitor muscle pathology, and to develop interventions, such as exercise, in order to improve muscle quality. Interventions that could improve muscle quality

may have a substantial impact on the health and wellbeing of individuals and could decrease the demands and financial burden on health systems (453).

The research within this thesis aims to provide a foundation for which to base future work on the investigation of muscle health in healthy individuals and patients with rheumatic disease. The work in this thesis has shown that quantitative MRI and muscle strength measurements are useful non-invasive tools which can provide information on muscle health. The results of the research studies within this thesis suggest that quantitative muscle strength and MRI measures, including T2, fat fraction, and muscle volume, are effective for identifying differences in muscle properties due to age and rheumatic disease, and would be suitable for further research. However, diffusion measurements within this thesis did not show clinically substantive differences within this setting. This work adds to the growing body of evidence that describes muscle changes due to age-related sarcopenia and rheumatic disease.

Although the research studies within this thesis were pilot studies, they provide compelling evidence in support of further research. Following further research, the described measurements within this thesis may present clinical value if they are confirmed to be able to identify significant and clinically meaningful differences in muscle health, and therefore, may be able to improve clinical management and patient quality of life.

References

1. Farrow M, Biglands J, Alfuraih AM, Wakefield RJ, Tan AL. Novel Muscle Imaging in Inflammatory Rheumatic Diseases-A Focus on Ultrasound Shear Wave Elastography and Quantitative MRI. Front Med (Lausanne). 2020;7(434):434.

2. Farrow M, Grainger AJ, Tan AL, Buch MH, Emery P, Ridgway JP, et al. Normal values and test-retest variability of stimulated-echo diffusion tensor imaging and fat fraction measurements in the muscle. Br J Radiol. 2019;92(1101):20190143.

3. Farrow M, Biglands J, Tanner SF, Clegg A, Brown L, Hensor EMA, et al. The effect of ageing on skeletal muscle as assessed by quantitative MR imaging: an association with frailty and muscle strength. Aging Clin Exp Res. 2020.

4. Farrow M, Biglands JD, Grainger AJ, O'Connor P, Hensor EMA, Ladas A, et al. Quantitative MRI in myositis patients: comparison with healthy volunteers and radiological visual assessment. Clin Radiol. 2020.

5. Farrow M, Biglands J, Tanner S, Hensor EMA, Buch MH, Emery P, et al. Muscle deterioration due to rheumatoid arthritis: assessment by quantitative MRI and strength testing. Rheumatology (Oxford). 2020.

6. Tan AL, Farrow M, Biglands J, Fernandes RJ, Abraldes JA, de Souza Castro FA, et al. Commentaries on Viewpoint: The interaction between SARS-CoV-2 and ACE2 may have consequences for skeletal muscle viral susceptibility and myopathies. J Appl Physiol (1985). 2020;129(4):868-71.

7. Burnett C, Wright P, Keenan AM, Redmond A, Ridgway J. Magnetic Resonance Imaging of synovitis in knees of patients with osteoarthritis without injected contrast agents using T1 quantification. Radiography (Lond). 2018;24(4):283-8.

8. Siddle HJ, Hensor EM, Hodgson RJ, Grainger AJ, Redmond AC, Wakefield RJ, et al. Anatomical location of erosions at the metatarsophalangeal joints in patients with rheumatoid arthritis. Rheumatology (Oxford). 2014;53(5):932-6.

9. Pinedo-Villanueva R, Westbury LD, Syddall HE, Sanchez-Santos MT, Dennison EM, Robinson SM, et al. Health Care Costs Associated With Muscle Weakness: A UK Population-Based Estimate. Calcif Tissue Int. 2019;104(2):137-44.

10. Candow DG, Chilibeck PD. Differences in size, strength, and power of upper and lower body muscle groups in young and older men. J Gerontol A Biol Sci Med Sci. 2005;60(2):148-56.

11. Lauretani F, Russo CR, Bandinelli S, Bartali B, Cavazzini C, Di Iorio A, et al. Age-associated changes in skeletal muscles and their effect on mobility: an operational diagnosis of sarcopenia. J Appl Physiol (1985). 2003;95(5):1851-60.

12. Ekdahl C, Broman G. Muscle strength, endurance, and aerobic capacity in rheumatoid arthritis: a comparative study with healthy subjects. Ann Rheum Dis. 1992;51(1):35-40.

13. Perrot S, Le Jeunne C. [Steroid-induced myopathy]. Presse Med. 2012;41(4):422-6.

14. Wolfe RR. The underappreciated role of muscle in health and disease. Am J Clin Nutr. 2006;84(3):475-82.

15. Dequeker J, Nijs J, Westhovens R, Taelman V. Body composition in rheumatoid arthritis. Rheumatology. 1997;36(4):444-8.

16. Terrier F, Hricak H, Revel D, Alpers CE, Reinhold CE, Levine J, et al. Magnetic resonance imaging and spectroscopy of the periarticular inflammatory soft-tissue changes in experimental arthritis of the rat. Invest Radiol. 1985;20(8):813-23.

17. Hatakenaka M, Matsuo Y, Setoguchi T, Yabuuchi H, Okafuji T, Kamitani T, et al. Alteration of proton diffusivity associated with passive muscle extension and contraction. J Magn Reson Imaging. 2008;27(4):932-7.

18. Shin D, Finni T, Ahn S, Hodgson JA, Lee HD, Edgerton VR, et al. Effect of chronic unloading and rehabilitation on human Achilles tendon properties: a velocity-encoded phase-contrast MRI study. J Appl Physiol (1985). 2008;105(4):1179-86.

19. Drace JE, Pelc NJ. Tracking the motion of skeletal muscle with velocity-encoded MR imaging. J Magn Reson Imaging. 1994;4(6):773-8.

20. Pappas GP, Asakawa DS, Delp SL, Zajac FE, Drace JE. Nonuniform shortening in the biceps brachii during elbow flexion. J Appl Physiol (1985). 2002;92(6):2381-9.

21. Maganaris CN, Baltzopoulos V, Sargeant AJ. In vivo measurements of the triceps surae complex architecture in man: implications for muscle function. J Physiol. 1998;512 (Pt 2):603-14.

22. Finni T, Hodgson JA, Lai AM, Edgerton VR, Sinha S. Nonuniform strain of human soleus aponeurosis-tendon complex during submaximal voluntary contractions in vivo. J Appl Physiol (1985). 2003;95(2):829-37.

23. Willis TA, Hollingsworth KG, Coombs A, Sveen ML, Andersen S, Stojkovic T, et al. Quantitative muscle MRI as an assessment tool for monitoring disease progression in LGMD2I: a multicentre longitudinal study. PLoS One. 2013;8(8):e70993.

24. Marcus RL, Addison O, Dibble LE, Foreman KB, Morrell G, Lastayo P. Intramuscular adipose tissue, sarcopenia, and mobility function in older individuals. J Aging Res. 2012;2012:629637.

25. Scheel M, von Roth P, Winkler T, Arampatzis A, Prokscha T, Hamm B, et al. Fiber type characterization in skeletal muscle by diffusion tensor imaging. NMR Biomed. 2013;26(10):1220-4.

26. Qi J, Olsen NJ, Price RR, Winston JA, Park JH. Diffusion-weighted imaging of inflammatory myopathies: polymyositis and dermatomyositis. J Magn Reson Imaging. 2008;27(1):212-7.

27. Mashhood A, Railkar R, Yokoo T, Levin Y, Clark L, Fox-Bosetti S, et al. Reproducibility of hepatic fat fraction measurement by magnetic resonance imaging. J Magn Reson Imaging. 2013;37(6):1359-70.

28. Reeder SB, Cruite I, Hamilton G, Sirlin CB. Quantitative Assessment of Liver Fat with Magnetic Resonance Imaging and Spectroscopy. J Magn Reson Imaging. 2011;34(4):729-49.

29. Warach S, Chien D, Li W, Ronthal M, Edelman RR. Fast magnetic resonance diffusion-weighted imaging of acute human stroke. Neurology. 1992;42(9):1717-23.

30. Neumann-Haefelin T, Wittsack HJ, Wenserski F, Siebler M, Seitz RJ, Modder U, et al. Diffusion- and perfusion-weighted MRI. The DWI/PWI mismatch region in acute stroke. Stroke. 1999;30(8):1591-7.

31. Assaf Y, Pasternak O. Diffusion tensor imaging (DTI)-based white matter mapping in brain research: a review. J Mol Neurosci. 2008;34(1):51-61.

32. Shenton ME, Hamoda HM, Schneiderman JS, Bouix S, Pasternak O, Rathi Y, et al. A review of magnetic resonance imaging and diffusion tensor imaging findings in mild traumatic brain injury. Brain Imaging Behav. 2012;6(2):137-92.

33. Bennett IJ, Rypma B. Advances in functional neuroanatomy: a review of combined DTI and fMRI studies in healthy younger and older adults. Neurosci Biobehav Rev. 2013;37(7):1201-10.

34. Lee MA, Smith S, Palace J, Matthews PM. Defining multiple sclerosis disease activity using MRI T2-weighted difference imaging. Brain. 1998;121 (Pt 11)(11):2095-102.

35. Metsios GS, Kitas GD. Physical activity, exercise and rheumatoid arthritis: Effectiveness, mechanisms and implementation. Best Pract Res Clin Rheumatol. 2018;32(5):669-82.

36. Hall JE. Guyton and Hall textbook of medical physiology. Textbook of medical physiology. 1. 13 ed. Philadelphia: Elsevier; 2016. p. 75-102.

37. Janssen I, Heymsfield SB, Wang ZM, Ross R. Skeletal muscle mass and distribution in 468 men and women aged 18-88 yr. J Appl Physiol (1985). 2000;89(1):81-8.

38. Woolf AD, Pfleger B. Burden of major musculoskeletal conditions. Bull World Health Organ. 2003;81(9):646-56.

39. Fessel WJ. Muscle diseases in rheumatology. Semin Arthritis Rheum. 1973;3(2):127-54.

40. Arnold JB, Halstead J, Grainger AJ, Keenan AM, Hill CL, Redmond AC. Foot and leg muscle weakness in people with midfoot osteoarthritis. Arthritis Care Res (Hoboken). 2020.

41. Hiscock A, Dewar L, Parton M, Machado P, Hanna M, Ramdharry G. Frequency and circumstances of falls in people with inclusion body myositis: a questionnaire survey to explore falls management and physiotherapy provision. Physiotherapy. 2014;100(1):61-5.

42. Pollard LC, Choy EH, Gonzalez J, Khoshaba B, Scott DL. Fatigue in rheumatoid arthritis reflects pain, not disease activity. Rheumatology (Oxford). 2006;45(7):885-9.

43. Graham CD, Rose MR, Grunfeld EA, Kyle SD, Weinman J. A systematic review of quality of life in adults with muscle disease. J Neurol. 2011;258(9):1581-92.

44. Tellnes G, Bjerkedal T. Epidemiology of sickness certification--a methodological approach based on a study from Buskerud County in Norway. Scand J Soc Med. 1989;17(3):245-51.

45. Szubert Z, Sobala W, Zycinska Z. [The effect of system restructuring on absenteeism due to sickness in the work place. I. Sickness absenteeism during the period 19989-1994]. Med Pr. 1997;48(5):543-51.

46. Brage S, Nygard JF, Tellnes G. The gender gap in musculoskeletal-related long-term sickness absence in Norway. Scand J Soc Med. 1998;26(1):34-43.

47. Rasker JJ. Rheumatology in general practice. Br J Rheumatol. 1995;34(6):494-7.

48. Jack J, Jones T, Hutchinson C, Bez H, Edirisinghe E. Automatic diagnosis of inflammatory muscle disease for MRI using computer-extracted features of bivariate histograms. Proc Spie Medical Imaging 2015: Computer-Aided Diagnosis. 2015:941402.

49. Altabas-Gonzalez I, Perez-Gomez N, Pego-Reigosa JM. How to investigate: Suspected systemic rheumatic diseases in patients presenting with muscle complaints. Best Pract Res Clin Rheumatol. 2019;33(4):101437.

50. Ostergaard M, Peterfy C, Conaghan P, McQueen F, Bird P, Ejbjerg B, et al. OMERACT Rheumatoid Arthritis Magnetic Resonance Imaging Studies. Core set of MRI acquisitions, joint pathology definitions, and the OMERACT RA-MRI scoring system. J Rheumatol. 2003;30(6):1385-6.

51. Halstead J, Martin-Hervas C, Hensor EMA, McGonagle D, Keenan AM, Redmond AC, et al. Development and Reliability of a Preliminary Foot Osteoarthritis Magnetic Resonance Imaging Score. J Rheumatol. 2017;44(8):1257-64.

52. Lieber RL, Friden J. Functional and clinical significance of skeletal muscle architecture. Muscle Nerve. 2000;23(11):1647-66.

53. Edgerton VR, Smith JL, Simpson DR. Muscle fibre type populations of human leg muscles. Histochem J. 1975;7(3):259-66.

54. Wang Y, Pessin JE. Mechanisms for fiber-type specificity of skeletal muscle atrophy. Curr Opin Clin Nutr Metab Care. 2013;16(3):243-50.

55. Alnaqeeb MA, Goldspink G. Changes in fibre type, number and diameter in developing and ageing skeletal muscle. J Anat. 1987;153:31-45.

56. Goldspink G, Ward PS. Changes in rodent muscle fibre types during post-natal growth, undernutrition and exercise. J Physiol. 1979;296(1):453-69.

57. Seene T, Umnova M, Alev K, Pehme A. Effect of glucocorticoids on contractile apparatus of rat skeletal muscle. J Steroid Biochem. 1988;29(3):313-7.

58. Edstrom L, Nordemar R. Differential changes in type I and type II muscle fibres in rheumatoid arthritis. A biopsy study. Scand J Rheumatol. 1974;3(3):155-60.

59. Quittan M, Wiesinger GF, Sturm B, Puig S, Mayr W, Sochor A, et al. Improvement of thigh muscles by neuromuscular electrical stimulation in patients with refractory heart failure: a single-blind, randomized, controlled trial. Am J Phys Med Rehabil. 2001;80(3):206-14; quiz 15-6, 24.

60. Dubowitz V, Sewry CA, Oldford A. Section 1 The Biopsy: Normal and Diseased Muscle. Muscle Biopsy: A Practical Approach. 1. 5 ed. China: Saunders Elsevier; 2020. p. 1-183.

61. Walsmith J, Roubenoff R. Cachexia in rheumatoid arthritis. Int J Cardiol. 2002;85(1):89-99.

62. Pincus T, Callahan LF, Sale WG, Brooks AL, Payne LE, Vaughn WK. Severe functional declines, work disability, and increased mortality in seventy-five rheumatoid arthritis patients studied over nine years. Arthritis Rheum. 1984;27(8):864-72.

63. Janssen I, Heymsfield SB, Ross R. Low relative skeletal muscle mass (sarcopenia) in older persons is associated with functional impairment and physical disability. J Am Geriatr Soc. 2002;50(5):889-96.

64. Clarke AE, Bloch DA, Medsger TA, Jr., Oddis CV. A longitudinal study of functional disability in a national cohort of patients with polymyositis/dermatomyositis. Arthritis Rheum. 1995;38(9):1218-24.

65. Michel J-P, Beattie L, Martin FC, Walston JD. Section 4 Age-related biological changes, altered physiology, and vulnerability to diseases and chronic conditions In: Walston JD, editor. Oxford Textbook of Geriatric Medicine. 1. 3 ed. Oxford: Oxford University Press; 2017. p. 303-23.

66. Khan AA, Iliescu DD, Hines EL, Hutchinson CE, Sneath RJS. Classification of Age-Related Changes in Lumbar Spine with the Help of MRI Scores. 2013 29th Southern Biomedical Engineering Conference; Miami, Florida, USA: IEEE; 2013. p. 121-2.

67. Rikli RE, Jones CJ. Assessing Physical Performance in Independent Older Adults: Issues and Guidelines. Journal of Aging and Physical Activity. 1997;5(3):244-61.

68. Pendergast DR, Fisher NM, Calkins E. Cardiovascular, neuromuscular, and metabolic alterations with age leading to frailty. J Gerontol. 1993;48 Spec No:61-7.

69. Chatterji S, Byles J, Cutler D, Seeman T, Verdes E. Health, functioning, and disability in older adults--present status and future implications. Lancet. 2015;385(9967):563-75.

70. Fielding RA, Vellas B, Evans WJ, Bhasin S, Morley JE, Newman AB, et al. Sarcopenia: an undiagnosed condition in older adults. Current consensus definition: prevalence, etiology, and consequences. International working group on sarcopenia. J Am Med Dir Assoc. 2011;12(4):249-56.

71. Cruz-Jentoft AJ, Baeyens JP, Bauer JM, Boirie Y, Cederholm T, Landi F, et al. Sarcopenia: European consensus on definition and diagnosis: Report of the European Working Group on Sarcopenia in Older People. Age Ageing. 2010;39(4):412-23.

72. Frontera WR, Hughes VA, Lutz KJ, Evans WJ. A cross-sectional study of muscle strength and mass in 45- to 78-yr-old men and women. J Appl Physiol (1985). 1991;71(2):644-50.

73. Ferrucci L, Guralnik JM, Buchner D, Kasper J, Lamb SE, Simonsick EM, et al. Departures from linearity in the relationship between measures of muscular strength and physical performance of the lower extremities: the Women's Health and Aging Study. J Gerontol A Biol Sci Med Sci. 1997;52(5):M275-85.

74. Whipple RH, Wolfson LI, Amerman PM. The relationship of knee and ankle weakness to falls in nursing home residents: an isokinetic study. J Am Geriatr Soc. 1987;35(1):13-20.

75. Nevitt MC, Cummings SR, Kidd S, Black D. Risk factors for recurrent nonsyncopal falls. A prospective study. JAMA. 1989;261(18):2663-8.

76. Gehlsen GM, Whaley MH. Falls in the elderly: Part II, Balance, strength, and flexibility. Arch Phys Med Rehabil. 1990;71(10):739-41.

77. Landi F, Liperoti R, Russo A, Giovannini S, Tosato M, Capoluongo E, et al. Sarcopenia as a risk factor for falls in elderly individuals: results from the ilSIRENTE study. Clin Nutr. 2012;31(5):652-8.

78. Chang SF, Lin PL. Systematic Literature Review and Meta-Analysis of the Association of Sarcopenia With Mortality. Worldviews Evid Based Nurs. 2016;13(2):153-62.

79. Buigues C, Padilla-Sanchez C, Garrido JF, Navarro-Martinez R, Ruiz-Ros V, Cauli O. The relationship between depression and frailty syndrome: a systematic review. Aging Ment Health. 2015;19(9):762-72.

80. Lynch GS. Tackling Australia's future health problems: developing strategies to combat sarcopenia--age-related muscle wasting and weakness. Intern Med J. 2004;34(5):294-6.

81. Ryall JG, Schertzer JD, Lynch GS. Cellular and molecular mechanisms underlying age-related skeletal muscle wasting and weakness. Biogerontology. 2008;9(4):213-28.

82. Arnold AS, Egger A, Handschin C. PGC-1alpha and myokines in the aging muscle - a mini-review. Gerontology. 2011;57(1):37-43.

83. Wenz T, Rossi SG, Rotundo RL, Spiegelman BM, Moraes CT. Increased muscle PGC-1alpha expression protects from sarcopenia and metabolic disease during aging. Proc Natl Acad Sci U S A. 2009;106(48):20405-10.

84. Zoico E, Corzato F, Bambace C, Rossi AP, Micciolo R, Cinti S, et al. Myosteatosis and myofibrosis: relationship with aging, inflammation and insulin resistance. Arch Gerontol Geriatr. 2013;57(3):411-6.

85. Reid MB, Lannergren J, Westerblad H. Respiratory and limb muscle weakness induced by tumor necrosis factor-alpha: involvement of muscle myofilaments. Am J Respir Crit Care Med. 2002;166(4):479-84.

86. Delbono O. Expression and regulation of excitation-contraction coupling proteins in aging skeletal muscle. Curr Aging Sci. 2011;4(3):248-59.

87. Kostek MC, Delmonico MJ. Age-related changes in adult muscle morphology. Curr Aging Sci. 2011;4(3):221-33.

88. D'Antona G, Pellegrino MA, Adami R, Rossi R, Carlizzi CN, Canepari M, et al. The effect of ageing and immobilization on structure and function of human skeletal muscle fibres. J Physiol. 2003;552(Pt 2):499-511.

89. Lexell J. Human aging, muscle mass, and fiber type composition. J Gerontol A Biol Sci Med Sci. 1995;50 Spec No:11-6.

90. Andersen JL. Muscle fibre type adaptation in the elderly human muscle. Scand J Med Sci Sports. 2003;13(1):40-7.

91. Frontera WR, Suh D, Krivickas LS, Hughes VA, Goldstein R, Roubenoff R. Skeletal muscle fiber quality in older men and women. Am J Physiol Cell Physiol. 2000;279(3):C611-8.

92. Maxwell LC, Faulkner JA, Lieberman DA. Histochemical manifestations of age and endurance training in skeletal muscle fibers. Am J Physiol. 1973;224(2):356-61.

93. Xie Y, Yao Z, Chai H, Wong WM, Wu W. Expression and role of low-affinity nerve growth factor receptor (p75) in spinal motor neurons of aged rats following axonal injury. Dev Neurosci. 2003;25(1):65-71.

94. Verdijk LB, Koopman R, Schaart G, Meijer K, Savelberg HH, van Loon LJ. Satellite cell content is specifically reduced in type II skeletal muscle fibers in the elderly. Am J Physiol Endocrinol Metab. 2007;292(1):E151-7.

95. Clark BC, Taylor JL. Age-related changes in motor cortical properties and voluntary activation of skeletal muscle. Curr Aging Sci. 2011;4(3):192-9.

96. Kalinkovich A, Livshits G. Sarcopenia--The search for emerging biomarkers. Ageing Res Rev. 2015;22:58-71.

97. Lourenco RA, Perez-Zepeda M, Gutierrez-Robledo L, Garcia-Garcia FJ, Rodriguez Manas L. Performance of the European Working Group on Sarcopenia in Older People algorithm in screening older adults for muscle mass assessment. Age Ageing. 2015;44(2):334-8.

98. Boutin RD, Yao L, Canter RJ, Lenchik L. Sarcopenia: Current Concepts and Imaging Implications. AJR Am J Roentgenol. 2015;205(3):W255-66.

99. Cruz-Jentoft AJ, Bahat G, Bauer J, Boirie Y, Bruyere O, Cederholm T, et al. Sarcopenia: revised European consensus on definition and diagnosis. Age Ageing. 2019;48(4):601.

100. Aagaard P, Suetta C, Caserotti P, Magnusson SP, Kjaer M. Role of the nervous system in sarcopenia and muscle atrophy with aging: strength training as a countermeasure. Scand J Med Sci Sports. 2010;20(1):49-64.

101. Runge M, Rittweger J, Russo CR, Schiessl H, Felsenberg D. Is muscle power output a key factor in the age-related decline in physical performance? A comparison of muscle cross section, chair-rising test and jumping power. Clin Physiol Funct Imaging. 2004;24(6):335-40.

102. Yamauchi J, Mishima C, Nakayama S, Ishii N. Force-velocity, force-power relationships of bilateral and unilateral leg multi-joint movements in young and elderly women. J Biomech. 2009;42(13):2151-7.

103. Korhonen MT, Cristea A, Alen M, Hakkinen K, Sipila S, Mero A, et al. Aging, muscle fiber type, and contractile function in sprint-trained athletes. J Appl Physiol (1985). 2006;101(3):906-17.

104. Cristea A, Korhonen MT, Hakkinen K, Mero A, Alen M, Sipila S, et al. Effects of combined strength and sprint training on regulation of muscle contraction at the whole-muscle and single-fibre levels in elite master sprinters. Acta Physiol (Oxf). 2008;193(3):275-89.

105. Chinoy H, Lilleker JB. Pitfalls in the diagnosis of myositis. Best Pract Res Clin Rheumatol. 2020;34(1):101486.

106. Day J, Patel S, Limaye V. The role of magnetic resonance imaging techniques in evaluation and management of the idiopathic inflammatory myopathies. Semin Arthritis Rheum. 2017;46(5):642-9.

107. Van De Vlekkert J, Maas M, Hoogendijk JE, De Visser M, Van Schaik IN. Combining MRI and muscle biopsy improves diagnostic accuracy in subacute-onset idiopathic inflammatory myopathy. Muscle Nerve. 2015;51(2):253-8.

108. Pipitone N. Value of MRI in diagnostics and evaluation of myositis. Curr Opin Rheumatol. 2016;28(6):625-30.

109. Kubinova K, Mann H, Vencovsky J. MRI scoring methods used in evaluation of muscle involvement in patients with idiopathic inflammatory myopathies. Curr Opin Rheumatol. 2017;29(6):623-31.

110. Connor A, Stebbings S, Anne Hung N, Hammond-Tooke G, Meikle G, Highton J. STIR MRI to direct muscle biopsy in suspected idiopathic inflammatory myopathy. J Clin Rheumatol. 2007;13(6):341-5.

111. Milisenda JC, Collado MV, Pinal-Fernandez I, Hormaza Jaramillo A, Faruch Bilfeld M, Cano MD, et al. Correlation between quantitative and semiquantitative magnetic resonance imaging and histopathology findings in dermatomyositis. Clin Exp Rheumatol. 2019;37(4):633-40.

112. Huang ZG, Gao BX, Chen H, Yang MX, Chen XL, Yan R, et al. An efficacy analysis of whole-body magnetic resonance imaging in the diagnosis and follow-up of polymyositis and dermatomyositis. PLoS One. 2017;12(7):e0181069.

113. Filli L, Maurer B, Manoliu A, Andreisek G, Guggenberger R. Whole-body MRI in adult inflammatory myopathies: Do we need imaging of the trunk? Eur Radiol. 2015;25(12):3499-507.

114. Kadoba K, Mizukawa K, Nishimura K, Murabe H. Large vessel giant cell arteritis suggested by magnetic resonance imaging of the thigh: a potential mimicker of myositis, fasciitis and skeletal muscle vasculitis. Rheumatology (Oxford). 2019;58(12):2211.

115. Yao L, Yip AL, Shrader JA, Mesdaghinia S, Volochayev R, Jansen AV, et al. Magnetic resonance measurement of muscle T2, fat-corrected T2 and fat fraction in the assessment of idiopathic inflammatory myopathies. Rheumatology (Oxford). 2016;55(3):441-9.

116. Ran J, Ji S, Morelli JN, Wu G, Li XM. The diagnostic value of T2 maps and rs-EPI DWI in dermatomyositis. Br J Radiol. 2019;92(1094):20180715.

117. Lemmey AB, Wilkinson TJ, Clayton RJ, Sheikh F, Whale J, Jones HS, et al. Tight control of disease activity fails to improve body composition or physical function in rheumatoid arthritis patients. Rheumatology (Oxford). 2016;55(10):1736-45.

118. Hanaoka BY, Ithurburn MP, Rigsbee CA, Bridges SL, Jr., Moellering DR, Gower B, et al. Chronic Inflammation in Rheumatoid Arthritis and Mediators of Skeletal Muscle Pathology and Physical Impairment: A Review. Arthritis Care Res (Hoboken). 2019;71(2):173-7.

119. Baker JF, Von Feldt J, Mostoufi-Moab S, Noaiseh G, Taratuta E, Kim W, et al. Deficits in muscle mass, muscle density, and modified associations with fat in rheumatoid arthritis. Arthritis Care Res (Hoboken). 2014;66(11):1612-8.

120. Ekdahl C, Andersson SI, Svensson B. Muscle function of the lower extremities in rheumatoid arthritis and osteoarthrosis. A descriptive study of patients in a primary health care district. J Clin Epidemiol. 1989;42(10):947-54.

121. Seifert O, Baerwald C. Impact of fatigue on rheumatic diseases. Best Pract Res Clin Rheumatol. 2019;33(3):101435.

122. Brooke MH, Kaplan H. Muscle pathology in rheumatoid arthritis, polymyalgia rheumatica, and polymyositis: a histochemical study. Arch Pathol. 1972;94(2):101-18.

123. Roubenoff R, Roubenoff RA, Cannon JG, Kehayias JJ, Zhuang H, Dawson-Hughes B, et al. Rheumatoid cachexia: cytokine-driven hypermetabolism accompanying reduced body cell mass in chronic inflammation. J Clin Invest. 1994;93(6):2379-86.

124. Engvall IL, Elkan AC, Tengstrand B, Cederholm T, Brismar K, Hafstrom I. Cachexia in rheumatoid arthritis is associated with inflammatory activity, physical disability, and low bioavailable insulin-like growth factor. Scand J Rheumatol. 2008;37(5):321-8.

125. Almeida C, Choy EH, Hewlett S, Kirwan JR, Cramp F, Chalder T, et al. Biologic interventions for fatigue in rheumatoid arthritis. Cochrane Database Syst Rev. 2016(6):CD008334.

126. Azeez M, Clancy C, O'Dwyer T, Lahiff C, Wilson F, Cunnane G. Benefits of exercise in patients with rheumatoid arthritis: a randomized controlled trial of a patient-specific exercise programme. Clin Rheumatol. 2020;39(6):1783-92.

127. Watts RA, Conaghan PG, Denton C, Foster H, Isaacs J, Müller-Ladner U. Oxford Textbook of Rheumatology. 1. 4 ed. Oxford: Oxford University Press; 2013. p. 500-1000.

128. Askari A, Vignos PJ, Jr., Moskowitz RW. Steroid myopathy in connective tissue disease. Am J Med. 1976;61(4):485-92.

129. Dasgupta B, Borg FA, Hassan N, Alexander L, Barraclough K, Bourke B, et al. BSR and BHPR guidelines for the management of giant cell arteritis. Rheumatology (Oxford). 2010;49(8):1594-7.

130. Harris E, Tiganescu A, Tubeuf S, Mackie SL. The prediction and monitoring of toxicity associated with long-term systemic glucocorticoid therapy. Curr Rheumatol Rep. 2015;17(6):513.

131. Minetto MA, Rainoldi A, Jabre JF. The clinical use of macro and surface electromyography in diagnosis and follow-up of endocrine and drug-induced myopathies. J Endocrinol Invest. 2007;30(9):791-6.

132. Schakman O, Kalista S, Barbe C, Loumaye A, Thissen JP. Glucocorticoid-induced skeletal muscle atrophy. Int J Biochem Cell Biol. 2013;45(10):2163-72.

133. Lofberg E, Gutierrez A, Wernerman J, Anderstam B, Mitch WE, Price SR, et al. Effects of high doses of glucocorticoids on free amino acids, ribosomes and protein turnover in human muscle. Eur J Clin Invest. 2002;32(5):345-53.

134. Mackie SL, Pease CT, Fukuba E, Harris E, Emery P, Hodgson R, et al. Whole-body MRI of patients with polymyalgia rheumatica identifies a distinct subset with complete patient-reported response to glucocorticoids. Ann Rheum Dis. 2015;74(12):2188-92.

135. McGonagle D, Pease C, Marzo-Ortega H, O'Connor P, Gibbon W, Emery P. Comparison of extracapsular changes by magnetic resonance imaging in patients with rheumatoid arthritis and polymyalgia rheumatica. J Rheumatol. 2001;28(8):1837-41.

136. Mori S, Koga Y, Ito K. Clinical characteristics of polymyalgia rheumatica in Japanese patients: evidence of synovitis and extracapsular inflammatory changes by fat suppression magnetic resonance imaging. Mod Rheumatol. 2007;17(5):369-75.

137. Danneskiold-Samsoe B, Grimby G. Isokinetic and isometric muscle strength in patients with rheumatoid arthritis. The relationship to clinical parameters and the influence of corticosteroid. Clin Rheumatol. 1986;5(4):459-67.

138. Rothstein JM, Delitto A, Sinacore DR, Rose SJ. Muscle function in rheumatic disease patients treated with corticosteroids. Muscle Nerve. 1983;6(2):128-35.

139. Baczynska AM, Shaw S, Roberts HC, Cooper C, Aihie Sayer A, Patel HP. Human Vastus Lateralis Skeletal Muscle Biopsy Using the Weil-Blakesley Conchotome. J Vis Exp. 2016(109):e53075.

140. Dengler J, Linke P, Gdynia HJ, Wolf S, Ludolph AC, Vajkoczy P, et al. Differences in pain perception during open muscle biopsy and Bergstroem needle muscle biopsy. J Pain Res. 2014;7:645-50.

141. Sadikoglu F, Kavalcioglu C, Dagman B. Electromyogram (EMG) signal detection, classification of EMG signals and diagnosis of neuropathy muscle disease. Procedia computer science. 2017;120:422-9.

142. Bohannon RW. Sit-to-stand test for measuring performance of lower extremity muscles. Percept Mot Skills. 1995;80(1):163-6.

143. Mathias S, Nayak US, Isaacs B. Balance in elderly patients: the "get-up and go" test. Arch Phys Med Rehabil. 1986;67(6):387-9.

144. McDonald CM, Abresch RT, Carter GT, Fowler WM, Jr., Johnson ER, Kilmer DD. Profiles of neuromuscular diseases. Becker's muscular dystrophy. Am J Phys Med Rehabil. 1995;74(5 Suppl):S93-103.

145. Winter EM, Jones AM, Sport BAo, Sciences E, Davison RCR. Strength testing. In: Cannavan ABaD, editor. Sport and Exercise Physiology Testing Guidelines: The British Association of Sport and Exercise Sciences Guide. 1. Abingdon: Routledge; 2007. p. 130-8.

146. Sapega AA, Drillings G. The definition and assessment of muscular power. J Orthop Sports Phys Ther. 1983;5(1):7-9.

147. Swash M, Brown MM, Thakkar C. CT muscle imaging and the clinical assessment of neuromuscular disease. Muscle Nerve. 1995;18(7):708-14.

148. Ten Dam L, van der Kooi AJ, Verhamme C, Wattjes MP, de Visser M. Muscle imaging in inherited and acquired muscle diseases. Eur J Neurol. 2016;23(4):688-703.

149. Levine JA, Abboud L, Barry M, Reed JE, Sheedy PF, Jensen MD. Measuring leg muscle and fat mass in humans: comparison of CT and dual-energy X-ray absorptiometry. J Appl Physiol (1985). 2000;88(2):452-6.

150. Tateyama M, Fujihara K, Misu T, Arai A, Kaneta T, Aoki M. Clinical values of FDG PET in polymyositis and dermatomyositis syndromes: imaging of skeletal muscle inflammation. BMJ Open. 2015;5(1):e006763.

151. Cimmino MA. Genetic and environmental factors in polymyalgia rheumatica. Ann Rheum Dis. 1997;56(10):576-7.

152. Koh ES, McNally EG. Ultrasound of skeletal muscle injury. Semin Musculoskelet Radiol. 2007;11(2):162-73.

153. Mayans D, Cartwright MS, Walker FO. Neuromuscular ultrasonography: quantifying muscle and nerve measurements. Phys Med Rehabil Clin N Am. 2012;23(1):133-48, xii.

154. Reimers CD, Finkenstaedt M. Muscle imaging in inflammatory myopathies. Curr Opin Rheumatol. 1997;9(6):475-85.

155. Ostergaard M, Pedersen SJ, Dohn UM. Imaging in rheumatoid arthritis--status and recent advances for magnetic resonance imaging, ultrasonography, computed tomography and conventional radiography. Best Pract Res Clin Rheumatol. 2008;22(6):1019-44.

156. Hayashi D, Hamilton B, Guermazi A, de Villiers R, Crema MD, Roemer FW. Traumatic injuries of thigh and calf muscles in athletes: role and clinical relevance of MR imaging and ultrasound. Insights Imaging. 2012;3(6):591-601.

157. Koulouris G, Connell D. Hamstring muscle complex: an imaging review. Radiographics. 2005;25(3):571-86.

158. Mercuri E, Jungbluth H, Muntoni F. Muscle imaging in clinical practice: diagnostic value of muscle magnetic resonance imaging in inherited neuromuscular disorders. Curr Opin Neurol. 2005;18(5):526-37.

159. Mercuri E, Pichiecchio A, Allsop J, Messina S, Pane M, Muntoni F. Muscle MRI in inherited neuromuscular disorders: past, present, and future. J Magn Reson Imaging. 2007;25(2):433-40.

160. Maillard SM, Jones R, Owens C, Pilkington C, Woo P, Wedderburn LR, et al. Quantitative assessment of MRI T2 relaxation time of thigh muscles in juvenile dermatomyositis. Rheumatology (Oxford). 2004;43(5):603-8.

161. Hashemi RH, Bradley WG, Lisanti CJ. MRI: The Basics: The Basics. 4 ed. China: Lippincott Williams & Wilkins; 2017. 17-391 p.

162. Nieminen MT, Rieppo J, Toyras J, Hakumaki JM, Silvennoinen J, Hyttinen MM, et al. T2 relaxation reveals spatial collagen architecture in articular cartilage: a comparative quantitative MRI and polarized light microscopic study. Magn Reson Med. 2001;46(3):487-93.

163. Burakiewicz J, Hooijmans MT, Webb AG, Verschuuren J, Niks EH, Kan HE. Improved olefinic fat suppression in skeletal muscle DTI using a magnitude-based dixon method. Magn Reson Med. 2018;79(1):152-9.

164. Milford D, Rosbach N, Bendszus M, Heiland S. Mono-Exponential Fitting in T2-Relaxometry: Relevance of Offset and First Echo. PLoS One. 2015;10(12):e0145255.

165. Pai A, Li X, Majumdar S. A comparative study at 3 T of sequence dependence of T2 quantitation in the knee. Magn Reson Imaging. 2008;26(9):1215-20.

166. McPhee KC, Wilman AH. Transverse relaxation and flip angle mapping: Evaluation of simultaneous and independent methods using multiple spin echoes. Magn Reson Med. 2017;77(5):2057-65.

167. Marty B, Baudin PY, Reyngoudt H, Azzabou N, Araujo EC, Carlier PG, et al. Simultaneous muscle water T2 and fat fraction mapping using transverse relaxometry with stimulated echo compensation. NMR Biomed. 2016;29(4):431-43.

168. Ma J. Dixon techniques for water and fat imaging. J Magn Reson Imaging. 2008;28(3):543-58.

169. Bydder M, Yokoo T, Hamilton G, Middleton MS, Chavez AD, Schwimmer JB, et al. Relaxation effects in the quantification of fat using gradient echo imaging. Magn Reson Imaging. 2008;26(3):347-59.

170. Hernando D, Liang ZP, Kellman P. Chemical shift-based water/fat separation: a comparison of signal models. Magn Reson Med. 2010;64(3):811-22.

171. Hu HH, Kim HW, Nayak KS, Goran MI. Comparison of fat-water MRI and single-voxel MRS in the assessment of hepatic and pancreatic fat fractions in humans. Obesity (Silver Spring). 2010;18(4):841-7.

172. Bernard CP, Liney GP, Manton DJ, Turnbull LW, Langton CM. Comparison of fat quantification methods: a phantom study at 3.0T. J Magn Reson Imaging. 2008;27(1):192-7.

173. Hines CD, Yu H, Shimakawa A, McKenzie CA, Brittain JH, Reeder SB. T1 independent, T2* corrected MRI with accurate spectral modeling for

quantification of fat: validation in a fat-water-SPIO phantom. J Magn Reson Imaging. 2009;30(5):1215-22.

174. Hines CD, Frydrychowicz A, Hamilton G, Tudorascu DL, Vigen KK, Yu H, et al. T(1) independent, T(2) (*) corrected chemical shift based fat-water separation with multi-peak fat spectral modeling is an accurate and precise measure of hepatic steatosis. J Magn Reson Imaging. 2011;33(4):873-81.

175. Hines CD, Yu H, Shimakawa A, McKenzie CA, Warner TF, Brittain JH, et al. Quantification of hepatic steatosis with 3-T MR imaging: validation in ob/ob mice. Radiology. 2010;254(1):119-28.

176. Levenson H, Greensite F, Hoefs J, Friloux L, Applegate G, Silva E, et al. Fatty infiltration of the liver: quantification with phase-contrast MR imaging at 1.5 T vs biopsy. AJR Am J Roentgenol. 1991;156(2):307-12.

177. McRobbie D, Moore E, Graves M, Prince M. MRI: From Picture to Proton. 2 ed. Cambridge: Cambridge University Press; 2006. 365 p.

178. Fischer MA, Nanz D, Shimakawa A, Schirmer T, Guggenberger R, Chhabra A, et al. Quantification of muscle fat in patients with low back pain: comparison of multi-echo MR imaging with single-voxel MR spectroscopy. Radiology. 2013;266(2):555-63.

179. Budzik JF, Balbi V, Verclytte S, Pansini V, Le Thuc V, Cotten A. Diffusion tensor imaging in musculoskeletal disorders. Radiographics. 2014;34(3):E56-72.

180. Pierpaoli C, Basser PJ. Toward a quantitative assessment of diffusion anisotropy. Magn Reson Med. 1996;36(6):893-906.

181. Van Donkelaar CC, Kretzers LJ, Bovendeerd PH, Lataster LM, Nicolay K, Janssen JD, et al. Diffusion tensor imaging in biomechanical studies of skeletal muscle function. J Anat. 1999;194 (Pt 1)(Pt 1):79-88.

182. Le Bihan D, Breton E, Lallemand D, Grenier P, Cabanis E, Laval-Jeantet M. MR imaging of intravoxel incoherent motions: application to diffusion and perfusion in neurologic disorders. Radiology. 1986;161(2):401-7.

183. Longwei X. Clinical application of diffusion tensor magnetic resonance imaging in skeletal muscle. Muscles Ligaments Tendons J. 2012;2(1):19-24.

184. Kim HK, Lindquist DM, Serai SD, Mariappan YK, Wang LL, Merrow AC, et al. Magnetic resonance imaging of pediatric muscular disorders: recent advances and clinical applications. Radiol Clin North Am. 2013;51(4):721-42.

185. Khalil C, Budzik JF, Kermarrec E, Balbi V, Le Thuc V, Cotten A. Tractography of peripheral nerves and skeletal muscles. Eur J Radiol. 2010;76(3):391-7.

186. Kuo GP, Carrino JA. Skeletal muscle imaging and inflammatory myopathies. Curr Opin Rheumatol. 2007;19(6):530-5.

187. Koltzenburg M, Yousry T. Magnetic resonance imaging of skeletal muscle. Curr Opin Neurol. 2007;20(5):595-9.

188. Noseworthy MD, Davis AD, Elzibak AH. Advanced MR imaging techniques for skeletal muscle evaluation. Semin Musculoskelet Radiol. 2010;14(2):257-68.

189. Heymsfield SB, Adamek M, Gonzalez MC, Jia G, Thomas DM. Assessing skeletal muscle mass: historical overview and state of the art. J Cachexia Sarcopenia Muscle. 2014;5(1):9-18.

190. Heemskerk AM, Strijkers GJ, Drost MR, van Bochove GS, Nicolay K. Skeletal muscle degeneration and regeneration after femoral artery ligation in mice: monitoring with diffusion MR imaging. Radiology. 2007;243(2):413-21.

191. Heemskerk AM, Drost MR, van Bochove GS, van Oosterhout MF, Nicolay K, Strijkers GJ. DTI-based assessment of ischemia-reperfusion in mouse skeletal muscle. Magn Reson Med. 2006;56(2):272-81.

192. Zhang H, Wang X, Guan M, Li C, Luo L. Skeletal muscle evaluation by MRI in a rabbit model of acute ischaemia. Br J Radiol. 2013;86(1026):20120042.

193. Yamabe E, Nakamura T, Oshio K, Kikuchi Y, Toyama Y, Ikegami H. Line scan diffusion spectrum of the denervated rat skeletal muscle. J Magn Reson Imaging. 2007;26(6):1585-9.

194. Saotome T, Sekino M, Eto F, Ueno S. Evaluation of diffusional anisotropy and microscopic structure in skeletal muscles using magnetic resonance. Magn Reson Imaging. 2006;24(1):19-25.

195. Zhang J, Zhang G, Morrison B, Mori S, Sheikh KA. Magnetic resonance imaging of mouse skeletal muscle to measure denervation atrophy. Exp Neurol. 2008;212(2):448-57.

196. Hara Y, Ikoma K, Kido M, Sukenari T, Arai Y, Fujiwara H, et al. Diffusion tensor imaging assesses triceps surae dysfunction after achilles tenotomy in rats. J Magn Reson Imaging. 2015;41(6):1541-8.

197. Fieremans E, Lemberskiy G, Veraart J, Sigmund EE, Gyftopoulos S, Novikov DS. In vivo measurement of membrane permeability and myofiber size in human muscle using time-dependent diffusion tensor imaging and the random permeable barrier model. NMR Biomed. 2017;30(3).

198. Sigmund EE, Novikov DS, Sui D, Ukpebor O, Baete S, Babb JS, et al. Time-dependent diffusion in skeletal muscle with the random permeable barrier model (RPBM): application to normal controls and chronic exertional compartment syndrome patients. NMR Biomed. 2014;27(5):519-28.

199. Malis V, Sinha U, Csapo R, Narici M, Smitaman E, Sinha S. Diffusion tensor imaging and diffusion modeling: Application to monitoring changes in the medial gastrocnemius in disuse atrophy induced by unilateral limb suspension. J Magn Reson Imaging. 2019;49(6):1655-64.

200. Alexander AL, Lee JE, Lazar M, Field AS. Diffusion tensor imaging of the brain. Neurotherapeutics. 2007;4(3):316-29.

201. Mukherjee P, McKinstry RC. Diffusion tensor imaging and tractography of human brain development. Neuroimaging Clin N Am. 2006;16(1):19-43, vii.

202. Le Bihan D. Molecular diffusion nuclear magnetic resonance imaging. Magn Reson Q. 1991;7(1):1-30.

203. Le Bihan D, Mangin JF, Poupon C, Clark CA, Pappata S, Molko N, et al. Diffusion tensor imaging: concepts and applications. J Magn Reson Imaging. 2001;13(4):534-46.

204. Qiu H, Hedlund LW, Gewalt SL, Benveniste H, Bare TM, Johnson GA. Progression of a focal ischemic lesion in rat brain during treatment with a novel

glycine/NMDA antagonist: an in vivo three-dimensional diffusion-weighted MR microscopy study. J Magn Reson Imaging. 1997;7(4):739-44.

205. Wangensteen A, Almusa E, Boukarroum S, Farooq A, Hamilton B, Whiteley R, et al. MRI does not add value over and above patient history and clinical examination in predicting time to return to sport after acute hamstring injuries: a prospective cohort of 180 male athletes. Br J Sports Med. 2015;49(24):1579-87.

206. Basser PJ, Mattiello J, LeBihan D. MR diffusion tensor spectroscopy and imaging. Biophys J. 1994;66(1):259-67.

207. van Doorn A, Bovendeerd PH, Nicolay K, Drost MR, Janssen JD. Determination of muscle fibre orientation using Diffusion-Weighted MRI. Eur J Morphol. 1996;34(1):5-10.

208. Cleveland GG, Chang DC, Hazlewood CF, Rorschach HE. Nuclear magnetic resonance measurement of skeletal muscle: anisotrophy of the diffusion coefficient of the intracellular water. Biophys J. 1976;16(9):1043-53.

209. Basser PJ, Pierpaoli C. Microstructural and physiological features of tissues elucidated by quantitative-diffusion-tensor MRI. 1996. J Magn Reson. 2011;213(2):560-70.

210. Fukunaga T, Miyatani M, Tachi M, Kouzaki M, Kawakami Y, Kanehisa H. Muscle volume is a major determinant of joint torque in humans. Acta physiologica scandinavica. 2001;172(4):249-55.

211. Holzbaur KR, Delp SL, Gold GE, Murray WM. Moment-generating capacity of upper limb muscles in healthy adults. J Biomech. 2007;40(11):2442-9.

212. Trappe SW, Trappe TA, Lee GA, Costill DL. Calf muscle strength in humans. Int J Sports Med. 2001;22(3):186-91.

213. Pons C, Sheehan FT, Im HS, Brochard S, Alter KE. Shoulder muscle atrophy and its relation to strength loss in obstetrical brachial plexus palsy. Clin Biomech (Bristol, Avon). 2017;48:80-7.

214. Tothill P, Stewart AD. Estimation of thigh muscle and adipose tissue volume using magnetic resonance imaging and anthropometry. J Sports Sci. 2002;20(7):563-76.

215. Nakatani M, Takai Y, Akagi R, Wakahara T, Sugisaki N, Ohta M, et al. Validity of muscle thickness-based prediction equation for quadriceps femoris volume in middle-aged and older men and women. Eur J Appl Physiol. 2016;116(11-12):2125-33.

216. Marcon M, Ciritsis B, Laux C, Nanz D, Nguyen-Kim TD, Fischer MA, et al. Cross-sectional area measurements versus volumetric assessment of the quadriceps femoris muscle in patients with anterior cruciate ligament reconstructions. Eur Radiol. 2015;25(2):290-8.

217. Nordez A, Jolivet E, Sudhoff I, Bonneau D, de Guise JA, Skalli W. Comparison of methods to assess quadriceps muscle volume using magnetic resonance imaging. J Magn Reson Imaging. 2009;30(5):1116-23.

218. Sudhoff I, de Guise JA, Nordez A, Jolivet E, Bonneau D, Khoury V, et al. 3D-patient-specific geometry of the muscles involved in knee motion from selected MRI images. Med Biol Eng Comput. 2009;47(6):579-87.

219. Jenkins TM, Burness C, Connolly DJ, Rao DG, Hoggard N, Mawson S, et al. A prospective pilot study measuring muscle volumetric change in amyotrophic lateral sclerosis. Amyotroph Lateral Scler Frontotemporal Degener. 2013;14(5-6):414-23.

220. Godi C, Ambrosi A, Nicastro F, Previtali SC, Santarosa C, Napolitano S, et al. Longitudinal MRI quantification of muscle degeneration in Duchenne muscular dystrophy. Ann Clin Transl Neurol. 2016;3(8):607-22.

221. Wu EX, Tang H, Tong C, Heymsfield SB, Vasselli JR. In vivo MRI quantification of individual muscle and organ volumes for assessment of anabolic steroid growth effects. Steroids. 2008;73(4):430-40.

222. Popadic Gacesa JZ, Kozic DB, Dragnic NR, Jakovljevic DG, Brodie DA, Grujic NG. Changes of functional status and volume of triceps brachii measured by magnetic resonance imaging after maximal resistance training. J Magn Reson Imaging. 2009;29(3):671-6.

223. Barendregt AM, Bray TJP, Hall-Craggs MA, Maas M. Emerging quantitative MR imaging biomarkers in inflammatory arthritides. Eur J Radiol. 2019;121:108707.

224. Maggi L, Moscatelli M, Frangiamore R, Mazzi F, Verri M, De Luca A, et al. Quantitative Muscle MRI Protocol as Possible Biomarker in Becker Muscular Dystrophy. Clin Neuroradiol. 2020.

225. Nunez-Peralta C, Alonso-Perez J, Llauger J, Segovia S, Montesinos P, Belmonte I, et al. Follow-up of late-onset Pompe disease patients with muscle magnetic resonance imaging reveals increase in fat replacement in skeletal muscles. J Cachexia Sarcopenia Muscle. 2020;11(4):1032-46.

226. D'Souza A, Bolsterlee B, Herbert RD. Architecture of the medial gastrocnemius muscle in people who have had a stroke: A diffusion tensor imaging investigation. Clin Biomech (Bristol, Avon). 2020;74:27-33.

227. Heskamp L, van Nimwegen M, Ploegmakers MJ, Bassez G, Deux JF, Cumming SA, et al. Lower extremity muscle pathology in myotonic dystrophy type 1 assessed by quantitative MRI. Neurology. 2019;92(24):e2803-e14.

228. Barnard AM, Willcocks RJ, Finanger EL, Daniels MJ, Triplett WT, Rooney WD, et al. Skeletal muscle magnetic resonance biomarkers correlate with function and sentinel events in Duchenne muscular dystrophy. PLoS One. 2018;13(3):e0194283.

229. Merboldt KD, Hanicke W, Frahm J. Diffusion imaging using stimulated echoes. Magn Reson Med. 1991;19(2):233-9.

230. Fischmann A, Kaspar S, Reinhardt J, Gloor M, Stippich C, Fischer D. Exercise might bias skeletal-muscle fat fraction calculation from Dixon images. Neuromuscul Disord. 2012;22 Suppl 2:S107-10.

231. Gaeta M, Scribano E, Mileto A, Mazziotti S, Rodolico C, Toscano A, et al. Muscle fat fraction in neuromuscular disorders: dual-echo dual-flip-angle spoiled gradient-recalled MR imaging technique for quantification--a feasibility study. Radiology. 2011;259(2):487-94.

232. Nozaki T, Tasaki A, Horiuchi S, Ochi J, Starkey J, Hara T, et al. Predicting Retear after Repair of Full-Thickness Rotator Cuff Tear: Two-Point Dixon MR Imaging Quantification of Fatty Muscle Degeneration-Initial Experience with 1-year Follow-up. Radiology. 2016;280(2):500-9.

233. Jellus V, inventor; 08/13/2009, assignee. Phase correction method Patent. Erlangen, DE2011.

234. Liu CY, McKenzie CA, Yu H, Brittain JH, Reeder SB. Fat quantification with IDEAL gradient echo imaging: correction of bias from T(1) and noise. Magn Reson Med. 2007;58(2):354-64.

235. Gold GE, Han E, Stainsby J, Wright G, Brittain J, Beaulieu C. Musculoskeletal MRI at 3.0 T: relaxation times and image contrast. AJR Am J Roentgenol. 2004;183(2):343-51.

236. Steidle G, Schick F. Addressing spontaneous signal voids in repetitive single-shot DWI of musculature: spatial and temporal patterns in the calves of healthy volunteers and consideration of unintended muscle activities as underlying mechanism. NMR Biomed. 2015;28(7):801-10.

237. Kjaer P, Bendix T, Sorensen JS, Korsholm L, Leboeuf-Yde C. Are MRI-defined fat infiltrations in the multifidus muscles associated with low back pain? BMC Med. 2007;5(1):2.

238. Kader DF, Wardlaw D, Smith FW. Correlation between the MRI changes in the lumbar multifidus muscles and leg pain. Clin Radiol. 2000;55(2):145-9.

239. Parkkola R, Rytokoski U, Kormano M. Magnetic resonance imaging of the discs and trunk muscles in patients with chronic low back pain and healthy control subjects. Spine (Phila Pa 1976). 1993;18(7):830-6.

240. Solgaard Sorensen J, Kjaer P, Jensen ST, Andersen P. Low-field magnetic resonance imaging of the lumbar spine: reliability of qualitative evaluation of disc and muscle parameters. Acta Radiol. 2006;47(9):947-53.

241. Research AaH. Allied Dunbar national fitness survey: main findings; summary. In: UK AaHR, editor. London, UK; Sports Council; London: Health Education Authority, England, UK; 1992. p. 160pp. + 11pp.

242. Julious SA. Sample size of 12 per group rule of thumb for a pilot study. Pharmaceutical Statistics. 2005;4(4):287-91.

243. Lancaster GA, Dodd S, Williamson PR. Design and analysis of pilot studies: recommendations for good practice. J Eval Clin Pract. 2004;10(2):307-12.

244. Edalati M, Hastings MK, Sorensen CJ, Zayed M, Mueller MJ, Hildebolt CF, et al. Diffusion Tensor Imaging of the Calf Muscles in Subjects With and Without Diabetes Mellitus. J Magn Reson Imaging. 2019;49(5):1285-95.

245. Zaraiskaya T, Kumbhare D, Noseworthy MD. Diffusion tensor imaging in evaluation of human skeletal muscle injury. J Magn Reson Imaging. 2006;24(2):402-8.

246. Giraudo C, Motyka S, Weber M, Karner M, Resinger C, Feiweier T, et al. Normalized STEAM-based diffusion tensor imaging provides a robust assessment of muscle tears in football players: preliminary results of a new approach to evaluate muscle injuries. Eur Radiol. 2018;28(7):2882-9.

247. Okamoto Y, Mori S, Kujiraoka Y, Nasu K, Hirano Y, Minami M. Diffusion property differences of the lower leg musculature between athletes and non-athletes using 1.5T MRI. MAGMA. 2012;25(4):277-84.

248. Okamoto Y, Kemp GJ, Isobe T, Sato E, Hirano Y, Shoda J, et al. Changes in diffusion tensor imaging (DTI) eigenvalues of skeletal muscle due to hybrid exercise training. Magn Reson Imaging. 2014;32(10):1297-300.

249. Froeling M, Oudeman J, Strijkers GJ, Maas M, Drost MR, Nicolay K, et al. Muscle changes detected with diffusion-tensor imaging after long-distance running. Radiology. 2015;274(2):548-62.

250. Mercier B, Granier P, Mercier J, Foucat L, Bielicki G, Pradere J, et al. Noninvasive skeletal muscle lactate detection between periods of intense exercise in humans. Eur J Appl Physiol Occup Physiol. 1998;78(1):20-7.

251. Williams SE, Heemskerk AM, Welch EB, Li K, Damon BM, Park JH. Quantitative effects of inclusion of fat on muscle diffusion tensor MRI measurements. J Magn Reson Imaging. 2013;38(5):1292-7.

252. Johnson MA, Polgar J, Weightman D, Appleton D. Data on the distribution of fibre types in thirty-six human muscles. An autopsy study. J Neurol Sci. 1973;18(1):111-29.

253. Polgar J, Johnson MA, Weightman D, Appleton D. Data on fibre size in thirty-six human muscles. An autopsy study. J Neurol Sci. 1973;19(3):307-18.

254. Li K, Dortch RD, Welch EB, Bryant ND, Buck AK, Towse TF, et al. Multi-parametric MRI characterization of healthy human thigh muscles at 3.0 T - relaxation, magnetization transfer, fat/water, and diffusion tensor imaging. NMR Biomed. 2014;27(9):1070-84.

255. Grimm A, Meyer H, Nickel MD, Nittka M, Raithel E, Chaudry O, et al. A Comparison between 6-point Dixon MRI and MR Spectroscopy to Quantify Muscle Fat in the Thigh of Subjects with Sarcopenia. J Frailty Aging. 2019;8(1):21-6.

256. Morrow JM, Sinclair CD, Fischmann A, Reilly MM, Hanna MG, Yousry TA, et al. Reproducibility, and age, body-weight and gender dependency of candidate skeletal muscle MRI outcome measures in healthy volunteers. Eur Radiol. 2014;24(7):1610-20.

257. Foure A, Ogier AC, Le Troter A, Vilmen C, Feiweier T, Guye M, et al. Diffusion Properties and 3D Architecture of Human Lower Leg Muscles Assessed with Ultra-High-Field-Strength Diffusion-Tensor MR Imaging and Tractography: Reproducibility and Sensitivity to Sex Difference and Intramuscular Variability. Radiology. 2018;287(2):592-607.

258. Froeling M, Oudeman J, van den Berg S, Nicolay K, Maas M, Strijkers GJ, et al. Reproducibility of diffusion tensor imaging in human forearm muscles at 3.0 T in a clinical setting. Magn Reson Med. 2010;64(4):1182-90.

259. Noble JJ, Keevil SF, Totman J, Charles-Edwards GD. In vitro and in vivo comparison of two-, three- and four-point Dixon techniques for clinical intramuscular fat quantification at 3 T. Br J Radiol. 2014;87(1036):20130761.

260. Fischer MA, Pfirrmann CW, Espinosa N, Raptis DA, Buck FM. Dixon-based MRI for assessment of muscle-fat content in phantoms, healthy volunteers and patients with achillodynia: comparison to visual assessment of calf muscle quality. Eur Radiol. 2014;24(6):1366-75.

261. Gaeta M, Messina S, Mileto A, Vita GL, Ascenti G, Vinci S, et al. Muscle fat-fraction and mapping in Duchenne muscular dystrophy: evaluation of disease distribution and correlation with clinical assessments. Preliminary experience. Skeletal Radiol. 2012;41(8):955-61.

262. Triplett WT, Baligand C, Forbes SC, Willcocks RJ, Lott DJ, DeVos S, et al. Chemical shift-based MRI to measure fat fractions in dystrophic skeletal muscle. Magn Reson Med. 2014;72(1):8-19.

263. Cicchetti DV. Guidelines, criteria, and rules of thumb for evaluating normed and standardized assessment instruments in psychology. Psychological assessment. 1994;6(4):284.

264. Yu H, Shimakawa A, McKenzie CA, Brodsky E, Brittain JH, Reeder SB. Multiecho water-fat separation and simultaneous R2* estimation with multifrequency fat spectrum modeling. Magn Reson Med. 2008;60(5):1122-34.

265. Sigmund EE, Sui D, Ukpebor O, Baete S, Fieremans E, Babb JS, et al. Stimulated echo diffusion tensor imaging and SPAIR T2 -weighted imaging in chronic exertional compartment syndrome of the lower leg muscles. J Magn Reson Imaging. 2013;38(5):1073-82.

266. Kumar D, Karampinos DC, MacLeod TD, Lin W, Nardo L, Li X, et al. Quadriceps intramuscular fat fraction rather than muscle size is associated with knee osteoarthritis. Osteoarthritis Cartilage. 2014;22(2):226-34.

267. Schick F, Machann J, Brechtel K, Strempfer A, Klumpp B, Stein DT, et al. MRI of muscular fat. Magn Reson Med. 2002;47(4):720-7.

268. Kermarrec E, Budzik JF, Khalil C, Le Thuc V, Hancart-Destee C, Cotten A. In vivo diffusion tensor imaging and tractography of human thigh muscles in healthy subjects. AJR Am J Roentgenol. 2010;195(5):W352-6.

269. Sinha S, Sinha U, Edgerton VR. In vivo diffusion tensor imaging of the human calf muscle. J Magn Reson Imaging. 2006;24(1):182-90.

270. Ponrartana S, Andrade KE, Wren TA, Ramos-Platt L, Hu HH, Bluml S, et al. Repeatability of chemical-shift-encoded water-fat MRI and diffusion-tensor imaging in lower extremity muscles in children. AJR Am J Roentgenol. 2014;202(6):W567-73.

271. Kinsella KG, Phillips DR. Global aging: The challenge of success. Washington, DC: Population Reference Bureau. 2005;60(1):3.

272. Visser M, Goodpaster BH, Kritchevsky SB, Newman AB, Nevitt M, Rubin SM, et al. Muscle mass, muscle strength, and muscle fat infiltration as predictors of incident mobility limitations in well-functioning older persons. J Gerontol A Biol Sci Med Sci. 2005;60(3):324-33.

273. Fantin F, Di Francesco V, Fontana G, Zivelonghi A, Bissoli L, Zoico E, et al. Longitudinal body composition changes in old men and women: interrelationships with worsening disability. J Gerontol A Biol Sci Med Sci. 2007;62(12):1375-81.

274. Bouchard DR, Janssen I. Dynapenic-obesity and physical function in older adults. J Gerontol A Biol Sci Med Sci. 2010;65(1):71-7.

275. Visser M, Deeg DJ, Lips P, Harris TB, Bouter LM. Skeletal muscle mass and muscle strength in relation to lower-extremity performance in older men and women. J Am Geriatr Soc. 2000;48(4):381-6.

276. Ferrucci L, Penninx BW, Volpato S, Harris TB, Bandeen-Roche K, Balfour J, et al. Change in muscle strength explains accelerated decline of physical function in older women with high interleukin-6 serum levels. J Am Geriatr Soc. 2002;50(12):1947-54.

277. Stalenhoef PA, Diederiks JP, Knottnerus JA, Kester AD, Crebolder HF. A risk model for the prediction of recurrent falls in community-dwelling elderly: a prospective cohort study. J Clin Epidemiol. 2002;55(11):1088-94.

278. Pluijm SM, Smit JH, Tromp EA, Stel VS, Deeg DJ, Bouter LM, et al. A risk profile for identifying community-dwelling elderly with a high risk of recurrent falling: results of a 3-year prospective study. Osteoporos Int. 2006;17(3):417-25.

279. Roubenoff R, Hughes VA. Sarcopenia: current concepts. J Gerontol A Biol Sci Med Sci. 2000;55(12):M716-24.

280. Rosenberg IH. Sarcopenia: origins and clinical relevance. J Nutr. 1997;127(5 Suppl):990S-1S.

281. Young A, Stokes M, Crowe M. Size and strength of the quadriceps muscles of old and young women. Eur J Clin Invest. 1984;14(4):282-7.

282. Young A, Stokes M, Crowe M. The size and strength of the quadriceps muscles of old and young men. Clin Physiol. 1985;5(2):145-54.

283. Overend TJ, Cunningham DA, Paterson DH, Lefcoe MS. Thigh composition in young and elderly men determined by computed tomography. Clin Physiol. 1992;12(6):629-40.

284. Kent-Braun JA, Ng AV, Young K. Skeletal muscle contractile and noncontractile components in young and older women and men. J Appl Physiol (1985). 2000;88(2):662-8.

285. Goodpaster BH, Park SW, Harris TB, Kritchevsky SB, Nevitt M, Schwartz AV, et al. The loss of skeletal muscle strength, mass, and quality in older adults: the health, aging and body composition study. J Gerontol A Biol Sci Med Sci. 2006;61(10):1059-64.

286. Mitchell WK, Williams J, Atherton P, Larvin M, Lund J, Narici M. Sarcopenia, dynapenia, and the impact of advancing age on human skeletal muscle size and strength; a quantitative review. Front Physiol. 2012;3:260.

287. Morley JE. Sarcopenia: diagnosis and treatment. J Nutr Health Aging. 2008;12(7):452-6.

288. von Haehling S, Morley JE, Anker SD. An overview of sarcopenia: facts and numbers on prevalence and clinical impact. J Cachexia Sarcopenia Muscle. 2010;1(2):129-33.

289. Newman AB, Kupelian V, Visser M, Simonsick EM, Goodpaster BH, Kritchevsky SB, et al. Strength, but not muscle mass, is associated with mortality in the health, aging and body composition study cohort. J Gerontol A Biol Sci Med Sci. 2006;61(1):72-7.

290. Gale CR, Martyn CN, Cooper C, Sayer AA. Grip strength, body composition, and mortality. Int J Epidemiol. 2007;36(1):228-35.

291. Janssen I, Shepard DS, Katzmarzyk PT, Roubenoff R. The healthcare costs of sarcopenia in the United States. J Am Geriatr Soc. 2004;52(1):80-5.

292. Welle S. Cellular and molecular basis of age-related sarcopenia. Can J Appl Physiol. 2002;27(1):19-41.

293. Lawler JM, Hindle A. Living in a box or call of the wild? Revisiting lifetime inactivity and sarcopenia. Antioxid Redox Signal. 2011;15(9):2529-41.

294. Lexell J, Taylor CC, Sjostrom M. What is the cause of the ageing atrophy? Total number, size and proportion of different fiber types studied in whole vastus lateralis muscle from 15- to 83-year-old men. J Neurol Sci. 1988;84(2-3):275-94.

295. Larsson L, Grimby G, Karlsson J. Muscle strength and speed of movement in relation to age and muscle morphology. J Appl Physiol Respir Environ Exerc Physiol. 1979;46(3):451-6.

296. Larsson L, Sjodin B, Karlsson J. Histochemical and biochemical changes in human skeletal muscle with age in sedentary males, age 22--65 years. Acta Physiol Scand. 1978;103(1):31-9.

297. Scelsi R, Marchetti C, Poggi P. Histochemical and ultrastructural aspects of m. vastus lateralis in sedentary old people (age 65--89 years). Acta Neuropathol. 1980;51(2):99-105.

298. Caccia MR, Harris JB, Johnson MA. Morphology and physiology of skeletal muscle in aging rodents. Muscle Nerve. 1979;2(3):202-12.

299. Jakobsson F, Borg K, Edstrom L, Grimby L. Use of motor units in relation to muscle fiber type and size in man. Muscle Nerve. 1988;11(12):1211-8.

300. Mantyvaara J, Sjoholm T, Pertovaara A. Masseter inhibitory reflex in humans: attempted modulation by various experimental parameters. Acta Physiol Scand. 1999;167(2):A21.

301. Tomonaga M. Histochemical and ultrastructural changes in senile human skeletal muscle. J Am Geriatr Soc. 1977;25(3):125-31.

302. Akasaki Y, Ouchi N, Izumiya Y, Bernardo BL, Lebrasseur NK, Walsh K. Glycolytic fast-twitch muscle fiber restoration counters adverse age-related changes in body composition and metabolism. Aging Cell. 2014;13(1):80-91.

303. Rice CL, Cunningham DA, Paterson DH, Lefcoe MS. Arm and leg composition determined by computed tomography in young and elderly men. Clin Physiol. 1989;9(3):207-20.

304. Forsberg AM, Nilsson E, Werneman J, Bergstrom J, Hultman E. Muscle composition in relation to age and sex. Clin Sci (Lond). 1991;81(2):249-56.

305. Heymsfield SB, Gonzalez MC, Lu J, Jia G, Zheng J. Skeletal muscle mass and quality: evolution of modern measurement concepts in the context of sarcopenia. Proc Nutr Soc. 2015;74(4):355-66.

306. Roubenoff R, Parise H, Payette HA, Abad LW, D'Agostino R, Jacques PF, et al. Cytokines, insulin-like growth factor 1, sarcopenia, and mortality in very old community-dwelling men and women: the Framingham Heart Study. Am J Med. 2003;115(6):429-35.

307. Bruunsgaard H, Pedersen M, Pedersen BK. Aging and proinflammatory cytokines. Curr Opin Hematol. 2001;8(3):131-6.

308. Fong Y, Moldawer LL, Marano M, Wei H, Barber A, Manogue K, et al. Cachectin/TNF or IL-1 alpha induces cachexia with redistribution of body proteins. Am J Physiol. 1989;256(3 Pt 2):R659-65.

309. Lang CH, Frost RA, Nairn AC, MacLean DA, Vary TC. TNF-alpha impairs heart and skeletal muscle protein synthesis by altering translation initiation. Am J Physiol Endocrinol Metab. 2002;282(2):E336-47.

310. Narici MV, Maffulli N. Sarcopenia: characteristics, mechanisms and functional significance. Br Med Bull. 2010;95(1):139-59.

311. Skelton DA, Greig CA, Davies JM, Young A. Strength, power and related functional ability of healthy people aged 65-89 years. Age Ageing. 1994;23(5):371-7.

312. Reeves D, Pye S, Ashcroft DM, Clegg A, Kontopantelis E, Blakeman T, et al. The challenge of ageing populations and patient frailty: can primary care adapt? BMJ. 2018;362:k3349.

313. Bauer JM, Sieber CC. Sarcopenia and frailty: a clinician's controversial point of view. Exp Gerontol. 2008;43(7):674-8.

314. Clegg A, Young J, Iliffe S, Rikkert MO, Rockwood K. Frailty in elderly people. Lancet. 2013;381(9868):752-62.

315. Fried LP, Tangen CM, Walston J, Newman AB, Hirsch C, Gottdiener J, et al. Frailty in older adults: evidence for a phenotype. J Gerontol A Biol Sci Med Sci. 2001;56(3):M146-56.

316. Song X, Mitnitski A, Rockwood K. Prevalence and 10-year outcomes of frailty in older adults in relation to deficit accumulation. J Am Geriatr Soc. 2010;58(4):681-7.

317. Han L, Clegg A, Doran T, Fraser L. The impact of frailty on healthcare resource use: a longitudinal analysis using the Clinical Practice Research Datalink in England. Age Ageing. 2019;48(5):665-71.

318. Reeves ND, Maganaris CN, Longo S, Narici MV. Differential adaptations to eccentric versus conventional resistance training in older humans. Exp Physiol. 2009;94(7):825-33.

319. Sinha U, Csapo R, Malis V, Xue Y, Sinha S. Age-related differences in diffusion tensor indices and fiber architecture in the medial and lateral gastrocnemius. J Magn Reson Imaging. 2015;41(4):941-53.

320. Yoon MA, Hong SJ, Ku MC, Kang CH, Ahn KS, Kim BH. Multiparametric MR Imaging of Age-related Changes in Healthy Thigh Muscles. Radiology. 2018;287(1):235-46.

321. McPhee JS, Hogrel JY, Maier AB, Seppet E, Seynnes OR, Sipila S, et al. Physiological and functional evaluation of healthy young and older men and women: design of the European MyoAge study. Biogerontology. 2013;14(3):325-37.

322. Heaven A, Brown L, Young J, Teale E, Hawkins R, Spilsbury K, et al. Community ageing research 75+ study (CARE75+): an experimental ageing and frailty research cohort. BMJ Open. 2019;9(3):e026744.

323. Gale CR, Mottus R, Deary IJ, Cooper C, Sayer AA. Personality and Risk of Frailty: the English Longitudinal Study of Ageing. Ann Behav Med. 2017;51(1):128-36.

324. Steptoe A, Breeze E, Banks J, Nazroo J. Cohort profile: the English longitudinal study of ageing. Int J Epidemiol. 2013;42(6):1640-8.

325. Hatakenaka M, Ueda M, Ishigami K, Otsuka M, Masuda K. Effects of aging on muscle T2 relaxation time: difference between fast- and slow-twitch muscles. Invest Radiol. 2001;36(12):692-8.

326. Schwenzer NF, Martirosian P, Machann J, Schraml C, Steidle G, Claussen CD, et al. Aging effects on human calf muscle properties assessed by MRI at 3 Tesla. J Magn Reson Imaging. 2009;29(6):1346-54.

327. Azzabou N, Hogrel JY, Carlier PG. NMR based biomarkers to study age-related changes in the human quadriceps. Exp Gerontol. 2015;70:54-60.

328. Stanisz GJ, Odrobina EE, Pun J, Escaravage M, Graham SJ, Bronskill MJ, et al. T1, T2 relaxation and magnetization transfer in tissue at 3T. Magn Reson Med. 2005;54(3):507-12.

329. Cesari M, Penninx BW, Pahor M, Lauretani F, Corsi AM, Rhys Williams G, et al. Inflammatory markers and physical performance in older persons: the InCHIANTI study. J Gerontol A Biol Sci Med Sci. 2004;59(3):242-8.

330. Cesari M, Fielding RA, Pahor M, Goodpaster B, Hellerstein M, van Kan GA, et al. Biomarkers of sarcopenia in clinical trials-recommendations from the International Working Group on Sarcopenia. J Cachexia Sarcopenia Muscle. 2012;3(3):181-90.

331. Carter CS, Justice JN, Thompson L. Lipotoxicity, aging, and muscle contractility: does fiber type matter? Geroscience. 2019;41(3):297-308.

332. Janovska A, Hatzinikolas G, Mano M, Wittert GA. The effect of dietary fat content on phospholipid fatty acid profile is muscle fiber type dependent. Am J Physiol Endocrinol Metab. 2010;298(4):E779-86.

333. Yanagisawa O, Kurihara T, Kobayashi N, Fukubayashi T. Strenuous resistance exercise effects on magnetic resonance diffusion parameters and muscle-tendon function in human skeletal muscle. J Magn Reson Imaging. 2011;34(4):887-94.

334. Ababneh ZQ, Ababneh R, Maier SE, Winalski CS, Oshio K, Ababneh AM, et al. On the correlation between T(2) and tissue diffusion coefficients in exercised muscle: quantitative measurements at 3T within the tibialis anterior. MAGMA. 2008;21(4):273-8.

335. Deux JF, Malzy P, Paragios N, Bassez G, Luciani A, Zerbib P, et al. Assessment of calf muscle contraction by diffusion tensor imaging. Eur Radiol. 2008;18(10):2303-10.

336. Kortebein P, Ferrando A, Lombeida J, Wolfe R, Evans WJ. Effect of 10 days of bed rest on skeletal muscle in healthy older adults. JAMA. 2007;297(16):1772-4.

337. Morley JE. Hormones and the aging process. J Am Geriatr Soc. 2003;51(7 Suppl):S333-7.

338. Visser M, Deeg DJ, Lips P, Longitudinal Aging Study A. Low vitamin D and high parathyroid hormone levels as determinants of loss of muscle strength and muscle mass (sarcopenia): the Longitudinal Aging Study Amsterdam. J Clin Endocrinol Metab. 2003;88(12):5766-72.

339. Cesari M, Kritchevsky SB, Baumgartner RN, Atkinson HH, Penninx BW, Lenchik L, et al. Sarcopenia, obesity, and inflammation--results from the Trial of Angiotensin Converting Enzyme Inhibition and Novel Cardiovascular Risk Factors study. Am J Clin Nutr. 2005;82(2):428-34.

340. Reijnierse EM, de Jong N, Trappenburg MC, Blauw GJ, Butler-Browne G, Gapeyeva H, et al. Assessment of maximal handgrip strength: how many attempts are needed? J Cachexia Sarcopenia Muscle. 2017;8(3):466-74.

341. Chinoy H, Cooper RG. Myositis. 1 ed. Oxford: Oxford University Press; 2017. 198 p.

342. Carstens PO, Schmidt J. Diagnosis, pathogenesis and treatment of myositis: recent advances. Clin Exp Immunol. 2014;175(3):349-58.

343. Dalakas MC. Inflammatory muscle diseases. N Engl J Med. 2015;372(18):1734-47.

344. Limaye V, Hakendorf P, Woodman RJ, Blumbergs P, Roberts-Thomson P. Mortality and its predominant causes in a large cohort of patients with biopsy-determined inflammatory myositis. Intern Med J. 2012;42(2):191-8.

345. Dalakas MC. Polymyositis, dermatomyositis and inclusion-body myositis. N Engl J Med. 1991;325(21):1487-98.

346. Dalakas MC, Hohlfeld R. Polymyositis and dermatomyositis. Lancet. 2003;362(9388):971-82.

347. Lundberg IE, Tjarnlund A, Bottai M, Werth VP, Pilkington C, Visser M, et al. 2017 European League Against Rheumatism/American College of Rheumatology classification criteria for adult and juvenile idiopathic inflammatory myopathies and their major subgroups. Ann Rheum Dis. 2017;76(12):1955-64.

348. Badrising UA, Maat-Schieman ML, Ferrari MD, Zwinderman AH, Wessels JA, Breedveld FC, et al. Comparison of weakness progression in inclusion body myositis during treatment with methotrexate or placebo. Ann Neurol. 2002;51(3):369-72.

349. Cox FM, Reijnierse M, van Rijswijk CS, Wintzen AR, Verschuuren JJ, Badrising UA. Magnetic resonance imaging of skeletal muscles in sporadic inclusion body myositis. Rheumatology (Oxford). 2011;50(6):1153-61.

350. Cox FM, Titulaer MJ, Sont JK, Wintzen AR, Verschuuren JJ, Badrising UA. A 12-year follow-up in sporadic inclusion body myositis: an end stage with major disabilities. Brain. 2011;134(Pt 11):3167-75.

351. Cortese A, Machado P, Morrow J, Dewar L, Hiscock A, Miller A, et al. Longitudinal observational study of sporadic inclusion body myositis: implications for clinical trials. Neuromuscul Disord. 2013;23(5):404-12.

352. Miller FW, Rider LG, Chung YL, Cooper R, Danko K, Farewell V, et al. Proposed preliminary core set measures for disease outcome assessment in adult and juvenile idiopathic inflammatory myopathies. Rheumatology (Oxford). 2001;40(11):1262-73.

353. Rider LG, Giannini EH, Brunner HI, Ruperto N, James-Newton L, Reed AM, et al. International consensus on preliminary definitions of improvement in adult and juvenile myositis. Arthritis Rheum. 2004;50(7):2281-90.

354. Rider LG, Giannini EH, Harris-Love M, Joe G, Isenberg D, Pilkington C, et al. Defining Clinical Improvement in Adult and Juvenile Myositis. J Rheumatol. 2003;30(3):603-17.

355. Harris-Love MO, Shrader JA, Koziol D, Pahlajani N, Jain M, Smith M, et al. Distribution and severity of weakness among patients with polymyositis, dermatomyositis and juvenile dermatomyositis. Rheumatology (Oxford). 2009;48(2):134-9.

356. Kendall F, McCreary E, Provance PJB, Maryland: Williams, Wilkins. Muscle testing and function 4th edition. Philadelphia: Lippincott Williams and Wilkins; 1993. 560 p.

357. Alexanderson H, Broman L, Tollback A, Josefson A, Lundberg IE, Stenstrom CH. Functional index-2: Validity and reliability of a disease-specific measure of impairment in patients with polymyositis and dermatomyositis. Arthritis Rheum. 2006;55(1):114-22.

358. Alexanderson H, Regardt M, Ottosson C, Alemo Munters L, Dastmalchi M, Dani L, et al. Muscle Strength and Muscle Endurance During the First Year of Treatment of Polymyositis and Dermatomyositis: A Prospective Study. J Rheumatol. 2018;45(4):538-46.

359. Moxley RT, 3rd. Evaluation of neuromuscular function in inflammatory myopathy. Rheum Dis Clin North Am. 1994;20(4):827-43.

360. Stoll T, Bruhlmann P, Stucki G, Seifert B, Michel BA. Muscle strength assessment in polymyositis and dermatomyositis evaluation of the reliability and clinical use of a new, quantitative, easily applicable method. J Rheumatol. 1995;22(3):473-7.

361. Bohan A, Peter JB, Bowman RL, Pearson CM. Computer-assisted analysis of 153 patients with polymyositis and dermatomyositis. Medicine (Baltimore). 1977;56(4):255-86.

362. Theodorou DJ, Theodorou SJ, Kakitsubata Y. Skeletal muscle disease: patterns of MRI appearances. Br J Radiol. 2012;85(1020):e1298-308.

363. Caetano AP, Alves P. Advanced MRI Patterns of Muscle Disease in Inherited and Acquired Myopathies: What the Radiologist Should Know. Semin Musculoskelet Radiol. 2019;23(3):e82-e106.

364. Ran J, Ji S, Morelli JN, Wu G, Li X. T2 mapping in dermatomyositis/polymyositis and correlation with clinical parameters. Clin Radiol. 2018;73(12):1057 e13- e18.

365. Jones TA, Wayte SC, Reddy NL, Adesanya O, Dimitriadis GK, Barber TM, et al. Identification of an optimal threshold for detecting human brown adipose tissue using receiver operating characteristic analysis of IDEAL MRI fat fraction maps. Magn Reson Imaging. 2018;51:61-8.

366. Meyer HJ, Ziemann O, Kornhuber M, Emmer A, Quaschling U, Schob S, et al. Apparent diffusion coefficient (ADC) does not correlate with different serological parameters in myositis and myopathy. Acta Radiol. 2018;59(6):694-9.

367. Pillen S, Arts IM, Zwarts MJ. Muscle ultrasound in neuromuscular disorders. Muscle Nerve. 2008;37(6):679-93.

368. Tomasova Studynkova J, Charvat F, Jarosova K, Vencovsky J. The role of MRI in the assessment of polymyositis and dermatomyositis. Rheumatology (Oxford). 2007;46(7):1174-9.

369. Maurer B, Walker UA. Role of MRI in diagnosis and management of idiopathic inflammatory myopathies. Curr Rheumatol Rep. 2015;17(11):67.

370. May DA, Disler DG, Jones EA, Balkissoon AA, Manaster BJ. Abnormal signal intensity in skeletal muscle at MR imaging: patterns, pearls, and pitfalls. Radiographics. 2000;20 Spec No(suppl_1):S295-315.

371. Fraser DD, Frank JA, Dalakas M, Miller FW, Hicks JE, Plotz P. Magnetic resonance imaging in the idiopathic inflammatory myopathies. J Rheumatol. 1991;18(11):1693-700.

372. Schiffenbauer A. Imaging: seeing muscle in new ways. Curr Opin Rheumatol. 2014;26(6):712-6.

373. Sigmund EE, Baete SH, Luo T, Patel K, Wang D, Rossi I, et al. MRI assessment of the thigh musculature in dermatomyositis and healthy subjects using diffusion tensor imaging, intravoxel incoherent motion and dynamic DTI. Eur Radiol. 2018;28(12):5304-15.

374. Ran J, Liu Y, Sun D, Morelli J, Zhang P, Wu G, et al. The diagnostic value of biexponential apparent diffusion coefficients in myopathy. J Neurol. 2016;263(7):1296-302.

375. Baumli HP, Mumenthaler M. The perifascicular atrophy factor. An aid in the histological diagnosis of polymyositis. J Neurol. 1977;214(2):129-36.

376. Bohan A, Peter JB. Polymyositis and dermatomyositis (first of two parts). N Engl J Med. 1975;292(7):344-7.

377. Kim HK, Laor T, Horn PS, Racadio JM, Wong B, Dardzinski BJ. T2 mapping in Duchenne muscular dystrophy: distribution of disease activity and correlation with clinical assessments. Radiology. 2010;255(3):899-908.

378. Yao L, Gai N. Fat-corrected T2 measurement as a marker of active muscle disease in inflammatory myopathy. AJR Am J Roentgenol. 2012;198(5):W475-81.

379. Schlaeger S, Weidlich D, Klupp E, Montagnese F, Deschauer M, Schoser B, et al. Decreased water T2 in fatty infiltrated skeletal muscles of patients with neuromuscular diseases. NMR Biomed. 2019;32(8):e4111.

380. Wokke BH, van den Bergen JC, Versluis MJ, Niks EH, Milles J, Webb AG, et al. Quantitative MRI and strength measurements in the assessment of muscle quality in Duchenne muscular dystrophy. Neuromuscul Disord. 2014;24(5):409-16.

381. Chen L, Nelson DR, Zhao Y, Cui Z, Johnston JA. Relationship between muscle mass and muscle strength, and the impact of comorbidities: a population-based, cross-sectional study of older adults in the United States. BMC Geriatr. 2013;13(1):74.

382. Ai T, Yu K, Gao L, Zhang P, Goerner F, Runge VM, et al. Diffusion tensor imaging in evaluation of thigh muscles in patients with polymyositis and dermatomyositis. Br J Radiol. 2014;87(1043):20140261.

383. Westhoff G, Listing J, Zink A. Loss of physical independence in rheumatoid arthritis: interview data from a representative sample of patients in rheumatologic care. Arthritis Care Res. 2000;13(1):11-22.

384. Hakkinen A, Sokka T, Kotaniemi A, Paananen ML, Malkia E, Kautiainen H, et al. Muscle strength characteristics and central bone mineral density in women with recent onset rheumatoid arthritis compared with healthy controls. Scand J Rheumatol. 1999;28(3):145-51.

385. Miro O, Pedrol E, Casademont J, Garcia-Carrasco M, Sanmarti R, Cebrian M, et al. Muscle involvement in rheumatoid arthritis: clinicopathological study of 21 symptomatic cases. Semin Arthritis Rheum. 1996;25(6):421-8.

386. Agrawal V, Husain N, Das SK, Bagchi M. Muscle involvement in rheumatoid arthritis: clinical and histological characteristics and review of literature. J Indian Rheumatol Assoc. 2003;11(4):98-103.

387. Li H, Malhotra S, Kumar A. Nuclear factor-kappa B signaling in skeletal muscle atrophy. J Mol Med (Berl). 2008;86(10):1113-26.

388. Schaap LA, Pluijm SM, Deeg DJ, Harris TB, Kritchevsky SB, Newman AB, et al. Higher inflammatory marker levels in older persons: associations with 5-year change in muscle mass and muscle strength. J Gerontol A Biol Sci Med Sci. 2009;64(11):1183-9.

389. Metsios GS, Stavropoulos-Kalinoglou A, Panoulas VF, Koutedakis Y, Nevill AM, Douglas KM, et al. New resting energy expenditure prediction equations for patients with rheumatoid arthritis. Rheumatology (Oxford). 2008;47(4):500-6.

390. Metsios GS, Stavropoulos-Kalinoglou A, Panoulas VF, Sandoo A, Toms TE, Nevill AM, et al. Rheumatoid cachexia and cardiovascular disease. Clin Exp Rheumatol. 2009;27(6):985-8.

391. Kremers HM, Nicola PJ, Crowson CS, Ballman KV, Gabriel SE. Prognostic importance of low body mass index in relation to cardiovascular mortality in rheumatoid arthritis. Arthritis Rheum. 2004;50(11):3450-7.

392. Giles JT, Bartlett SJ, Andersen RE, Fontaine KR, Bathon JM. Association of body composition with disability in rheumatoid arthritis: impact of appendicular fat and lean tissue mass. Arthritis Rheum. 2008;59(10):1407-15.

393. Biolo G, Cederholm T, Muscaritoli M. Muscle contractile and metabolic dysfunction is a common feature of sarcopenia of aging and chronic diseases: from sarcopenic obesity to cachexia. Clin Nutr. 2014;33(5):737-48.

394. Saraux A, Berthelot JM, Chales G, Le Henaff C, Thorel JB, Hoang S, et al. Ability of the American College of Rheumatology 1987 criteria to predict rheumatoid arthritis in patients with early arthritis and classification of these patients two years later. Arthritis Rheum. 2001;44(11):2485-91.

395. D'Agostino MA, Terslev L, Aegerter P, Backhaus M, Balint P, Bruyn GA, et al. Scoring ultrasound synovitis in rheumatoid arthritis: a EULAR-OMERACT ultrasound taskforce-Part 1: definition and development of a standardised, consensus-based scoring system. RMD Open. 2017;3(1):e000428.

396. Terslev L, Naredo E, Aegerter P, Wakefield RJ, Backhaus M, Balint P, et al. Scoring ultrasound synovitis in rheumatoid arthritis: a EULAR-OMERACT ultrasound taskforce-Part 2: reliability and application to multiple joints of a standardised consensus-based scoring system. RMD Open. 2017;3(1):e000427.

397. Just SA, Nielsen C, Werlinrud JC, Larsen PV, Klinkby CS, Schroder HD, et al. Six-month prospective trial in early and long-standing rheumatoid arthritis: evaluating disease activity in the wrist through sequential synovial

histopathological analysis, RAMRIS magnetic resonance score and EULAR-OMERACT ultrasound score. RMD Open. 2019;5(2):e000951.

398. Lisbona MP, Solano A, Ares J, Almirall M, Salman-Monte TC, Maymo J. ACR/EULAR Definitions of Remission Are Associated with Lower Residual Inflammatory Activity Compared with DAS28 Remission on Hand MRI in Rheumatoid Arthritis. J Rheumatol. 2016;43(9):1631-6.

399. Carstensen SMD, Terslev L, Jensen MP, Ostergaard M. Future use of musculoskeletal ultrasonography and magnetic resonance imaging in rheumatoid arthritis. Curr Opin Rheumatol. 2020;32(3):264-72.

400. Aletaha D, Neogi T, Silman AJ, Funovits J, Felson DT, Bingham CO, 3rd, et al. 2010 Rheumatoid arthritis classification criteria: an American College of Rheumatology/European League Against Rheumatism collaborative initiative. Arthritis Rheum. 2010;62(9):2569-81.

401. Taylor R. Interpretation of the Correlation Coefficient: A Basic Review. Journal of Diagnostic Medical Sonography. 2016;6(1):35-9.

402. Borenstein M. The case for confidence intervals in controlled clinical trials. Control Clin Trials. 1994;15(5):411-28.

403. Khoja SS, Patterson CG, Goodpaster BH, Delitto A, Piva SR. Skeletal muscle fat in individuals with rheumatoid arthritis compared to healthy adults. Exp Gerontol. 2020;129:110768.

404. Helliwell PS, Jackson S. Relationship between weakness and muscle wasting in rheumatoid arthritis. Ann Rheum Dis. 1994;53(11):726-8.

405. Pereira RM, Freire de Carvalho J. Glucocorticoid-induced myopathy. Joint Bone Spine. 2011;78(1):41-4.

406. Tomaszewski M, Stepien KM, Tomaszewska J, Czuczwar SJ. Statin-induced myopathies. Pharmacol Rep. 2011;63(4):859-66.

407. Cooney JK, Law RJ, Matschke V, Lemmey AB, Moore JP, Ahmad Y, et al. Benefits of exercise in rheumatoid arthritis. J Aging Res. 2011;2011:681640.

408. Coath F, Gillbert K, Griffiths B, Hall F, Kay L, Lanyon P, et al. Giant cell arteritis: new concepts, treatments and the unmet need that remains. Rheumatology (Oxford). 2019;58(7):1123-5.

409. Liddle J, Bartlam R, Mallen CD, Mackie SL, Prior JA, Helliwell T, et al. What is the impact of giant cell arteritis on patients' lives? A UK qualitative study. BMJ Open. 2017;7(8):e017073.

410. Aiello PD, Trautmann JC, McPhee TJ, Kunselman AR, Hunder GG. Visual prognosis in giant cell arteritis. Ophthalmology. 1993;100(4):550-5.

411. Hellmich B, Agueda A, Monti S, Buttgereit F, de Boysson H, Brouwer E, et al. 2018 Update of the EULAR recommendations for the management of large vessel vasculitis. Ann Rheum Dis. 2020;79(1):19-30.

412. Gupta A, Gupta Y. Glucocorticoid-induced myopathy: Pathophysiology, diagnosis, and treatment. Indian J Endocrinol Metab. 2013;17(5):913-6.

413. Hasselgren PO. Glucocorticoids and muscle catabolism. Curr Opin Clin Nutr Metab Care. 1999;2(3):201-5.

414. Dekhuijzen PN, Gayan-Ramirez G, Bisschop A, De Bock V, Dom R, Decramer M. Corticosteroid treatment and nutritional deprivation cause a different pattern of atrophy in rat diaphragm. J Appl Physiol (1985). 1995;78(2):629-37.

415. Levine A, Broide E, Stein M, Bujanover Y, Weizman Z, Dinari G, et al. Evaluation of oral budesonide for treatment of mild and moderate exacerbations of Crohn's disease in children. J Pediatr. 2002;140(1):75-80.

416. Walsh LJ, Wong CA, Oborne J, Cooper S, Lewis SA, Pringle M, et al. Adverse effects of oral corticosteroids in relation to dose in patients with lung disease. Thorax. 2001;56(4):279-84.

417. Levin OS, Polunina AG, Demyanova MA, Isaev FV. Steroid myopathy in patients with chronic respiratory diseases. J Neurol Sci. 2014;338(1-2):96-101.

418. Pons C, Borotikar B, Garetier M, Burdin V, Ben Salem D, Lempereur M, et al. Quantifying skeletal muscle volume and shape in humans using MRI: A systematic review of validity and reliability. PLoS One. 2018;13(11):e0207847.

419. Marie I. Morbidity and mortality in adult polymyositis and dermatomyositis. Curr Rheumatol Rep. 2012;14(3):275-85.

420. Powers SK, Lynch GS, Murphy KT, Reid MB, Zijdewind I. Disease-Induced Skeletal Muscle Atrophy and Fatigue. Med Sci Sports Exerc. 2016;48(11):2307-19.

421. Aghdam KA, Sanjari MS, Manafi N, Khorramdel S, Alemzadeh SA, Navahi RAA. Temporal Artery Biopsy for Diagnosing Giant Cell Arteritis: A Ten-year Review. J Ophthalmic Vis Res. 2020;15(2):201-9.

422. Hedges LV. Distribution Theory for Glass's Estimator of Effect size and Related Estimators. Journal of Educational Statistics. 2016;6(2):107-28.

423. McGraw KO, Wong SP. A common language effect size statistic. Psychological Bulletin. 1992;111(2):361-5.

424. Reed RL, Pearlmutter L, Yochum K, Meredith KE, Mooradian AD. The relationship between muscle mass and muscle strength in the elderly. J Am Geriatr Soc. 1991;39(6):555-61.

425. Mackie SL, Mallen CD. Polymyalgia rheumatica. BMJ. 2013;347(dec03 1):f6937.

426. Jin J, Sklar GE, Min Sen Oh V, Chuen Li S. Factors affecting therapeutic compliance: A review from the patient's perspective. Ther Clin Risk Manag. 2008;4(1):269-86.

427. Nagy S, Schädelin S, Hafner P, Bonati U, Scherrer D, Ebi S, et al. Longitudinal reliability of outcome measures in patients with Duchenne muscular dystrophy. Muscle Nerve. 2020;61(1):63-8.

428. Goubert D, Oosterwijck JV, Meeus M, Danneels L. Structural Changes of Lumbar Muscles in Non-specific Low Back Pain: A Systematic Review. Pain Physician. 2016;19(7):E985-E1000.

429. Wendling D, Hory B, Guidet M, Saint-Hillier Y, Cassou M, Perol C. [Unusual muscular manifestations in a case of Horton's disease]. Sem Hop. 1983;59(39):2713-5.

430. Herbison GJ, Ditunno JF, Jaweed MM. Muscle atrophy in rheumatoid arthritis. J Rheumatol Suppl. 1987;14 Suppl 15:78-81.

431. Lassche S, Küsters B, Heerschap A, Schyns MVP, Ottenheijm CAC, Voermans NC, et al. Correlation Between Quantitative MRI and Muscle Histopathology in Muscle Biopsies from Healthy Controls and Patients with IBM, FSHD and OPMD. J Neuromuscul Dis. 2020;7(4):495-504.

432. Marcus RL, Addison O, Kidde JP, Dibble LE, Lastayo PC. Skeletal muscle fat infiltration: impact of age, inactivity, and exercise. J Nutr Health Aging. 2010;14(5):362-6.

433. Heskamp L, Okkersen K, van Nimwegen M, Ploegmakers MJ, Bassez G, Deux JF, et al. Quantitative Muscle MRI Depicts Increased Muscle Mass after a Behavioral Change in Myotonic Dystrophy Type 1. Radiology. 2020;297(1):132-42.

434. Hirano T, Matsuda T, Turner M, Miyasaka N, Buchan G, Tang B, et al. Excessive production of interleukin 6/B cell stimulatory factor-2 in rheumatoid arthritis. Eur J Immunol. 1988;18(11):1797-801.

435. Woods JA, Wilund KR, Martin SA, Kistler BM. Exercise, inflammation and aging. Aging Dis. 2012;3(1):130-40.

436. Haddad F, Zaldivar F, Cooper DM, Adams GR. IL-6-induced skeletal muscle atrophy. J Appl Physiol (1985). 2005;98(3):911-7.

437. Beavers KM, Brinkley TE, Nicklas BJ. Effect of exercise training on chronic inflammation. Clin Chim Acta. 2010;411(11-12):785-93.

438. Clarkson PM, Hubal MJ. Exercise-induced muscle damage in humans. Am J Phys Med Rehabil. 2002;81(11 Suppl):S52-69.

439. Steensberg A, Keller C, Starkie RL, Osada T, Febbraio MA, Pedersen BK. IL-6 and TNF-alpha expression in, and release from, contracting human skeletal muscle. Am J Physiol Endocrinol Metab. 2002;283(6):E1272-8.

440. Fu C, Xia Y, Meng F, Li F, Liu Q, Zhao H, et al. MRI Quantitative Analysis of Eccentric Exercise-induced Skeletal Muscle Injury in Rats. Acad Radiol. 2020;27(4):e72-e9.

441. Proske U, Morgan DL. Muscle damage from eccentric exercise: mechanism, mechanical signs, adaptation and clinical applications. J Physiol. 2001;537(Pt 2):333-45.

442. Ropars J, Gravot F, Ben Salem D, Rousseau F, Brochard S, Pons C. Muscle MRI: A biomarker of disease severity in Duchenne muscular dystrophy? A systematic review. Neurology. 2020;94(3):117-33.

443. Dahlqvist JR, Widholm P, Leinhard OD, Vissing J. MRI in Neuromuscular Diseases: An Emerging Diagnostic Tool and Biomarker for Prognosis and Efficacy. Ann Neurol. 2020;88(4):669-81.

444. Chrzanowski SM, Darras BT, Rutkove SB. The Value of Imaging and Composition-Based Biomarkers in Duchenne Muscular Dystrophy Clinical Trials. Neurotherapeutics. 2020;17(1):142-52.

445. Naarding KJ, Reyngoudt H, van Zwet EW, Hooijmans MT, Tian C, Rybalsky I, et al. MRI vastus lateralis fat fraction predicts loss of ambulation in Duchenne muscular dystrophy. Neurology. 2020;94(13):e1386-e94.

446. Goodall AF, Broadbent DA, Dumitru RB, Buckley DL, Tan AL, Buch MH, et al. Feasibility of MRI based extracellular volume fraction and partition coefficient measurements in thigh muscle. Br J Radiol. 2020;93(1111):20190931.

447. Miokovic T, Armbrecht G, Felsenberg D, Belavy DL. Heterogeneous atrophy occurs within individual lower limb muscles during 60 days of bed rest. J Appl Physiol (1985). 2012;113(10):1545-59.

448. Craig CL, Marshall AL, Sjostrom M, Bauman AE, Booth ML, Ainsworth BE, et al. International physical activity questionnaire: 12-country reliability and validity. Med Sci Sports Exerc. 2003;35(8):1381-95.

449. Marty B, Lopez Kolkovsky AL, Araujo ECA, Reyngoudt H. Quantitative Skeletal Muscle Imaging Using 3D MR Fingerprinting With Water and Fat Separation. J Magn Reson Imaging. 2020.

450. Nuñez-Peralta C, Alonso-Pérez J, Díaz-Manera J. The increasing role of muscle MRI to monitor changes over time in untreated and treated muscle diseases. Curr Opin Neurol. 2020;33(5):611-20.

451. Stoel B. Use of artificial intelligence in imaging in rheumatology - current status and future perspectives. RMD Open. 2020;6(1).

452. Trombetti A, Reid KF, Hars M, Herrmann FR, Pasha E, Phillips EM, et al. Age-associated declines in muscle mass, strength, power, and physical performance: impact on fear of falling and quality of life. Osteoporos Int. 2016;27(2):463-71.

453. Mijnarends DM, Luiking YC, Halfens RJG, Evers S, Lenaerts ELA, Verlaan S, et al. Muscle, Health and Costs: A Glance at their Relationship. J Nutr Health Aging. 2018;22(7):766-73.